Scattering Problems in Generalized Continua

MSc Thesis

By
Epameinondas Alevras

Supervised by
Thanasis Zisis
Panagiotis Gourgiotis

National Technical University of Athens
School of Applied Mathematical and Physical Sciences
Department of Mechanics
MSc Applied Mechanics

Athens, September 2024

Προβλήματα Σκέδασης σε Γενικευμένα Συνεχή Μέσα

Μεταπτυχιακή Διπλωματική Εργασία

Εκπόνηση
Επαμεινώνδας Αλευράς

Επίβλεψη
Θανάσης Ζήσης
Παναγιώτης Γουργιώτης

Εθνικό Μετσόβιο Πολυτεχνείο
Σχολή Εφαρμοσμένων Μαθηματικών και Φυσικών Επιστημών
Τομέας Μηχανικής
ΔΠΜΣ Εφαρμοσμένη Μηχανική

Αθήνα, Σεπτέμβριος 2024

Acknowledgements

With this work, my postgraduate studies come to an end, marking what has undoubtedly been the best part of my academic journey so far. My time as a postgraduate student in the MSc Applied Mechanics program has been especially productive, and I would like to extend my gratitude to everyone in the Department of Mechanics with whom I had the pleasure of collaborating during the years of my studies. First and foremost, I feel deeply obliged to thank the supervising professors of my Master Thesis, Thanasis, Zisis, and Panagiotis Gourgiotis, for their constant guidance and support. Their contribution was essential, and I can confidently say that the completion of this work would not have been possible without their involvement. I would also like to extend my gratitude to Professor Antonis Giannakopoulos for the private plasticity courses he gave during the spring semester of the 2022-2023 academic year, which were both enjoyable and unique in the topics covered. Finally, I would like to thank my parents for their unwavering support throughout my life.

Epameinondas Alevras

Ευχαριστίες

Με αυτή την εργασία ολοκληρώνονται οι μεταπτυχιακές μου σπουδές, σηματοδοτώντας αυτό που αναμφίβολα ήταν το καλύτερο μέρος της ακαδημαϊκής μου διαδρομής μέχρι τώρα. Ο χρόνος μου ως μεταπτυχιακός φοιτητής στο ΔΠΜΣ Εφαρμοσμένη Μηχανική ήταν ιδιαίτερα παραγωγικός και θα ήθελα να εκφράσω τις ευχαριστίες μου σε όλους τους ανθρώπους του Τομέα Μηχανικής με τους οποίους είχα τη χαρά να συνεργαστώ κατά τα χρόνια των σπουδών μου. Καταρχήν, αισθάνομαι βαθιά την υποχρέωση να ευχαριστήσω τους επιβλέποντες καθηγητές της Μεταπτυχιακής μου εργασίας, Θανάση, Ζήση και Παναγιώτη Γουργιώτη, για τη συνεχή καθοδήγηση και υποστήριξή τους. Η συμβολή τους ήταν ουσιαστική και μπορώ με βεβαιότητα να πω ότι η ολοκλήρωση αυτής της εργασίας δεν θα ήταν δυνατή χωρίς τη συμβολή τους. Θα ήθελα επίσης να εκφράσω τις ευχαριστίες μου στον καθηγητή Αντώνη Γιαννακόπουλο για τα ιδιαίτερα μαθήματα πλαστικότητας που έδωσε κατά το εαρινό εξάμηνο του ακαδημαϊκού έτους 2022-2023, τα οποία ήταν απολαυστικά και μοναδικά όσο αφορά τα θέματα που καλύφθηκαν. Τέλος, θα ήθελα να ευχαριστήσω τους γονείς μου για την αμέριστη συμπαράστασή τους σε όλη μου τη ζωή.

Επαμεινώνδας Αλευράς

Abstract

This work focuses on wave propagation in generalized continua governed by sub-theories of Mindlin's general one. The primary focus is given on deriving new analytical solutions (i.e., Green's functions) for infinite domains, which serve as a foundation for addressing problems where body waves are confined within configurations of obstacle points (pins). The pins are modelled as concentrated body forces, utilizing the displacement Green's functions derived in the work. The first chapter provides a brief overview of the key concepts presented in the work and discusses potential applications. In the second chapter, Mindlin's general theory is thoroughly presented, beginning with the most general non-linear micromorphic theory. The third chapter introduces the three simplified versions of Mindlin's general theory, known as Forms I, II, and III. Additionally, a brief overview of dipolar gradient elasticity, which represents the simplest version of Mindlin's general theory, is provided. This chapter also includes a section dedicated to the elastodynamics of gradient continua, with a particular focus on the formulation and proof of the completeness theorem, which the author believes is a gap in the current literature. In the fourth chapter, two analytical solutions for infinite domains under plane strain and anti-plane shear are derived using integral transform techniques. Unlike their classical elasticity counterparts, these solutions are non-singular, which makes them suitable for formulating various problems where waves are trapped inside configurations of pins. In the fifth and final chapter, scattering problems are formulated using the aforementioned Green's functions. Due to the relatively low computational load of the anti-plane shear Green's function, complex geometries such as fractals can be considered The results specifically address the case where Koch's snowflake is generated through an iterative process and due to the fractal nature of the configuration, the system's response reveals many intriguing phenomena.

Keywords: Bessel functions, Dispersion, Double Fourier transform, Form II, Fractals, Green's function, Hankel transform, Infinite domain, Koch snowflake, Microinertia, Microstructure, Mindlin's general theory, Scattering.

Περίληψη

Αυτή η εργασία εστιάζει στη διάδοση κυμάτων σε γενικευμένα συνεχή μέσα που διέπονται από υποθεωρίες της γενικής θεωρίας του Mindlin. Κύρια έμφαση δίνεται στην εξαγωγή νέων αναλυτικών λύσεων (δηλαδή, συναρτήσεων Green) για άπειρα χωρία, οι οποίες χρησιμεύουν ως βάση για την αντιμετώπιση προβλημάτων όπου κύματα όγκου εγκλωβίζονται εντός σχηματισμών που ορίζονται από σημειακά εμπόδια (ακίδες). Οι ακίδες μοντελοποιούνται ως συγκεντρωμένες καθολικές δυνάμεις, χρησιμοποιώντας τις συναρτήσεις Green για τις μετατοπίσεις που εξάγονται στην εργασία. Το πρώτο κεφάλαιο παρέχει μια σύντομη επισκόπηση των βασικών εννοιών που παρουσιάζονται στην εργασία και συζητά πιθανές εφαρμογές. Στο δεύτερο κεφάλαιο παρουσιάζεται διεξοδικά η γενική θεωρία του Mindlin, ξεκινώντας από την πιο γενική μη-γραμμική μικρομορφική θεωρία. Το τρίτο κεφάλαιο εισάγει τις τρεις απλοποιημένες εκδοχές της γενικής θεωρίας του Mindlin, γνωστές ως Μορφές I, II και III. Επιπλέον, παρέχεται μια σύντομη επισκόπηση της διπολικής ελαστικότητας βαθμίδας, η οποία αντιστοιχεί στην απλούστερη εκδοχή της γενικής θεωρίας του Mindlin. Αυτό το κεφάλαιο περιλαμβάνει επίσης μια ενότητα αφιερωμένη στην ελαστοδυναμική των ελαστικών υλικών βαθμίδας, με ιδιαίτερη έμφαση να δίνεται στη διατύπωση και την απόδειξη του θεωρήματος πληρότητας, το οποίο ο συγγραφέας πιστεύει ότι είναι ένα κενό στην τρέχουσα βιβλιογραφία. Στο τέταρτο κεφάλαιο, εξάγονται δύο αναλυτικές λύσεις για άπειρα χωρία υπό επίπεδη παραμόρφωση και αντί-επίπεδη διάτμηση χρησιμοποιώντας τεχνικές ολοκληρωτικών μετασχηματισμών. Σε αντίθεση με τις αντίστοιχες λύσεις της κλασσικής ελαστικότητας, αυτές οι λύσεις δεν είναι ιδιόμορφες, γεγονός που τις καθιστά κατάλληλες για τη διατύπωση διαφόρων προβλημάτων όπου κύματα παγιδεύονται μέσα σε σχηματισμούς ακίδων. Στο πέμπτο και τελευταίο κεφάλαιο, διατυπώνονται προβλήματα σκέδασης χρησιμοποιώντας τις προαναφερθείσες συναρτήσεις Green . Λόγω του σχετικά χαμηλού υπολογιστικού φόρτου της συνάρτησης Green της αντι-επίπεδης διάτμησης, μπορούν να ληφθούν υπόψη πολύπλοκες γεωμετρίες όπως τα φράκταλ. Τα αποτελέσματα αφορούν συγκεκριμένα την περίπτωση όπου η νιφάδα του Koch δημιουργείται μέσω μιας επαναληπτικής διαδικασίας και λόγω της κλασματικής φύσης του σχηματισμού, η απόκριση του συστήματος αποκαλύπτει πολλά ενδιαφέροντα φαινόμενα.

Λέξεις κλειδιά: Απειρο χωρίο, Γενική θεωρία του Mindlin, Διασπορά, Διπλός μετασχηματισμός Fourier, Φράκταλς, Μίκροαδράνεια, Μίκροδομη, Μετασχηματισμός Hankel, Μορφή II, Νιφάδα του Koch, Σκέδαση, Συναρτήσεις Bessel, Συνάρτηση Green.

Contents

1 Setting the Stage

1.1 Introduction

As the title indicates, this thesis focuses on wave scattering in generalized continua governed by specific sub-theories of Mindlin's general theory, with the primary focus given on deriving new closed-form analytical solutions that can be utilized to model wave scattering. Providing a concise summary of the concepts presented here is challenging without delving into details. The title also raises several questions, such as why a more advanced theory than the one of Cauchy is adopted and what leads to wave scattering. Therefore, the first chapter is dedicated entirely to addressing these questions and providing examples of potential applications for this research.

1.2 Conceptual Framework

We consider the scenario where an infinite domain, governed by a generalized continuum theory, is subjected to deformation due to the propagation of body waves. Within this infinite domain, there exists a configuration of point obstacles (pins), which are assumed to be undeformable. The objective is to explore how this configuration of pins can be tuned to modify the characteristics of wave propagation according to our desired outcomes. In other words, we aim to examine how the geometry of the pins, along with the parameters introduced through the generalized continuum theories, influences the system's response. In the following section, a brief overview of generalized continua is provided, focusing on their historical development and foundational concepts. For a more comprehensive understanding of the topic, the reader is referred to the first chapter of [1].

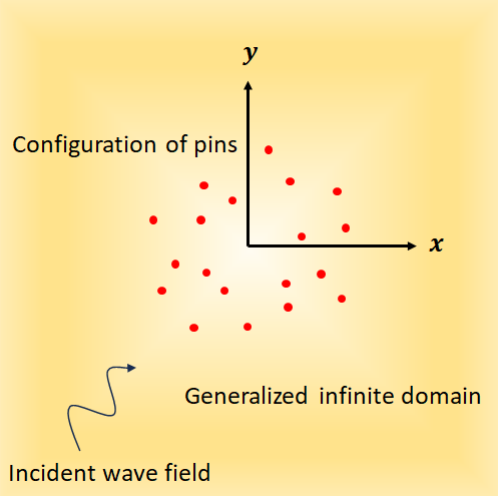

Figure 1.2.1: Problem statement.

1.3 A Concise Overview of Generalized Continua

One of the earliest works on generalized continua was a paper published in 1839 by MacCullagh [2], where he developed a theoretical framework to understand how light behaves when interacting with crystalline materials. In this paper, MacCullagh sought to extend the understanding of light reflection and refraction from isotropic media where properties are uniform in all directions to anisotropic or crystalline media, where properties vary with direction. He proposed a dynamical theory that explained how light waves are reflected and refracted at the boundaries of crystals, which exhibit different optical properties depending on the direction of the light's propagation. At that time, wave theories of light were often based on the concept of the luminiferous ether a hypothetical medium thought to enable light waves to propagate through a vacuum, despite the absence of any physical medium. However, MacCullagh's theory did not rely on the luminiferous ether, setting it apart from other theories of the era. His work laid the foundation for future developments in electromagnetism and the theory of light, particularly contributing to the understanding of light polarization and the behaviour of light in various media.

Same forty years latter Lord Kelvin [3] proposed a mechanical model that was based on MacCullagh generalized continuum and in 1887 Voigt [4] constructed an elastic continuum where each point of the continuum is supplied with a triad (directors) capable for describing polar molecules in crystallography. In this work, Voigt introduced the concept of anisotropic elasticity, where the elastic response of a material varies depending on the direction of the applied stress. He systematically explored how crystals deform under mechanical forces and derived equations that describe the relationship between stress and strain in crystalline materials. This work is significant because it expanded the understanding of elasticity from isotropic materials (where properties are uniform in all directions) to anisotropic crystals, which have directionally dependent properties. Voigt's work laid the foundation for the modern field of crystal elasticity and is particularly known for introducing the Voigt notation, which simplifies the mathematical representation of the elasticity tensor in crystalline materials.

The most significant contribution to the field of generalized continua was made in 1909 by the Cosserat brothers [5], who introduced a generalized theory of elasticity that expanded upon classical continuum mechanics. In this ground-breaking work, they developed the concept of micropolar or Cosserat continua, which considers the internal structure of materials by incorporating additional degrees of freedom beyond those in traditional theories. Specifically, they proposed that each point in a material has not only translational motion but also rotational motion. This led to the introduction of couple stresses and rotational inertia. Their framework enables the modelling of materials with complex internal structures, such as granular materials, composites, and other heterogeneous media, marking a significant advancement in the study of deformable bodies and continuum mechanics.

After World War II, a significant resurgence in this field occurred, marked by the publication of Ericksen and Truesdell in 1958. Further advancements were driven by the foundational contributions of researchers such as Kröner [6], Aero and Kuvshinskil [7], Nowacki [8] and

Maugin [9]. This revival was motivated by the limitations of classical models in explaining certain mechanical behaviours of solids and fluids. Notable examples include the turbulence of fluids and the behaviour of solids with complex microstructures. The 1960s are often considered the heyday of generalized continua, as most of the seminal works in this field were published during that decade. An incomplete couple stress theory was initially formulated in 1960 by Truesdell and Toupin [10], and it was later corrected and completed in 1962 by Mindlin and Tiersten [11], Toupin [12], and Eringen [13] and became known as the "indeterminate" couple stress theory.

In 1964, Eringen and Suhubi [14], [15] and Eringen [16], [17] introduced a new general theory of non-linear micromorphic continua. This theory extends traditional balance laws by incorporating additional ones and considering the intrinsic deformations and motions of the body's micro-constituents. It includes, as a special case, both the Cosserat continuum and the indeterminate couple stress theory. That same year, Mindlin [18] published a linear microstructure theory of elasticity, and Green and Rivlin [19] introduced a multipolar theory. Additionally, Palmov [20] recapitulated the Cosserat continuum in 1964. These theories, along with the micromorphic theory, are closely related. Since then, research in this area has intensified, resulting in an abundance of papers on this topic and related fields.

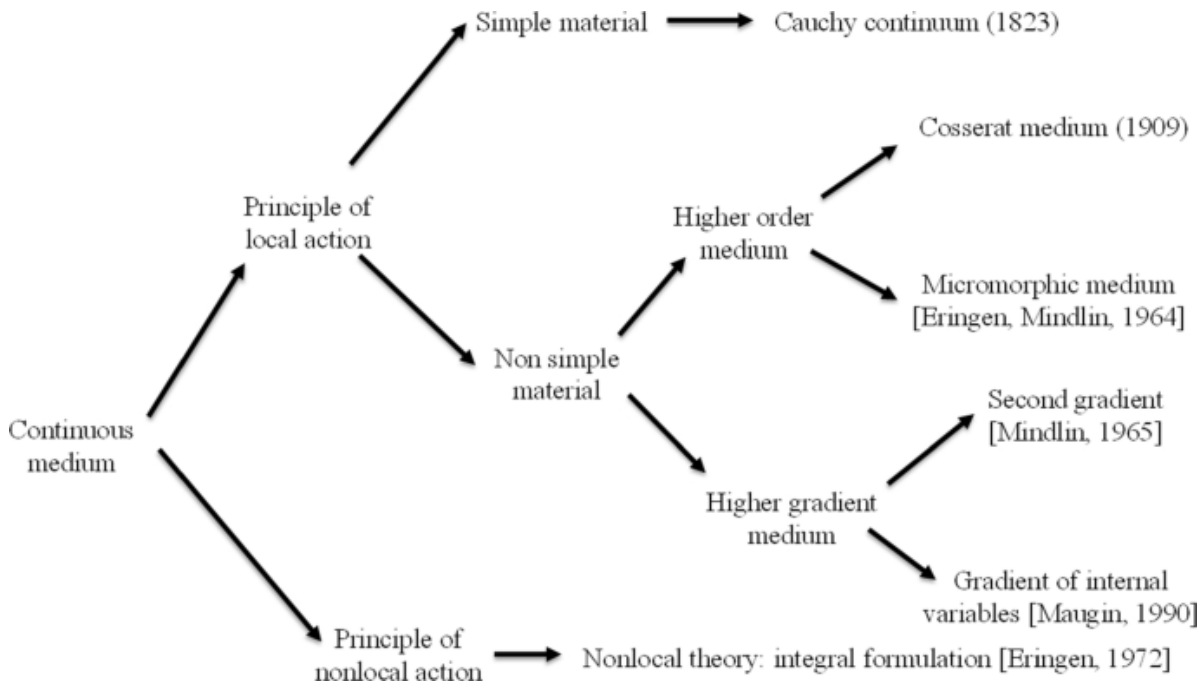

Figure 1.3.1: Classification of generalized continua into higher-order and higher-grade media [21].

The models proposed initially met all the requirements of Continuum Thermomechanics, including the formulation of balance laws and general representations of constitutive equations. This initially satisfied the scientific community. However, the models fell short in practical applications. The main issue was the gap between the formulated constitutive equations and the ability to identify the necessary material parameters. These models often involved many

more parameters compared to classical models, making them difficult to apply. Additionally, computational resources and available technology at the time were limited. Consequently, from the late 1960s until the 1990s, only a small number of researchers in the scientific and engineering communities continued to work in the field of Generalized Continua.

In the past twenty years, the landscape has transformed dramatically. Advances in computational capabilities have revitalized interest in previously overlooked models, allowing for the numerical simulation of very complex problems. Additionally, increased focus on materials with intricate microstructures and a better understanding of material parameters (including scale effects) have significantly improved the accuracy of material identification. As a result, we now have contributions that detail both micro and macro-behaviour, new theorems on existence and uniqueness, and the formulation of multiscale problems. These developments allow us to reassess the state of matter and explore emerging trends and applications.

As noted, there are various types of generalized continuum theories. The theory applied in this work is Mindlin's general theory [18], which is part of a broader class of generalized continua known as micromorphic continua. Micromorphic continua poses the following very interesting features [1]

• Inevitable introduction of characteristic lengths.

• Appearance of so-called capillarity effects (surface tension) due to the explicit intervening of curvature of surfaces.

• Correlative boundary layers effects.

• Dispersion of waves with a possible competition and balance between non-linearity and and dispersion, and the existence of solitonic structures [22].

• Intimate relationship with the Ginzburg–Landau theory of phase transitions [23], [24] and for fluids, van der Waals' theory [25], [26].

To clearly demonstrate the characteristics of the micromorphic continua, it is necessary to present the governing equations. However, this will be addressed later in the context of this work.

1.4 Applications

1.4.1 Applications of Generalized Continuum Theories

Generalized continuum theories expand upon classical continuum mechanics by introducing additional elements like microstructure effects, size dependencies, and higher-order gradients. These advanced theories are especially valuable for modelling materials and phenomena that classical methods cannot accurately capture. Key applications of generalized continuum theories include:

1. **Advanced Material Design**

   • **Metamaterials**: Generalized continuum theories, such as micropolar or micromorphic theories, are used to design and analyse metamaterials, which have unusual properties like negative refractive index, anisotropy, or tailored mechanical behaviour. These materials are crucial in applications like superlenses, cloaking devices, and vibration control [27].

   • **Composite Materials**: In the study of composites, generalized continuum theories help model the interactions between different phases at the microscopic level, improving predictions of overall material properties such as stiffness, strength, and toughness [28].

2. **Micro and Nano Scale Mechanics**

   • **Micromechanical Systems (MMS) and Nanomechanical Systems (NMS)**: Generalized continuum theories are essential for accurately modelling the mechanical behaviour of structures at micro and nano scales, where surface effects, size dependencies, and material microstructure play significant roles. These theories are used in the design and optimization of MMS and NMS devices [29].

   • **Crystalline Materials**: In materials science, generalized continuum theories help describe the behaviour of crystals, particularly at small scales where dislocation dynamics, grain boundaries, and other microstructural features influence the material's mechanical properties [30].

3. **Biomechanics**

   • **Soft Tissue Modelling**: Generalized continuum theories are used to model the complex behaviour of biological tissues, which often exhibit non-classical mechanical responses due to their hierarchical structure. These models are important in understanding soft tissue mechanics, aiding in medical device design, surgical planning, and injury analysis [31].

   • **Bone Mechanics**: In biomechanics, generalized continuum theories help simulate the behaviour of bone, which has a complex microstructure. These models are used to predict bone strength, understand fracture mechanisms, and design implants [31].

4. **Geomechanics**

   • **Seismic Wave Propagation**: In geomechanics, generalized continuum theories are applied to model seismic wave propagation through complex geological media. These theories account for the microstructure of rocks and soils, leading to more accurate predictions of seismic behaviour and better earthquake-resistant design [32].

   • **Landslide and Subsidence Modelling**: These theories help in the study of phenomena like landslides or ground subsidence, where the microstructure of soil and rock layers affects the overall stability and deformation patterns [32].

5. **Structural Engineering**

   • **Fracture Mechanics**: Generalized continuum theories are applied to model the initiation and propagation of cracks in materials, particularly in situations where traditional fracture mechanics fails. These theories can predict fracture behaviour in materials with complex microstructures, such as composites, ceramics, and certain alloys [33].

   • **Damage Mechanics**: In structural engineering, generalized continuum theories are used to model damage and failure in materials under various loading conditions. This is especially relevant in predicting the lifespan of structures and materials subject to fatigue, impact, or high-temperature environments [34].

6. **Multiscale Modelling**

   • **Bridging Scales**: Generalized continuum theories provide a framework for multiscale modelling, where behaviour at the microscopic level influences macroscopic responses. This is important in fields like materials science, where understanding how nanoscale features affect bulk properties is crucial for developing new materials [35].

These applications demonstrate the versatility and importance of generalized continuum theories in advancing our understanding of complex materials and systems, leading to innovations across multiple scientific and engineering disciplines. However, among the possible applications, the ones that intrigue the author the most are those related to controlling extreme natural events such as earthquakes and tsunamis:

• **Controlling Earthquakes**: The principles of generalized continua can be used to protect civil structures and in some cases even entire cities. By modifying the soil a metamaterial is created. This metamaterial can be engineered to have properties that mitigate the negative effects of seismic waves. Prominent contributions to this field come from the research of Brûlé, Javelaud, Enoch, and Guenneau [36], [37]. In 2012, they presented groundbreaking work on using seismic metamaterials to control surface seismic waves. Through large-scale experiments, they demonstrated how arrays of vertical boreholes, acting as metamaterials, can manipulate seismic wave propagation. Their findings confirmed that seismic metamaterials can effectively redirect, attenuate, or block seismic waves, offering a novel method for seismic protection. This research has significant implications for earthquake engineering, potentially leading to new strategies for safeguarding buildings and infrastructure from seismic hazards.

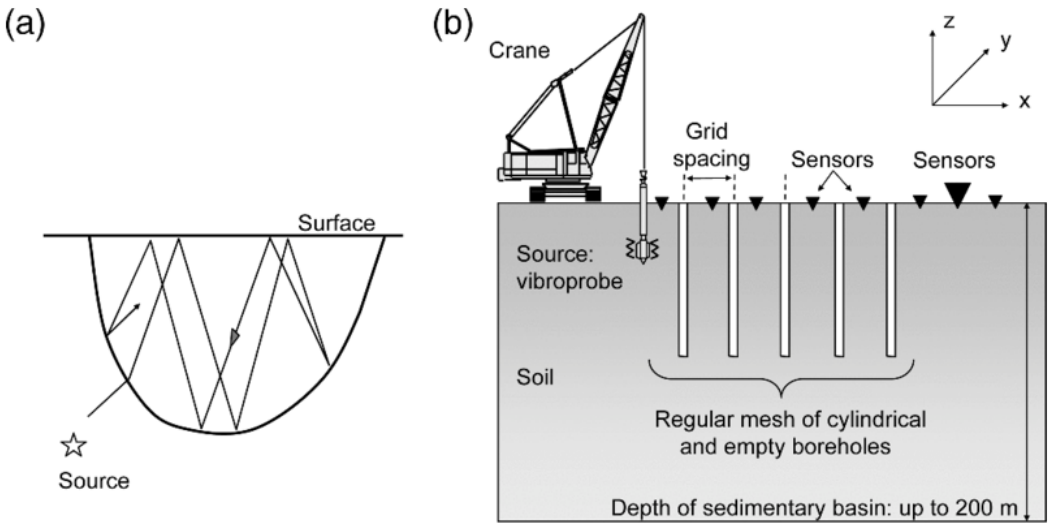

Figure 1.4.1.1: Schematics of (a) a seismic wave in an alluvium basin and (b) the seismic testing device cross section in the $x - z$ plane [36].

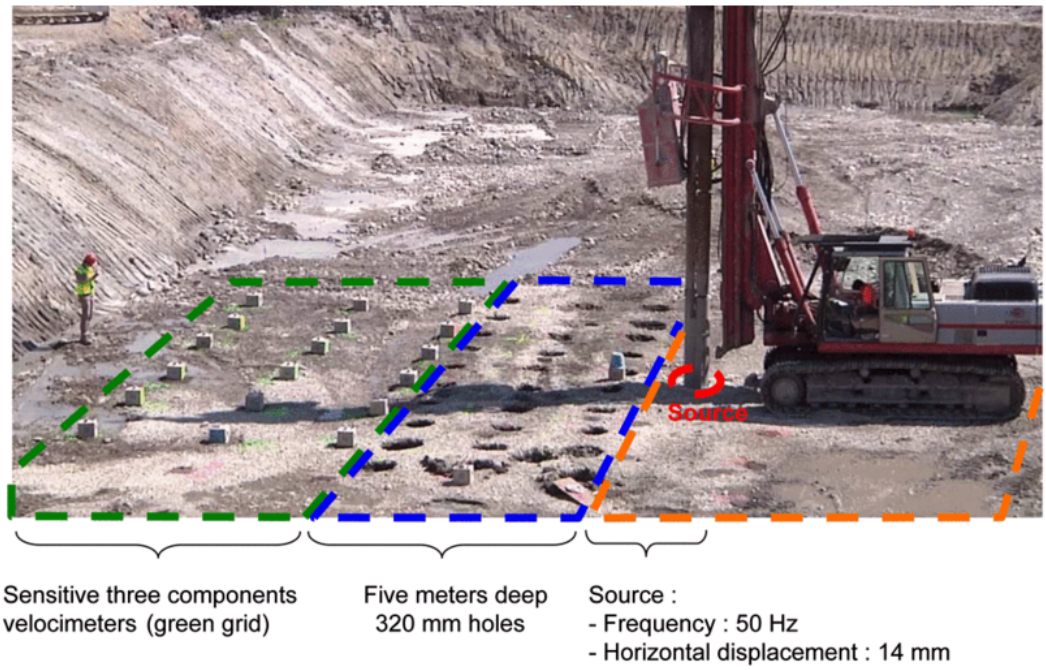

Figure 1.4.1.2: Photograph of the seismic metamaterial experiment from Ménard. The three dashed perimeters account for the location of sensors [measuring the three components of wave velocity (green area on this photograph)], seismic metamaterial [5 m deep self-stable holes of diameter 0.32 m with center-to-center spacing of 1.73 m (blue area)], and rotating source (a vibrating probe set on a crane) with a horizontal displacement of 0.014 m generating an elastic wave at frequency 50 Hz [36].

In 2016, Achaoui, Ungureanu, Enoch, Brûlé, and Guenneau [38] conducted notable research exploring the use of arrays of inertial resonators to dampen seismic waves. The study investigates the potential of these resonators—structures that vibrate at specific frequencies to reduce the amplitude of seismic waves as they travel through the ground. By strategically placing these resonators in the soil, they created a type of seismic metamaterial that can effectively mitigate the impact of earthquakes, enhancing the protection of structures. Their research combines theoretical analysis, numerical simulations, and experimental validations to demonstrate the feasibility of this innovative approach.

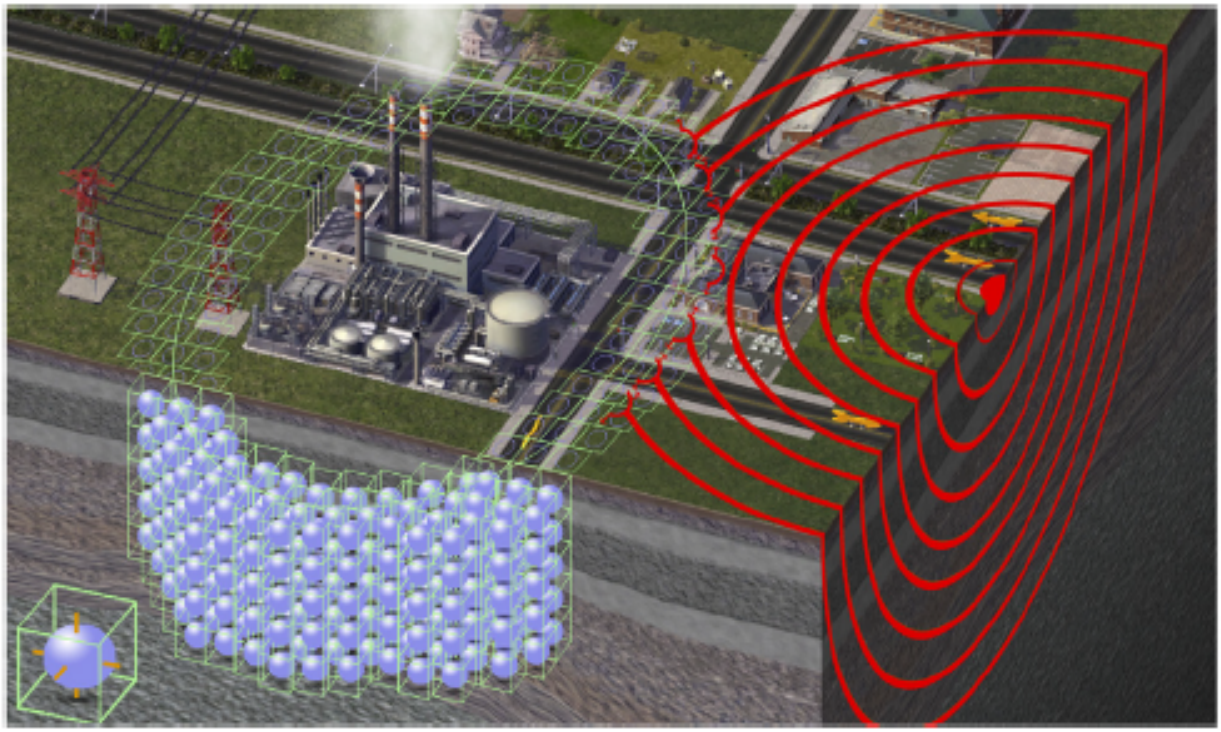

Figure 1.4.1.3: Schematic diagram of a seismic wave shield consisting of inertial resonators placed around the foundations of a large civil infrastructure. Inset shows a periodic cell with an iron sphere connected to a bulk of concrete or soil through six iron or rubber ligaments [38].

In 2019 Brûlé, Enoch, and Guenneau [39] examined how integrating nanophotonic materials and devices into seismic engineering can lead to innovative approaches for mitigating seismic risks and improving structural resilience. Nanophotonic materials have unique properties, such as the ability to manipulate electromagnetic waves with high precision. This capability allows engineers to develop advanced sensors, actuators, and damping mechanisms that can significantly improve the effectiveness of seismic protection systems. Their study highlights the potential of these cutting-edge technologies to revolutionize seismic design, offering new solutions for safeguarding infrastructure against the challenges of earthquake-induced forces. With the integration of nanophotonics into seismic engineering a significant advancement is

made in the field, promising to push the boundaries of what is possible in creating resilient and adaptive seismic megastructures.

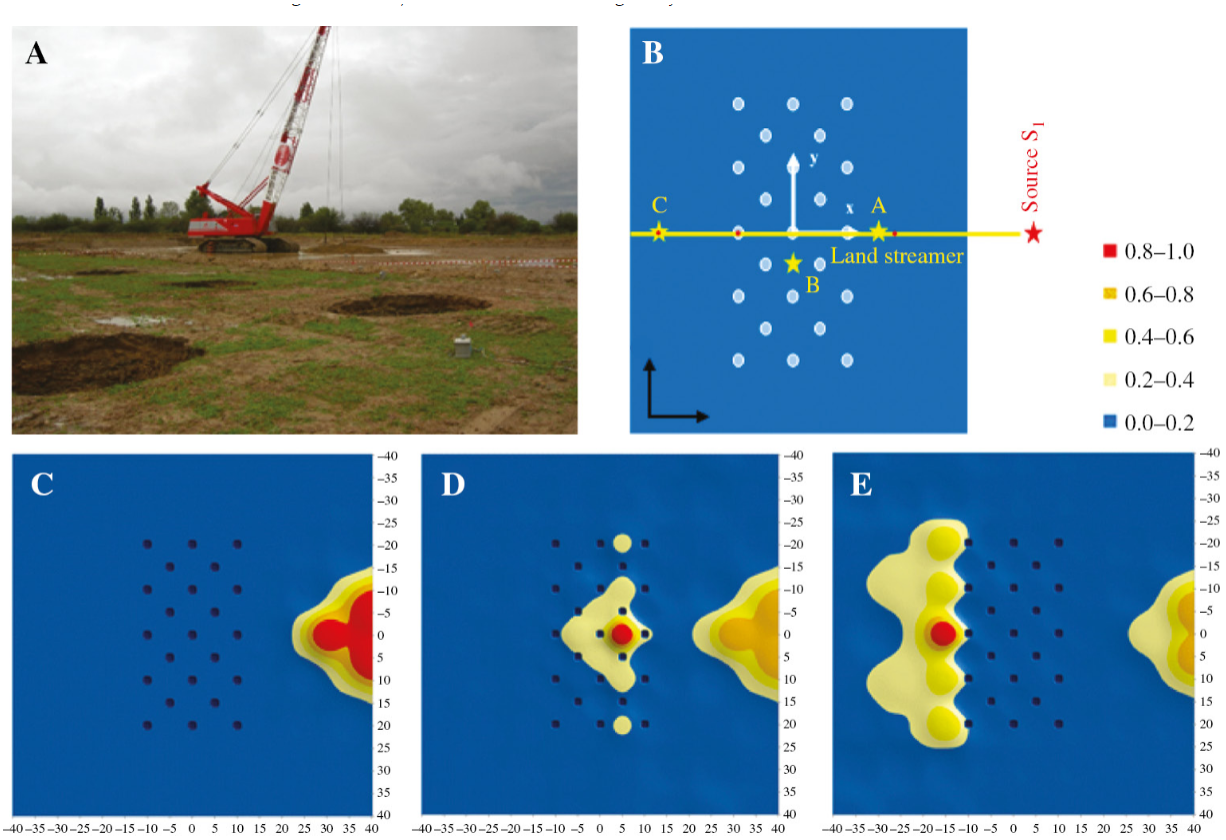

Figure 1.4.1.4: Experiment on a flat seismic lens: (A) Photo (courtesy of S. Brûlé) of the array of boreholes, (B), (C–E) Chronology of the x–y spatial distribution of normalized $v^2(t)$ from (C) 1.900 s to (D) 2.124 s to (E) 2.345 s [39].

In all the examples that were given above, classical plate theory (CPT) was used as the theoretical framework. There are many similarities between CPT and generalized continuum theories, which will be further analysed later in this work.

• **Controlling Tsunamis**: History has shown that planting trees with complex root systems, such as mangroves, around coastlines can help control the impact of tsunamis. Mangrove trees play a crucial role in protecting coastal areas from the devastating impact of tsunamis. The dense root systems of mangroves act as a natural barrier, reducing the energy and speed of incoming tsunami waves before they reach inland areas. Scientific studies have shown that mangroves can significantly reduce wave height and energy, providing a buffer that minimizes coastal erosion and the impact on human settlements. According to research by Kathiresan and Rajendran (2005) [40], mangroves can reduce the height of tsunami waves by up to 50% over short distances, depending on the density and width of the mangrove forest. Another study by Danielsen et al. (2005) [41] highlighted that areas with healthy mangrove forests experienced less damage during the 2004 Indian Ocean tsunami compared to regions where mangroves had been cleared.

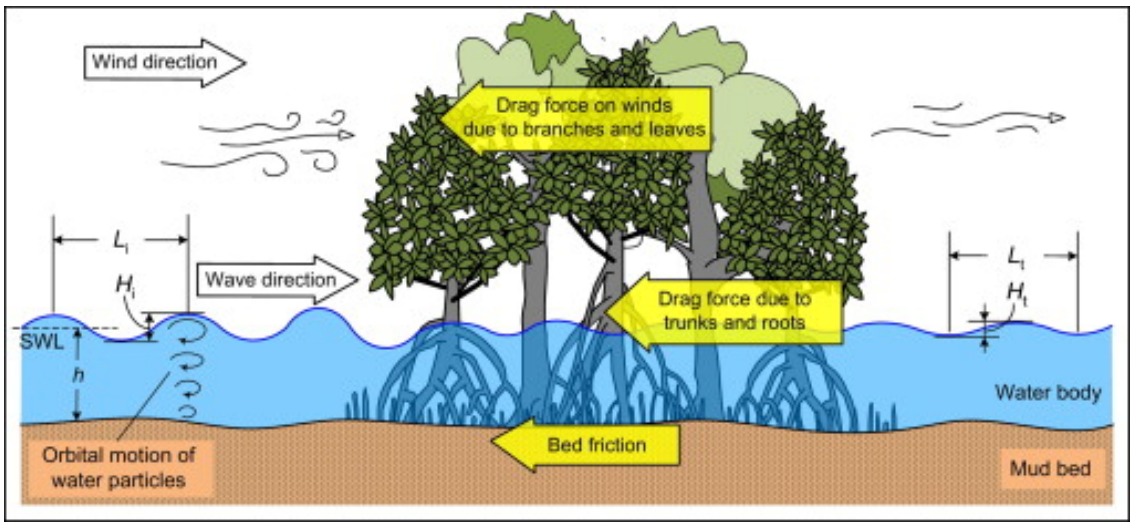

Figure 1.4.1.5: Wave propagation through a mangrove forest [42].

The effectiveness of mangroves in protecting coasts from tsunamis is largely due to their complex and extensive root systems. Mangrove roots, particularly the stilt and prop roots, are adept at trapping sediments and stabilizing the coastline. These roots interlock to form a dense network that absorbs and dissipates the energy of the waves, reducing their force as they move inland. Additionally, the roots help to reduce soil erosion by anchoring the soil and preventing it from being washed away by the waves. This not only protects the coastline but also helps maintain the health of the mangrove ecosystem itself, ensuring its continued effectiveness as a natural tsunami barrier (Alongi, 2008 [43]).

In summary, mangrove forests serve as a vital natural defence against tsunamis, with their root systems playing a key role in reducing wave energy and protecting coastal regions. The preservation and restoration of mangrove forests are therefore essential for enhancing coastal resilience against future tsunami events.

The concept of generalized continua can be applied to study wave propagation through a mangrove forest. Traditional models often oversimplify the interaction between tsunami waves and the complex root systems of mangroves, potentially missing important microstructural behaviours. Generalized continuum theories allow for a more precise representation of energy dissipation, wave attenuation, and momentum exchange as the tsunami moves through the dense root network. This approach leads to more accurate predictions of how mangrove forests reduce wave intensity, providing valuable insights for designing coastal protection strategies that leverage natural defences.

1.4.2 Modelling Crystal Latices With Fractals

Given that the problems under examination involve configurations of fractals, it is fitting to discuss a few applications of fractals. Many applications of fractals in mechanics involve

modelling crystal lattices. Although challenging, using fractals to model crystal lattices can offer valuable insights, particularly when capturing the complexity, self-similarity, and hierarchical structures found in certain materials. Traditional crystal lattices are often periodic with regular, repeating patterns, but fractals can serve as effective conceptual or quantitative models for specific types of crystal structures or related phenomena. Below are some examples of fractals that can be useful in modelling or representing aspects of crystal lattices:

1. **Sierpinski Triangle (or Gasket)**: The Sierpinski triangle can be used to model the hierarchical structure of certain quasicrystals or fractal-like defects within a crystal lattice. It's a 2D fractal that exhibits self-similarity, where each triangle is composed of smaller triangles that repeat at different scales [44]. This fractal can help visualize how a crystal might form or break down in a self-similar manner, or how defects might distribute across scales within the crystal.

2. **Koch Snowflake**: The Koch snowflake is a fractal curve that represents the concept of infinite perimeter within a finite area. It's useful for modelling interfaces or boundaries in crystal lattices, particularly in cases where the surface exhibits complex, self-similar roughness, such as grain boundaries or crack fronts in polycrystalline materials [45]. It can be used to understand the growth patterns of crystals or the development of surface roughness during processes like solidification or phase transitions.

3. **Cantor Set**: The Cantor set is a 1D fractal that can be extended to higher dimensions. It's useful in modelling atomic distributions in disordered systems or in studying the distribution of vacancies, impurities, or defects within a crystal lattice [45]. The Cantor set's fractal nature can represent how certain atomic sites might be occupied or unoccupied across different scales, leading to a fractal distribution of defects or dopants.

4. **Mandelbrot Set**: Although primarily a mathematical construct, the Mandelbrot set can be used to explore the concept of fractal boundaries and phase transitions in materials. It's particularly useful in studying systems that exhibit chaotic behaviour or complex boundary conditions [46]. The Mandelbrot set can model the complex and chaotic behaviour of interfaces in crystal lattices, particularly in systems near critical points or undergoing phase transitions.

5. **Penrose Tiling**: While not a fractal in the strictest sense, Penrose tiling exhibits non-periodic order and is used to model quasicrystals, which have a structure that is ordered but not periodic. Penrose tiling can be extended to exhibit self-similar properties, making it relevant to fractal concepts [47]. This tiling is crucial in understanding the atomic arrangement of quasicrystals, which can have fractal-like hierarchical structures without repeating periodically.

6. **Apollonian Gasket**: The Apollonian gasket is a fractal generated by repeatedly filling the gaps between circles (or spheres in 3D) with smaller circles (or spheres). It can be used to model the packing of atoms in a crystal lattice, particularly in systems where the atomic arrangement is non-regular or hierarchical. The Apollonian gasket can

represent how atoms or particles pack in certain disordered or amorphous materials, where space-filling and hierarchical organization are important [45].

7. **Gosper Curve (or Gosper Island)**: The Gosper curve is a space-filling fractal that can model certain aspects of crystal lattices, particularly those with hexagonal symmetry or those that exhibit self-similar tiling patterns [48]. It can be used to model the distribution of atoms in materials with hexagonal structures or to explore the arrangement of defects or inclusions within such lattices.

8. **Fractal Aggregation Models (e.g., Diffusion-Limited Aggregation - DLA)**: DLA is a process that generates fractal patterns through the aggregation of particles undergoing random motion. It's used to model crystal growth, particularly in systems where the growth is irregular or where particles aggregate in a fractal manner [49]. This model is relevant in studying the formation of dendritic crystals or the growth of colloidal crystals, where the aggregation process leads to a fractal structure.

9. **Vicsek Fractal**: The Vicsek fractal is a self-similar fractal that can be used to model the hierarchical and recursive nature of certain crystal structures, particularly in materials that form through recursive processes or that have fractal-like defects [45]. It can be applied in studying materials that exhibit hierarchical porosity or in understanding the recursive nature of certain defect patterns within crystal lattices [50].

Fractals are powerful tools for modelling and understanding complex structures and behaviours in crystal lattices, especially in cases where traditional periodic models fall short. While these fractals might not replicate the exact atomic positions in a lattice, they provide insights into the hierarchical, self-similar, and irregular features that can occur in real-world materials.

1.4.3 Applications of Fractals in Continuum Theories

In addition to modelling crystal lattices, fractals have many other applications in classical and generalized continua, including:

1. **Modelling Microstructural Effects**: Fractals can be used to model complex microstructures in materials where classical continuum theories might fall short. The self-similar nature of fractals allows for the representation of hierarchical structures and variations at different scales, which is particularly useful in understanding materials with complex internal structures like porous media or composites. Fractal-based models are especially effective in capturing the microstructures of porous materials or foams. Fractals can help in simulating how such materials behave under various stress conditions and predict their mechanical properties more accurately than traditional methods [51], [52].

2. **Enhanced Modelling of Damage and Failure**: In the study of damage and failure in materials, fractal models can represent the distribution of cracks and defects. The fractal dimension can be used to characterize the irregularities and complexity of crack patterns, providing more detailed insights into the damage evolution process. Applying fractal geometry to describe the crack patterns in brittle materials. By incorporating fractal dimensions into generalized continuum theories, researchers can improve predictions of crack growth and material failure [53], [54].

3. **Predicting Fractal-like Defects in Materials**: Fractals are useful for modelling defects and irregularities in materials that exhibit self-similar patterns. Generalized continuum theories that include fractal descriptions can better capture the behaviour of materials with complex defect structures, such as certain types of polycrystalline materials [55]. Using fractal models to predict the behaviour of materials with fractal-like defects, such as grain boundaries in polycrystalline materials or dislocations in crystals. These models help in understanding how such defects influence the overall mechanical properties [56].

4. **Simulating Material Behaviour at Multiple Scales**: Fractals can aid in bridging scales between micro and macro levels in generalized continuum theories. They provide a framework for incorporating scale effects and hierarchical structures into continuum models, improving the accuracy of simulations for materials with complex hierarchical features. Integrating fractal geometry into multiscale models to simulate the mechanical behaviour of materials with hierarchical structures, such as hierarchical composites or biological tissues. This approach helps in understanding how microstructural features affect the macroscopic properties [57], [58].

5. **Designing Metamaterials**: Fractals are used in the design and analysis of metamaterials, which are engineered to have specific properties not found in natural materials. Fractal patterns can be incorporated into the design of metamaterials to achieve desired mechanical or optical properties. For instance, fractal designs can be used to create materials with negative refraction or other unique characteristics. By using fractal geometry in the design process, engineers can create materials with enhanced or tailored properties [59], [60].

2 Mindlin's General Theory

2.1 Introduction

In this section a brief presentation of Mindlin's general theory is made, despite the fact that only form II is used in this work. Mindlin's general theory is an elasticity theory that takes the existence of microstructure into account from the macroscopic point of view, (which is the point of view of a continuum theory). By doing so, the continuum is now described with more variables, in this way, the filed equations that arise are more detailed compared to those of classical elasticity, which in many cases results in a more realistic response of the material in relation to that predicted by the classical theory of Cauchy. Initially, the kinematics are presented from a general point of view, which accounts for every micromorphic continuum, (in this work the word micromorphic is used to indicate a generalized continuum with microstructure). In this way, the kinematics of Mindlin's general theory can be formulated in a rational way. Having formulated the kinematics, we continue by defining the kinetic and potential energy of the continuum, the expressions of which will be used for the variational formulation of the equations of motion and boundary conditions through Hamilton's Principle. The constitutive laws are formulated for the general case of anisotropic materials. These equations are quite extensive, however they can be significantly simplified in the case of isotropic materials. Finally, the displacement equations of motion are being derived which will be used extensively latter in the problems, as they will function as a reference point in the search of analytical solutions.

2.2 Kinematics

2.2.1 Non – Linear Kinematics of Micromorphic Continua

Consider a body $\mathbb{B}$ whose particles occupy the points of a region of a Euclidean point space $\mathbb{E}$. During the motion of $\mathbb{B}$, a point P of the reference configuration $\mathbb{B}_0$ with position vector $\mathbf{X}$ measured from a fixed origin O is mapped into a point on the spatial configuration $\mathbb{B}_t$ with position vector $\mathbf{x}$ relative at an origin o. The origin O from which $\mathbf{X}$ is measured does not need to coincide with o. In a continuum theory that takes microstructure into account a point P (respectively p) is manifested as a particle, which on the microscopic level appears as a continuum of small extent. In each particle of $\mathbb{B}$ corresponds a micro – configuration, the notations $\mathbb{B}'_0$, $\mathbb{B}'_t$ are used in order to indicate the reference and spatial micro – configurations. Let P' be a point of $\mathbb{B}'_0$ that during the motion of $\mathbb{B}$ is mapped into a point p' on $\mathbb{B}'_t$. The position vectors of points P', p' are $\mathbf{X}'$, $\mathbf{x}'$ with respect to the macro – frame of reference, while the same points are also measured with respect to a micro – frame of reference by two other position vectors $\boldsymbol{\Xi}'$, $\boldsymbol{\xi}'$. The axis of $\boldsymbol{\Xi}'$, $\boldsymbol{\xi}'$ are parallel to those of $\mathbf{X}$, $\mathbf{x}$, with origin fixed to the centroid of the micro – configuration, denoted by C (respectively c), so that the origin of the coordinates ξ'_i moves with the displacement $\mathbf{u}$. It is clear that

in micromorphic theories we are obliged to consider at least two frames of reference even for the case of small deformations, one which describes the motion of the macro – medium and another that describes the motion of the micro – medium.

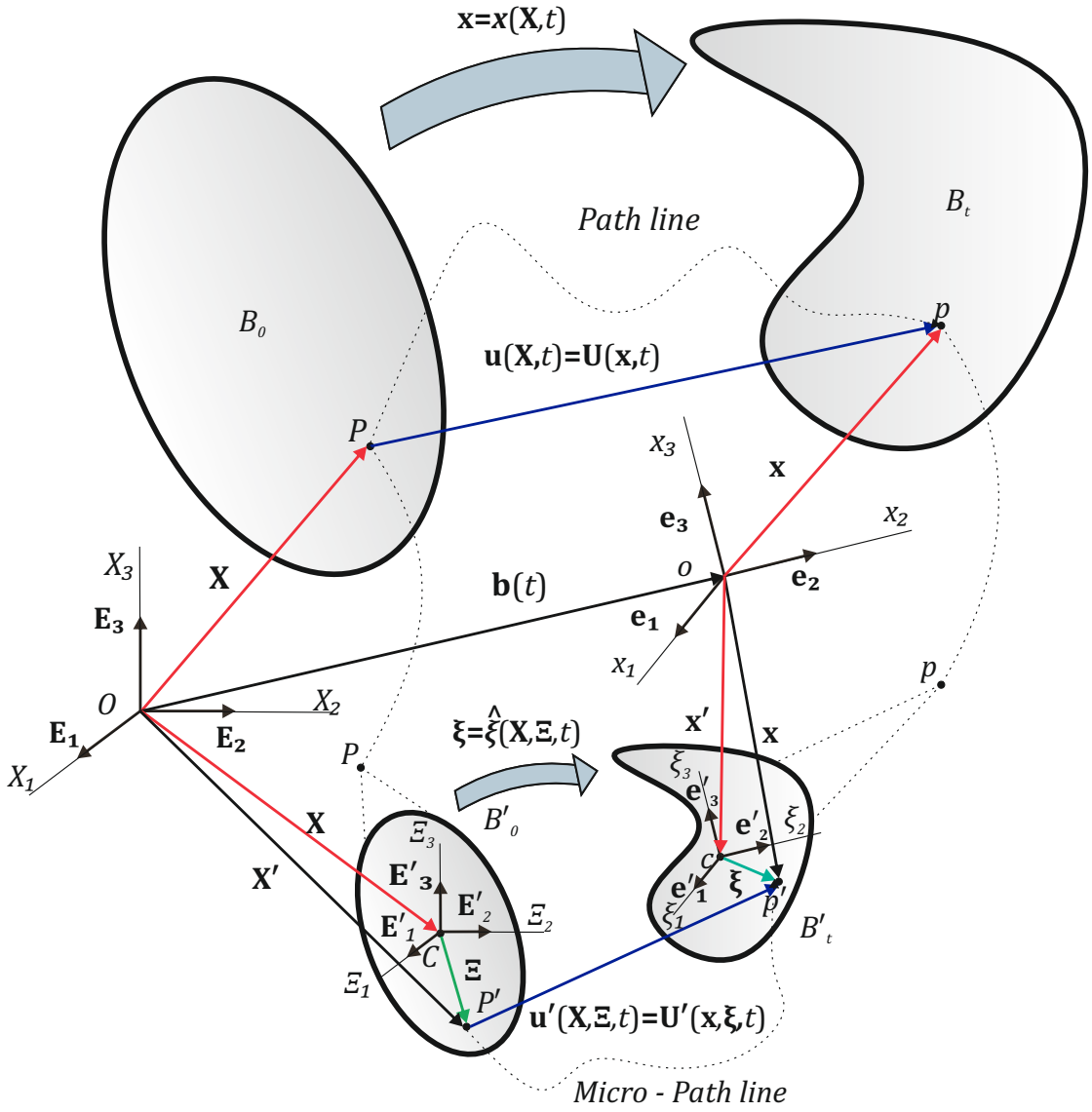

Figure 2.2.1.1: Motion of a continuum body with microstructure.

The motion of the macro – medium can be described by the same placement functions as in classical continuum mechanic:

$$\mathbf{x} = \boldsymbol{\chi}(\mathbf{X}, t) \tag{2.2.1.1}$$

$$\mathbf{X} = \boldsymbol{X}(\mathbf{x}, t) \tag{2.2.1.2}$$

While the motion of the micro – medium can be described by two other placement functions that will depend on both the micro and the macro - coordinates:

$$\boldsymbol{\xi} = \hat{\boldsymbol{\xi}}(\mathbf{X}, \boldsymbol{\Xi}, t) \tag{2.2.1.3}$$

$$\boldsymbol{\Xi} = \hat{\boldsymbol{\Xi}}(\mathbf{x}, \boldsymbol{\xi}, t) \tag{2.2.1.4}$$

In accordance with the impenetrability and indestructibly of matter, it is assumed that (2.2.1.1), (2.2.1.3) and their unique inverse (2.2.2.1), (2.2.1.4) exist at all points of $\mathbb{B}_0$, $\mathbb{B}_t$ and $\mathbb{B}'_0$, $\mathbb{B}'_t$ respectively at every time t. This is valid when $\partial\mathbf{x}/\partial\mathbf{X}$ and $\partial\boldsymbol{\xi}/\partial\boldsymbol{\Xi}$ are continuous functions of $\mathbf{X}$, $\boldsymbol{\Xi}$ and t and the Jacobians satisfy the following conditions:

$$J = det\left(\frac{\partial \mathbf{x}}{\partial \mathbf{X}}\right) \neq 0 \quad \forall \mathbf{X} \in \mathbb{B}_0 \quad \forall t \tag{2.2.1.5}$$

$$J' = det\left(\frac{\partial \boldsymbol{\xi}}{\partial \boldsymbol{\Xi}}\right) \neq 0 \quad \forall \boldsymbol{\Xi} \in \mathbb{B}'_0 \quad \forall t \tag{2.2.1.6}$$

Equations (2.2.1.1), (2.2.1.2) represent the spatial and referential form of the motion of the macro – medium, whereas, equations (2.2.1.3), (2.2.1.4) represent the spatial and referential form of the motion of the micro – medium.

From Figure (2.2.1.1), it is very easy to obtain the following equations:

$$\mathbf{x}' = \mathbf{x} + \boldsymbol{\xi} \tag{2.2.1.7}$$

$$\mathbf{X}' = \mathbf{X} + \boldsymbol{\Xi} \tag{2.2.1.8}$$

Also, the placement functions (2.2.1.1), (2.2.1.2) can be expressed in terms of $\mathbf{x}'$, $\mathbf{X}'$ as:

$$\mathbf{x}' = \boldsymbol{\chi}(\mathbf{X}', t) = \boldsymbol{\chi}(\mathbf{X} + \boldsymbol{\Xi}, t) \tag{2.2.1.9}$$

$$\mathbf{X}' = \boldsymbol{X}(\mathbf{x}', t) = \boldsymbol{X}(\mathbf{x} + \boldsymbol{\xi}, t) \tag{2.2.1.10}$$

Substituting (2.2.1.1), (2.2.1.3) into (2.2.1.9) and (2.2.1.2), (2.2.1.4) into (2.2.1.10) yields:

$$\boldsymbol{\chi}(\mathbf{X}+\boldsymbol{\Xi},t)=\boldsymbol{\chi}(\mathbf{X},t)+\hat{\boldsymbol{\xi}}(\mathbf{X},\boldsymbol{\Xi},t) \tag{2.2.1.11}$$

$$\boldsymbol{X}(\mathbf{x}+\boldsymbol{\xi},t)=\boldsymbol{X}(\mathbf{x},t)+\hat{\boldsymbol{\Xi}}(\mathbf{x},\boldsymbol{\xi},t) \tag{2.2.1.12}$$

Evaluating (2.2.1.11) at $\boldsymbol{\Xi}=\mathbf{0}$ and (2.2.1.12) at $\boldsymbol{\xi}=\mathbf{0}$ gives:

$$\hat{\boldsymbol{\xi}}(\mathbf{X},0,t)=0 \tag{2.2.1.13}$$

$$\hat{\boldsymbol{\Xi}}(\mathbf{x},0,t)=0 \tag{2.2.1.14}$$

In order to formulate an equation for the motion of the micro – medium in spatial form we can expand (2.2.1.3) in terms of Taylor series about point $\boldsymbol{\Xi}=\mathbf{0}$:

$$\boldsymbol{\xi}=\hat{\boldsymbol{\xi}}(\mathbf{X},0,t)+\frac{\partial\hat{\boldsymbol{\xi}}}{\partial\boldsymbol{\Xi}}\Big|_{\boldsymbol{\Xi}=\mathbf{0}}\cdot\boldsymbol{\Xi}+\frac{1}{2!}\frac{\partial^2\hat{\boldsymbol{\xi}}}{\partial\boldsymbol{\Xi}^2}\Big|_{\boldsymbol{\Xi}=\mathbf{0}}:(\boldsymbol{\Xi}\otimes\boldsymbol{\Xi})+\ldots+\frac{1}{n!}\frac{\partial^n\hat{\boldsymbol{\xi}}}{\partial\boldsymbol{\Xi}^n}\Big|_{\boldsymbol{\Xi}=\mathbf{0}}\bullet\underbrace{(\boldsymbol{\Xi}\otimes\ldots\otimes\boldsymbol{\Xi})}_{(n-1)\quad\text{times}} \tag{2.2.1.15}$$

In (2.2.1.15) the $\bullet$ symbol denotes n contractions. We can also formulate an equation for the motion of the micro – medium in referential form by expanding (2.2.1.4) in terms of Taylor series about point $\boldsymbol{\xi}=\mathbf{0}$:

$$\boldsymbol{\Xi}=\hat{\boldsymbol{\Xi}}(\mathbf{x},0,t)+\frac{\partial\hat{\boldsymbol{\Xi}}}{\partial\boldsymbol{\xi}}\Big|_{\boldsymbol{\xi}=\mathbf{0}}\cdot\boldsymbol{\xi}+\frac{1}{2!}+\frac{\partial^2\hat{\boldsymbol{\Xi}}}{\partial\boldsymbol{\xi}^2}\Big|_{\boldsymbol{\xi}=\mathbf{0}}:(\boldsymbol{\xi}\otimes\boldsymbol{\xi})+\ldots+\frac{1}{n!}\frac{\partial^n\hat{\boldsymbol{\Xi}}}{\partial\boldsymbol{\xi}^n}\Big|_{\boldsymbol{\xi}=\mathbf{0}}\bullet\underbrace{(\boldsymbol{\xi}\otimes\ldots\otimes\boldsymbol{\xi})}_{(n-1)\quad\text{times}} \tag{2.2.1.16}$$

Because of (2.2.1.13), (2.2.1.14) the constant term in (2.2.1.15), (2.2.1.16) vanish, thus we have:

$$\boldsymbol{\xi}=\frac{\partial\hat{\boldsymbol{\xi}}}{\partial\boldsymbol{\Xi}}\Big|_{\boldsymbol{\Xi}=\mathbf{0}}\cdot\boldsymbol{\Xi}+\frac{1}{2!}\frac{\partial^2\hat{\boldsymbol{\xi}}}{\partial\boldsymbol{\Xi}^2}\Big|_{\boldsymbol{\Xi}=\mathbf{0}}:(\boldsymbol{\Xi}\otimes\boldsymbol{\Xi})+\ldots+\frac{1}{n!}\frac{\partial^n\hat{\boldsymbol{\xi}}}{\partial\boldsymbol{\Xi}^n}\Big|_{\boldsymbol{\Xi}=\mathbf{0}}\bullet\underbrace{(\boldsymbol{\Xi}\otimes\ldots\otimes\boldsymbol{\Xi})}_{(n-1)\quad\text{times}} \tag{2.2.1.17}$$

$$\boldsymbol{\Xi}=\frac{\partial\hat{\boldsymbol{\Xi}}}{\partial\boldsymbol{\xi}}\Big|_{\boldsymbol{\xi}=\mathbf{0}}\cdot\boldsymbol{\xi}+\frac{1}{2!}+\frac{\partial^2\hat{\boldsymbol{\Xi}}}{\partial\boldsymbol{\xi}^2}\Big|_{\boldsymbol{\xi}=\mathbf{0}}:(\boldsymbol{\xi}\otimes\boldsymbol{\xi})+\ldots+\frac{1}{n!}\frac{\partial^n\hat{\boldsymbol{\Xi}}}{\partial\boldsymbol{\xi}^n}\Big|_{\boldsymbol{\xi}=\mathbf{0}}\bullet\underbrace{(\boldsymbol{\xi}\otimes\ldots\otimes\boldsymbol{\xi})}_{(n-1)\quad\text{times}} \tag{2.2.1.18}$$

At this point we introduce a few definitions regarding macromorphic continua [61]

Definition 2.2.1.1. *A deformable body $\mathbb{B}$ is called micromorphic continuum of grade n if its motion in spatial form is described by (2.2.1.1) and (2.2.1.17), which are C^n class with respect to the variables $\mathbf{X}$, t and the inverse motion is given by (2.2.1.2), (2.2.1.18).*

If the microstructure is considered small with respect the macroscopic scale of the body, then we can assume a linear approximation of (2.2.1.17), (2.2.1.18):

$$\boldsymbol{\xi} = \mathbf{P} \cdot \boldsymbol{\Xi} \tag{2.2.1.19}$$

$$\boldsymbol{\Xi} = \mathbf{P}^{-1} \cdot \boldsymbol{\xi} \tag{2.2.1.20}$$

Where the micromorphic deformation gradient of each microstructure is defined as:

$$\mathbf{P} = \frac{\partial \hat{\boldsymbol{\xi}}}{\partial \boldsymbol{\Xi}}\Big|_{\boldsymbol{\Xi}=\mathbf{0}}, \quad \mathbf{P} = \mathbf{P}(\mathbf{X}, t) \tag{2.2.1.21}$$

While the inverse micromorphic deformation gradient is defined as:

$$\mathbf{P}^{-1} = \frac{\partial \hat{\boldsymbol{\Xi}}}{\partial \boldsymbol{\xi}}\Big|_{\boldsymbol{\xi}=\mathbf{0}}, \quad \mathbf{P}^{-1} = \mathbf{P}^{-1}(\mathbf{X}, t) \tag{2.2.1.22}$$

The existence of $\mathbf{P}^{-1}$ is ensured due to (2.2.1.6).

Definition 2.2.1.2. *A deformable body $\mathbb{B}$ is called micromorphic continuum of grade one if its motion in spatial form is described by (2.2.1.1) and (2.2.1.21), which are C^1 class with respect to the variables $\mathbf{X}$, t and the inverse motion is given by (2.2.1.2), (2.2.1.22).*

From equations (2.2.1.1), (2.2.1.1) and (2.2.1.21), (2.2.1.22) it is obvious that the motion of a micromorphic continuum of grade one can be completely described by a vector function $\mathbf{x} = \boldsymbol{\chi}(\mathbf{X}, t)$ (respectively $\mathbf{X} = \boldsymbol{X}(\mathbf{x}, t)$) and a tensor function $\mathbf{P} = \mathbf{P}(\mathbf{X}, t)$ (respectively $\mathbf{P}^{-1}(\mathbf{X}, t)$). Thus, such a continuum in the most general case has 12 kinematic degrees of freedom.

From (2.2.1.1), it is also easy to express the macro – displacement and micro- displacement vectors in terms of the material coordinates:

$$\mathbf{u} = \mathbf{b} + \mathbf{x} - \mathbf{X}, \quad \mathbf{u} = \mathbf{u}(\mathbf{X}, t) \tag{2.2.1.23}$$

$$\mathbf{u}' = \mathbf{u} + \boldsymbol{\xi} - \boldsymbol{\Xi}, \quad \mathbf{u}' = \mathbf{u}'(\mathbf{X}, \boldsymbol{\Xi}, t) \tag{2.2.1.24}$$

Where $\mathbf{b} = \mathbf{b}(t)$ is the displacement vector representing rigid body motion, $\mathbf{u}$ is the macro – displacement vector in material description and $\mathbf{u}'$ is the micro – displacement vector in material description.

Equations (2.2.1.23) – (2.2.1.24) can be written using index notation as:

$$u_i = a_{iJ} b_J + x_i - a_{iJ} X_J \tag{2.2.1.25}$$

$$u'_i = u_i + \xi_i - a'_{iJ} \Xi_J \tag{2.2.1.26}$$

Where a_{iJ} are the direction cosines between the spatial and material macro – coordinate systems with unit vectors $\mathbf{e}_i$ and $\mathbf{E}_J$ respectively and a'_{iJ} are the direction cosines between the spatial and material micro – coordinate systems with unit vectors $\mathbf{e}'_i$ and $\mathbf{E}'_J$.

$$a_{iJ} = \mathbf{e}_i \cdot \mathbf{E}_J = \mathbf{E}_J \cdot \mathbf{e}_i \tag{2.2.1.27}$$

$$a'_{iJ} = \mathbf{e}'_i \cdot \mathbf{E}'_J = \mathbf{E}'_J \cdot \mathbf{e}'_i \tag{2.2.1.28}$$

It was mentioned earlier that the axis of $\boldsymbol{\Xi}$, $\boldsymbol{\xi}$ are parallel to those of $\mathbf{X}$, $\mathbf{x}$, which results in:

$$a_{iJ} = a'_{iJ} \tag{2.2.1.29}$$

In order to examine the pure deformation, it is convenient to superimpose the coordinates systems for the reference and spatial macro – configurations, which results in $\mathbf{b} = \mathbf{0}$. In this case the direction cosines degenerate into Kronecker deltas ($a_{iJ} = a'_{iJ} = \delta_{iJ}$) and as a result (2.2.1.23) – (2.2.1.24) become:

$$\mathbf{u} = \mathbf{x} - \mathbf{X} \tag{2.2.1.30}$$

$$\mathbf{u}' = \mathbf{x} - \mathbf{X} + \boldsymbol{\xi} - \boldsymbol{\Xi} \tag{2.2.1.31}$$

or using index notation:

$$u_i = x_i - \delta_{iJ} X_J = x_i - X_i \tag{2.2.1.32}$$

$$u'_i = x_i - \delta_{iJ} X_J + \xi_i - \delta_{iJ} \Xi_J = x_i - X_i + \xi_i - \Xi_i \tag{2.2.1.33}$$

By differentiating equations (2.2.1.30), (2.2.1.31) with respect to the material position vectors $\mathbf{X}$, $\boldsymbol{\Xi}$ respectively, we define the material macro and micro – displacement gradients:

$$\nabla_{\mathbf{X}} \mathbf{u} = \mathbf{F} - \mathbf{I} \tag{2.2.1.34}$$

$$\nabla_{\boldsymbol{\Xi}} \mathbf{u}' = \mathbf{F}' - \mathbf{I} \tag{2.2.1.35}$$

Where $\mathbf{F}$ is the classical deformation gradient (now the macro – gradient of the macro deformation) and $\mathbf{F}'$ is the micro – deformation gradient (the micro – gradient of the micro deformation):

$$\mathbf{F} = \nabla_{\mathbf{X}} \mathbf{x}, \quad \mathbf{F} = \mathbf{F}(\mathbf{X}, t) \tag{2.2.1.36}$$

$$\mathbf{F}' = \nabla_{\boldsymbol{\Xi}} \boldsymbol{\xi}, \quad \mathbf{F}' = \mathbf{F}'(\mathbf{X}, \boldsymbol{\Xi}, t) \tag{2.2.1.37}$$

An essential assumption of the micromorphic theories is that the micro – deformation is taken to be homogenous in the micro – medium and non – homogenous in the macro – medium, which means that $\mathbf{F}'$ must not depend from the micro – coordinates $\boldsymbol{\Xi}$. Thus, in view of (2.2.1.21), (2.2.1.37) we can write:

$$\mathbf{P}(\mathbf{X}, t) = \mathbf{F}'(\mathbf{X}, t) \tag{2.2.1.38}$$

Equation (2.2.1.35) can be expressed in terms of $\mathbf{P}$ as:

$$\boldsymbol{\psi}^{\mathbf{T}} = \mathbf{P} - \mathbf{I} \tag{2.2.1.39}$$

Where $\boldsymbol{\psi}$ is the micromorphic displacement gradient, also commonly refereed in the literature as the micro – deformation:

$$\boldsymbol{\psi} = (\nabla_{\boldsymbol{\Xi}} \mathbf{u}')^{\mathbf{T}}, \quad \boldsymbol{\psi} = \boldsymbol{\psi}(\mathbf{X}, t) \tag{2.2.1.40}$$

Equations (2.2.1.34), (2.2.1.35) are the fundamental relations that describe the deformation and motion of a micromorphic continuum locally. Because (2.2.1.34), (2.2.1.35) are identical, we can conclude that whatever holds for $\mathbf{F}$ regarding the polar decomposition will also hold for $\mathbf{P}$, meaning we can define deformation measures for the micro – deformation identical to those of the macro – deformation in terms of $\mathbf{P}$.

We now define the Green – Saint – Venant strain tensor $\mathbf{E}$ in the same way as in classical continuum mechanics:

$$\mathbf{E} = \frac{1}{2}\left(\mathbf{F}^{\mathbf{T}}\mathbf{F} - \mathbf{I}\right) \tag{2.2.1.41}$$

In a similar fashion, we define a corresponding deformation metric tensor that measures how much a given micro – displacement differs locally from a rigid body micro – displacement [61].

$$\mathbf{M} = \frac{1}{2}\left(\mathbf{P}^{\mathbf{T}}\mathbf{P} - \mathbf{I}\right) \tag{2.2.1.42}$$

$\mathbf{M}$ is known as the micromorphic Green – Saint – Venant strain tensor.

It is also useful to define a strain measure that takes into account the differential deformations of the continuum element and the microstructure by the name relative micro – macro – Green – Saint – Venant strain tensor [61]:

$$\mathbf{Y} = \left(\mathbf{I} - \mathbf{P}^{\mathbf{T}}\mathbf{F}^{-\mathbf{T}}\right) \tag{2.2.1.43}$$

It is noted that tensor $\mathbf{Y}$ takes into account the differential rotation between the micro and macro-scale, since when applying the polar decomposition theorem in (2.2.1.43) the rotation does not vanish, however we will see later that this problem is sorted within the three forms of Mindlin's general theory.

We also define the following third-order tensor, called the first nonlinear micro-deformation gradient [61]:

$$\boldsymbol{\Lambda} = \left(\mathbf{F}^{-1}\nabla_{\mathbf{X}}\mathbf{P}\right)^{\mathbf{T_{13}}} \tag{2.2.1.44}$$

With T_{13} indicating the transpose operator with respect to the first and third indices of $\boldsymbol{\Lambda}$.

In equations (2.2.1.41) – (2.2.1.44) appear three independent strain measures $\mathbf{F}$, $\mathbf{P}$, $\nabla_{\mathbf{X}}\mathbf{P}$, which means that in order to describe the deformation of a micromorphic continuum we must use only three of the aforementioned four strain tensors. Since $\mathbf{E}$ is the only tensor that measures the deformation of the macro – medium and $\mathbf{Y}$ is the only one of them that measures the relative deformation of the microstructure with respect to the macro – medium we are obliged to consider them, also since the tensor $\nabla_{\mathbf{X}}\mathbf{P}$ appears only through $\boldsymbol{\Lambda}$ we come to the conclusion that our deformation measures will be $\mathbf{E}$, $\mathbf{Y}$ and $\boldsymbol{\Lambda}$. In the next chapter we will see that the strain tensors that are defined in Mindlin's general theory (which is a geometrically linear theory) will be derived by linearizing the expressions of $\mathbf{E}$, $\mathbf{Y}$ and $\boldsymbol{\Lambda}$.

2.2.2 Kinematics of Mindlin's General Theory

Up to this point the kinematics has been presented from a general point of view which does not only hold for Mindlin's general theory but also applies in geometrically nonlinear micromorphic continua. From this point on, we will continue by invoking the assumptions regarding the kinematics of Mindlin's general theory. We begin by considering the case of small deformations, so the absolute values of the displacement gradients are assumed to be small in comparison with unity:

$$\left|\frac{\partial u_i}{\partial X_j}\right| \ll 1 \tag{2.2.2.1}$$

$$|\psi_{ij}| = \left|\frac{\partial u'_j}{\partial \Xi_i}\right| \ll 1 \tag{2.2.2.2}$$

The above assumptions imply that there is little difference in the material and spatial coordinates of a given material point in the continuum, thus the referential and spatial description are approximately the same:

$$\frac{\partial u_i}{\partial X_j} \approx \frac{\partial u_i}{\partial x_j}, \quad u_j = u_j(x_i, t) \tag{2.2.2.3}$$

$$\psi_{ij} = \frac{\partial u'_j}{\partial \Xi_i} = \frac{\partial u'_j}{\partial \xi_i}, \quad u'_j = u'_j(x_i, \xi_i, t) \tag{2.2.2.4}$$

The linearization process is performed by initially expressing (2.2.1.41) – (2.2.1.44) in terms of the displacement and micro – displacement gradients and then taking into account (2.2.2.3), (2.2.2.4):

$$\begin{aligned}\mathbf{E} &= \frac{1}{2}\left[\left(\nabla_{\mathbf{X}}\mathbf{u}+\mathbf{I}\right)^{\mathbf{T}}\left(\nabla_{\mathbf{X}}\mathbf{u}+\mathbf{I}\right)-\mathbf{I}\right] \\ &+ \frac{1}{2}\left[\nabla_{\mathbf{X}}\mathbf{u}+\left(\nabla_{\mathbf{X}}\mathbf{u}\right)^{\mathbf{T}}+\left(\nabla_{\mathbf{X}}\mathbf{u}\right)^{\mathbf{T}}\nabla_{\mathbf{X}}\mathbf{u}\right] \\ &\approx \frac{1}{2}\left[\nabla_{\mathbf{X}}\mathbf{u}+\left(\nabla_{\mathbf{X}}\mathbf{u}\right)^{\mathbf{T}}\right] \\ &\approx \frac{1}{2}\left[\nabla_{\mathbf{x}}\mathbf{u}+\left(\nabla_{\mathbf{x}}\mathbf{u}\right)^{\mathbf{T}}\right]=\boldsymbol{\varepsilon}\end{aligned} \tag{2.2.2.5}$$

$$\begin{aligned}\mathbf{M} &= \frac{1}{2}\left(\boldsymbol{\psi}+\boldsymbol{\psi}^{\mathbf{T}}+\boldsymbol{\psi}\boldsymbol{\psi}^{\mathbf{T}}\right) \\ &\approx \frac{1}{2}\left(\boldsymbol{\psi}+\boldsymbol{\psi}^{\mathbf{T}}\right)=sym(\boldsymbol{\psi})\end{aligned} \tag{2.2.2.6}$$

$$\begin{aligned}\mathbf{Y} &= \left[\mathbf{I}-\left(\boldsymbol{\Psi}^{\mathbf{T}}+\mathbf{I}\right)^{\mathbf{T}}\left(\nabla_{\mathbf{X}}\mathbf{u}+\mathbf{I}\right)^{\mathbf{T}}\right] \\ &\approx \left[\left(\nabla_{\mathbf{X}}\mathbf{u}\right)^{\mathbf{T}}-\boldsymbol{\psi}+\boldsymbol{\psi}\left(\nabla_{\mathbf{X}}\mathbf{u}\right)^{\mathbf{T}}\right] \\ &\approx \left[\left(\nabla_{\mathbf{X}}\mathbf{u}\right)^{\mathbf{T}}-\boldsymbol{\psi}\right]=\boldsymbol{\gamma}\end{aligned} \tag{2.2.2.7}$$

For the linearization of $\boldsymbol{\Lambda}$ it is convenient to use index notation.

$$\begin{aligned}\lambda_{ijk} &= F^{-1}_{kl}P_{lj,i} \\ &\approx \left(\delta_{kl}-u_{k,l}P_{lj,i}\right) \\ &= P_{kj,i}-u_{k,l}P_{lj,i} \\ &\approx P_{kj,i}=\psi_{jk,i}=k_{ijk}\end{aligned} \tag{2.2.2.8}$$

Where $\boldsymbol{\varepsilon}$ is the infinitesimal strain tensor, $\boldsymbol{\psi}$ is the symmetric part of the micro – deformation, $\boldsymbol{\gamma}$ is the linearized micro – macro – Green – Saint – Venant strain tensor, k_{ijk} is the macro – gradient of the micro - deformation and the comma symbol denotes differentiation with respect to the coordinate x_i or ξ_i. Tensors $\boldsymbol{\varepsilon}$, $sym(\boldsymbol{\psi})$ and $\boldsymbol{\gamma}$ can be expressed using index notation as:

$$\varepsilon_{ij} = \frac{1}{2}\left(\frac{\partial u_i}{\partial x_j} + \frac{\partial u_j}{\partial x_i}\right) \tag{2.2.2.9}$$

$$\psi_{(ij)} = \frac{1}{2}\left(\psi_{ij} + \psi_{ji}\right) \tag{2.2.2.10}$$

$$\gamma_{ij} = \left(\frac{\partial u_i}{\partial x_j} - \psi_{ij}\right) \tag{2.2.2.11}$$

From classical continuum mechanics we know that in small deformations the symmetric part of the displacement gradient is the infinitesimal strain tensor ε_{ij}, defined in (2.2.2.9) (now the macro – strain) and the antisymmetric part of the displacement gradient is the infinitesimal rotation tensor ω_{ij} (now the macro - rotation).

$$\omega_{ij} = \left(\frac{\partial u_i}{\partial x_j} - \frac{\partial u_j}{\partial x_i}\right) \tag{2.2.2.12}$$

In the same sense the micro – deformation can be decomposed uniquely as the sum of a symmetric and an antisymmetric second order tensor. The symmetric part of ψ_{ij} is the micro – strain $\psi_{(ij)}$, defined in (2.2.2.10) and the antisymmetric part is the macro – rotation:

$$\psi_{[ij]} = \frac{1}{2}\left(\psi_{ij} - \psi_{ji}\right) \tag{2.2.2.13}$$

Because u_i and ψ_{ij} are assumed to be continuous and single valued functions of the macro – coordinates x_i, the following compatibility equations are obtained for simply connected bodies.

$$e_{mik}e_{nlj}\frac{\partial^2 \varepsilon_{kl}}{\partial x_i \partial x_j} = 0 \tag{2.2.2.14}$$

$$e_{mij}\frac{\partial k_{jkl}}{\partial x_i} = 0 \tag{2.2.2.15}$$

$$\frac{\partial}{\partial x_i}(\varepsilon_{jk} + \omega_{jk} - \gamma_{jk}) = k_{ijk} \tag{2.2.2.16}$$

Where ε_{ijk} is the alternating tensor.

2.3 Energetics

2.3.1 Kinetic Energy

In Mindlin's general theory the micro – medium is considered as a parallelepiped with volume V' and edges of lengths $2d_i$ and direction cosines l_{ij} with respect to the axis ξ_i. Let ξ_i' be oblique Cartesian coordinates parallel to the edges d_i respectively. Then:

$$\xi_i = l_{ij}\xi_j' \tag{2.3.1.1}$$

The volume of a parallelepiped can be calculated as the mixed product of three vectors parallel with the edges of the parallelepiped, with length equal to that of the edges.

$$V' = 8\|l_{ij}l_{ik}\|^{1/2}d_1d_2d_3 \tag{2.3.1.2}$$

$$dV' = \|l_{ij}l_{ik}\|^{1/2}d\xi_1'd\xi_2'd\xi_3' \tag{2.3.1.3}$$

In his general theory Mindlin defined the kinetic energy density (kinetic energy per unit macro – volume) as:

$$T = \frac{1}{2}\rho_M\dot{u}_j\dot{u}_j + \frac{1}{V'}\int_{V'}\frac{1}{2}\rho'(\dot{u}_j + \dot{u}_j')(\dot{u}_j + \dot{u}_j')\,dV' \tag{2.3.1.4}$$

Where ρ_M is the mass of the macro – material per unit macro – volume, ρ' is the mass of the micro – material per unit micro – volume and the dot symbol designates differentiation with respect to time. As we know from classical mechanics, the speed and thus the kinetic energy of a system depends on the frame of reference. If one notices carefully the above equation, then it is will be obvious that the first term represents the kinetic energy density of a particle of the macro – medium with respect to the origin of the macro – frame of reference, while the second term represent the kinetic energy density of the micro medium

that at the macroscopic scale corresponds to the same particle, again with respect to the macro – frame of reference.

By substituting (2.3.1.2), (2.3.1.3) into (2.3.1.4) and performing the integration we obtain:

$$T = \frac{1}{2}\rho \dot{u}_j \dot{u}_j + \frac{1}{6}\rho' d_{kl}^2 \dot{\psi}_{lj} \dot{\psi}_{lj} \tag{2.3.1.5}$$

where:

$$\rho = \rho_M + \rho' \tag{2.3.1.6}$$

$$d_{kl}^2 = d_p d_q (\delta_{p1}\delta_{q1} l_{k1} l_{l1} + \delta_{p2}\delta_{q2} l_{k2} l_{l2} + \delta_{p3}\delta_{q3} l_{k3} l_{l3}) = d_{lk}^2 \tag{2.3.1.7}$$

From (2.3.1.7) it is clear that the expression of d_{kl}^2 depends from the geometry of the micro – structure. In Mindlin's general theory the unit cell is taken to be a parallelepiped in order to represent the unit cell of a crystal lattice. If another shape is considered then the only expression that changes is that of d_{kl}^2. Also, the cell can be interpreted as a molecule of a polymer, a crystallite of a polycrystal or a grain of a granular material.

2.3.2 Potential Energy

Regarding the potential energy density (potential energy per unit macro – volume), it is assumed that a function of ϵ_{ij}, γ_{ij}, k_{ijk} exists.

$$W = W(\epsilon_{ij}, \gamma_{ij}, k_{ijk}) \tag{2.3.2.1}$$

At first glance, one could argue that it is absurd for W to depend from the entire γ_{ij}. It is reminded that γ_{ij} is the linearized relative micro – macro – Green – Saint – Venant strain tensor $\mathbf{Y}$, defined in (2.2.1.43) that takes into account the differential rotation between the micro and macro-scale, which means that $\mathbf{Y}$ apart from pure deformations also measures rigid body motion. It will be proved later in the kinematics of form I that a small rigid rotation of the deformed body produces an equal rotation of the micro – material, meaning that $\omega_{ij} = \psi_{[ij]}$. Consequently, the antisymmetric parts of the tensors that appear in (2.2.2.11) vanish, making γ_{ij} an appropriate variable for the potential energy density. However, at the moment the problem that was mentioned earlier regarding the rotation continues to exist.

2.4 Variational Approach in Mindlin's General Theory

2.4.1 Formulation of the Equations of Motion and Boundary Conditions

Instead of applying the conservation laws of linear and angular momentum the equations of motion are formulated using Hamilton's principle, since in this way, the boundary conditions are also derived simultaneously. According to Bedford [62], for the case of a micromorphic continuum Hamilton's principle states:

Theorem 2.4.1.1 (Hamilton's Principle for Micromorphic Continua)

Among admissible comparison motions (2.2.1.1), (2.2.1.2) and micro – motions (2.2.1.3), (2.2.1.4), the actual motion of the system is such that:

$$\int_{t_1}^{t_2} [\delta(\mathscr{J} - \mathscr{W}) + \delta W_{ext}]\, dt = 0$$

Where δ denotes the variation, t_1, t_2 are fixed times with $t_1 < t_2$ at which we suppose that the configuration of the system is prescribed, $\mathscr{J}$ is the total kinetic energy, $\mathscr{W}$ is the total potential energy and δW_{ext} is the work of the external forces.

The major advantage of Hamilton's principle when it comes to formulating equations of motion and boundary conditions is that the quantities that appear in the above expression are all scalar, which means that the principle is independent of the geometry of the system. Equivalently, the equations of motion can be formulated using the balance of linear and angular momentum, but first the relations that connect the multi – polar traction vectors with the multi – polar stress tensors must be derived. This can be achieved using the idea of Cauchy's tetrahedron as in classical continuum mechanics, with the difference being that the multi – polar forces that act in each face of the tetrahedron should also be considered.

The variation of the kinetic energy term in Hamilton's principle is:

$$\begin{aligned}
\int_{t_1}^{t_2} \delta \mathscr{J}\, dt &= \int_{t_1}^{t_2} \delta \int_{\mathbb{B}_0} T\, dV\, dt \\
&= \int_{t_1}^{t_2} \delta \int_{\mathbb{B}_0} \left(\frac{1}{2}\rho \dot{u}_j \dot{u}_j + \frac{1}{6}\rho' d_{kl}^2 \dot{\psi}_{lj} \dot{\psi}_{lj} \right) dV\, dt \\
&= \int_{t_1}^{t_2} \int_{\mathbb{B}_0} \left(\rho \dot{u}_j \delta \dot{u}_j + \frac{1}{3}\rho' d_{kl}^2 \dot{\psi}_{lj} \delta \dot{\psi}_{lj} \right) dV\, dt \qquad (2.4.1.1)
\end{aligned}$$

By integrating (2.4.1.1) by parts with respect to time and taking also into account the conditions $\delta u_i|_{t=t1} = \delta u_i|_{t=t2} = 0$ and $\delta \psi_{ij}|_{t=t1} = \delta \psi_{ij}|_{t=t2} = 0$ we obtain:

$$\int_{t_1}^{t_2} \delta \mathscr{J}\, dt = \int_{t_1}^{t_2} \int_{\mathbb{B}_0} \left(\rho \dot{u}_j \delta \dot{u}_j + \frac{1}{3} \rho' d_{kl}^2 \dot{\psi}_{lj} \delta \dot{\psi}_{lj} \right) dV\, dt$$
$$= - \int_{t_1}^{t_2} \int_{\mathbb{B}_0} \left(\rho \ddot{u}_j \delta u_j + \frac{1}{3} \rho' d_{kl}^2 \ddot{\psi}_{lj} \delta \psi_{lj} \right) dV\, dt \qquad (2.4.1.2)$$

In order to determine the variation of the potential energy, we define the following stress tensors, the interpretation of which will be given later:

$$\tau_{ij} = \frac{\partial W}{\partial \varepsilon_{ij}} \qquad (2.4.1.3)$$

$$\sigma_{ij} = \frac{\partial W}{\partial \gamma ij} \qquad (2.4.1.4)$$

$$\mu_{ijk} = \frac{\partial W}{\partial k_{ijk}} \qquad (2.4.1.5)$$

In view of (2.3.2.1), (2.4.1.3) – (2.4.1.5) we can write the variation of the potential energy density in the form of:

$$\delta W = \tau_{ij} \delta \varepsilon_{ij} + \sigma_{ij} \delta \gamma_{ij} + \mu_{ijk} \delta k_{ijk} \qquad (2.4.1.6)$$

Using the definitions of ε_{ij}, γij, k_{ijk}, (2.4.1.6) can be written as:

$$\delta W = \tau_{ij} \frac{\partial \delta u_j}{\delta x_i} + \sigma_{ij} \left(\frac{\partial \delta u_j}{\delta x_i} - \delta \psi_{ij} \right) + \mu_{ijk} \frac{\partial \delta \psi_{jk}}{\delta x_i} \qquad (2.4.1.7)$$

The variation of the potential energy term in Hamilton's principle is:

$$\begin{aligned}\int_{t_1}^{t_2} \delta\mathscr{W}\, dt &= \int_{t_1}^{t_2} \delta \int_{\mathbb{B}_0} W\, dV\, dt \\ &= \int_{t_1}^{t_2} \int_{\mathbb{B}_0} \left(\tau_{ij} \frac{\partial \delta u_j}{\delta x_i} + \sigma_{ij} \left(\frac{\partial \delta u_j}{\delta x_i} - \delta\psi_{ij} \right) + \mu_{ijk} \frac{\partial \delta \psi_{jk}}{\delta x_i} \right) dV\, dt \\ &= \int_{t_1}^{t_2} \int_{\mathbb{B}_0} \left\{ \frac{\partial}{\partial x_i} \left[(\tau_{ij} + \sigma_{ij}) \delta u_j \right] - \frac{\partial}{\partial x_i} (\tau_{ij} + \sigma_{ij}) \delta u_j \right\} dV\, dt \\ &+ \int_{t_1}^{t_2} \int_{\mathbb{B}_0} \left[\frac{\partial}{\partial x_i} \left(\mu_{ijk} \delta \psi_{jk} \right) - \sigma_{ij} \delta \psi_{ij} - \frac{\partial \mu_{ijk}}{\partial x_i} \delta \psi_{jk} \right] dV\, dt \end{aligned} \tag{2.4.1.8}$$

We will continue from here by applying a well – known theorem of vector calculus.

Theorem 2.4.1.2 (Divergence Theorem)

Let R be a regular area of an Euclidean space with boundary ∂R, let $\mathbf{n}$ be the outward pointing unit normal vector at each point on the boundary and let $\mathbf{T}$ be a n – order tensor field continuous on R and continuously differentiable at every point in its interior. Then:

$$\int_R \frac{\partial T_{i_1,i_2,\ldots,i_q,\ldots,i_n}}{i_q}\, dV = \int_{\partial R} T_{i_1,i_2,\ldots,i_q,\ldots,i_n} n_{i_q}\, dS$$

Applying the divergence theorem in (2.4.1.8) yields:

$$\begin{aligned}\int_{t_1}^{t_2} \delta\mathscr{W}\, dt &= \int_{t_1}^{t_2} \int_{\partial\mathbb{B}_0} (\tau_{ij} + \sigma_{ij}) n_i \delta u_j\, dS\, dt + \int_{t_1}^{t_2} \int_{\partial\mathbb{B}_0} \mu_{ijk} n_i \delta\psi_{jk}\, dS\, dt \\ &- \int_{t_1}^{t_2} \int_{\mathbb{B}_0} \frac{\partial}{\partial x_i} (\tau_{ij} + \sigma_{ij}) \delta u_j\, dV\, dt - \int_{t_1}^{t_2} \int_{\mathbb{B}_0} \left(\frac{\partial \mu_{ijk}}{\partial x_i} + \sigma_{jk} \right) \delta\psi_{jk}\, dV\, dt \end{aligned} \tag{2.4.1.9}$$

The work of the external forces is:

$$W_{ext} = \int_{\mathbb{B}_0} f_j u_j\, dV + \int_{\mathbb{B}_0} F_{jk} \psi_{jk}\, dV + \int_{\partial\mathbb{B}_0} t_j u_j\, dS + \int_{\partial\mathbb{B}_0} T_{jk} \psi_{jk}\, dS \tag{2.4.1.10}$$

Where f_j is the body force per unit volume, t_j is the surface force per unit area, F_{jk} is the double force per unit volume and T_{jk} is the double force per unit area. The double (or dipolar) forces are antiparallel forces acting between the micromedia contained in the continuum with microstructure. The diagonal terms of F_{jk}, T_{jk} are double forces without moment and the off – diagonal terms are double forces with moment. The antisymmetric part $F_{[jk]}$ of F_{jk} is the body double, while the antisymmetric part $T_{[jk]}$ of T_{jk} Is the Cosserat couple

– stress vector. As for the notation of the double forces, the first index of the forces denotes the orientation of the lever arm between the forces and the second index the orientation of the pair of the forces.

The variation of the work of the external forces is:

$$\delta W_{ext} = \int_{\mathbb{B}_0} f_j \delta u_j \, dV + \int_{\mathbb{B}_0} F_{jk} \delta \psi_{jk} \, dV + \int_{\partial \mathbb{B}_0} t_j \delta u_j \, dS + \int_{\partial \mathbb{B}_0} T_{jk} \delta \psi_{jk} \, dS \tag{2.4.1.11}$$

By substituting equations (2.4.1.2), (2.4.1.9), (2.4.1.11) into Hamilton's principle, we obtain:

$$\begin{aligned} &\int_{t_1}^{t_2} \int_{\mathbb{B}_0} \left[\frac{\partial}{\partial x_i} (\tau_{ij} + \sigma_{ij}) + f_j - \rho \ddot{u}_j \right] \delta u_j \, dV \, dt \\ &\int_{t_1}^{t_2} \int_{\mathbb{B}_0} \left(\frac{\partial \mu_{ijk}}{\partial x_i} + \sigma_{jk} + F_{jk} - \frac{1}{3} \rho' d_{jl}^2 \ddot{\psi}_{jk} \right) \delta \psi_{jk} \, dV \, dt \\ &+ \int_{t_1}^{t_2} \int_{\partial \mathbb{B}_0} \left[t_j - (\tau_{ij} + \sigma_{ij}) \, n_i \right] \delta u_j \, dS \, dt \\ &+ \int_{t_1}^{t_2} \int_{\partial \mathbb{B}_0} (T_{jk} - \mu_{ijk} n_i) \, \delta \psi_{jk} \, dS \, dt = 0 \end{aligned} \tag{2.4.1.12}$$

Due to the independence of the fields δu_j, $\delta \psi_{jk}$, equation (2.4.1.12) yields the differential equations of motions:

$$\frac{\partial}{\partial x_i} (\tau_{ij} + \sigma_{ij}) + f_j = \rho \ddot{u}_j \tag{2.4.1.13}$$

$$\frac{\partial \mu_{ijk}}{\partial x_i} + \sigma_{jk} + \Phi_{jk} = \frac{1}{3} \rho' d_{jl}^2 \ddot{\psi}_{lk} \tag{2.4.1.14}$$

As well as the boundary conditions.

$$t_j = (\tau_{ij} + \sigma_{ij}) n_i \tag{2.4.1.15}$$

$$T_{jk} = \mu_{ijk} n_i \tag{2.4.1.16}$$

Taking into consideration equations (2.4.1.3) – (2.4.1.5), (2.4.1.15), (2.4.1.16) as well as the definitions of ϵ_{ij}, γ_{ij}, k_{ijk} it appears that an appropriate terminology for the three stress

tensors is: Cauchy stress for τ_{ij}, relative stress for σ_{ij} and double (or dipolar) stress for μ_{ijk}. As for the notation of the double stresses, the first index denotes the orientation of the outward pointing unit normal vector to the surface on which the double stress acts, while the significance of the other two indices is the same as that of the indices of the double forces T_{jk}.

2.4.2 Linear Stability Analysis

The stability of a micromorphic system can be described by the action functional $S = S(u_i, \psi_{ij})$, which is defined as:

$$S = \int_{t_1}^{t_2} (\mathscr{T} - \mathscr{W} + W_{ext})\, dt \tag{2.4.2.1}$$

Setting the first variation of the action functional equal to zero ensures the equations of motion and boundary conditions through Hamilton's principle. Regarding the stability of the system, it is determined by the second variation of the action functional. By expanding S in terms of Taylor series about the point (u_i, ψ_{ij}) we obtain:

$$\begin{aligned} S(u_i + \delta u_i, \psi_{ij} + \delta\psi_{ij}) = S(u_i, \psi_{ij}) + \left(\frac{\partial S}{\partial ui}\delta u_i + \frac{\partial S}{\partial \psi ij}\delta\psi_{ij}\right) \\ + \frac{1}{2}\left[\frac{\partial^2 S}{\partial u_i \partial u_j}\delta u_i \delta u_j + 2\frac{\partial^2 S}{\partial u_i \partial \psi_{jk}}\delta u_i \psi u_{jk} + \frac{\partial^2 S}{\partial \psi_{ij}\partial\psi_{kl}}\delta\psi_{ij}\delta\psi_{kl}\right] + ... \end{aligned} \tag{2.4.2.2}$$

According to (2.4.2.2), the change of the action $\Delta S \equiv S(u_i + \delta u_i, \psi_{ij} + \delta\psi_{ij}) - S(u_i, \psi_{ij})$ can be expressed as:

$$\Delta S = \delta S + \frac{1}{2}\delta^2 S + ... \tag{2.4.2.3}$$

Where the first variation δS must be equal to zero due to Hamilton's principle:

$$\delta S = \frac{\partial S}{\partial ui}\delta u_i + \frac{\partial S}{\partial \psi ij}\delta\psi_{ij} \tag{2.4.2.4}$$

Whereas the second variation is defined as:

$$\delta^2 S = \frac{\partial^2 S}{\partial u_i \partial u_j}\delta u_i \delta u_j + 2\frac{\partial^2 S}{\partial u_i \partial \psi_{jk}}\delta u_i \psi u_{jk} + \frac{\partial^2 S}{\partial \psi_{ij}\partial \psi_{kl}}\delta\psi_{ij}\delta\psi_{kl} \tag{2.4.2.5}$$

From equations (2.4.2.3) – (2.4.2.5) it is clear that the sign of δS is determined by the first non – zero term in the Taylor series. If $\delta^2 S > 0$, then $\Delta S > 0$ and therefore S exhibits a relative minimum, meaning that the equilibrium state (dynamic or static) is stable. If $\delta^2 S < 0$, then $\Delta S < 0$, in this case S exhibits a relative maximum, meaning that the state is unstable. Finally, known as neutral stability a special case occurs when the second and all the higher order variations are equal to zero. When a system is in this state under the influence of a virtual displacement field, it remains in this state without being able to return to its original state due to zero restoring forces.

2.5 Constitutive Equations

2.5.1 Anisotropic Materials

From the previous analysis we derived 12 equations of motion (equations (2.4.1.13), (2.4.1.14)) using Hamilton's Principle. The number of unknown functions that appear in (2.4.1.13), (2.4.1.14)) are 54 and so the problem is undefined. We also have the kinematic equations that relate the displacements with the strains. However, the stresses do not appear in these equations, which means that in order to solve a problem in the context of Mindlin's general theory we need additional equations that relate the stresses with the strains. In order to formulate these equations, we start by expanding (2.3.2.1) in terms of Taylor series about the point $(\epsilon_{ij}, \gamma_{ij}, k_{ijk}) = (0, 0, 0)$.

$$\begin{aligned} W = W_0 &+ \left(\frac{\partial W}{\partial \epsilon_{ij}}\epsilon_{ij} + \frac{\partial W}{\partial \gamma ij}\gamma_{ij} + \frac{\partial W}{\partial k_{ijk}}k_{ijk}\right) \\ &+ \frac{1}{2}\left[\frac{\partial^2 W}{\partial \epsilon_{ij}\partial\epsilon_{kl}}\epsilon_{ij}\epsilon_{kl} + \frac{\partial^2 W}{\partial \gamma_{ij}\partial\gamma_{kl}}\gamma_{ij}\gamma_{kl} + \frac{\partial^2 W}{\partial k_{ijk}\partial k_{lmn}}k_{ijk}k_{lmn}\right. \\ &\left. + 2\frac{\partial^2 W}{\partial \gamma_{ij}\partial k_{klm}}\gamma_{ij}k_{klm} + 2\frac{\partial^2 W}{\partial k_{ijk}\partial\epsilon_{lm}}k_{ijk}\epsilon_{lm} + 2\frac{\partial^2 W}{\partial\gamma_{ij}\epsilon_{kl}}\gamma_{ij}\epsilon_{kl}\right] + ... \end{aligned} \tag{2.5.1.1}$$

By setting $a_{ijk} = \partial W/\partial k_{ijk}$, $b_{ij} = \partial W/\partial\gamma_{ij}$, $c_{ij} = \partial W/\partial\epsilon_{ij}$, $a_{ijklmn} = \partial^2 W/\partial k_{ijk}\partial k_{lmn}$, $b_{ijkl} = \partial^2 W/\partial\gamma_{ij}\partial\gamma_{kl}$, $c_{ijkl} = \partial^2 W/\partial\epsilon_{ij}\partial\epsilon_{kl}$, $d_{ijklm} = \partial^2 W/\partial\gamma_{ij}\partial k_{klm}$, $f_{ijklm} = \partial^2 W/\partial k_{ijk}\partial\epsilon_{lm}$, $g_{ijkl} = \partial^2 W/\partial\gamma_{ij}\partial\epsilon_{kl}$ equation (2.5.1.1) can be written as:

$$\begin{aligned} W = W_0 &+ (c_{ij}\epsilon_{ij} + b_{ij}\gamma ij + a_{ijk}k_{ijk}) \\ &+ \frac{1}{2}\left[c_{ijkl}\epsilon_{ij}\epsilon_{kl} + b_{ijkl}\gamma_{ij}\gamma_{kl} + a_{ijklmn}k_{ijk}k_{lmn}\right. \\ &\left.+2d_{ijklm}\gamma_{ij}k_{klm} + 2f_{ijklm}k_{ijk}\epsilon_{lm} + 2g_{ijkl}\gamma_{ijkl}\epsilon_{kl}\right] + ... \end{aligned} \tag{2.5.1.2}$$

In (2.5.1.2) W_0 is a constant, the terms inside the parenthesis express the potential energy density due to residual stresses, the terms within the bracket express the potential energy density due to linear elastic deformations, while the higher order terms that are not shown express the potential energy density due to non – linear response of the material and in the context of a constitutive linear theory can be neglected. Also, since in most engineering problems the residual stresses are not taken into consideration, the terms inside the parenthesis can also be neglected. Taking the aforementioned into account, we can write (2.5.1.2) in the form of:

$$\begin{aligned} W = &\frac{1}{2}c_{ijkl}\epsilon_{ij}\epsilon_{kl} + \frac{1}{2}b_{ijkl}\gamma_{ij}\gamma_{kl} + \frac{1}{2}a_{ijklmn}k_{ijk}k_{lmn} \\ &+ d_{ijklm}\gamma_{ij}k_{klm} + f_{ijklm}k_{ijk}\epsilon_{lm} + g_{ijkl}\gamma_{ijkl}\epsilon_{kl} \end{aligned} \tag{2.5.1.3}$$

In (2.5.1.3) the number of coefficients that seem to appear are 1764, however not all of them are independent. Due to the symmetry of ϵ_{ij} and the fact that interchanging the indices i, j with k, l in the first and second terms and the indices i, j, k with l, m, n in the third term does not change the potential energy density, the following symmetries result and so, the number of unknowns is reduced to 903:

$$c_{ijkl} = c_{klij} = c_{jikl} \tag{2.5.1.4}$$

$$b_{ijkl} = b_{klij} \tag{2.5.1.5}$$

$$a_{ijklmn} = a_{lmnijk} \tag{2.5.1.6}$$

$$f_{ijklm} = f_{ijklm} \tag{2.5.1.7}$$

$$g_{ijkl} = g_{ijlk} \tag{2.5.1.8}$$

Using (2.4.1.3) – (2.4.1.5) and (2.5.1.3) – (2.5.1.8), the following three constitutive equations are obtained:

$$\tau_{pq} = c_{pqij}\epsilon_{ij} + g_{ijpq}\gamma_{ij} + f_{ijkpq}k_{ijk} \tag{2.5.1.9}$$

$$\sigma_{pq} = g_{pqij}\epsilon_{ij} + b_{ijpq}\gamma_{ij} + d_{pqijk}k_{ijk} \tag{2.5.1.10}$$

$$\mu_{pqr} = f_{pqrij}\epsilon_{ij} + d_{ijpqr}\gamma_{ij} + a_{pqrijk}k_{ijk} \tag{2.5.1.11}$$

Equations (2.5.1.9) – (2.5.1.11) are the three constitutive laws that relate the stresses with the strains in Mindlin's general theory for the most general case of an anisotropic materials.

2.5.2 Higher Order Isotropic Tensors

In the case of isotropic materials, the number of independent coefficients is greatly reduced. In order to illustrate this, we will use the definition of isotropic tensors. However, it is deemed necessary to first give o few formal definitions regarding group theory. (Definitions 2.5.2.3 - 2.5.2.6 here are the same as Definitions 2.1 – 2.4 of [63]).

Let $\mathbb{V}$ be a vector space of dimension $m = 3$ on the real field, equipped with an inner product and referred to an orthogonal basis. Let $\mathbb{T}_n(V)$ denote the vector space of tensors of order n on $\mathbb{V}$ and let $\mathbf{I}$ be the identity tensor of $\mathbb{T}_2(\mathbb{V})$.

Definition 2.5.2.1. *The orthogonal group $O(3)$ of a three – dimensional vector space $\mathbb{V}$ is defined as:*

$$O(3) = \left\{\mathbf{Q} \in \mathbb{T}_n(V) | \mathbf{Q}\mathbf{Q}^{\mathsf{T}} = \mathbf{Q}^{\mathsf{T}}\mathbf{Q} = \mathbf{I}\right\}$$

Definition 2.5.2.2. *The rotation group $O^+(3)$ of a three – dimensional vector space $\mathbb{V}$ is defined as:*

$$O^+(3) = \{\mathbf{Q} \in O(3) | det(\mathbf{Q}) = 1\}$$

Definition 2.5.2.3. *Let $\mathscr{T}$ be a subset of $O(3)$. A Cartesian tensor $\mathbf{T} \in \mathbb{T}_n(V)$ is said to be $\mathscr{T}$ – invariant if:*

$$T_{j_1,j_2,\ldots,j_n} = Q_{i_1j_1}Q_{i_2j_2}\ldots Q_{i_nj_n}T_{i_1,i_2,\ldots,i_n}$$

With the help of the above definitions, we can now define the different types of isotropic tensors.

Definition 2.5.2.4. *A Cartesian tensor* $\mathbf{T} \in \mathbb{T}_n(V)$ *is called isotropic if it is* $O(3)$ *– invariant. (The notation* $O(3)$ *– invariant means orthogonally invariant).*

Definition 2.5.2.5. *A Cartesian tensor* $\mathbf{T} \in \mathbb{T}_n(V)$ *is called weakly isotropic if it is* $O^+(3)$ *– invariant. (The notation* $O^+(3)$ *– invariant means rotationally invariant).*

Definition 2.5.2.6. *A Cartesian tensor* $\mathbf{T} \in \mathbb{T}_n(V)$ *is called skew – isotropic if it is* $O^+(3)$ *– invariant and further more if it satisfies the equality:*

$$T_{j_1,j_2,\ldots,j_n} = -Q_{i_1j_1}Q_{i_2j_2}\ldots Q_{i_nj_n}T_{i_1,i_2,\ldots,i_n}, \quad \forall \mathbf{Q} \in O(3), \quad det(\mathbf{Q}) = -1$$

Using the above definitions Montanaro and Pigozzi [63] proved the following Lemma's that will appear very useful when constructing constitutive laws for isotropic materials:

Lemma 2.5.2.1. *Let* $\mathbf{T} \in \mathbb{T}_n(V)$*, with* n *even. If* $\mathbf{T}$ *is weakly isotropic, then* $\mathbf{T}$ *is isotropic. If* $\mathbf{T}$ *is skew – isotropic, then* $\mathbf{T} = \mathbf{0}$*.*

Lemma 2.5.2.2. *Let* $\mathbf{T} \in \mathbb{T}_n(V)$*, with* n *odd. If* $\mathbf{T}$ *is weakly isotropic, then* $\mathbf{T}$ *is skew – isotropic. If* $\mathbf{T}$ *is isotropic, then* $\mathbf{T} = \mathbf{0}$*.*

Based on Lemma 2.5.2.2 we are led to the conclusion that isotropic tensors of odd order do not exist, however there exist weakly isotropic tensors. Using the definitions of the various types of isotropic tensors, it is not difficult to show that there is no Cartesian isotropic tensor of order 1, as well as all isotropic tensors of order 2 are in the form of $\kappa\delta_{ij}$ and all weakly isotropic tensors of order 3 are in the form of $\lambda\epsilon_{ijk}$, with $\kappa, \lambda \in \mathbb{R}$. Later in this work we will consider only the case of "pure" isotropic tensors, nonetheless, a few things regarding weakly isotropic tensors of higher order will also be mentioned for the sake of completeness.

When it comes to higher order tensors Weyl [64] proved that every weakly isotropic Cartesian tensor of even order can be expressed as a linear combination of products of the Kronecker deltas δ_{ij}, δ_{kl},…,δ_{pq} and every weakly isotropic Cartesian tensor of odd order is given by a linear combination of terms formed of products of an appropriate number of Kronecker deltas with an altering tensor ϵ_{ijk}. Such products of Kronecker deltas with or without the alternating tensor ϵ_{ijk} are referred as fundamental (weakly) isotropic Cartesian tensors (abbreviation FICT's) [65]. For every order $n > 1$, the number $N(n)$ of such tensors can be calculated from the following formulas:

$$N(n) = \frac{n!}{\left(\frac{n}{2}\right)!2^{n/2}}, \quad \text{For n even} \tag{2.5.2.1}$$

$$M(n) = \frac{n!}{3!\left(\frac{n-3}{2}\right)!2^{(n-3)/2}}, \quad \text{For n odd} \tag{2.5.2.2}$$

However, Racah [66] using concepts of group theory for the three – dimensional rotational group $O^+(3)$, showed that $N(n)$ in general exceeds the total number of linearly independent fundamental weakly isotropic Cartesian tensors $M(n)$:

$$M(n) = \sum_{k=0}^{[\frac{n+1}{2}]} \left\{ \left[\binom{n}{2k} - \frac{1}{2}\binom{n}{2k-1} \right] \binom{2k}{k} \right\} \tag{2.5.2.3}$$

Order n	2	3	4	5	6	7	8
Number of Distinct FICT's $N(n)$	1	1	3	10	15	105	105
Number of Linearly Independent FICT's $M(n)$	1	1	3	6	15	365	91

Table 2.5.2.1: Values of $N(n)$ and $M(n)$ for different order FICT's.

Table (2.5.2.1) shows that for odd order tensors with $n \geq 5$ and for even rank tensors with $n \geq 8$, there exist linear combinations among fundamental weakly isotropic Cartesian tensors which are identically zero. This can be understood very easily by observing the following two properties:

$$\begin{Vmatrix} \delta_{ip} & \delta_{iq} & \delta_{ir} \\ \delta_{jp} & \delta_{jq} & \delta_{jr} \\ \delta_{kp} & \delta_{kq} & \delta_{kr} \end{Vmatrix} = \epsilon_{ijk}\epsilon_{pqr} \tag{2.5.2.4}$$

$$\begin{Vmatrix} \delta_{ip} & \delta_{iq} & \delta_{ir} & \delta_{is} \\ \delta_{jp} & \delta_{jq} & \delta_{jr} & \delta_{js} \\ \delta_{kp} & \delta_{kq} & \delta_{kr} & \delta_{ks} \\ \delta_{mp} & \delta_{mq} & \delta_{mr} & \delta_{ms} \end{Vmatrix} = 0 \tag{2.5.2.5}$$

Identity (2.5.2.4) is a well – known result of linear algebra and can be verified directly by expanding the 3×3 determinant. The interpretation of identity (2.5.2.5) is that since there are only three possible values of the indices in a three – dimensional space and since there are four columns on the left – hand side, the indices of at least two columns must be equal [65]. Hence the determinant in (2.5.2.5) must vanish.

Order n	Distinct and Linearly Independent Fundamental Isotropic Tensors
2	δ_{ij}
4	$\delta_{ij}\delta_{km}$, $\delta_{ik}\delta_{jm}$, $\delta_{im}\delta_{jk}$
6	$\delta_{ij}\delta_{km}\delta_{pq}$, $\delta_{ij}\delta_{kp}\delta_{mq}$, $\delta_{ij}\delta_{kq}\delta_{mp}$, $\delta_{ik}\delta_{jm}\delta_{pq}$, $\delta_{ik}\delta_{jp}\delta_{mq}$ $\delta_{ik}\delta_{jq}\delta_{mp}$, $\delta_{im}\delta_{jk}\delta_{pq}$, $\delta_{im}\delta_{jp}\delta_{kq}$, $\delta_{im}\delta_{jq}\delta_{kp}$, $\delta_{ip}\delta_{jk}\delta_{mq}$ $\delta_{ip}\delta_{jm}\delta_{kq}$, $\delta_{ip}\delta_{jq}\delta_{km}$, $\delta_{iq}\delta_{jk}\delta_{mp}$, $\delta_{iq}\delta_{jm}\delta_{kp}$, $\delta_{iq}\delta_{jp}\delta_{km}$

Table 2.5.2.2: Expressions for distinct and linearly independent FICT's.

The distinct and linearly independent isotropic tensors of even order are presented in Table (2.5.2.2).

2.5.3 Isotropic Materials

In the previous analysis we showed that there are no isotropic Cartesian tensors of odd order. Taking this into account we can eliminate tensors d_{ijpqr}, f_{ijkpq} from equations (2.5.1.9) – (2.5.1.11) for the case of isotropic materials. The remaining tensors can be constructed as linear combinations of the Kronecker deltas that appear in Table (2.5.2.2). Hence:

$$c_{ijkl} = \lambda\delta_{ij}\delta_{kl} + \mu_1\delta_{ij}\delta_{kl} + \mu_2\delta_{ij}\delta_{kl} \tag{2.5.3.1}$$

$$b_{ijkl} = b_1\delta_{ij}\delta_{kl} + b_2\delta_{ij}\delta_{kl} + b_3\delta_{ij}\delta_{kl} \tag{2.5.3.2}$$

$$g_{ijkl} = g_1\delta_{ij}\delta_{kl} + g_2\delta_{ij}\delta_{kl} + g_3\delta_{ij}\delta_{kl} \tag{2.5.3.3}$$

$$\begin{aligned} a_{ijklmn} = {} & a_1\delta_{ij}\delta_{kl}\delta_{mn} + a_2\delta_{ij}\delta_{km}\delta_{nl} + a_3\delta_{ij}\delta_{kn}\delta_{lm} \\ & + a_4\delta_{jk}\delta_{il}\delta_{mn} + a_5\delta_{jk}\delta_{im}\delta_{nl} + a_6\delta_{jk}\delta_{in}\delta_{lm} \\ & + a_7\delta_{jk}\delta_{il}\delta_{mn} + a_8\delta_{jk}\delta_{im}\delta_{nl} + a_9\delta_{jk}\delta_{in}\delta_{lm} \\ & + a_{10}\delta_{jk}\delta_{il}\delta_{mn} + a_{11}\delta_{jk}\delta_{im}\delta_{nl} + a_{12}\delta_{jk}\delta_{in}\delta_{lm} \\ & + a_{13}\delta_{jk}\delta_{il}\delta_{mn} + a_{14}\delta_{jk}\delta_{im}\delta_{nl} + a_{15}\delta_{jk}\delta_{in}\delta_{lm} \end{aligned} \tag{2.5.3.4}$$

The following relationships are obtained thanks of the symmetries of the tensors c_{ijkl}, b_{ijkl}, g_{ijkl}, a_{ijklmn}.

$$\mu_1 = \mu_2 \equiv \mu \tag{2.5.3.5}$$

$$g_2 = g_3 \tag{2.5.3.6}$$

$$a_1 = a_6, \quad a_2 = a_9, \quad a_5 = a_7, \quad a_{11} = a_{12} \tag{2.5.3.7}$$

Thus, the expression of the potential energy density reduces to:

$$\begin{aligned} W = & \frac{1}{2}\lambda\delta_{pq}\epsilon_{ii} + \mu\epsilon_{ij}\epsilon_{ij} + \frac{1}{2}b_1\gamma_{ii}\gamma_{jj} + \frac{1}{2}b_2\gamma_{ij}\gamma_{ij} \\ & + \frac{1}{2}b_3\gamma_{ij}\gamma_{ji} + \frac{1}{2}g_1\gamma_{ii}\epsilon_{jj} + g_2(\gamma_{ij} + \gamma_{ji})\epsilon_{ij} \\ & + a_1 k_{iik}k_{kjj} + a_2 k_{iik}k_{jkj} + \frac{1}{2}a_3 k_{iik}k_{jjk} + \frac{1}{2}a_4 k_{ijj}k_{ikk} \\ & + a_5 k_{ijj}k_{kik} + \frac{1}{2}a_8 k_{iji}k_{kjk} + \frac{1}{2}a_{10}k_{ijk}k_{ijk} + a_{11}k_{ijk}k_{jki} \\ & + \frac{1}{2}a_{13}k_{ijk}k_{ikj} + \frac{1}{2}a_{14}k_{ijk}k_{jik} + \frac{1}{2}a_{15}k_{ijk}k_{kji} \end{aligned} \tag{2.5.3.8}$$

The constitutive equations are also reduced to:

$$\tau_{pq} = \lambda\delta_{pq}\epsilon_{ii} + 2\mu\epsilon_{pq} + g_1\delta_{pq}\gamma_{ii} + g_2\left(\gamma_{pq} + \gamma_{qp}\right) \tag{2.5.3.9}$$

$$\sigma_{pq} = g_1\delta_{pq}\epsilon_{ii} + 2g_2\epsilon_{pq} + b_1\delta_{pq}\gamma_{ii} + b_2\gamma_{pq} + b_3\gamma_{qp} \tag{2.5.3.10}$$

$$\begin{aligned} \mu_{pqr} = & a_1\left(k_{iip}\delta_{qr} + k_{rii}\delta_{pq}\right) + a_2\left(k_{iiq}\delta_{pr} + k_{iri}\delta_{pq}\right) + a_3 k_{iir}\delta_{pq} \\ & + a_4 k_{pii}\delta_{qr} + a_5\left(k_{qii}\delta_{pr} + k_{ipi}\delta_{qr}\right) + a_8 k_{iqi}\delta_{pr} + a_{10}k_{pqr} \\ & + a_{11}\left(k_{rpq} + k_{qrp}\right) + a_{13}k_{prq} + a_{14}k_{qpr} + a_{15}k_{rqp} \end{aligned} \tag{2.5.3.11}$$

Equations (2.5.3.8) – (2.5.3.11) are the simplest expressions for the potential energy density and the constitutive laws that can be generated in the context of Mindlin's general theory. Later we will see that by making some additional assumptions we can formulate three sub - theories which are much simpler compared to the general one. These sub - theories are known as the three forms of Mindlin's general theory and in all three of them equations (2.5.3.8) – (2.5.3.11) are greatly reduced.

2.6 Displacement - Strain Formulation

2.6.1 Displacement Equations of Motion

In classical elasticity we can express the equations of motion in terms of the displacements only, this form of the equations of motion is known as the Navier – Cauchy equations

and can be formulated by first substituting the kinematic equation that relate the strains with the displacements into the constitutive equations and then the latter into the stress equations of motion. In the same sense, we can formulate an equivalent set of equations in Mindlin's general theory, one for the macro – displacement u_i and another one for the micro – deformation ψ_{ij}. These equations are derived inserting (2.2.2.8), (2.2.2.9), (2.2.2.11) into (2.5.3.9) – (2.5.3.11) and then the latter into (2.4.1.13), (2.4.1.14).

$$\begin{aligned}&(\mu + 2g_2 + b_2)\frac{\partial^2 u_i}{\partial x_j \partial x_j} + (\lambda + \mu + 2g_1 + 2g_2 + b_1 + b_3)\frac{\partial^2 u_j}{\partial x_i \partial x_j} \\ &- (g_1 + b_1)\frac{\partial \psi_{ij}}{\partial x_i} - (g_2 + b_2)\frac{\partial \psi_{ji}}{\partial x_j} - (g_2 + b_3)\frac{\partial \psi_{ij}}{\partial x_j} + f_i = \rho \ddot{u}_i\end{aligned} \tag{2.6.1.1}$$

$$\begin{aligned}&(a_1 + a_5)\left(\frac{\partial^2 \psi_{kl}}{\partial x_k \partial x_l}\delta_{ij} + \frac{\partial^2 \psi_{kk}}{\partial x_i \partial x_j}\right) + (a_2 + a_{11})\left(\frac{\partial^2 \psi_{ki}}{\partial x_k \partial x_j} + \frac{\partial^2 \psi_{jl}}{\partial x_i \partial x_k}\right) \\ &+ (a_3 + a_{14})\frac{\partial^2 \psi_{kj}}{\partial x_i \partial x_k} + a_4 \frac{\partial^2 \psi_{ll}}{\partial x_k \partial x_k} + (a_8 + a_{15})\frac{\partial^2 \psi_{ik}}{\partial x_j \partial x_k} + a_{10}\frac{\partial^2 \psi_{ij}}{\partial x_k \partial x_k} \\ &+ a_{13}\frac{\partial^2 \psi_{ji}}{\partial x_k \partial x_k} + g_1 \frac{\partial u_k}{\partial x_k}\delta_{ij} + g_2\left(\frac{\partial u_j}{\partial x_i} + \frac{\partial u_i}{\partial x_j}\right) + b_1\left(\frac{\partial u_k}{\partial x_k} - \psi_{kk}\right)\delta_{ij} \\ &+ b_2\left(\frac{\partial u_j}{\partial x_i} - \psi_{ik}\right) + b_3\left(\frac{\partial u_i}{\partial x_j} - \psi_{ji}\right) + \Phi_{ij} = \frac{1}{3}\rho' d^2 \ddot{\psi}_{ij}\end{aligned} \tag{2.6.1.2}$$

2.6.2 Stress Compatibility Equations

In the same sense as in classical elasticity, the compatibility equations presented in (2.2.2.14) - (2.2.2.16) can be expressed in terms of the stresses. This approach would allow the development of a set of differential equations akin to the Beltrami-Michell compatibility equations or the Ignaczak equation of elastodynamics. However, to the authors' knowledge, this has not yet been explored within the context of Mindlin's general theory, though it has been addressed in other generalized theories. For further information, the reader is referred to [67].

3 The Three Forms of Mindlin's General Theory

3.1 Introduction

Mindlin's general theory is quite complicated both from a physical and a mathematical point of view and as result its application are limited. In order to make things simpler Mindlin proposed three simplified versions of his theory, known as form I, II and III. Even though the three forms are restricted to low frequency motions, they are much more applicable compared to the general theory, since the field equations that arise can now be solved much easier and in some cases, where the analyzed domain has a relatively simple geometry analytical solutions are obtainable (see, e.g., [68], [69], [70], [71]). The idea behind the three forms is that by setting a few kinematical constraints regarding the connection between the macro – displacement u_i and the micro – deformation ψ_{ij} the field equations can be greatly simplified. The assumptions of form I imply that the macro – gradient of the micro deformation k_{ijk} is the second gradient of displacement, as a result the potential energy density can be expressed as a function of the classical strains and the second gradient of displacement. In form II the second gradient of displacement is considered to be a linear function of the gradient of strains and thus the potential energy density is a function of the classical strains and the gradient of the strains, while in form III the potential energy density is written in terms of the infinitesimal strain tensor, the gradient of rotation and the fully symmetric part of the gradient of strain. The three forms conclude to equivalent equations of motion, however form II has a better algebraic structure, since in this case the total stress tensor is symmetric in contrast with the other two forms, which include all the problems associated with non – symmetric stress tensors as in the case of Cosserat and couple stress theories.

3.2 Form I

3.2.1 Assumptions

In the following two sections the governing equations of forms I, II and III are rederived. The concept of the three forms is to formulate a set of displacement equations of motion that are much simpler than (2.6.1.1) and (2.6.1.2). Even though in this work only form II and dipolar gradient elasticity are implemented, it is essential to present form I in detail since the equations of forms II and III are formulated based on the assumptions and the equations of form I. Thus, we begin by stating the assumptions of form I.

$$\sigma_{(ij)} = 0 \tag{3.2.1.1}$$

$$b_2 - b_3 \to \infty \tag{3.2.1.2}$$

$$\gamma_{[ij]} \to 0 \tag{3.2.1.3}$$

In view of (3.2.1.1) - (3.2.1.3) the isotropic constitutive equations of the general theory for τ_{pq} and σ_{pq} presented in (2.5.3.9) and (2.5.3.10) degenerate to:

$$\tau_{pq} = \lambda\delta_{pq}\epsilon_{ii} + 2\mu\epsilon_{pq} + g_1\delta_{pq}\gamma_{ii} + 2g_2\gamma_{pq} \tag{3.2.1.4}$$

$$\sigma_{(pq)} = g_1\delta_{pq}\epsilon_{ii} + 2g_2\epsilon_{pq} + b_1\delta_{pq}\gamma_{ii} + (b_2 + b_3)\gamma_{(pq)} \tag{3.2.1.5}$$

$$\sigma_{[pq]} = (b_2 - b_3)\gamma_{[pq]} \tag{3.2.1.6}$$

By observing (3.2.1.2) and (3.2.1.3), it is clear that $\sigma_{[pq]}$ is indeterminate in (3.2.1.6).

3.2.2 Form I Kinematics

We continue by examining the consequences of the assumptions (3.2.1.1) – (3.2.1.3) in the strain measures ϵ_{ij}, ψ_{ij}, γ_{ij} and k_{ijk}. In view of (3.2.1.1), (3.2.1.4) we obtain:

$$g_1 + \delta_{pq}\epsilon_{ii} + 2g_2\epsilon_{pq} + b_1\delta_{pq}\gamma_{ii} + (b_2 + b_3)\gamma_{(pq)} = 0 \tag{3.2.2.1}$$

Multiplying (3.2.2.1) with δ_{pq} gives:

$$g_1 + \delta_{pp}\epsilon_{ii} + 2g_2\epsilon_{pp} + b_1\delta_{pp}\gamma_{ii} + (b_2 + b_3)\gamma_{pp} = 0 \tag{3.2.2.2}$$

Since $\delta_{pp} = 3$ and by setting the repeated indices in (3.2.2.2) equal to i, we obtain:

$$\gamma_{ii} = \frac{3g_1 + 2g_2}{3b_1 + b_2 + b_3}\epsilon_{ii} \tag{3.2.2.3}$$

By substituting (3.2.2.3) into (3.2.2.1), we can express $\gamma_{(pq)}$ in terms of the components of the infinitesimal strain tensor only:

$$\gamma_{(pq)} = \alpha\delta_{pq}\epsilon_{ii} + (1-\beta)\epsilon_{pq} \tag{3.2.2.4}$$

Where the expressions of α,β are given by:

$$\alpha = \frac{1}{b_2 + b_3}\left[g_1 - \frac{b_1(3g1 + 2g_2)}{3b1 + b_2 + b3}\right] \tag{3.2.2.5}$$

$$\beta = 1 + \frac{2g_2}{b_2 + b_3} \tag{3.2.2.6}$$

Regarding k_{ijk}, we begin by decomposing ψ_{ij} in (2.2.2.16) into a symmetric and an anti – symmetric part:

$$\psi_{(pq)} = \epsilon_{pq} - \gamma_{(pq)} \tag{3.2.2.7}$$

$$\psi_{[pq]} = \omega_{pq} \tag{3.2.2.8}$$

Where for the derivation of (3.2.2.8), assumption (3.2.1.3) has been taken into account. We can also formulate an expression for $\psi_{(pq)}$ in terms of the components of the infinitesimal strain tensor only by substituting equation (3.2.2.4) into (3.2.2.7):

$$\psi_{(pq)} = \alpha\delta_{pq}\epsilon_{ii} + \beta\epsilon_{pq} \tag{3.2.2.9}$$

In view of (2.2.2.8) k_{ijk} can be expressed as:

$$k_{ijk} \equiv \frac{\partial\psi_{jk}}{\partial x_i} = \frac{\partial\psi_{(jk)}}{\partial x_i} + \frac{\partial\psi_{[jk]}}{\partial x_i} \tag{3.2.2.10}$$

Inserting (3.2.2.7), (3.2.2.8) into (3.2.2.10) gives:

$$k_{ijk} = \frac{\alpha\delta_{jk}\epsilon_{ll}}{\partial x_i} + \frac{\omega_{jk}}{\partial x_i} \tag{3.2.2.11}$$

Substituting (2.2.2.9), (2.2.2.12) into (3.2.2.11) gives:

$$k_{ijk} = \alpha \frac{\partial u_l}{\partial x_i \partial x_l} \delta_{jk} + \frac{1}{2}(1+\beta)\frac{\partial u_j}{\partial x_i \partial x_k} - \frac{1}{2}(1-\beta)\frac{\partial u_k}{\partial x_i \partial x_j} \tag{3.2.2.12}$$

The above equation can equivalently be written as:

$$\tilde{k}_{ijk} = \alpha \tilde{k}_{ill} \delta_{jk} + \frac{1}{2}(1+\beta)\tilde{k}_{ijk} - \frac{1}{2}(1-\beta)\tilde{k}_{ikj} \tag{3.2.2.13}$$

where $\tilde{k}_{ijk}$ is the second gradient of the macro – displacement vector $\mathbf{u}$.

$$\tilde{k}_{ijk} = \frac{\partial u_k}{\partial x_i \partial x_j} = \tilde{k}_{ikj} \tag{3.2.2.14}$$

3.2.3 Form I Energetics

In the previous paragraph it was shown that the assumptions of form I imply that the symmetric part of the relative deformation tensor can be expressed in terms of the components of the infinitesimal strain tensor, while the micro – deformation gradient is a function of $\tilde{k}_{ijk}$ only. This means that the kinetic energy density will now be a function of the macro velocity only, while, the part of the potential energy density that is a function of k_{ijk} in the general theory becomes a function of $\tilde{k}_{ijk}$ in form I.

In order to formulate the expression of the kinetic energy density, we begin by decomposing the micro – deformation into a symmetric and an anti – symmetric part:

$$\psi_{pq} = \psi_{(pq)} + \psi_{[pq]} \tag{3.2.3.1}$$

By substituting (3.2.2.8), (3.2.2.9) into (3.2.3.1) we obtain:

$$\psi_{pq} = \alpha \delta_{pq} \epsilon_{ll} + \beta \epsilon_{pq} + \omega_{pq} \tag{3.2.3.2}$$

Using the definitions of ϵ_{ij} and ω_{ij}, we can write the above equation as:

$$\psi_{pq} = \alpha \delta_{pq} \frac{\partial u_l}{\partial x_l} + \frac{1}{2}\beta\left(\frac{\partial u_p}{\partial x_q} + \frac{\partial u_q}{\partial x_p}\right) + \frac{1}{2}\left(\frac{\partial u_q}{\partial x_p} - \frac{\partial u_p}{\partial x_q}\right) \tag{3.2.3.3}$$

Differentiating (3.2.3.3) with respect to time gives:

$$\dot{\psi}_{pq} = \alpha\delta_{pq}\frac{\partial \dot{u}_l}{\partial x_l} + \frac{1}{2}\beta(\frac{\partial \dot{u}_p}{\partial x_q} + \frac{\partial \dot{u}_q}{\partial x_p}) + \frac{1}{2}(\frac{\partial \dot{u}_q}{\partial x_p} - \frac{\partial \dot{u}_p}{\partial x_q}) \tag{3.2.3.4}$$

The following expression is obtained by multiplying equation (3.2.3.4) with $\delta_{ip}\delta_{jq}$ and then factorizing the terms:

$$\dot{\psi}_{pq} = [\frac{1}{2}(\delta_{ik}\delta_{jl} - \delta_{il}\delta_{jk}) + \alpha\delta_{ij}\delta_{kl} + \frac{1}{2}\beta(\delta_{ik}\delta_{jl} + \delta_{il}\delta_{jk})]\frac{\partial \dot{u}_l}{\partial x_k} \tag{3.2.3.5}$$

The above expression can equivalently be written as:

$$\dot{\psi}_{pq} = h_{ijkl}\frac{\partial \dot{u}_l}{\partial x_k} \tag{3.2.3.6}$$

Where:

$$h_{ijkl} = \frac{1}{2}(\delta_{ik}\delta_{jl} - \delta_{il}\delta_{jk}) + \alpha\delta_{ij}\delta_{kl} + \frac{1}{2}\beta(\delta_{ik}\delta_{jl} + \delta_{il}\delta_{jk}) \tag{3.2.3.7}$$

By inserting (3.2.3.6), (3.2.3.7) into (2.3.1.5) we obtain the formula for the kinetic energy density function of form I.

$$\begin{aligned}\tilde{T} &= \frac{1}{2}\rho\dot{u}_j\dot{u}_j + \frac{1}{6}\rho'\tilde{d}^2_{pkmn}\frac{\partial \dot{u}_n}{\partial x_m}\frac{\partial \dot{u}_k}{\partial x_p} \\ &= \frac{1}{2}\rho\dot{u}_j\dot{u}_j + \frac{1}{6}\frac{\partial}{\partial x_p}\left[\rho'\tilde{d}^2_{pkmn}\left(\frac{\partial \dot{u}_n}{\partial x_m}\right)\dot{u}_k\right] - \frac{1}{6}\frac{\partial}{\partial x_p}\left[\rho'\tilde{d}^2_{pkmn}\left(\frac{\partial \dot{u}_n}{\partial x_m}\right)\right]\dot{u}_k\end{aligned} \tag{3.2.3.8}$$

Where:

$$\begin{aligned}\tilde{d}^2_{pkmn} &= d^2_{jl}h_{lqpk}h_{jqmn} = \tilde{d}^2_{mnpk} \\ &= \frac{1}{2}d^2[\delta_{pm}\delta_{kn} - \delta_{pn}\delta_{km} + 2\alpha(3\alpha + 2\beta)\delta_{pk}\delta_{mn} + \beta^2(\delta_{pm}\delta_{kn} + \delta_{pn}\delta_{km})]\end{aligned} \tag{3.2.3.9}$$

Regarding the potential energy density, it was explained before why in the context of form I it is a function of ϵ_{ij} and $\tilde{k}_{ijk}$ only.

$$\tilde{W} = \tilde{W}(\epsilon_{ij}, \tilde{k}_{ijk}) \tag{3.2.3.10}$$

The eighteen independent components of $\tilde{k}_{ijk}$ may be resolved, in more than one way, into tensors whose components are independent linear combinations of $\partial_i \partial_j u_k$, so that other forms of the potential energy density, for the law frequency approximation are possible. These are the so – called forms II, III of Mindlin's general theory and will be presented later in this work.

3.2.4 Form I Constitutive Equations

The expression of the potential energy density for isotropic materials in the context of form I can be obtained by inserting (3.2.1.3), (3.2.2.4), (3.2.2.12) into (2.5.3.8) and also taking (3.2.1.2) into account:

$$\tilde{W} = \frac{1}{2}\tilde{\lambda}\epsilon_{ii}\epsilon_{jj} + \tilde{\mu}\epsilon_{ij}\epsilon_{ij} + \tilde{a}_1\tilde{k}_{iik}\tilde{k}_{kjj} + \tilde{a}_2\tilde{k}_{ijj}\tilde{k}_{ikk} + \tilde{a}_3\tilde{k}_{iik}\tilde{k}_{jjk} + \tilde{a}_4\tilde{k}_{ijk}\tilde{k}_{ijk} + \tilde{a}_5\tilde{k}_{iik}\tilde{k}_{kji} \tag{3.2.4.1}$$

Where $\tilde{\lambda}$, $\tilde{\mu}$, $\tilde{a}_1 - \tilde{a}_5$ are defined as:

$$\tilde{\lambda} = \lambda + 2\mu - \frac{8g_2^2}{3(b_2+b_3)} - \frac{(3g_1+2g_2)^2}{3(3b_1+b_2+b3)} \tag{3.2.4.2}$$

$$\tilde{\mu} = \mu - \frac{2g_2^2}{b_2+b_3} \tag{3.2.4.3}$$

$$\begin{aligned}\tilde{a}_1 = \frac{1}{2}\Big[&(1+\beta)(3\alpha+\beta)a_1 + (1+2\alpha\beta+\beta^2)a_2 - \frac{1}{2}(1+\beta)(1-2\alpha-\beta)a_3 \\ &-(1-\beta)(3\alpha+\beta)a_5 - \frac{1}{2}(1-\beta)(1+2\alpha+\beta)a_6 + 2\alpha\beta a_{11} - \alpha(1-\beta)a_{14} \\ &+\alpha(1+\beta)a_{15}\Big]\end{aligned} \tag{3.2.4.4}$$

$$\begin{aligned}\tilde{a}_1 = \frac{1}{2}\Big\{&-(1-2\alpha-\beta)(3\alpha+\beta)a_1 - \frac{1}{2}[1-(2\alpha+\beta)^2]a_2 - \frac{1}{4}(1-2\alpha-\beta)^2 a_3 \\ &+ (3\alpha+\beta)^2 a_4 + (3\alpha+\beta)(1+2\alpha+\beta)a_5 + \frac{1}{4}(1+2\alpha+\beta)^2 a_8 + \alpha(3\alpha+2\beta)a_{10} \\ &+ 2\alpha(\alpha+\beta)a_{11} - \alpha(3\alpha+2\beta)a_{13} + \alpha(1+\alpha+\beta)a_{14} - \alpha(1-\alpha-\beta)a_{15}\Big\}\end{aligned} \tag{3.2.4.5}$$

$$\tilde{a}_3 = \frac{1}{4}\left[-(1-\beta)^2 a_2 + \frac{1}{2}(1+\beta)^2 a_3 + \frac{1}{2}(1-\beta)^2 a_8\right] \tag{3.2.4.6}$$

$$\tilde{a}_4 = \frac{1}{4}\left[(1+\beta)^2 a_{10} - (1-\beta)^2(a_{11}+a_{13}) + \frac{1}{2}(1+\beta)^2 a_{14} + \frac{1}{2}(1-\beta)^2 a_{15}\right] \tag{3.2.4.7}$$

$$\begin{aligned}\tilde{a}_5 = \frac{1}{4}\Bigg[&-(1-\beta)^2 a_{10} + (1+3\beta^2)a_{11} + (1+\beta^2)a_{13} - \frac{1}{2}(1+2\beta-3\beta^2)a_{14} \\ &-\frac{1}{2}(1-2\beta-3\beta^2)a_{15}\Bigg]\end{aligned} \tag{3.2.4.8}$$

The stress tensors are defined as:

$$\tilde{\tau}_{ij} \equiv \frac{\partial \tilde{W}}{\partial \epsilon_{ij}} = \tilde{\tau}_{ji} \tag{3.2.4.9}$$

$$\tilde{\mu}_{ijk} \equiv \frac{\partial \tilde{W}}{\partial k_{ijk}} = \tilde{\mu}_{jik} \tag{3.2.4.10}$$

Using (3.2.4.1), (3.2.4.9), (3.2.4.10) the following two constitutive equations are obtained:

$$\tilde{\tau}_{pq} = \tilde{\lambda}\delta_{pq}\epsilon_{ii} + 2\tilde{\mu}\epsilon_{pq} \tag{3.2.4.11}$$

$$\begin{aligned}\tilde{\mu}_{pqr} = &\frac{1}{2}\tilde{a}_1(\tilde{k}_{iip}\delta_{qr}2\tilde{k}_{rii}\delta_{pq}\tilde{k}_{iiq}\delta_{pr}) + \tilde{a}_2(\tilde{k}_{pii}\delta_{qr} + \tilde{k}_{qii}\delta_{pr}) \\ &+ 2\tilde{a}_3\tilde{k}_{iir}\delta_{pq} + 2\tilde{a}_4\tilde{k}_{pqr} + \tilde{a}_5(\tilde{k}_{rqp} + \tilde{k}_{rpq})\end{aligned} \tag{3.2.4.12}$$

3.2.5 Form I Field Equations

The equations of motion and boundary conditions will be formulated using Hamilton's principle as in the case of the general theory. However, from (3.2.3.3) and (3.2.3.4) it is clear that the fields u_i and ψ_{ij} are now coupled, meaning that Hamilton's principle will be expressed with one independent variation, which is chosen to be δu_i.

In view of (3.2.3.8), the total kinetic energy term in Hamilton's principle is:

$$\begin{aligned}\tilde{\mathscr{J}} &= \int_{\mathbb{B}_0} \tilde{T}\, dV \\ &= \int_{\mathbb{B}_0} \left\{\frac{1}{2}\rho\dot{u}_j\dot{u}_j + \frac{1}{6}\frac{\partial}{\partial x_p}\left[\rho' \tilde{d}^2_{pkmn}\left(\frac{\partial \dot{u}_n}{\partial x_m}\right)\dot{u}_k\right] - \frac{1}{6}\frac{\partial}{\partial x_p}\left[\rho' \tilde{d}^2_{pkmn}\left(\frac{\partial \dot{u}_n}{\partial x_m}\right)\right]\dot{u}_k\right\} dV\end{aligned} \tag{3.2.5.1}$$

Applying the divergence theorem in (3.2.5.1) yields:

$$\begin{aligned}\tilde{\mathscr{J}} = &\int_{\mathbb{B}_0} \left\{ \frac{1}{2}\rho \dot{u}_j \dot{u}_j - \frac{1}{6}\frac{\partial}{\partial x_p}\left[\rho' \tilde{d}^2_{pkmn} \left(\frac{\partial \dot{u}_n}{\partial x_m} \right) \right] \dot{u}_k \right\} dV \\ &+ \int_{\partial\mathbb{B}_0} \frac{1}{6} n_p \rho' \tilde{d}^2_{pkmn} \left(\frac{\partial \dot{u}_n}{\partial x_m} \right) \dot{u}_k \, dS\end{aligned} \tag{3.2.5.2}$$

The variation of the kinetic energy term in Hamilton's principle is:

$$\begin{aligned}\int_{t_1}^{t_2} \delta \tilde{\mathscr{J}} \, dt = &\int_{t_1}^{t_2} \delta \int_{\mathbb{B}_0} \left\{ \frac{1}{2}\rho \dot{u}_j \dot{u}_j - \frac{1}{6}\frac{\partial}{\partial x_p}\left[\rho' \tilde{d}^2_{pkmn} \left(\frac{\partial \dot{u}_n}{\partial x_m} \right) \right] \dot{u}_k \right\} dV \, dt \\ &+ \int_{t_1}^{t_2} \delta \int_{\partial\mathbb{B}_0} \frac{1}{6} n_p \rho' \tilde{d}^2_{pkmn} \left(\frac{\partial \dot{u}_n}{\partial x_m} \right) \dot{u}_k \, dS \, dt\end{aligned} \tag{3.2.5.3}$$

By executing the variations in (3.2.5.3) and then performing integration by parts with respect to time we obtain:

$$\begin{aligned}\int_{t_1}^{t_2} \delta \tilde{\mathscr{J}} \, dt = &- \int_{t_1}^{t_2} \int_{\mathbb{B}_0} \left[\frac{1}{2}\rho \ddot{u}_k - \frac{1}{3}\frac{\partial}{\partial x_p}\left(\rho' \tilde{d}^2_{pkmn} \frac{\partial \dot{u}_n}{\partial x_m} \right) \right] \delta u_k \, dV \, dt \\ &- \int_{t_1}^{t_2} \delta \int_{\partial\mathbb{B}_0} \frac{1}{3} n_p \rho' n_p \tilde{d}^2_{pkmn} \left(D_m \ddot{u}_n + n_m D \ddot{u}_n \right) \delta u_k \, dS \, dt\end{aligned} \tag{3.2.5.4}$$

Where D_m is the surface gradient operator and D is the normal gradient operator, which are defined as:

$$D_m \equiv (\delta_{ml} - n_m n_l)\frac{\partial}{\partial x_l} \tag{3.2.5.5}$$

$$D \equiv n_l \frac{\partial}{\partial x_l} \tag{3.2.5.6}$$

In view of (3.2.3.10), (3.2.4.9), (3.2.4.10) we can write the variation of the potential energy in the form of:

$$\delta \tilde{W} = \tilde{\tau}_{ij} \delta \epsilon_{ij} + \tilde{\mu}_{ijk} \delta \tilde{k}_{ijk} \tag{3.2.5.7}$$

Using the definitions of ϵ_{ij}, $\tilde{k}_{ijk}$, (3.2.5.7) can be written as:

$$\delta\tilde{W} = \tilde{\tau}_{ij}\frac{\partial\delta u_j}{\partial x_i} + \tilde{\mu}_{ijk}\frac{\partial\delta u_k}{\partial x_i\partial x_j} \tag{3.2.5.8}$$

The variation of the potential energy term in Hamilton's principle is:

$$\begin{aligned}\int_{t_1}^{t_2}\delta\tilde{\mathscr{W}}\,dt &= \int_{t_1}^{t_2}\delta\int_{\mathbb{B}_0}\tilde{W}\,dV\,dt = \int_{t_1}^{t_2}\int_{\mathbb{B}_0}\left(\tilde{\tau}_{ij}\frac{\partial\delta u_j}{\partial x_i} + \tilde{\mu}_{ijk}\frac{\partial\delta u_k}{\partial x_i\partial x_j}\right)dV\,dt \\ &= \int_{t_1}^{t_2}\int_{\mathbb{B}_0}\left\{\frac{\partial}{\partial x_j}\left[\left(\tilde{\tau}_{ij} - \frac{\partial\tilde{\mu}_{ijk}}{\partial x_i}\right)\delta u_k\right] - \frac{\partial}{\partial x_j}\left(\tilde{\tau}_{jk} - \frac{\partial\tilde{\mu}_{ijk}}{\partial x_i}\right)\delta u_k\right. \\ &\quad \left. + \frac{\partial}{\partial x_i}\left(\tilde{\mu}_{ijk}\frac{\partial\delta u_k}{\partial x_j}\right)\right\}dV\,dt\end{aligned} \tag{3.2.5.9}$$

Applying the divergence theorem in (3.2.5.9) yields:

$$\begin{aligned}\int_{t_1}^{t_2}\delta\tilde{\mathscr{W}}\,dt &= \int_{t_1}^{t_2}\int_{\partial\mathbb{B}_0}\left(\tilde{\tau}_{ij} - \frac{\partial\tilde{\mu}_{ijk}}{\partial x_i}\right)n_j\delta u_k\,dS\,dt \\ &\quad - \int_{t_1}^{t_2}\int_{\mathbb{B}_0}\frac{\partial}{\partial x_j}\left(\tilde{\tau}_{jk} - \frac{\tilde{\mu}_{ijk}}{\partial x_i}\right)\delta u_k\,dV\,dt + \int_{t_1}^{t_2}\int_{\partial\mathbb{B}_0}\tilde{\mu}_{ijk}n_i\frac{\partial\delta u_k}{\partial x_j},dS\,dt\end{aligned} \tag{3.2.5.10}$$

In the last integral of (3.2.5.10), only the normal component of the variation $\partial\delta u_k/\partial x_j$ is independent of δu_j on S. Having this in mind, we decompose the term inside the integral as:

$$\tilde{\mu}_{ijk}n_i\frac{\partial\delta u_k}{\partial x_j} = \tilde{\mu}_{ijk}n_iD_j\delta u_k + \tilde{\mu}_{ijk}n_in_jD\delta u_k \tag{3.2.5.11}$$

Following Toupin [12], we express the first term on the right – hand side of (3.2.5.11), which contains the non – independent variation $D_j\delta u_k$, in the form of:

$$\tilde{\mu}_{ijk}n_iD_j\delta u_k = D_j(\tilde{\mu}_{ijk}n_i\delta u_k) - n_iD_j\tilde{\mu}_{ijk}\delta u_k - (D_jn_i)\tilde{\mu}_{ijk}\delta u_k \tag{3.2.5.12}$$

The last two terms in (3.2.5.12) contain the independent variation δu_k, the preceding term, on the surface $\partial\mathbb{B}_0$ can be written as:

$$D_j(\tilde{\mu}_{ijk}n_i\delta u_k) = (D_l n_l)n_j n_i\tilde{\mu}_{ijk}\delta u_k + e_{pqm}n_q\frac{\partial}{\partial x_p}(e_{mlj}n_l n_i\tilde{\mu}_{ijk}\delta u_k) \tag{3.2.5.13}$$

Equation (3.2.5.11) can be expressed with the help of (3.2.5.12), (3.2.5.13) as:

$$\begin{aligned}\tilde{\mu}_{ijk}n_i\frac{\partial\delta u_k}{\partial x_j} = {} & (D_l n_l)n_j n_i\tilde{\mu}_{ijk}\delta u_k + e_{pqm}n_q\frac{\partial}{\partial x_p}(e_{mlj}n_l n_i\tilde{\mu}_{ijk}\delta u_k) \\ & - n_i D_j\tilde{\mu}_{ijk}\delta u_k - (D_j n_i)\tilde{\mu}_{ijk}\delta u_k + \tilde{\mu}_{ijk}n_i n_j D\delta u_k\end{aligned} \tag{3.2.5.14}$$

While the term inside the first surface integral in (3.2.5.10) can be written as:

$$\left(\tilde{\tau}_{ij} - \frac{\tilde{\mu}_{ijk}}{\partial x_i}\right)n_j\delta u_k = \tilde{\tau}_{ij}n_j\delta u_k - n_j D_i\tilde{\mu}_{ijk} - n_i n_j D\tilde{\mu}_{ijk} \tag{3.2.5.15}$$

The following result arises by inserting (3.2.5.14), (3.2.5.15) into (3.2.5.10) and then performing a bit of algebra:

$$\begin{aligned}\int_{t_1}^{t_2}\delta\tilde{\mathscr{W}}\,dt = {} & -\int_{t_1}^{t_2}\int_{\mathbb{B}_0}\frac{\partial}{\partial x_j}\left(\tilde{\tau}_{ij} - \frac{\partial\tilde{\mu}_{ijk}}{\partial x_i}\right)\delta u_k\,dV\,dt \\ & + \int_{t_1}^{t_2}\int_{\partial\mathbb{B}_0}\left[n_j\tilde{\tau}_{jk} - n_i n_j D\tilde{\mu}_{ijk} - 2n_j D_i\tilde{\mu}_{ijk} + (n_i n_j D_l n_l - D_j n_i)\,\tilde{\mu}_{ijk}\right]\delta u_k\,dS\,dt \\ & + \int_{t_1}^{t_2}\int_{\partial\mathbb{B}_0} n_i n_j\tilde{\mu}_{ijk}D\delta u_k\,dS\,dt \\ & + \int_{t_1}^{t_2}\int_{\partial\mathbb{B}_0} e_{pqm}n_q\frac{\partial}{\partial x_p}\left(\epsilon_{mlj}n_l n_i\tilde{\mu}_{ijk}\delta u_k\right)\,dS\,dt\end{aligned} \tag{3.2.5.16}$$

In order to factorize the variation δu_k in the final integral of the above expression, we invoke Stoke's theorem:

Theorem 3.2.5.1 (Stoke's Theorem)

Let Λ be a regular surface bounded by a closed curve Γ and let $\mathbf{v}$ be a vector field whose components have continuous partials derivatives on a region that contains Λ. Then:

$$\int_{\Lambda} \epsilon_{ijk} \frac{\partial v_k}{\partial x_j}\, dS = \oint_{\Gamma} v_i n_i\, ds$$

Where Γ is positive oriented with respect to the unit vector $\mathbf{n}$, normal to Λ.

If the surface $\partial\mathbb{B}_0$ has an edge C, formed by the intersection of two parts $\partial\mathbb{B}_1$ and $\partial\mathbb{B}_2$ of $\partial\mathbb{B}_0$, then applying Stoke's theorem in the final (inner) integral of (3.2.5.16) yields:

$$\int_{t_1}^{t_2} \int_{\partial\mathbb{B}_0} e_{pqm} n_q \frac{\partial}{\partial x_p} \left(\epsilon_{mlj} n_l n_i \tilde{\mu}_{ijk} \delta u_k\right)\, dS\, dt = \oint_C \left[\left[n_i m_j \tilde{\mu}_{ijk}\right]\right] \delta u_k\, ds \tag{3.2.5.17}$$

Where $m_j = \epsilon_{mlj} s_m n_l$ is a vector being tangential to the corner, s_m are the components of the unit vector tangent to C and the double brackets $[[\star]]$ indicate that the enclosed quantity is the difference between its values taken at the two sides of the corner line.

Finally, by substituting (3.2.5.17) into (3.2.5.16) we obtain the following expression for the variation of the total potential energy density:

$$\begin{aligned}
\int_{t_1}^{t_2} \delta\tilde{\mathscr{W}}\, dt = &- \int_{t_1}^{t_2} \int_{\mathbb{B}_0} \frac{\partial}{\partial x_j} \left(\tilde{\tau}_{ij} - \frac{\partial \tilde{\mu}_{ijk}}{\partial x_i}\right) \delta u_k\, dV\, dt \\
&+ \int_{t_1}^{t_2} \int_{\partial\mathbb{B}_0} \left[n_j \tilde{\tau}_{jk} - n_i n_j D\tilde{\mu}_{ijk} - 2 n_j D_i \tilde{\mu}_{ijk} + \left(n_i n_j D_l n_l - D_j n_i\right) \tilde{\mu}_{ijk}\right] \delta u_k\, dS\, dt \\
&+ \int_{t_1}^{t_2} \int_{\partial\mathbb{B}_0} n_i n_j \tilde{\mu}_{ijk} D\delta u_k\, dS\, dt + \oint_C \left[\left[n_i m_j \tilde{\mu}_{ijk}\right]\right] \delta u_k\, ds
\end{aligned} \tag{3.2.5.18}$$

The above expression of the variation of the total potential energy density suggests that the work of the external forces has to be in the form:

$$W_{ext} = \int_{\mathbb{B}_0} F_k u_k\, dV + \int_{\partial\mathbb{B}_0} \tilde{P}_k u_k\, dS + \int_{\partial\mathbb{B}_0} \tilde{R}_k D u_k\, dS + \oint_C \tilde{E}_k u_k\, ds \tag{3.2.5.19}$$

Where F_k is the body force per unit volume, while $\tilde{P}_k$, $\tilde{R}_k$ and $\tilde{E}_k$ represent surface forces per unit are and their interpretation will be given later:

The variation of the work of the external forces is:

$$\delta W_{ext} = \int_{\mathbb{B}_0} F_k \delta u_k \, dV + \int_{\partial\mathbb{B}_0} \tilde{P}_k \delta u_k \, dS + \int_{\partial\mathbb{B}_0} \tilde{R}_k D\delta u_k \, dS + \oint_C \tilde{E}_k \delta u_k \, ds \tag{3.2.5.20}$$

The equations of motion and boundary conditions of form I of Mindlin's general theory are obtained by substituting equations (3.2.5.4), (3.2.5.18), (3.2.5.20) into Hamilton's principle and performing afterwards a few operations:

$$\frac{\partial}{\partial x_j}\left(\tilde{\tau}_{ij} - \frac{\partial \tilde{\mu}_{ijk}}{\partial x_i}\right) + F_k = \rho \ddot{u}_k - \frac{1}{3}\frac{\partial}{\partial x_j}\left(\rho' \tilde{d}^2_{pkmn} \frac{\ddot{u}_n}{\partial x_m}\right) \tag{3.2.5.21}$$

$$\begin{aligned}\tilde{P}_k = {} & n_j \tilde{\tau}_{jk} - n_i n_j D\tilde{\mu}_{ijk} - 2n_j D_i \tilde{\mu_{ijk}} + (n_i n_j D_l n_l - D_j n_i)\,\tilde{\mu}_{ijk} \\ & + \frac{1}{3}\rho' n_p \tilde{d}^2_{pkmn}\,(D_m \ddot{u}_n + n_m \ddot{u}_n)\end{aligned} \tag{3.2.5.22}$$

$$\tilde{R}_k = n_i n_j \tilde{\mu}_{ijk} \tag{3.2.5.23}$$

$$\tilde{E}_k = [[n_i m_j \tilde{\mu}_{ijk}]] \tag{3.2.5.24}$$

Taking into consideration equations (3.2.5.19), (3.2.5.22) – (3.2.5.24) it appears that an appropriate terminology for the three traction vectors of form I is: Traction vector for $\tilde{P}_k$, double traction vector for $\tilde{R}_k$ and jump traction vector for $\tilde{E}_k$.

The displacement equations of motion can be obtained by inserting (2.2.2.9), (3.2.2.4) into (3.2.4.11), (3.2.4.12) and then substituting the later into (3.2.5.21):

$$\begin{aligned}&(\tilde{\lambda} + 2\tilde{\mu})(1 - \tilde{l}_1^2 \nabla^2)\nabla\nabla \cdot \mathbf{u} - \tilde{\mu}(1 - \tilde{l}_2^2 \nabla^2)\nabla \times \nabla \times \mathbf{u} + \mathbf{F} \\ &= \rho(\ddot{\mathbf{u}} - h_1^2 \nabla\nabla \cdot \ddot{\mathbf{u}} + h_2^2 \nabla \times \nabla \times \ddot{\mathbf{u}})\end{aligned} \tag{3.2.5.25}$$

Where the expressions of $\tilde{l}_i^2$, h_i^2 are given by:

$$\tilde{l}_1^2 = \frac{2(\tilde{a}_1 + \tilde{a}_2 + \tilde{a}_3 + \tilde{a}_4 + \tilde{a}_5)}{\tilde{\lambda} + 2\tilde{\mu}} \tag{3.2.5.26}$$

$$\tilde{l}_2^2 = \frac{2(\tilde{a}_3 + \tilde{a}_4)}{\tilde{\mu}} \tag{3.2.5.27}$$

$$h_1^2 = \frac{\rho' d^2 [2\alpha^2 + (\alpha + \beta)^2]}{3\rho} \tag{3.2.5.28}$$

$$h_1^2 = \frac{\rho' d^2 (1+\beta^2)}{6\rho} \tag{3.2.5.29}$$

The positive definiteness of W requires $\tilde{\mu} > 0$, $\tilde{\lambda} + 2\tilde{\mu} > 0$, $\tilde{l}_i^2 > 0$. It is also reasonable to assume that $h_i^2 > 0$. This can be justified since h_i is related to the length of the edges of the material's cell which is an observable quantity through (3.2.5.28), (3.2.5.29). Generally, $\tilde{l}_i^2 > 0$ and $h_i^2 > 0$ are treated as positive quantities that express length properties of the material and are known in the literature as the gradient coefficients $(\tilde{\lambda}_1, \tilde{\lambda}_2)$ and the characteristic lengths of the material (h_1, h_2). These intrinsic parameters have units of length square and represent the effect of the stiffness $\tilde{\lambda}_1^2, \tilde{\lambda}_2^2$ and the inertia h_1^2, h_2^2 of the microstructure on the macrostructural response of the gradient elastic material [18]. It will also be shown latter that $\tilde{\lambda}_1^2$, h_1^2 are related to longitudinal deformations, while $\tilde{\lambda}_2^2$, h_2^2 to shear ones.

3.3 Forms II, III

3.3.1 The Equations of Form II

It was mentioned earlier that the eighteen independent components of $\tilde{k}_{ijk}$ may be resolved, in more than one way, into tensors whose components are independent linear combinations of $\partial_i \partial_j u_k$. One such, indicated by Toupin [12] is the gradient of the infinitesimal strain tensor:

$$\hat{k}_{ijk} \equiv \frac{\partial \epsilon_{jk}}{\partial x_i} = \frac{1}{2}\left(\frac{\partial u_k}{\partial x_i \partial x_j} + \frac{\partial u_j}{\partial x_i \partial x_k}\right) \tag{3.3.1.1}$$

The gradient of the strain is assumed to be related with $\tilde{k}_{ijk}$ as:

$$\tilde{k}_{ijk} = \hat{k}_{ijk} + \hat{k}_{jki} - \hat{k}_{kij} \tag{3.3.1.2}$$

The expression of the potential energy density function of form II is obtained by substituting (3.3.1.2) into (3.2.4.1):

$$\hat{W} = \frac{1}{2}\tilde{\lambda}\epsilon_{ii}\epsilon_{jj} + \tilde{\mu}\epsilon_{ij}\epsilon_{ij} + \hat{a}_1 \hat{k}_{iik}\hat{k}_{kjj} + \hat{a}_2 \hat{k}_{ijj}\hat{k}_{ikk} + \hat{a}_3 \hat{k}_{iik}\hat{k}_{jjk} + \hat{a}_4 \hat{k}_{ijk}\hat{k}_{ijk} + \hat{a}_5 \hat{k}_{iik}\hat{k}_{kji} \tag{3.3.1.3}$$

Where the constants $\hat{a}_1 - \hat{a}_5$ are given by:

$$\begin{aligned} &\hat{a}_1 = 2\tilde{a}_1 - 4\tilde{a}_3, \quad \hat{a}_2 = -\tilde{a}_1 + \tilde{a}_2 + \tilde{a}_3 \\ &\hat{a}_3 = 4\tilde{a}_3, \quad \hat{a}_4 = 3\tilde{a}_4 - \tilde{a}_5, \quad \hat{a}_5 = -2\tilde{a}_4 + 2\tilde{a}_5 \end{aligned} \tag{3.3.1.4}$$

The stress tensors of form II are defined as:

$$\hat{\tau}_{ij} \equiv \frac{\partial \hat{W}}{\partial \epsilon_{ij}} = \hat{\tau}_{ji} \tag{3.3.1.5}$$

$$\hat{\mu}_{ijk} \equiv \frac{\partial \hat{W}}{\partial \hat{k}_{ijk}} = \hat{\mu}_{ikj} \tag{3.3.1.6}$$

While the constitutive equations are:

$$\hat{\tau}_{pq} = \tilde{\lambda}\delta_{pq}\epsilon_{ii} + 2\tilde{\mu}\epsilon_{pq} \tag{3.3.1.7}$$

$$\begin{aligned} \hat{\mu}_{pqr} = &\frac{1}{2}\hat{a}_1(\hat{k}_{rii}\delta_{pq} + 2\hat{k}_{iip}\delta_{qr} + \hat{k}_{qii}\delta_{rp}) + 2\hat{a}_2\hat{k}_{pii}\delta_{qr} + 2\hat{a}_3(\hat{k}_{iir}\delta_{pq} + \hat{k}_{iiq}\delta_{pr}) \\ &+ 2\hat{a}_4\hat{k}_{pqr} + \hat{a}_5(\hat{k}_{rpq} + \hat{k}_{qrp}) \end{aligned} \tag{3.3.1.8}$$

In view of (3.3.1.3), (3.3.1.5), (3.3.1.6) we can write the variation of the potential energy in the form of:

$$\delta\hat{\mathscr{W}} = \hat{\tau}_{ij}\delta\epsilon_{ij} + \hat{\mu}_{ijk}\delta\hat{k}_{ijk} \tag{3.3.1.9}$$

Using the definitions of ϵ_{ij}, $\hat{k}_{ijk}$, (3.3.1.9) can be written as:

$$\begin{aligned} \delta\hat{\mathscr{W}} &= \hat{\tau}_{ij}\frac{\partial \delta u_j}{\partial x_i} + \hat{\mu}_{ijk}\frac{\partial \delta u_k}{\partial x_i x_j} \\ &= \frac{\partial}{\partial x_j}\left[\left(\hat{\tau}_{ij} - \frac{\partial \hat{\mu}_{ijk}}{\partial x_i}\right)\delta u_k\right] + \frac{\partial}{\partial x_j}\left(\hat{\tau}_{ij} - \frac{\partial \hat{\mu}_{ijk}}{\partial x_i}\right)\delta u_k + \frac{\partial}{\partial x_i}\left(\hat{\mu}_{ijk}\frac{\partial \delta u_k}{\partial x_j}\right) \end{aligned} \tag{3.3.1.10}$$

The equations of motion and boundary conditions can once again be formulated using Hamilton's principle. The procedure will not be shown analytically this time due to the fact that the expression of the kinetic energy is unchanged compared to form I, while equation (3.3.1.10) has the same form as (3.2.5.8), which implies that that the expression of the work of the external forces in both sub – theories is also identical. Having the aforementioned in

mind we come to the conclusion that in form II the boundary conditions and the equations of motion are the same as in form I with the only difference being that $\tilde{\tau}_{ij}$ and $\tilde{\mu}_{ijk}$ are replaced by $\hat{\tau}_{ij}$ and $\hat{\mu}_{ijk}$ respectively:

$$\frac{\partial}{\partial x_j}\left(\hat{\tau}_{ij}-\frac{\partial \hat{\mu}_{ijk}}{\partial x_i}\right)+F_k=\rho\ddot{u}_k-\frac{1}{3}\frac{\partial}{\partial x_j}\left(\rho' \tilde{d}^2_{pkmn}\frac{\ddot{u}_n}{\partial x_m}\right) \tag{3.3.1.11}$$

$$\begin{aligned}\hat{P}_k=&\, n_j\hat{\tau}_{jk}-n_in_jD\hat{\mu}_{ijk}-2n_jD_i\hat{\mu}_{ijk}+\left(n_in_jD_ln_l-D_jn_i\right)\hat{\mu}_{ijk}\\&+\frac{1}{3}\rho' n_p\tilde{d}^2_{pkmn}\left(D_m\ddot{u}_n+n_m\ddot{u}_n\right)\end{aligned} \tag{3.3.1.12}$$

$$\hat{R}_k=n_in_j\hat{\mu}_{ijk} \tag{3.3.1.13}$$

$$\hat{E}_k=[[n_im_j\hat{\mu}_{ijk}]] \tag{3.3.1.14}$$

At this point the major advantage of form II over the other two forms of Mindlin's general theory can be illustrated. It was mentioned before and it will be shown latter that the three forms conclude to identical equations of motion. However, the fact that $\tilde{\mu}_{ijk}=\tilde{\mu}_{jik}$, whereas $\hat{\mu}_{ijk}=\hat{\mu}_{ikj}$ implies that the quantity inside the parenthesis on the left – hand side of (3.2.5.21), (i.e. the total stress tensor) is not symmetric, but the corresponding quantity in (3.3.1.11) is symmetric as in the case of classical elasticity, thus avoiding problems associated with non – symmetric stress tensors introduced by Cosserat and couple stress theories.

The displacement equations of motion can be obtained by inserting (3.3.1.1), (2.2.2.9) into (3.3.1.7), (3.3.1.8) and then substituting the later into (3.3.1.11):

$$\begin{aligned}&(\tilde{\lambda}+2\tilde{\mu})(1-\hat{l}_1^2\nabla^2)\nabla\nabla\cdot\mathbf{u}-\tilde{\mu}(1-\hat{l}_2^2\nabla^2)\nabla\times\nabla\times\mathbf{u}+\mathbf{F}\\&=\rho(\ddot{\mathbf{u}}-h_1^2\nabla\nabla\cdot\ddot{\mathbf{u}}+h_2^2\nabla\times\nabla\times\ddot{\mathbf{u}})\end{aligned} \tag{3.3.1.15}$$

Where:

$$\hat{l}_1^2=\frac{2(\hat{a}_1+\hat{a}_2+\hat{a}_3+\hat{a}_4+\hat{a}_5)}{\tilde{\lambda}+2\tilde{\mu}} \tag{3.3.1.16}$$

$$\hat{l}_2^2=\frac{\hat{a}_3+2\hat{a}_4+\hat{a}_5}{2\tilde{\mu}} \tag{3.3.1.17}$$

From (3.2.5.26), (3.2.5.27), (3.2.5.4) we observe that $\hat{l}_i^2=\tilde{l}_i^2$, which means that the displacement equations of motion (3.2.5.25) and (3.3.1.15) of form I and II respectively are identical.

3.3.2 The Equations of Form III

In form III the potential energy density is a function of the infinitesimal strain tensor, the gradient of rotation and the fully symmetric part of the gradient of strain. Even though in this work form III is not implemented the governing equations are presented briefly for the shake of completeness. We begin by defining the curl of the strain:

$$\bar{k}_{ij} \equiv e_{jlm}\frac{\partial \epsilon_{mi}}{\partial x_l} \tag{3.3.2.1}$$

By substituting (2.2.2.9) into (3.3.2.1) we can also express the curl of the strain as:

$$\bar{k}_{ij} = \frac{1}{2}e_{jlm}\frac{\partial^2 u_m}{\partial x_i \partial x_l} \tag{3.3.2.2}$$

From the last two equations it is clear that $\bar{k}_{ij}$ is the part of $\partial x_i \partial x_j \partial u_k$ that generates couple - stresses. Also, $\bar{k}_{ii} = 0$, which means that $\bar{k}_{ij}$ has only eight independent components. In his original work Mindlin defined the fully symmetric part of the gradient of strain as:

$$\bar{\bar{k}}_{ijk} = \hat{k}_{ijk} + \frac{1}{3}e_{ilj}\bar{k}_{kl} + \frac{1}{3}e_{ilk}\bar{k}_{jl} \tag{3.3.2.3}$$

Alternatively, $\bar{\bar{k}}_{ijk}$ can be expressed in terms of the displacement vector only be substituting (3.3.1.1), (3.3.2.2) into (3.3.2.3):

$$\bar{\bar{k}}_{ijk} = \frac{1}{3}\left(\frac{\partial^2 u_k}{\partial x_i \partial x_j} + \frac{\partial^2 u_j}{\partial x_k \partial x_i} + \frac{\partial^2 u_i}{\partial x_j \partial x_k}\right) \tag{3.3.2.4}$$

The potential energy expression of form III can be obtained by solving (3.3.2.4) with respect to $\hat{k}_{ijk}$ and substituting the latter into (3.3.1.3):

$$\bar{W} = \frac{1}{2}\tilde{\lambda}\epsilon_{ii}\epsilon_{jj} + \mu\epsilon_{ij}\epsilon_{ij} + 2\bar{d}_1\bar{k}_{ij}\bar{k}_{ij} + 2\bar{d}_1\bar{k}_{ij}\bar{k}_{ji} + \frac{3}{2}\bar{a}_1\bar{\bar{k}}_{iij}\bar{\bar{k}}_{kkj} + \bar{a}_2\bar{\bar{k}}_{ijk}\bar{\bar{k}}_{ijk} + \bar{f}e_{ijk}\bar{k}_{ij}\bar{\bar{k}}_{kll} \tag{3.3.2.5}$$

Where the constants $\bar{a}_1$, $\bar{a}_2$, $\bar{d}_1$, $\bar{d}_2$, $\bar{f}$ given by:

$$\begin{aligned} 18\bar{d}_1 &= -2\hat{a}_1 + 4\hat{a}_2 + \hat{a}_3 + 6\hat{a}_4 - 3\hat{a}_5, \quad 18\bar{d}_2 = 2\hat{a}_1 - 4\hat{a}_2 - \hat{a}_3 \\ 3\bar{a}_1 &= 2(\hat{a}_1 + \hat{a}_2 + \hat{a}_3), \quad \bar{a}_1 = \hat{a}_4 + \hat{a}_5, \quad 3\bar{f} = \hat{a}_1 + 4\hat{a}_2 - 2\hat{a}_3 \end{aligned} \tag{3.3.2.6}$$

The stress tensors of form III are defined as:

$$\bar{\tau}_{ij} \equiv \frac{\partial \bar{W}}{\partial \epsilon_{ij}} = \bar{\tau}_{ji} \tag{3.3.2.7}$$

$$\bar{\mu}_{ij} \equiv \frac{\partial \bar{W}}{\partial \bar{k}_{ij}}, \quad \bar{\mu}_{ii} = 0 \tag{3.3.2.8}$$

$$\bar{\bar{\mu}}_{ijk} \equiv \frac{\partial \bar{W}}{\partial \bar{\bar{k}}_{ijk}} = \bar{\bar{\mu}}_{kij} = \bar{\bar{\mu}}_{jki} = \bar{\bar{\mu}}_{jik} \tag{3.3.2.9}$$

Where $\bar{\mu}_{ij}$ is the couple - stress deviator. The constitutive equations that arise are:

$$\bar{\tau}_{pq} = \tilde{\lambda}\delta_{pq}\epsilon_{ii} + 2\tilde{\mu}\epsilon_{pq} \tag{3.3.2.10}$$

$$\bar{\mu}_{pq} = 4\bar{d}_1\bar{k}_{pq} + 4\bar{d}_2\bar{k}_{qp} + \bar{f}e_{pqi}\bar{\bar{k}}_{ijj} \tag{3.3.2.11}$$

$$\bar{\bar{\mu}}_{pqr} = \bar{a}_1\left(\bar{\bar{k}}_{iir}\delta_{pq} + \bar{\bar{k}}_{iip}\delta_{qr} + \bar{\bar{k}}_{iiq}\delta_{rp}\right) + 2\bar{a}_2\bar{\bar{k}}_{pqr} + \frac{1}{3}\bar{f}\bar{k}_{ij}\left(\delta_{pq}e_{ijr} + \delta_{qr}e_{ijp} + \delta_{rp}e_{ijq}\right) \tag{3.3.2.12}$$

In view of (3.3.2.5), (3.3.2.7) - (3.3.2.9) we can write the variation of the potential energy in the form of:

$$\delta\bar{W} = \bar{\tau}_{ij}\delta\epsilon_{ij} + \bar{\mu}_{ij}\delta\bar{k}_{ij} + \bar{\bar{\mu}}_{ijk}\delta\bar{\bar{k}}_{ijk} \tag{3.3.2.13}$$

Using the definitions of ϵ_{ij}, $\bar{k}_{ij}$, $\bar{k}_{ijk}$, (3.3.2.13) can be written as:

$$\delta\bar{W} = \frac{\partial}{\partial x_j}\left[\left(\bar{\tau}_{jk} - \frac{\partial\bar{\mu}^*_{ijk}}{\partial x_i}\right)\delta u_k\right] - \frac{\partial}{\partial x_j}\left(\bar{\tau}_{jk} - \frac{\partial\bar{\mu}^*_{ijk}}{\partial x_i}\right)\delta u_k + \frac{\partial\bar{\mu}^*_{ij}\delta u_k}{\partial x_i} \tag{3.3.2.14}$$

Where:

$$\bar{\mu}^*_{ijk} \equiv \frac{1}{2}e_{jkl}\bar{\mu}_{il} + \bar{\bar{\mu}}_{ijk} \tag{3.3.2.15}$$

In order to derive this time stress equations of motion and boundary conditions different than those of form I and II we resolve (3.2.5.11) with respect to $D\delta u_k$:

$$D\delta u_k = 2\delta w_i n_j e_{ijk} + D_k\left(n_i \delta u_i\right) - \left(D_k n_i\right)\delta u_i + n_k \delta \epsilon_{nn} \tag{3.3.2.16}$$

Where w_i is the axial vector of the rotation tensor and ϵ_{nn} is the normal component of the strain tensor:

$$w_i \equiv \frac{1}{2} e_{ilm} \frac{\partial u_m}{\partial x_l} \tag{3.3.2.17}$$

$$\epsilon_{nn} \equiv n_i n_j \epsilon_{ij}, \quad \text{no summation over the n indices} \tag{3.3.2.18}$$

By integrating (3.3.1.14) by parts and applying the divergence theorem and Stoke's theorem, the following expression for the variation of the potential energy density:

$$\begin{aligned}
\delta\bar{\mathscr{W}} = &-\int_{\mathbb{B}_0}\left(\nabla\cdot\bar{\boldsymbol{\tau}} + \frac{1}{2}\nabla\times\nabla\cdot\bar{\boldsymbol{\mu}} - \nabla\cdot\bar{\bar{\boldsymbol{\mu}}}\cdot\nabla\right)\delta\mathbf{u}\,dV \\
&+\int_{\partial\mathbb{B}_0}\{\mathbf{n}\cdot\bar{\boldsymbol{\tau}} + \frac{1}{2}\mathbf{n}\times\left(\nabla\cdot\bar{\boldsymbol{\mu}} - \nabla tr\bar{\boldsymbol{\mu}}\right) - \left(\nabla\times\bar{\bar{\boldsymbol{\mu}}}\right)\cdot\mathbf{n} \\
&-\mathbf{n}\cdot\nabla\times[\mathbf{n}\times\left(\mathbf{n}\cdot\bar{\bar{\boldsymbol{\mu}}} + \mathbf{n}\cdot\bar{\bar{\boldsymbol{\mu}}}\cdot\mathbf{n}\otimes\mathbf{n}\right)]\}\delta\mathbf{u}\,dS \\
&+\int_{\partial\mathbb{B}_0}\left[\mathbf{n}\cdot\bar{\boldsymbol{\tau}}\times\mathbf{n} + 2\mathbf{n}\times\left(\mathbf{n}\cdot\bar{\bar{\boldsymbol{\mu}}}\cdot\mathbf{n}\right)\times\mathbf{n}\right]\cdot\left(\delta\mathbf{w}\times\mathbf{n}\right)\,dS \\
&+\int_{\partial\mathbb{B}_0}\mathbf{n}\otimes\mathbf{n}:\bar{\bar{\boldsymbol{\mu}}}\cdot\mathbf{n}\left(\delta tr\boldsymbol{\epsilon}\right)\,dS \\
&+\oint_C\left[\frac{1}{2}\left(tr\bar{\boldsymbol{\mu}}\otimes\mathbf{s}\right) + \left(\mathbf{s}\times\mathbf{n}\right)\cdot\left(\mathbf{n}\bar{\bar{\boldsymbol{\mu}}} + \mathbf{n}\cdot\bar{\bar{\boldsymbol{\mu}}}:\mathbf{n}\otimes\mathbf{n}\right)\right]\delta\mathbf{u}\,ds
\end{aligned} \tag{3.3.2.19}$$

In (3.3.2.19) $\mathbf{s}$ represents the unit vector tangent to the edge C. The above expression of the variation of the total potential energy suggests that the work of the external forces has to be in the form of:

$$W_{ext} = \int_{\mathbb{B}_0}\mathbf{F}\delta\mathbf{u}\,dV + \int_{\partial\mathbb{B}_0}\left[\mathbf{P}\cdot\delta\mathbf{u} + \mathbf{Q}\cdot\delta\mathbf{w}\times\mathbf{n} + R\delta\left(tr\boldsymbol{\epsilon}\right)\right]\,dS + \oint_C\mathbf{E}\cdot\delta\mathbf{u}\,ds \tag{3.3.2.20}$$

Where $\mathbf{Q}$ is the tangential component of the couple - stress vector and R denotes a double force per unit area, without moment, normal to S.

As in the previous cases the equations of motion and boundary conditions are formulated by substituting (3.2.5.4), (3.3.2.19), (3.3.2.20) into Hamilton's principle. It is noted that the expression of the kinetic energy is the same as in form I

$$\nabla \cdot \bar{\boldsymbol{\tau}} + \frac{1}{2}\nabla \times \nabla \cdot \bar{\boldsymbol{\mu}} - \nabla \cdot \bar{\bar{\boldsymbol{\mu}}} \cdot \nabla + \mathbf{F} = \rho \ddot{\mathbf{u}} - \frac{1}{3}\nabla \cdot \left(\rho' \tilde{\mathbf{d}}^2 : \nabla \ddot{\mathbf{u}}\right) \tag{3.3.2.21}$$

$$\begin{aligned} &\mathbf{n} \cdot \bar{\boldsymbol{\tau}} + \frac{1}{2}\mathbf{n} \times (\nabla \cdot \bar{\boldsymbol{\mu}} - \nabla tr\bar{\boldsymbol{\mu}}) - (\nabla \times \bar{\bar{\boldsymbol{\mu}}}) \cdot \mathbf{n} \\ &- \mathbf{n} \cdot \nabla \times [\mathbf{n} \times (\mathbf{n} \cdot \bar{\bar{\boldsymbol{\mu}}} + \mathbf{n} \cdot \bar{\bar{\boldsymbol{\mu}}} \cdot \mathbf{n} \otimes \mathbf{n})] + \frac{1}{3}\rho' \mathbf{n} \cdot \tilde{\mathbf{d}}^2 : \nabla \ddot{\mathbf{u}} = \mathbf{P} \end{aligned} \tag{3.3.2.22}$$

$$\mathbf{n} \cdot \bar{\boldsymbol{\mu}} \times \mathbf{n} + 2\mathbf{n} \times (\mathbf{n} \cdot \bar{\bar{\boldsymbol{\mu}}} \cdot \mathbf{n}) \times \mathbf{n} = \mathbf{Q} \tag{3.3.2.23}$$

$$\mathbf{n} \otimes \mathbf{n} : \bar{\bar{\boldsymbol{\mu}}} \cdot \mathbf{n} = R \tag{3.3.2.24}$$

$$\left[\frac{1}{2}\left(tr\bar{\boldsymbol{\mu}} \otimes \mathbf{s}\right) + (\mathbf{s} \times \mathbf{n}) \cdot (\mathbf{n}\bar{\bar{\boldsymbol{\mu}}} + \mathbf{n} \cdot \bar{\bar{\boldsymbol{\mu}}} : \mathbf{n} \otimes \mathbf{n})\right] = \mathbf{E} \tag{3.3.2.25}$$

The displacement equations of motion can be obtained by inserting (2.2.2.9), (3.3.2.2) and (3.3.2.4) into (3.3.2.7) - (3.3.2.9) and then substituting the latter into (3.3.2.22):

$$\begin{aligned} &(\tilde{\lambda} + 2\tilde{\mu})(1 - \bar{l}_1^2\nabla^2)\nabla\nabla \cdot \mathbf{u} - \tilde{\mu}(1 - \bar{l}_2^2\nabla^2)\nabla \times \nabla \times \mathbf{u} + \mathbf{F} \\ &= \rho(\ddot{\mathbf{u}} - h_1^2\nabla\nabla \cdot \ddot{\mathbf{u}} + h_2^2\nabla \times \nabla \times \ddot{\mathbf{u}}) \end{aligned} \tag{3.3.2.26}$$

Where:

$$\bar{l}_1^2 = \frac{3\bar{a}_1 + \bar{a}_2}{\tilde{\lambda} + 2\tilde{\mu}} \tag{3.3.2.27}$$

$$\bar{l}_2^2 = \frac{3\bar{d}_1 + \bar{a}_1 + 2\bar{a}_2 - \bar{f}}{3\tilde{\mu}} \tag{3.3.2.28}$$

Using (3.3.1.4), (3.3.1.16), (3.3.1.17), (3.3.2.6), (3.3.2.27), (3.3.2.28) it can be shown that $\bar{l}_i^2 = \hat{l}_i^2$, while it was previously proved that $\hat{l}_i^2 = \tilde{l}_i^2$ meaning that the displacement equations of motion (3.2.5.25), (3.3.1.15), (3.3.2.26) of forms forms I, II and III are identical. Having the aforementioned in mind, from now on we will not distinguished between the intrinsic gradient parameters $\tilde{l}_i^2$, $\hat{l}_i^2$, $\bar{l}_i^2$ and we will write the equations of motion as:

$$(\tilde{\lambda}+2\tilde{\mu})(1-l_1^2\nabla^2)\nabla\nabla\cdot\mathbf{u}-\tilde{\mu}(1-l_2^2\nabla^2)\nabla\times\nabla\times\mathbf{u}+\mathbf{F} \\ =\rho(\ddot{\mathbf{u}}-h_1^2\nabla\nabla\cdot\ddot{\mathbf{u}}+h_2^2\nabla\times\nabla\times\ddot{\mathbf{u}}) \tag{3.3.2.29}$$

The above differential equation is indeed much simpler compared to (2.6.1.1), (2.6.1.2) and in some cases closed form analytical solution can be obtained, however by making a few more assumptions regarding the material properties (3.3.2.29) can be simplified even further as it will be shown in the following section.

3.3.3 Dipolar Gradient Elasticity

Dipolar gradient elasticity was presented in 2003 by Georgiadis [72] and corresponds to the simplest possible version of Mindlin's general theory. This theory has been implemented multiple times (see, e.g., [73], [74], [75], [76]) and can be easily formulated by setting $\rho'=\rho$, $\hat{a}_1=\hat{a}_3=\hat{a}_5=0$, $\hat{a}_2=\tilde{\lambda}l^2/2$, $\hat{a}_4=\tilde{\mu}l^2$, $g_1^2=g_2^2=0$. In this case, equations (3.2.2.5), (3.2.2.6), (3.2.4.2) - (3.2.4.8), (3.2.5.26) - (3.2.5.29) imply that $\tilde{\lambda}=\lambda$, $\tilde{\mu}=\mu$, $\alpha=0$, $\beta=1$, $\tilde{d}^2_{pkmn}=h^2\delta_{pm}\delta_{kn}$, $\hat{l}_1^2=\hat{l}_2^2=l^2$, $h_1^2=h_2^2=h^2=d^2/3$. In this work dipolar gradient elasticity is formulated having form II as a background for the kinematics and the potential energy density, however versions of this sub - theory can be formulated using either form I or form III.

By setting the above values in (3.2.3.8), (3.3.1.3) the following expressions for the kinetic energy density and the potential energy density are obtained:

$$\tilde{T}=\frac{1}{2}\rho\dot{u}_j\dot{u}_j+\frac{1}{6}\rho h^2\frac{\partial\dot{u}_k}{\partial x_p}\frac{\partial\dot{u}_k}{\partial x_p} \tag{3.3.3.1}$$

$$\hat{W}=\frac{1}{2}\lambda\epsilon_{ii}\epsilon_{jj}+\mu\epsilon_{ij}\epsilon_{ij}+\frac{\lambda l^2}{2}\hat{k}_{ijj}\hat{k}_{ikk}+\frac{\mu l^2}{2}\hat{k}_{ijk}\hat{k}_{ijk} \tag{3.3.3.2}$$

The constitutive equations (3.3.1.7), (3.3.1.8) now become:

$$\hat{\tau}_{pq}=\lambda\delta_{pq}\epsilon_{ii}+2\mu\epsilon_{pq} \tag{3.3.3.3}$$

$$\hat{\mu}_{pqr}=l^2\frac{\partial}{\partial x_p}\left(\lambda\delta_{qr}\epsilon_{ii}+2\mu\epsilon_{qr}\right) \tag{3.3.3.4}$$

Because in this case the kinematics as well as the potential energy density are the same as in form II, the equations of motion and boundary conditions can be formulated by setting the values of the gradient parameters into the corresponding equations of form II. By setting

$\rho' = \rho$, $\tilde{\lambda} = \lambda$, $\tilde{\mu} = \mu$, $\tilde{d}^2_{pkmn} = h^2\delta_{pm}\delta_{kn}$, $\hat{l}_1^2 = \hat{l}_2^2 = l^2$, $h_1^2 = h_2^2 = h^2 = d^2/3$ into (3.3.1.11) - (3.3.1.14) the following equations are obtained :

$$\frac{\partial}{\partial x_j}\left(\hat{\tau}_{kj} - \frac{\partial \hat{\mu}_{ijk}}{\partial x_i}\right) + F_k = \rho\ddot{u}_k - \frac{1}{3}\rho h^2\left(\frac{\ddot{u}_n}{\partial x_p \partial_p}\right) \tag{3.3.3.5}$$

$$\hat{P}_k = n_j\hat{\tau}_{jk} - n_i n_j D\hat{\mu}_{ijk} - 2n_j D_i\hat{\mu}_{ijk} + \left(n_i n_j D_l n_l - D_j n_i\right)\hat{\mu}_{ijk} + \frac{1}{3}\rho h^2 n_p \frac{\ddot{u}_k}{\partial x_p} \tag{3.3.3.6}$$

While the boundary conditions (3.3.1.13), (3.3.1.14) remain invariant.

Finally, the displacement equations of motion are obtained by setting in (3.3.1.15) $\hat{l}_1^2 = \hat{l}_2^2 = l^2$, $h_1^2 = h_2^2 = h^2 = d^2/3$:

$$(\lambda + \mu)(1 - l^2\nabla^2)\nabla\nabla \cdot \mathbf{u} + \mu(1 - l^2\nabla^2)\nabla^2\mathbf{u} + \mathbf{F} = \rho\ddot{\mathbf{u}} - I\nabla^2\ddot{\mathbf{u}} \tag{3.3.3.7}$$

Where I is the micro-inertia coefficient defined as:

$$I = \rho h^2 = \frac{1}{3}\rho d^2 \tag{3.3.3.8}$$

Because d has a geometric representation it can be considered as a real positive quantity. It is reminded that $2d$ is the length of the edges of the cells that compose the microstructure, for this reason it can be justified that $I > 0$.

Equation (3.3.3.7) corresponds to the simplest possible governing equation that can describe the motion of a gradient material in the context of Mindlin's general theory. Both (3.3.2.29) and (3.3.3.8) will be used in this work for solving different problems with infinite domains.

3.4 Elastodynamics of Gradient Continua

3.4.1 Lamé Potentials

The system of displacement equations of motion (3.3.2.29) has a disadvantageous feature in that it couples the three displacement components. The aforementioned equations can be uncoupled with Lamé type potentials as in the case of Navier – Cauchy equations, which is the equivalent system of equations in classical elasticity.

Let us consider a decomposition of the displacement vector of the form of:

$$\mathbf{u} = \nabla\phi + \nabla \times \boldsymbol{\psi} \tag{3.4.1.1}$$

$$\nabla \cdot \boldsymbol{\psi} = \mathbf{0} \tag{3.4.1.2}$$

It will be shown that the above vector field indeed satisfies the displacement equations of motion (3.3.2.29), however before we begin the decomposition proses it is necessary to quote a theorem that will be used in order to decompose the body force vector in (3.3.2.29).

Theorem 3.4.1.1 (Helmholtz Decomposition Theorem)

Let $\mathbf{p}(\mathbf{x})$ be a vector field on a bounded domain $V \subseteq \mathbb{R}^3$, which is twice piecewise differentiable inside V and let S be the surface that encloses V. Then $\mathbf{p}(\mathbf{x})$ can be decomposed into an irrotational (curl – free) component and a solenoidal (divergence – free) component as:

$$\mathbf{p} = -\nabla P + \nabla \times \mathbf{Q}$$

Where:

$$P(\mathbf{x}) = \frac{1}{4\pi}\int_V \frac{\nabla_{\boldsymbol{\xi}} \cdot \mathbf{p}(\boldsymbol{\xi})}{|\mathbf{x}-\boldsymbol{\xi}|}\, dV' - \frac{1}{4\pi}\oint_S \mathbf{n}' \cdot \frac{\mathbf{p}(\boldsymbol{\xi})}{|\mathbf{x}-\boldsymbol{\xi}|}\, dS'$$

$$\mathbf{Q}(\mathbf{x}) = \frac{1}{4\pi}\int_V \frac{\nabla_{\boldsymbol{\xi}} \times \mathbf{p}(\boldsymbol{\xi})}{|\mathbf{x}-\boldsymbol{\xi}|}\, dV' - \frac{1}{4\pi}\oint_S \mathbf{n}' \times \frac{\mathbf{p}(\boldsymbol{\xi})}{|\mathbf{x}-\boldsymbol{\xi}|}\, dS'$$

$$\nabla \cdot \mathbf{Q} = 0$$

In the above equations ∇' is the gradient operator with respect to $\boldsymbol{\xi}$ and $\mathbf{n}'$ is the outward pointing unit normal vector at each point of the surface S'.

The physical interpretation of $\nabla \cdot \mathbf{Q} = 0$ is that it acts as a closure condition. Since $\mathbf{p}(\mathbf{x})$ is a vector function when decomposed it must be replaced by three equations. Also, it was mentioned before that by performing Helmholtz decomposition, a vector filed is decomposed

into an irrotational component and a solenoidal component. This can be easily be noticed since the vector identities $\nabla \times \nabla a = 0$, $\forall a$ and $\nabla \cdot \nabla \times \mathbf{v} = 0$, $\forall \mathbf{v}$ hold, as long as a,$\mathbf{v}$ are twice differentiable.

In the problems that are presented in this work the analyzed domain is always considered as an infinite domain. In this case the expressions of P, $\mathbf{Q}$ that are given above are significantly simplified.

Corollary 3.4.1.1. *Let* $\mathbf{p}(\mathbf{x})$ *be a vector field on* $V = \mathbb{R}^3$ *(in this case* V *is unbounded), which is twice piecewise differentiable, if* $\mathbf{p}(\mathbf{x})$ *vanishes faster than* $1/x$ *as* $x \to \infty$*. Then* $\mathbf{p}(\mathbf{x})$ *can be decomposed into an irrotational component and a solenoidal component as:*

$$\mathbf{p} = -\nabla P + \nabla \times \mathbf{Q}$$

Where:

$$P(\mathbf{x}) = \frac{1}{4\pi} \int_V \frac{\nabla_{\boldsymbol{\xi}} \cdot \mathbf{p}(\boldsymbol{\xi})}{|\mathbf{x} - \boldsymbol{\xi}|} \, dV'$$

$$\mathbf{Q}(\mathbf{x}) = \frac{1}{4\pi} \int_V \frac{\nabla_{\boldsymbol{\xi}} \times \mathbf{p}(\boldsymbol{\xi})}{|\mathbf{x} - \boldsymbol{\xi}|} \, dV'$$

$$\nabla \cdot \mathbf{Q} = 0$$

Using Helmholtz decomposition, we can express the body force vector in the form of:

$$\mathbf{F} = (\tilde{\lambda} + 2\tilde{\mu}) \nabla F + \tilde{\mu} \nabla \times \mathbf{G} \tag{3.4.1.3}$$

Where the coefficients in front of the differential operators in (3.4.1.3) are placed for dimensionality reasons.

We continue by inserting equations (3.4.1.1), (3.4.1.3) into (3.3.2.29):

$$\begin{aligned} &(\tilde{\lambda} + 2\tilde{\mu})(1 - l_1^2 \nabla^2) \nabla \nabla \cdot (\nabla \phi + \nabla \times \boldsymbol{\psi}) - \tilde{\mu}(1 - l_2^2 \nabla^2) \nabla \times \nabla \times (\nabla \phi + \nabla \times \boldsymbol{\psi}) \\ &+ (\tilde{\lambda} + 2\tilde{\mu}) \nabla F + \tilde{\mu} \nabla \times \mathbf{G} \\ &= \rho [(\nabla \ddot{\phi} + \nabla \times \ddot{\boldsymbol{\psi}}) - h_1^2 \nabla \nabla \cdot (\nabla \ddot{\phi} + \nabla \times \ddot{\boldsymbol{\psi}}) + h_2^2 \nabla \times \nabla \times (\nabla \ddot{\phi} + \nabla \times \ddot{\boldsymbol{\psi}})] \end{aligned} \tag{3.4.1.4}$$

The above equation can be simplified with the help of the following vector identities:

$$\nabla \cdot \nabla a = \nabla^2 a, \quad \forall a \tag{3.4.1.5}$$

$$\nabla \cdot \nabla \times \mathbf{v} = 0, \quad \forall \mathbf{v} \tag{3.4.1.6}$$

$$\nabla \times \nabla a = \mathbf{0}, \quad \forall a \tag{3.4.1.7}$$

Due to (3.4.1.5), (3.4.1.6), equation (3.4.1.4) takes the form:

$$\begin{aligned}&(\tilde{\lambda} + 2\tilde{\mu})(\nabla\nabla^2\phi - l_1^2\nabla^2\nabla\nabla^2\phi) - \tilde{\mu}(1 - l_2^2\nabla^2)\nabla \times \nabla \times \nabla \times \boldsymbol{\psi} + (\tilde{\lambda} + 2\tilde{\mu}) \\ &\nabla F + \tilde{\mu}\nabla \times \mathbf{G} = \rho[(\nabla\ddot{\phi} + \nabla \times \ddot{\boldsymbol{\psi}}) - h_1^2\nabla\nabla^2\ddot{\phi} + h_2^2 + \nabla \times \nabla \times \nabla \times \ddot{\boldsymbol{\psi}}]\end{aligned} \tag{3.4.1.8}$$

The terms with the multiple curl operators in (3.4.1.8) can be further simplified due to the following identity:

$$\nabla \times \nabla \times \mathbf{v} = \nabla\nabla \cdot \mathbf{v} - \nabla^2\mathbf{v}, \quad \forall \mathbf{v} \tag{3.4.1.9}$$

Substituting (3.4.1.9) into (3.4.1.8) and taking also (3.4.1.7) into account yields:

$$\begin{aligned}&(\tilde{\lambda} + 2\tilde{\mu})(\nabla\nabla^2\phi - l_1^2\nabla^2\nabla\nabla^2\phi) + \tilde{\mu}(\nabla \times \nabla^2\boldsymbol{\psi} - l_2^2\nabla^2\nabla \times \nabla^2\boldsymbol{\psi}) \\ &+ (\tilde{\lambda} + 2\tilde{\mu})\nabla F + \tilde{\mu}\nabla \times \mathbf{G} = \rho[(\nabla\ddot{\phi} + \nabla \times \ddot{\boldsymbol{\psi}}) - h_1^2\nabla\nabla^2\ddot{\phi} - h_2^2 + \nabla \times \nabla^2\ddot{\boldsymbol{\psi}}]\end{aligned} \tag{3.4.1.10}$$

By assuming that ϕ is of C^5 (it will be shown latter that this is not necessary) we can interchange the Laplacian and the gradient operators, as well as the Laplacian and curl operators in (3.4.1.10):

$$\begin{aligned}&(\tilde{\lambda} + 2\tilde{\mu})(\nabla\nabla^2\phi - l_1^2\nabla\nabla^4\phi) + \tilde{\mu}(\nabla \times \nabla^2\boldsymbol{\psi} - l_2^2\nabla \times \nabla^4\boldsymbol{\psi}) \\ &+ (\tilde{\lambda} + 2\tilde{\mu})\nabla F + \tilde{\mu}\nabla \times \mathbf{G} = \rho[(\nabla\ddot{\phi} + \nabla \times \ddot{\boldsymbol{\psi}}) - h_1^2\nabla\nabla^2\ddot{\phi} - h_2^2 + \nabla \times \nabla^2\ddot{\boldsymbol{\psi}}]\end{aligned} \tag{3.4.1.11}$$

Where ∇^4 is the biharmonic operator defined as:

$$\nabla^4 = \nabla^2\nabla^2 \tag{3.4.1.12}$$

By rearranging the terms in (3.4.1.11), the following equation is obtained:

$$\begin{aligned}&\nabla[-(\tilde{\lambda}+2\tilde{\mu})l_1^2\nabla^4\phi+(\tilde{\lambda}+2\tilde{\mu})\nabla^2\phi+\rho h_1^2\nabla^2\ddot{\phi}+(\tilde{\lambda}+2\tilde{\mu})F-\rho h_1^2\ddot{\phi}]\\&+\nabla\times[-l_2^2\tilde{\mu}\nabla^4\boldsymbol{\psi}+\tilde{\mu}\nabla^2\boldsymbol{\psi}+\rho h_2^2\ddot{\boldsymbol{\psi}}+\tilde{\mu}\mathbf{G}-\rho\ddot{\boldsymbol{\psi}}]=\mathbf{0}\end{aligned}\tag{3.4.1.13}$$

By applying the divergence operator in (3.4.1.13) and taking into account (3.4.1.5), (3.4.1.6) we obtain:

$$\nabla^2[-(\tilde{\lambda}+2\tilde{\mu})l_1^2\nabla^4\phi+(\tilde{\lambda}+2\tilde{\mu})\nabla^2\phi+\rho h_1^2\nabla^2\ddot{\phi}+(\tilde{\lambda}+2\tilde{\mu})F-\rho\ddot{\phi}]=0\tag{3.4.1.14}$$

By applying the curl operator in (3.4.1.13) and taking into account (3.4.1.7), we obtain:

$$\nabla\times\nabla\times[-l_2^2\tilde{\mu}\nabla^4\boldsymbol{\psi}+\tilde{\mu}\nabla^2\boldsymbol{\psi}+\rho h_2^2\nabla\ddot{\boldsymbol{\psi}}+\tilde{\mu}\mathbf{G}-\rho\ddot{\boldsymbol{\psi}}]=\mathbf{0}\tag{3.4.1.15}$$

The order of the final two differential equations can be reduced if we manage two prove that the terms inside the brackets in (3.4.1.14), (3.4.1.15) are equal to zero. This idea is known in the literature as the completeness theorem and the next paragraph of this work is entirely devoted to formulating and proving this theorem.

3.4.2 The Generalized Completeness Theorem

According to Achenbach [77], the question of the completeness of the representation (3.4.1.1) in the context of classical elasticity was first raised by Clebsch. Clebsch asserted that every solution of the Navier-Cauchy equations of motion could be expressed using the representation (3.4.1.1) for $l_i = h_i = 0$. The work of Clebsch and others, particularly Duhem, was discussed by Sternberg [78]. As far as the author is concerned all the work that has been made regarding the completeness theorem is in the context of classical elasticity and no one has ever attempted officially to generalize the theorem in a more complicated theory than the one of Cauchy. The formulation and proof of the theorem are presented below and are identical to those of Achenbach but for the case of classical elasticity [77].

Theorem 3.4.2.1 (Completeness Generalized Theorem)

Let $\mathbf{u}(\mathbf{x},t)$ and $\mathbf{F}(\mathbf{x},t)$ satisfy the conditions:

$$\mathbf{u} \in \mathcal{B}^4(V \times T)$$

$$\mathbf{F} \in \mathcal{B}(V \times T)$$

As well as the displacement equation of motion (3.3.2.29), in a region of a space V and in a closed time interval T. Also let $\mathbf{F}$ be given by (3.4.1.3). Then there exists a scalar function $\phi(\mathbf{x},t)$ and a vector function $\boldsymbol{\psi}(\mathbf{x},t)$ such that $\mathbf{u}(\mathbf{x},t)$ is represented by (3.4.1.1), (3.4.1.2). Where $\phi(\mathbf{x},t)$ and $\boldsymbol{\psi}(\mathbf{x},t)$ satisfy the following forth order differential equations:

$$\nabla^4\phi - \frac{1}{l_1^2}\nabla^2(\phi + \frac{h_1^2}{\tilde{v}_1^2}\ddot{\phi}) - \frac{1}{l_1^2}F = -\frac{1}{l_1^2\tilde{v}_1^2}\ddot{\phi}$$

$$\nabla^4\boldsymbol{\psi} - \frac{1}{l_2^2}\nabla^2(\boldsymbol{\psi} + \frac{h_2^2}{\tilde{v}_2^2}\ddot{\boldsymbol{\psi}}) - \frac{1}{l_2^2}\mathbf{G} = -\frac{1}{l_2^2\tilde{v}_2^2}\ddot{\boldsymbol{\psi}}$$

Proof: We begin by replacing the Laplacian operator in (3.3.2.29) with the expression given in (3.4.1.9):

$$\begin{aligned}&(\tilde{\lambda}+2\tilde{\mu})[\nabla\nabla\cdot\mathbf{u} - l_1^2(\nabla\nabla\cdot\nabla\nabla\cdot\mathbf{u} - \nabla\times\nabla\times\nabla\nabla\cdot\mathbf{u})]\\ &-\tilde{\mu}[\nabla\times\nabla\times\mathbf{u} - l_2^2(\nabla\nabla\cdot\nabla\times\nabla\times\mathbf{u} - \nabla\times\nabla\times\nabla\times\nabla\times\mathbf{u}) + \mathbf{F}]\\ &= \rho(\ddot{\mathbf{u}} - h_1^2\nabla\nabla\cdot\ddot{\mathbf{u}} + h_2^2\nabla\times\nabla\times\cdot\ddot{\mathbf{u}})\end{aligned} \tag{3.4.2.1}$$

Equation (3.4.2.1) can be simplified with the help of (3.4.1.5) – (3.4.1.7)

$$\begin{aligned}&(\tilde{\lambda}+2\tilde{\mu})(\nabla\nabla\cdot\mathbf{u} - l_1^2\nabla\nabla^2\nabla\cdot\mathbf{u}) - \tilde{\mu}(\nabla\times\nabla\times\mathbf{u} + l_2^2\nabla\times\nabla\times\nabla\times\nabla\times\mathbf{u}) + \mathbf{F}\\ &= \rho(\ddot{\mathbf{u}} - h_1^2\nabla\nabla\cdot\ddot{\mathbf{u}} + h_2^2\nabla\times\nabla\times\cdot\ddot{\mathbf{u}})\end{aligned} \tag{3.4.2.2}$$

The above equation can equivalently be written as:

$$\begin{aligned}&\ddot{\mathbf{u}} - h_1^2\nabla\nabla\cdot\ddot{\mathbf{u}} + h_2^2\nabla\times\nabla\times\cdot\ddot{\mathbf{u}}\\ &= -v_2^2l_2^2\nabla\times\nabla\times\nabla\times\nabla\times\mathbf{u} - v_1^2l_2^1\nabla\nabla^2\nabla\cdot\mathbf{u} + v_1^2\nabla\nabla\cdot\mathbf{u} - v_2^2\nabla\times\nabla\times\mathbf{u} + \mathbf{f}\end{aligned} \tag{3.4.2.3}$$

Where $\tilde{v}_1$, $\tilde{v}_2$ are material's constants that when the microstructural parameters are set equal to zero, degenerate to the wave velocities of the primary and the secondary waves of classical

elasticity and $\mathbf{f} = \mathbf{F}/\rho$ is the body force per unit mass, which according to (3.4.1.3) can be expressed as:

$$\tilde{v}_1 = \sqrt{\frac{\tilde{\lambda} + 2\tilde{\mu}}{\rho}} \tag{3.4.2.4}$$

$$\tilde{v}_2 = \sqrt{\frac{\tilde{\mu}}{\rho}} \tag{3.4.2.5}$$

$$\mathbf{f} = \tilde{v}_1^2 \nabla F + \tilde{v}_2^2 \nabla \times \mathbf{G} \tag{3.4.2.6}$$

By integrating (3.4.2.3) two times with respect to time we obtain:

$$\begin{aligned}
&\mathbf{u} - h_1^2 \nabla\nabla \cdot \mathbf{u} + h_2^2 \nabla \times \nabla \times \cdot\mathbf{u} \\
&= -\tilde{v}_2^2 l_2^2 \nabla \times \int_0^t \int_0^\tau (\nabla \times \nabla \times \nabla \times \mathbf{u})\, ds\, d\tau - \tilde{v}_1^2 l_2^1 \nabla \int_0^t \int_0^\tau (\nabla^2 \nabla \cdot \mathbf{u})\, ds\, d\tau \\
&+ \tilde{v}_1^2 \nabla \int_0^t \int_0^\tau (\nabla \cdot \mathbf{u})\, ds\, d\tau - \tilde{v}_2^2 \nabla \times \int_0^t \int_0^\tau (\nabla \times \mathbf{u})\, ds\, d\tau + \int_0^t \int_0^\tau \mathbf{f}\, ds\, d\tau \\
&+ \tilde{\mathbf{v}}(\mathbf{x}) t + \tilde{\mathbf{u}}(\mathbf{x})
\end{aligned} \tag{3.4.2.7}$$

Where $\tilde{\mathbf{v}}(\mathbf{x})$ and $\tilde{\mathbf{u}}(\mathbf{x})$ are the initial conditions for the velocity and the displacement respectively ($\tilde{\mathbf{v}}(\mathbf{x}) = \mathbf{v}(\mathbf{x}, 0)$, $\tilde{\mathbf{u}}(\mathbf{x}) = \mathbf{u}(\mathbf{x}, 0)$). Also, the initial conditions of the velocity and the displacement can be expressed in terms of (3.4.1.1) as:

$$\tilde{\mathbf{v}}(\mathbf{x}) = \nabla \dot{\phi}_0 + \nabla \times \dot{\boldsymbol{\psi}}_0 \tag{3.4.2.8}$$

$$\tilde{\mathbf{u}}(\mathbf{x}) = \nabla \phi_0 + \nabla \times \boldsymbol{\psi}_0 \tag{3.4.2.9}$$

Where:

$$\phi_0 = \phi_0(\mathbf{x}) = \phi(\mathbf{x}, 0), \quad \dot{\phi}_0 = \dot{\phi}_0(\mathbf{x}) = \dot{\phi}(\mathbf{x}, 0) \tag{3.4.2.10}$$

$$\boldsymbol{\psi}_0 = \boldsymbol{\psi}_0(\mathbf{x}) = \boldsymbol{\psi}(\mathbf{x}, 0), \quad \dot{\boldsymbol{\psi}}_0 = \dot{\boldsymbol{\psi}}_0(\mathbf{x}) = \dot{\boldsymbol{\psi}}(\mathbf{x}, 0) \tag{3.4.2.11}$$

Substituting (3.4.2.6), (3.4.2.8), (3.4.2.9) into (3.4.2.7) yields:

$$\begin{aligned}\mathbf{u} = &-\tilde{v}_2^2 l_2^2 \nabla \times \int_0^t \int_0^\tau (\nabla \times \nabla \times \nabla \times \mathbf{u})\, ds\, d\tau - \tilde{v}_1^2 l_1^2 \nabla \int_0^t \int_0^\tau (\nabla^2 \nabla \cdot \mathbf{u})\, ds\, d\tau \\ &+ \tilde{v}_1^2 \nabla \int_0^t \int_0^\tau (\nabla \cdot \mathbf{u})\, ds\, d\tau - \tilde{v}_2^2 \nabla \times \int_0^t \int_0^\tau (\nabla \times \mathbf{u})\, ds\, d\tau \\ &- h_2^2 \nabla \times \nabla \times \cdot \mathbf{u} + h_1^2 \nabla \nabla \cdot \mathbf{u} + \int_0^t \int_0^\tau (\tilde{v}_1^2 \nabla F + \tilde{v}_2^2 \nabla \times \mathbf{G})\, ds\, d\tau \\ &+ (\nabla \dot{\phi}_0 + \nabla \times \dot{\boldsymbol{\psi}}_0) t + (\nabla \phi_0 + \nabla \times \boldsymbol{\psi}_0)\end{aligned} \tag{3.4.2.12}$$

Due to the similarity between (3.4.1.1), (3.4.2.12) we define:

$$\begin{aligned}\phi = &-\tilde{v}_1^2 l_1^2 \int_0^t \int_0^\tau (\nabla^2 \nabla \cdot \mathbf{u})\, ds\, d\tau + \tilde{v}_1^2 \int_0^t \int_0^\tau (\nabla \cdot \mathbf{u})\, ds\, d\tau \\ &+ h_1^2 \nabla \cdot \mathbf{u} + \tilde{v}_1^2 \int_0^t \int_0^\tau F\, ds\, d\tau + \dot{\phi}_0 t + \phi_0\end{aligned} \tag{3.4.2.13}$$

$$\begin{aligned}\boldsymbol{\psi} = &-\tilde{v}_2^2 l_2^2 \int_0^t \int_0^\tau (\nabla \times \nabla \times \nabla \times \mathbf{u})\, ds\, d\tau - \tilde{v}_2^2 \int_0^t \int_0^\tau (\nabla \times \mathbf{u})\, ds\, d\tau \\ &- h_2^2 \nabla \times \cdot \mathbf{u} + \tilde{v}_2^2 \int_0^t \int_0^\tau \mathbf{G}\, ds\, d\tau + \dot{\boldsymbol{\psi}}_0 t + \boldsymbol{\psi}_0\end{aligned} \tag{3.4.2.14}$$

By differentiating (3.4.2.13), (3.4.2.14) two times with respect to time we obtain:

$$\ddot{\phi} = -\tilde{v}_1^2 l_1^2 \nabla^2 \nabla \cdot \mathbf{u} + \tilde{v}_1^2 \nabla \cdot \mathbf{u} + h_1^2 \nabla \cdot \ddot{\mathbf{u}} + \tilde{v}_1^2 F \tag{3.4.2.15}$$

$$\ddot{\boldsymbol{\psi}} = -\tilde{v}_2^2 l_2^2 \nabla \times \nabla \times \nabla \times \mathbf{u} - \tilde{v}_2^2 \nabla \times \mathbf{u} - h_2^2 \nabla \times \ddot{\mathbf{u}} + \tilde{v}_2^2 \mathbf{G} \tag{3.4.2.16}$$

By substituting (3.3.1.1) into (3.4.2.15) and taking into account (3.4.1.5), (3.4.1.6), (3.4.1.9) we obtain:

$$\ddot{\phi} = -\tilde{v}_1^2 l_1^2 \nabla^4 \phi + \tilde{v}_1^2 \nabla^2 \phi + h_1^2 \nabla^2 \ddot{\phi} + \tilde{v}_1^2 F \tag{3.4.2.17}$$

By substituting (3.3.1.1) into (3.4.2.16) and taking into account (3.3.1.7) we obtain:

$$\ddot{\boldsymbol{\psi}} = -\tilde{v}_2^2 l_2^2 \nabla \times \nabla \times \nabla \times \nabla \times \mathbf{u} - \tilde{v}_2^2 \nabla \times \nabla \times \mathbf{u} - h_2^2 \nabla \times \nabla \times \ddot{\mathbf{u}} + \tilde{v}_2^2 \mathbf{G} \tag{3.4.2.18}$$

Inserting (3.3.1.9) into (3.4.2.18) yields:

$$\ddot{\boldsymbol{\psi}} = -\tilde{v}_2^2 l_2^2(\nabla\nabla\cdot-\nabla^2)(\nabla\nabla\cdot\boldsymbol{\psi}-\nabla^2\boldsymbol{\psi})-\tilde{v}_2^2(\nabla\nabla\cdot\boldsymbol{\psi}-\nabla^2\boldsymbol{\psi})-h_2^2(\nabla\nabla\cdot\ddot{\boldsymbol{\psi}}-\nabla^2\ddot{\boldsymbol{\psi}})+\tilde{v}_2^2\mathbf{G} \quad (3.4.2.19)$$

However, since one of the assumptions of the completeness theorem is, $\nabla\cdot\boldsymbol{\psi}=0$ the above equation is simplified to:

$$\ddot{\boldsymbol{\psi}} = -\tilde{v}_2^2 l_2^2(\nabla\nabla\cdot\nabla^2\boldsymbol{\psi}+\nabla^2\nabla^2\boldsymbol{\psi})+\tilde{v}_2^2\nabla^2\boldsymbol{\psi}+h_2^2\nabla^2\ddot{\boldsymbol{\psi}}+\tilde{v}_2^2\mathbf{G} \quad (3.4.2.20)$$

By interchanging the divergence and the Laplacian operators, the first term inside the parenthesis in (3.4.2.20) vanishes, since $\nabla\cdot\boldsymbol{\psi}=0$ and in view of (3.4.1.12) the above equation can be written as:

$$\ddot{\boldsymbol{\psi}} = -\tilde{v}_2^2 l_2^2\nabla^4\boldsymbol{\psi}+\tilde{v}_2^2\nabla^2\boldsymbol{\psi}+h_2^2\nabla^2\ddot{\boldsymbol{\psi}}+\tilde{v}_2^2\mathbf{G} \quad (3.4.2.21)$$

Dividing (3.4.2.17) with $-v_1^2\hat{l}_1^2$ and (3.4.2.21) with $-v_2^2\hat{l}^2$ gives:

$$\nabla^4\phi-\frac{1}{l_1^2}\nabla^2(\phi+\frac{h_1^2}{\tilde{v}_1^2}\ddot{\phi})-\frac{1}{l_1^2}F=-\frac{1}{l_1^2\tilde{v}_1^2}\ddot{\phi} \quad (3.4.2.22)$$

$$\nabla^4\boldsymbol{\psi}-\frac{1}{l_2^2}\nabla^2(\boldsymbol{\psi}+\frac{h_2^2}{\tilde{v}_2^2}\ddot{\boldsymbol{\psi}})-\frac{1}{l_2^2}\mathbf{G}=-\frac{1}{l_2^2\tilde{v}_2^2}\ddot{\boldsymbol{\psi}} \quad (3.4.2.23)$$

And in this way the proof of the theorem is completed.

3.4.3 Wave Propagation in Gradient Continua

The only thing that remains to be considered before deriving analytical solutions, is to examine what happens when plane waves propagate inside a gradient continuum. Unlike classical elasticity, in the context of the three forms of Mindlin's general the body waves are dispersive, meaning that waves of different wavelengths travel at different phase speeds. To illustrate this we begin by applying the divergence and the curl operator in the homogeneous version of (3.3.2.29) and with the help of (3.4.1.6), we can obtain the equations that describe the propagation of dilatation and rotation respectively.

$$\tilde{v}_1^2(1-l_1^2\nabla^2)\nabla^2(\nabla\cdot\mathbf{u})=(1-h_1^2\nabla^2)\nabla\cdot\ddot{\mathbf{u}} \tag{3.4.3.1}$$

$$\tilde{v}_2^2(1-l_2^2\nabla^2)\nabla\times(\nabla\times\nabla\times\mathbf{u})=(1+h_2^2\nabla\times\nabla\times)\nabla\times\ddot{\mathbf{u}} \tag{3.4.3.2}$$

Using (3.4.1.9) and taking also into account (3.4.1.6), (3.4.3.2) can equivalently be written as:

$$\tilde{v}_2^2(1-l_2^2\nabla^2)\nabla^2(\nabla\times\mathbf{u})=(1+h_2^2\nabla^2)\nabla\times\ddot{\mathbf{u}} \tag{3.4.3.3}$$

Where the expressions of the material's constants $\tilde{v}_1$ and $\tilde{v}_2$ are given by (3.4.2.4), (3.4.2.5). Also, it is worth mentioning that in contrast with the corresponding relations of classical elasticity, the differential equations presented in (3.4.3.1), (3.4.3.3) of the forth order. This implies that wave signals emitted from a disturbance point propagate at different velocities. At this point, the dispersion relations can be determined by considering time - harmonic plane wave solution of (3.4.3.1), (3.4.3.3) in the form of:

$$\mathbf{u}=A\mathbf{d}e^{i[q(\mathbf{n}\cdot\mathbf{x})-\omega t]} \tag{3.4.3.4}$$

Where A denotes the amplitude, $(\mathbf{d},\mathbf{n})$ are unit vectors along the directions of motion and propagation, respectively ($\mathbf{n}$ should not be confused with the outward unit vector normal to a boundary of the body), $\mathbf{x}$ is the position vector, q is the wavenumber and ω is the circular frequency of the plane wave. Upon substituting (3.4.3.4) into (3.4.3.1), (3.4.3.3), the following dispersion equations are obtained for the primary and the secondary waves:

$$\omega^2=\tilde{v}_1^2q_1^2\left(1+l_1^2q_1^2\right)\left(1+h_1^2q_1^2\right)^{-1} \tag{3.4.3.5}$$

$$\omega^2=\tilde{v}_2^2q_2^2\left(1+l_2^2q_2^2\right)\left(1+h_2^2q_2^2\right)^{-1} \tag{3.4.3.6}$$

Where q_1 and q_2 are wavenumbers that describe the motions of the primary and the secondary waves. Accordingly, the phase velocities of the longitudinal and shear waves $\tilde{v}_i^p$, $i=1,2$ in either of the three forms of Mindlin's general theory are given by:

$$\tilde{v}_1^p\equiv\frac{\omega}{q_1}=\tilde{v}_1^2\left(1+l_1^2q_1^2\right)^{1/2}\left(1+h_1^2q_1^2\right)^{-1/2} \tag{3.4.3.7}$$

$$\tilde{v}_2^p \equiv \frac{\omega}{q_2} = \tilde{v}_2^2 \left(1 + l_2^2 q_2^2\right)^{1/2} \left(1 + h_2^2 q_2^2\right)^{-1/2} \tag{3.4.3.8}$$

Equations (3.4.3.7), (3.4.3.8) show that the propagation velocities of body waves depend on the respective wavenumber. Hence, both waves are dispersive in the context of the three forms of Mindlin's general theory. To investigate further the nature of the dispersion relations (3.4.3.5), (3.4.3.6), we consider the group velocity $\tilde{v}_i^g = d\omega/dq_i$ at which the energy propagates in a dispersive medium [77]. By differentiating (3.4.3.6), (3.4.3.7) with respect to q_i and with the help of (3.4.3.5), (3.4.3.6), we obtain:

$$\tilde{v}_1^g = \tilde{v}_1^p + \left(l_1^2 - h_1^2\right) \tilde{v}_1 q_1^2 \left(1 + l_1^2 q_1^2\right)^{-1/2} \left(1 + h_1^2 q_1^2\right)^{-3/2} \tag{3.4.3.9}$$

$$\tilde{v}_2^g = \tilde{v}_2^p + \left(l_2^2 - h_2^2\right) \tilde{v}_2 q_2^2 \left(1 + l_2^2 q_2^2\right)^{-1/2} \left(1 + h_2^2 q_2^2\right)^{-3/2} \tag{3.4.3.10}$$

The following three cases are distinguished [79], which will appear very important later in the analysis of the scattering problems.

• For $l_i^2 < h_i^2$, equations (3.4.3.9), (3.4.3.10) imply that $\tilde{v}_i^g < \tilde{v}_i^p$, thus the dispersion is normal.

• For $l_i^2 > h_i^2$, equations (3.4.3.9), (3.4.3.10) imply that $\tilde{v}_i^g > \tilde{v}_i^p$, this case is characterized as anomalous dispersion.

• Finally, for $l_i^2 = h_i^2$, or ($l_i^2 \to 0$, $h_i^2 \to 0$), the wave velocities degenerate into the non-dispersive velocities of classical elastodynamics. This case presents a lot of interest, as it combines aspects of both classical elasticity (i.e., non-dispersion) and gradient elasticity (i.e., the existence of microstructure).

4 Fundamental Solutions

4.1 Introduction

In this chapter the process of deriving two new analytical solutions in the context of sub-theories that are generated from Mindlin's general theory is presented in great detail. We consider a problem where plane waves generated by body forces propagate through an infinite domain and we distinguish between the two cases of anti – plane shear and plain strain. In both cases the analytical solutions are derived using purely displacement formulation and the displacement equations of motion are solved analytically using integral transforms techniques. Because in the plane strain problem the equations that arise are quite extensive, the theory of dipolar gradient elasticity is adopted which represents the simplest possible version of Mindlin's general theory. In both cases the displacement Green's functions are given in closed form and their validity is ensured by the fact that they satisfy the displacement equations of motion, while the corresponding solutions of classical elasticity can be obtained as a special case when the microstructure parameters approach to zero. These Green's functions will appear very useful later when formulating the scattering problems because the pins will be modelled as concentrated body forces and due to the principle of superposition which generally applies to linear elasticity regardless whether the system is a Cauchy type continuum or not, we can determine the displacement fields even for cases where the pins define complex configurations.

4.2 Infinite Domain Under Anti - Plane Shear

4.2.1 Problem Statement

The first problem we will deal with pertains to the case where SH waves generated by a concentrated body force, propagate in a infinite domain that is described by form II of Mindlin's general theory. In order to formulate the equations that describe the problem we consider the case of anti-plane shear deformation, in this special case the displacements and the body forces have the following forms:

$$u_x = u_y = 0, \quad u_z = u_z(x, y, t) \tag{4.2.1.1}$$

$$F_x = F_y = 0, \quad F_z = F_z(x, y, t) \tag{4.2.1.2}$$

Under this circumstances the displacement equations of motion of form II given by (3.3.1.15), (3.3.2.29) degenerate to a single scalar differential equation. In order to illustrate this we begin by expanding the divergence of the displacement vector:

$$\nabla \cdot \mathbf{u} = \frac{\partial u_x}{\partial x} + \frac{\partial u_y}{\partial y} + \frac{\partial u_z}{\partial z} = 0 \tag{4.2.1.3}$$

By substituting (4.2.1.1) - (4.2.1.3) into (3.3.2.29) and taking also (3.4.1.9) into account we obtain the following equation, which describes the motion of a form II gradient material under anti - plane conditions:

$$\tilde{\mu}\left(1 - l_2^2\nabla^2\right)\nabla^2 u_z + \rho h_2^2 \nabla^2 \ddot{u}_z - \rho \ddot{u}_z + F_z = 0 \tag{4.2.1.4}$$

From (4.2.1.4) it is noticeable that the particles motion is polarized in the z direction, meaning that the resulting waves are shear waves SH. The SH notation refers to shear waves (or secondary waves). In the context of this work the displacement u_z and the body force F_z are supposed to have a harmonic time variation:

$$u_z(x, y, t) = U_z(x, y)e^{-i\omega t} \tag{4.2.1.5}$$

$$F_z(x, y, t) = P_z(x, y)e^{-i\omega t} \tag{4.2.1.6}$$

The equation of motion for time harmonic conditions is obtained by substituting (4.2.1.5), (4.2.1.6) into (4.2.1.4):

$$\tilde{\mu}\left(1 - l_2^2\nabla^2\right)\nabla^2 U_z - \rho h_2^2 \omega^2 \nabla^2 U_z + \rho\omega^2 U_z + P_z = 0 \tag{4.2.1.7}$$

It is also convenient to express (4.2.1.7) in Cartesian coordinates x, y, since it will be the main frame of reference that will be adopted in the analyses:

$$\begin{aligned} &- l_2^2\tilde{\mu}\left(\frac{\partial^4 U_z}{\partial x^4} + 2\frac{\partial^4 U_z}{\partial x^2 \partial y^2} + \frac{\partial^4 U_z}{\partial y^4}\right) + \left(\tilde{\mu} - \rho h_2^2\omega^2\right)\left(\frac{\partial^2 U_z}{\partial x^2} + \frac{\partial^2 U_z}{\partial y^2}\right) \\ &+ \rho\omega^2 U_z + P_z = 0 \end{aligned} \tag{4.2.1.8}$$

The displacement U_z will be determined by solving (4.2.1.8). However, this is not necessary since the equation of motion of Kirchhoff plates under certain conditions which will be stated later is practically the same as (4.2.1.4). Nevertheless, the procedure of solving (4.2.1.8) will be presented in detail for the sake of completeness.

4.2.2 Correspondence to Classical Plate Theory

Another mechanical system that is described by a differential equation of motion in the form of (4.2.1.4) is the Kirchhoff plate, when an isotropic prestress is also taken into account. The Kirchhoff - Love theory of plates, also known as the classical plate theory (CPT) was developed in 1888 by Love [80] using assumptions proposed by Kirchhoff [81] in 1850 and is an extension of the Euler - Bernoulli beam theory to plates. The development of the classical (Kirchhoff - Love) plate theory is based on three basic assumptions:

(1) Straight lines perpendicular to the mid-surface (i.e., transverse normals) before deformation remain straight after deformation,

(2) The transverse normals do not experience elongation (i.e., they are inextensible).

(3) The transverse normals rotate such that they remain perpendicular to the mid-surface after deformation.

To examine the consequences of the Kirchhoff hypothesis, we consider a plate of uniform thickness h. We use as a frame of reference rectangular Cartesian coordinates (x, y, z) with the xy plane coinciding with the middle plane of the plate. The total displacement components of a point of the plate are (u, v, w). When deformed a material point with coordinates (x, y, z) in the unreformed pate moves to the position $(x + u, y + v, z + w)$ in the deformed plate. Assumptions (1), (2) imply that the normal strain along the thickness direction is zero:

$$\epsilon_{zz} = \frac{\partial w}{\partial z} = 0 \tag{4.2.2.1}$$

Equation (4.2.2.1) implies that w is independent of the coordinate z, while assumption (3) results in zero traverse shear strains:

$$\epsilon_{xz} = \frac{\partial u}{\partial z} + \frac{\partial w}{\partial x} = 0, \quad \epsilon_{yz} = \frac{\partial v}{\partial z} + \frac{\partial w}{\partial y} = 0 \tag{4.2.2.2}$$

By integrating equations (4.2.2.2) with respect to z and taking into account that w is independent of z, we obtain the following form for the displacement field:

$$u(x, y, z, t) = u_0(x, y, t) - z\frac{\partial w(x, y, z, t)}{\partial x} \tag{4.2.2.3}$$

$$v(x, y, z, t) = v_0(x, y, t) - z\frac{\partial w(x, y, z, t)}{\partial y} \tag{4.2.2.4}$$

$$w(x,y,z,t) = w_0(x,y,t) \tag{4.2.2.5}$$

Where (u_0, v_0, w_0) denote the displacements of a material point on the middle plane $(x, y, 0)$. It is also noted that u_0, v_0 are associated with extensional deformation of the plate, while w_0 denotes the bending deflection. For the general case of a prestressed Kirchhoff plate on top of elastic springs where thermal effects are also taken into account, the equation of motion in the transverse direction is given by Reddy, (equation (3.4.17) in [82]).

$$\begin{aligned} &- D_{11}\frac{\partial^4 w_0}{\partial x^4} - 2\left(D_{12}+2D_{66}\right)\frac{\partial^4 w_0}{\partial x^2 \partial y^2} - D_{22}\frac{\partial^4 w_0}{\partial y^4} - k w_0 \\ &- \left(\frac{\partial^2 M_{xx}^T}{\partial x^2} + 2\frac{\partial^2 M_{xy}^T}{\partial x \partial y} + \frac{\partial^2 M_{yy}^T}{\partial y^2}\right) + \mathscr{N}(u_0, v_0, w_0) + q \\ &= I_0 \frac{\partial^2 w_0}{\partial t^2} - I_2 \frac{\partial^2}{\partial t^2}\left(\frac{\partial^2 w_0}{\partial x^2} + \frac{\partial^2 w_0}{\partial y^2}\right) \end{aligned} \tag{4.2.2.6}$$

In (4.2.2.6) D_{ij} are the bending stiffness coefficients, k is the springs coefficient, M_{ij}^T are the thermal moments, q is a distributed surface load, $I_0 = \rho h$, $I_2 = \rho h^3/12$ and $\mathscr{N}$ is given by:

$$\mathscr{N} = \frac{\partial}{\partial x}\left(N_{xx} + \frac{\partial w_0}{\partial x} + N_{xy} + \frac{\partial w_0}{\partial y}\right) + \frac{\partial}{\partial y}\left(N_{xy} + \frac{\partial w_0}{\partial x} + N_{yy} + \frac{\partial w_0}{\partial y}\right) \tag{4.2.2.7}$$

The terms N_{ij} that appear in (4.2.2.7) represent the normal and shear prestress forces that act on the plate. For the case where the prestress is isotropic (i.e., $N_{xx} = N_{yy} = N$, $N_{xy} = 0$), (4.2.2.7) yields:

$$\mathscr{N} = N\left(\frac{\partial^2 w_0}{\partial x^2} + \frac{\partial^2 w_0}{\partial y^2}\right) = N\nabla^2 w_0 \tag{4.2.2.8}$$

Also if the plate is isotropic then the bending stiffness coefficients that appear in (4.2.2.6) are: $D_{11} = D_{22} = D$, $D_{12} = vD$, $2D_{66} = (1-v)D$, where D is the flexural rigidity of the isotropic plate:

$$D = \frac{Eh^3}{12(1-v^2)} \tag{4.2.2.9}$$

By substituting the above expressions into (4.2.2.6) and ignoring the thermal moments and the existence of the springs, we obtain:

$$\begin{aligned} &- D\left(\frac{\partial^4 w_0}{\partial x^4} - 2\frac{\partial^4 w_0}{\partial x^2 \partial y^2} - \frac{\partial^4 w_0}{\partial y^4}\right) + N\left(\frac{\partial^2 w_0}{\partial x^2} + \frac{\partial^2 w_0}{\partial y^2}\right) + q \\ &= \rho h\left[1 - \frac{h^2}{12}\left(\frac{\partial^2}{\partial x^2} + \frac{\partial^2}{\partial y^2}\right)\right]\frac{\partial^2 w_0}{\partial t^2} \end{aligned} \tag{4.2.2.10}$$

Or using vector notation:

$$N\left(1 - \frac{D}{N}\nabla^2\right)\nabla^2 w_0 + q = \rho h\left(1 - \frac{h^2}{12}\nabla^2\right)\ddot{w}_0 \tag{4.2.2.11}$$

Equation (4.2.2.11) is identical to (4.2.1.4), with the only difference being the coefficients upfront of the derivatives, meaning that the Green's function of a form II infinite domain under anti - plane shear will be the same as that of a prestressed Kirchhoff plate. Also by comparing (4.2.2.11) and (4.2.1.4) it is easy to find the correspondence between the microstructure parameters and the quantities that appear in classical plate theory. Specifically, the gradient coefficient l_2^2 can be correlated with D/N, while the characteristic length of the material h_2^2 has a similar role as the thickness of the plate h. Equation (4.2.2.11) has been solved for various types of loads including the time harmonic case which is of particular interest. In this case (4.2.2.11) degenerates into a bi - Helmholtz differential equation similar to (4.2.1.8) the general solution of which can be found in many textbooks. Nevertheless the procedure of deriving the general solution of (4.2.2.8) will be presented in detail.

4.2.3 Derivation of the Green's Function

The differential equation presented in (4.2.1.8) will be solved using the double Fourier transform, which is defined as:

$$\hat{\hat{f}}(\xi,\eta) = \int_{-\infty}^{+\infty}\int_{-\infty}^{+\infty} f(x,y)e^{-i(\xi x+\eta y)}\,dx\,dy \tag{4.2.3.1}$$

The inverse double Fourier transform is respectively defined as:

$$f(x,y) = \frac{1}{4\pi^2}\int_{-\infty}^{+\infty}\int_{-\infty}^{+\infty} \hat{\hat{f}}(\xi,\eta)e^{i(\xi x+\eta y)}\,d\xi\,d\eta \tag{4.2.3.2}$$

By applying the double Fourier transform in (4.2.1.8) for the case where $P_z(x,y) = \delta(x)\delta(y)p_z$, we obtain the following expression for the transformed displacement:

$$\hat{\hat{U}}_z = \frac{\hat{\hat{p}}_z}{\tilde{\mu}(\xi^2+\eta^2)[l_2^2(\xi^2+\eta^2)+1] - [h_2^2(\xi^2+\eta^2)+1]\rho\omega^2} \tag{4.2.3.3}$$

Applying the double inverse Fourier transform in (4.2.3.3) yields:

$$\hat{\hat{U}}_z = \frac{p_z}{4\pi^2}\int_{-\infty}^{+\infty}\int_{-\infty}^{+\infty} \frac{e^{i(\xi x+\eta y)}}{\tilde{\mu}(\xi^2+\eta^2)[l_2^2(\xi^2+\eta^2)+1] - [h_2^2(\xi^2+\eta^2)+1]\rho\omega^2}\, d\xi\, d\eta \tag{4.2.3.4}$$

In order to determine the integral presented in (4.2.3.4) it is convenient to use as a frame of reference polar coordinates. The spatial coordinates (x,y) and the components of the wavenumber (ξ,η) can be transformed into polar coordinates as:

$$x = r\cos(\theta), \quad y = r\sin(\theta), \quad r^2 = x^2+y^2 \tag{4.2.3.5}$$

$$\xi = k\cos(\phi), \quad \eta = k\sin(\phi), \quad k^2 = \xi^2+\eta^2 \tag{4.2.3.6}$$

Using (4.2.3.5), (4.2.3.6) as well as the fact that the Jacobian of the above transformation is $J = k$, (4.2.3.4) can be written as.

$$\hat{\hat{U}}_z = \frac{p_z}{4\pi^2}\int_0^{2\pi}\int_0^{\infty} \frac{e^{-ikr[\cos(\phi)\cos(\theta)+\sin(\phi)\sin(\theta)]}}{\tilde{\mu}(l_2^2k^2+1)k^2 - (h_2^2k^2+1)\rho\omega^2} k\, dk\, d\phi \tag{4.2.3.7}$$

The above integral can be simplified thanks to the following trigonometric identity:

$$\cos(\phi)\cos(\theta) + \sin(\phi)\sin(\theta) = \cos(\phi-\theta) \tag{4.2.3.8}$$

By substituting (4.2.3.8) into (4.2.3.7) we obtain:

$$\hat{\hat{U}}_z = \frac{p_z}{4\pi^2}\int_0^{2\pi}\int_0^{\infty} \frac{e^{-ikr\cos(\phi-\theta)}}{\tilde{\mu}(l_2^2k^2+1)k^2 - (h_2^2k^2+1)\rho\omega^2} k\, dk\, d\phi \tag{4.2.3.9}$$

While the integral can be simplified even further by just rearranging the terms:

$$\hat{\tilde{U}}_z = \frac{p_z}{2\pi}\int_0^{\infty} \frac{k}{\tilde{\mu}(l_2^2k^2+1)k^2-(h_2^2k^2+1)\rho\omega^2}\left[\frac{1}{2\pi}\int_0^{2\pi} e^{-ikr\cos(\phi-\theta)}\,d\phi\right]dk \tag{4.2.3.10}$$

The term inside the brackets in (4.2.3.10) corresponds to the Bessel function of the first kind of order zero $J_0(kr)$. Therefore (4.2.3.10) becomes:

$$\hat{\tilde{U}}_z = \frac{p_z}{2\pi}\int_0^{\infty} \frac{k}{\tilde{\mu}(l_2^2k^2+1)k^2-(h_2^2k^2+1)\rho\omega^2}J_0(kr)\,dk \tag{4.2.3.11}$$

Where:

$$J_0(kr) = \frac{1}{2\pi}\int_0^{2\pi} e^{-ikr\cos(\phi-\theta)}\,d\phi \tag{4.2.3.12}$$

The following result arises by inserting (3.4.2.5) into (4.2.3.11):

$$\hat{\tilde{U}}_z = \frac{p_z}{2\pi\tilde{\mu}}\int_0^{\infty} \frac{k}{(l_2^2k^2+1)k^2-(h_2^2k^2+1)\tilde{k}_2^2}J_0(kr)\,dk \tag{4.2.3.13}$$

The quantity $\tilde{k}_2$ denotes the wave number along the direction that the SH wave propagates:

$$\tilde{k}_2 = \frac{\omega}{\tilde{v}_2} \tag{4.2.3.14}$$

The roots of the denominator in (4.2.3.13) are:

$$p = \pm\sqrt{\frac{h_2^2\tilde{k}_2^2-1-\sqrt{4l_2^2\tilde{k}_2^2+\left(h_2^2\tilde{k}_2^2-1\right)^2}}{2l_2^2}} \tag{4.2.3.15}$$

$$q = \pm\sqrt{\frac{h_2^2\tilde{k}_2^2-1+\sqrt{4l_2^2\tilde{k}_2^2+\left(h_2^2\tilde{k}_2^2-1\right)^2}}{2l_2^2}} \tag{4.2.3.16}$$

It is noted that the denominator in (4.2.3.13) is the same as the dispersion equation (3.4.3.6), while the roots p, q correspond to q_2 in (4.2.3.6). By applying partial fraction decomposition the transformed function in (4.2.3.13) can be expressed as:

$$\frac{k}{\tilde{\mu}(l_2^2k^2+1)k^2-(h_2^2k^2+1)\tilde{k}_2^2}=\frac{k}{l_2^2}\left(\frac{A}{k-p}+\frac{B}{k+p}+\frac{\Gamma}{k-q}+\frac{\Delta}{k+q}\right) \tag{4.2.3.17}$$

Where the coefficients A, B, Γ, Δ are given by:

$$\begin{aligned} A&=\frac{1}{2p\,(p^2-q^2)}, \quad B=-\frac{1}{2p\,(p^2-q^2)},\\ \Gamma&=\frac{1}{2q\,(q^2-p^2)}, \quad \Delta=-\frac{1}{2q\,(q^2-p^2)} \end{aligned} \tag{4.2.3.18}$$

Therefore the transformed function in (4.2.3.13) can be written as:

$$\frac{k}{\tilde{\mu}(l_2^2k^2+1)k^2-(h_2^2k^2+1)\tilde{k}_2^2}=\frac{1}{l_2^2}\left[\frac{k}{(k^2-p^2)\,(p^2-q^2)}+\frac{k}{(k^2-q^2)\,(q^2-p^2)}\right] \tag{4.2.3.19}$$

By substituting (4.2.3.19) into (4.2.3.13) we obtain:

$$\hat{\hat{U}}_z=\frac{p_z}{2\pi\tilde{\mu}l_2^2\,(p^2-q^2)}\left[\int_0^\infty\frac{k}{(k^2-p^2)}J_0(kr)\,dk-\frac{k}{(k^2-q^2)}J_0(kr)\,dk\right] \tag{4.2.3.20}$$

The integrals that appear in (4.2.3.20) can be determined using the following identity that relates Bessel functions of the same order but of different kind, (see formula 1, page 424 in [83]).

$$\begin{aligned} &\int_0^\infty[(1+e^{i(b-n)})J_n(kr)+i(1-e^{i(b-n)})Y_n(kr)]\frac{k^{b-1}}{(k^2-\lambda^2)^{m+1}}\,dk\\ &=\frac{i\pi}{2^m m!}\left(\frac{d}{\lambda d\lambda}\right)^m\lambda^{b-2}H_n^{(1)}(\lambda r) \end{aligned} \tag{4.2.3.21}$$

Where Y_n is the Bessel function of the second kind of order n, $H_n^{(1)}$ is the Hankel function of the first kind (or equivalently the Bessel function of the third kind), r is a real positive

number, m is a positive integer or zero and λ is a complex number with positive imaginary part, while the following inequalities must also hold for (4.2.3.21) to be applicable:

$$|\Re(n)| < \Re(b) < 2m + \frac{7}{2} \tag{4.2.3.22}$$

Equation (4.2.3.21) for $b = 2$, $n = m = 0$ yields:

$$\int_0^\infty [(1 + e^{2i\pi})J_0(kr) + i(1 - e^{2i\pi})Y_0(kr)]\frac{k}{k^2 - \lambda^2}\, dk = i\pi H_0^{(1)}(\lambda r) \tag{4.2.3.23}$$

The above expression can be simplified with the help of Euler's formula:

$$e^{ix} = \cos(x) + i\sin(x) \tag{4.2.3.24}$$

By setting into (4.2.3.24) $x = 2\pi$, we obtain $e^{i2\pi} = 1$, so due to this result (4.2.3.23) becomes:

$$\int_0^\infty \frac{k}{k^2 - \lambda^2} J_0(kr)\, dk = \frac{i\pi}{2} H_0^1(\lambda r) \tag{4.2.3.25}$$

The expression of U_z is finally obtained by applying (4.2.3.25) twice for $\lambda = p$, $\lambda = q$ and then substituting the results into (4.2.3.20):

$$U_z(r) = \frac{p_z}{4l_2^2\tilde{\mu}\,(p^2 - q^2)} i \left[H_0^{(1)}(pr) - H_0^{(1)}(qr)\right] \tag{4.2.3.26}$$

From (4.2.3.15), (4.2.3.16) it is clear that $\pm q$ are the real routes of the dispersion equation, while $\pm p$ are the imaginary routes of the dispersion equation. Having this in mind, (4.2.3.26) can be written in terms of Hankel functions and modified Bessel functions with real arguments as presented bellow:

$$U_z(r) = \frac{p_z}{4l_2^2\tilde{\mu}\pi\,(P^2 + q^2)} \left[i\pi H_0^{(1)}(qr) - 2K_0(Pr)\right] \tag{4.2.3.27}$$

Where $p = iP$ and K_0 is the modified Bessel function of order n, which is related to the Hankel functions $H_n^{(1)}$, $H_n^{(2)}$ as:

$$K_n(x) = \begin{cases} \frac{\pi}{2} i^{n+1} H_n^{(1)}(ix), & -\pi \leq arg(x) \leq \frac{\pi}{2} \\ \frac{\pi}{2}(-i)^{n+1} H_n^{(2)}(-ix), & -\frac{\pi}{2} \leq arg(x) \leq \pi \end{cases} \tag{4.2.3.28}$$

From (4.2.3.27) it can be seen that the $H_0^{(1)}$ term is associated with outgoing waves while the K_0 term is associated with evanescent modes. Another major advantage that (4.2.3.27) offers compared to (4.2.3.26) is that it is much more appropriate for performing computations, since in (4.2.3.27) all the arguments are real, while in (4.2.3.26) p is imaginary. Using (4.2.3.27) we can express the problem's Green's function by performing a coordinate system shift:

$$g(\mathbf{r};\mathbf{r}') = \frac{p_z}{4l_2^2\tilde{\mu}\pi\left(P^2+q^2\right)}\left[i\pi H_0^{(1)}(qs) - 2K_0(Ps)\right] \tag{4.2.3.29}$$

Where $s = |\mathbf{r} - \mathbf{r}'|$ The Green's function $g(\mathbf{r};\mathbf{r}')$ expresses the displacement of a point with position vector $\mathbf{r}$ in the z direction due to a concentrated force of magnitude p_z at a point with position vector $\mathbf{r}'$ along the same direction. It is also noted that (4.2.3.29) is bounded in the limit where $\mathbf{r} \to \mathbf{r}'$:

$$g(\mathbf{r};\mathbf{r}') \sim \frac{p_z}{l_2^2\tilde{\mu}}\left[\frac{i\pi + 2\ln\left(P/q\right)}{4\pi\left(P^2+q^2\right)} + \frac{s^2 ln(s)}{8\pi}\right] + O(s^2) \tag{4.2.3.30}$$

4.2.4 Displacement Contours

For plotting the displacement contours it is convenient to introduce the following non-dimensional variables:

$$H = \frac{h_2}{l_2} \tag{4.2.4.1}$$

$$K_2 = l_2\tilde{k}_2 \tag{4.2.4.2}$$

$$R = \frac{r}{l_2} = \frac{s\tilde{k}_2}{K_2} \tag{4.2.4.3}$$

$$\bar{U}_z = \frac{\tilde{\mu}U_z}{p_z} \tag{4.2.4.4}$$

Where H is the non-dimensional characteristic length of the material, K_2 is a non-dimensional wave number, R is the non-dimensional radial coordinate and $\bar{U}_z$ is the non-dimensional

displacement. By substituting (4.2.4.1) - (4.2.4.3) into (4.2.3.15), (4.2.3.16) the following expressions for the roots of the dispersion equation arise:

$$p=\pm\sqrt{\frac{H^2K_2^2-1-\sqrt{4K_2^2+\left(H^2K_2^2-1\right)^2}}{2K_2^2}\tilde{k}_2^2} \tag{4.2.4.5}$$

$$q=\pm\sqrt{\frac{H^2K_2^2-1+\sqrt{4K_2^2+\left(H^2K_2^2-1\right)^2}}{2K_2^2}\tilde{k}_2^2} \tag{4.2.4.6}$$

In view of (4.2.3.27), (4.2.4.1) - (4.2.4.4) the non - dimensional Green's function is:

$$\bar{g}(\mathbf{r};\mathbf{r}')=\frac{1}{4\pi\left(P^2+q^2\right)}\left[i\pi H_0^{(1)}(qs)-2K_0(Ps)\right] \tag{4.2.4.7}$$

Where:

$$p^2-q^2=-\sqrt{\frac{4K_2^2+\left(H^2K_2^2-1\right)^2}{l_2^2}} \tag{4.2.4.8}$$

$$ps=\pm\sqrt{\frac{H^2K_2^2-1-\sqrt{4K_2^2+\left(H^2K_2^2-1\right)^2}}{2}R} \tag{4.2.4.9}$$

$$ps=\pm\sqrt{\frac{H^2K_2^2-1+\sqrt{4K_2^2+\left(H^2K_2^2-1\right)^2}}{2}R} \tag{4.2.4.10}$$

The expressions of p, q are now given by (4.2.4.9), (4.2.4.10) and when (4.2.4.7), (or (4.2.3.26), (4.2.3.27), (4.2.3.29)) are used only the positive roots are taken into account. It is also noted that in view of (4.2.4.8) - (4.2.4.10), the radial coordinate r and the gradient coefficient l_2 do not appear in (4.2.4.7). The non-dimensional displacement contours are determined using (4.2.4.7), we distinguish the cases of normal ($H>1$), anomalous ($H<1$) and no dispersion ($H=1$) by adjusting the value of H and for each one of the three cases we examine the effect of the parameter K_2. In the figures that follow the contours for the real part, the imaginary part and the norm of the non-dimensional displacement $\bar{U}_z$ are presented, for the case where the body force is applied at the origin of the coordinate system.

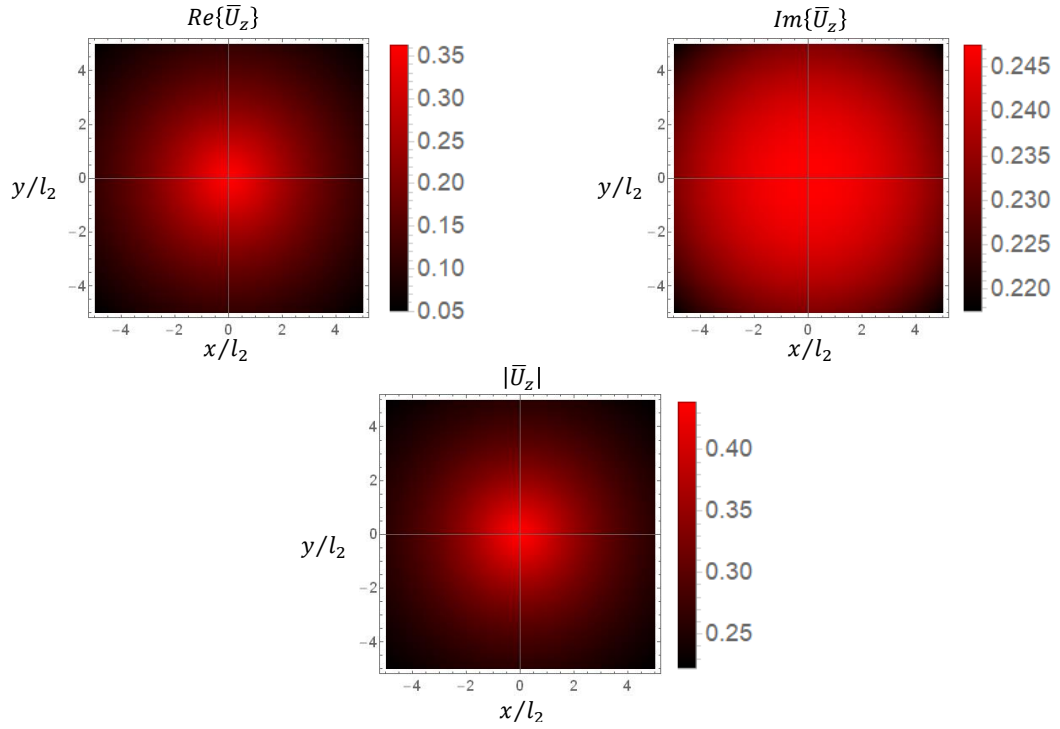

Figure 4.2.4.1: Displacement contours for $H = 1$, $K_2 = 0.1$, (no dispersion).

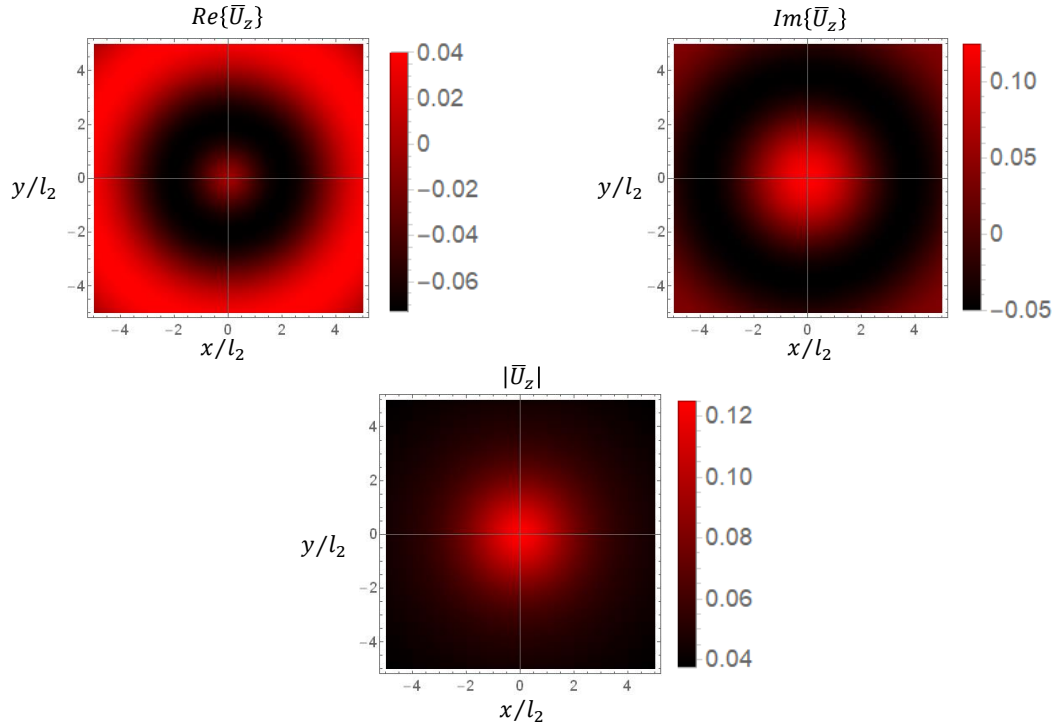

Figure 4.2.4.2: Displacement contours for $H = 1$, $K_2 = 1$, (no dispersion).

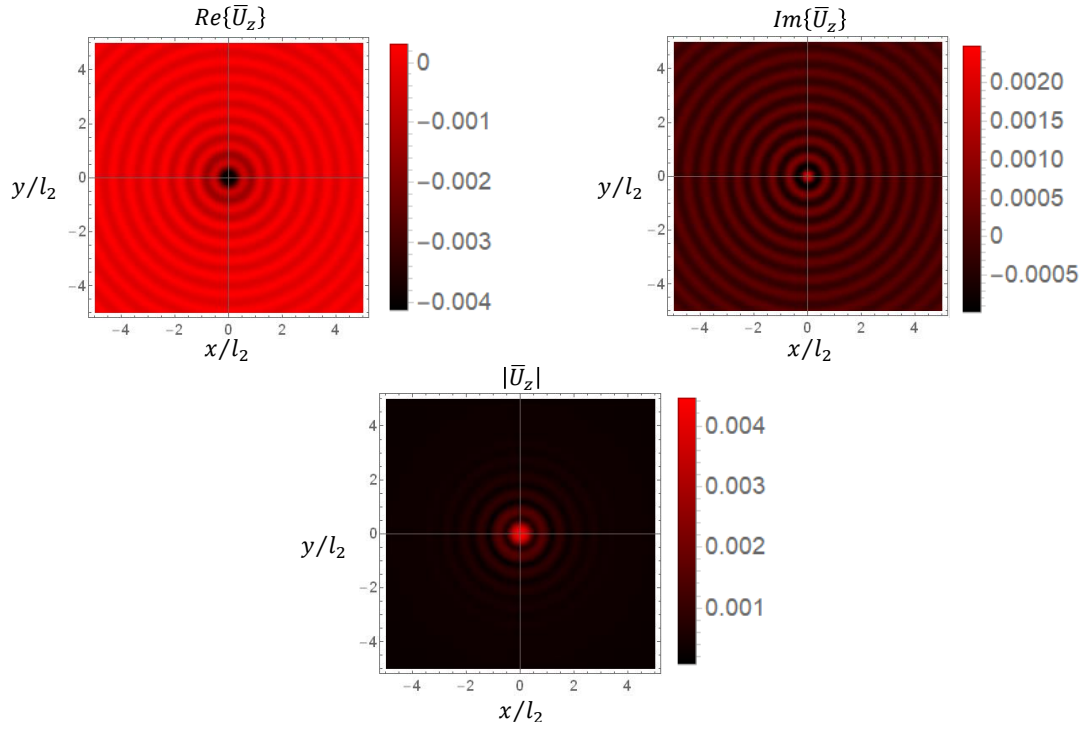

Figure 4.2.4.3: Displacement contours for $H = 1$, $K_2 = 10$, (no dispersion).

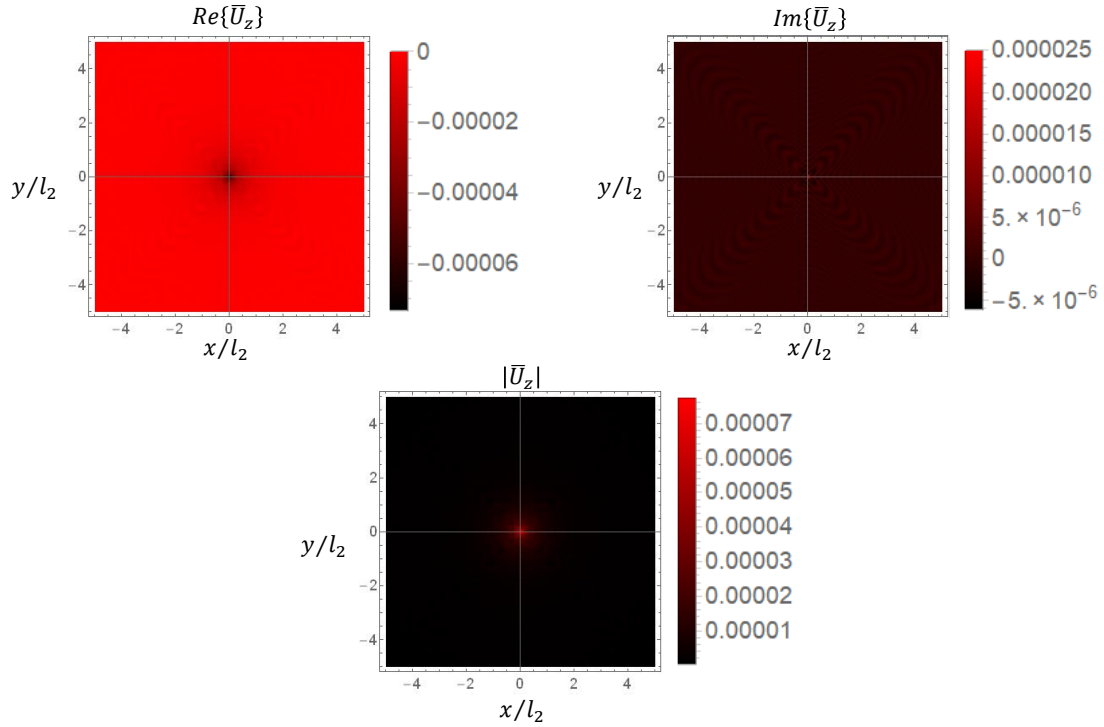

Figure 4.2.4.4: Displacement contours for $H = 1$, $K_2 = 100$, (no dispersion).

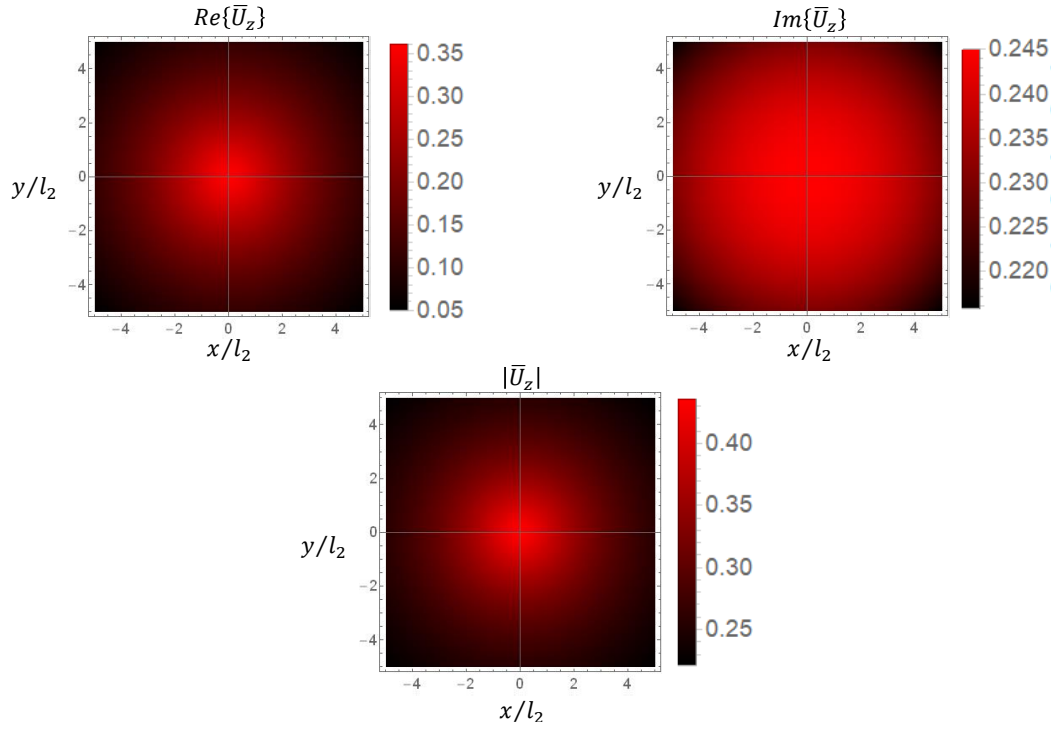

Figure 4.2.4.5: Displacement contours for $H = 0.1$, $K_2 = 0.1$, (anomalous dispersion).

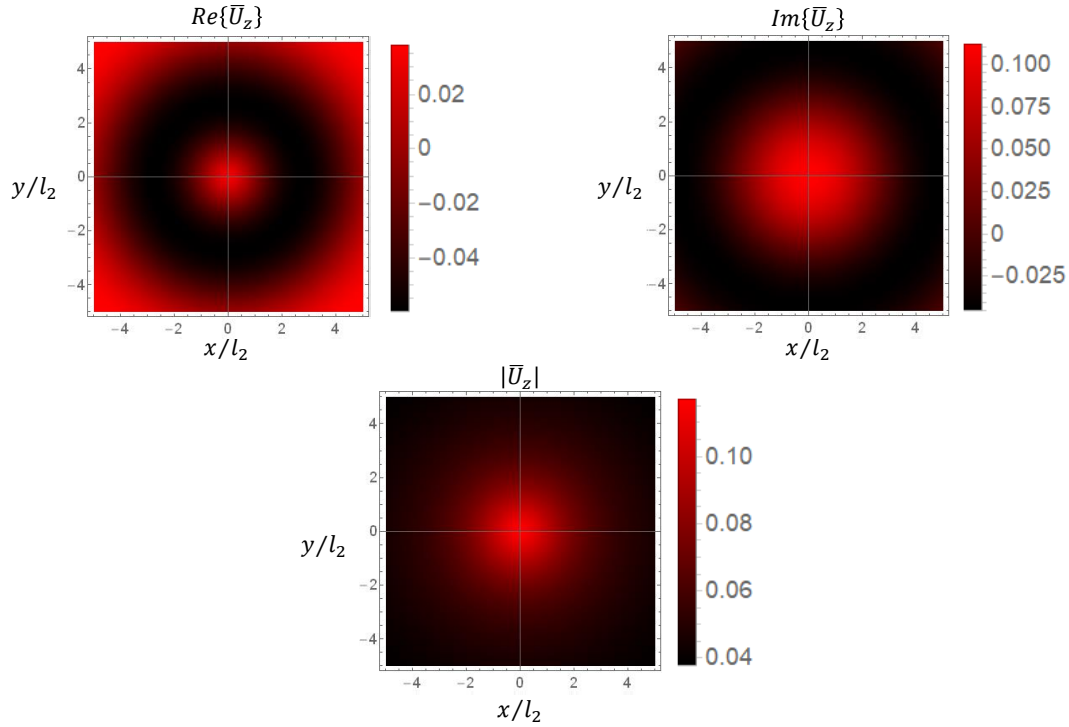

Figure 4.2.4.6: Displacement contours for $H = 0.1$, $K_2 = 1$, (anomalous dispersion).

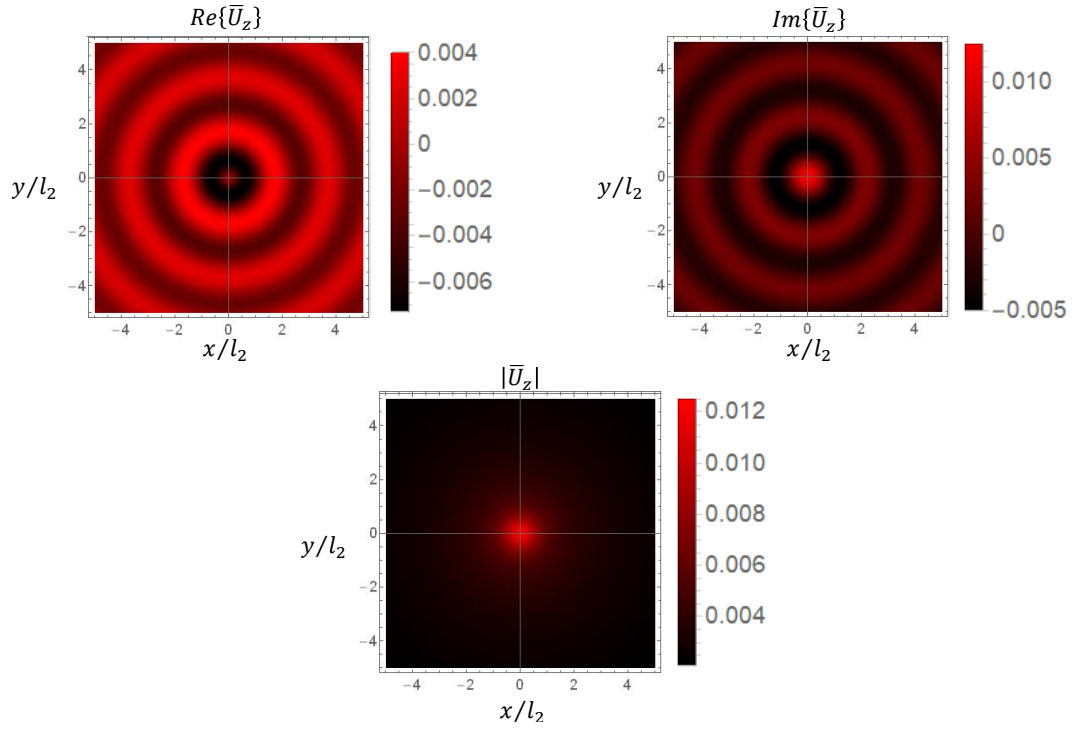

Figure 4.2.4.7: Displacement contours for $H = 0.1$, $K_2 = 10$, (anomalous dispersion).

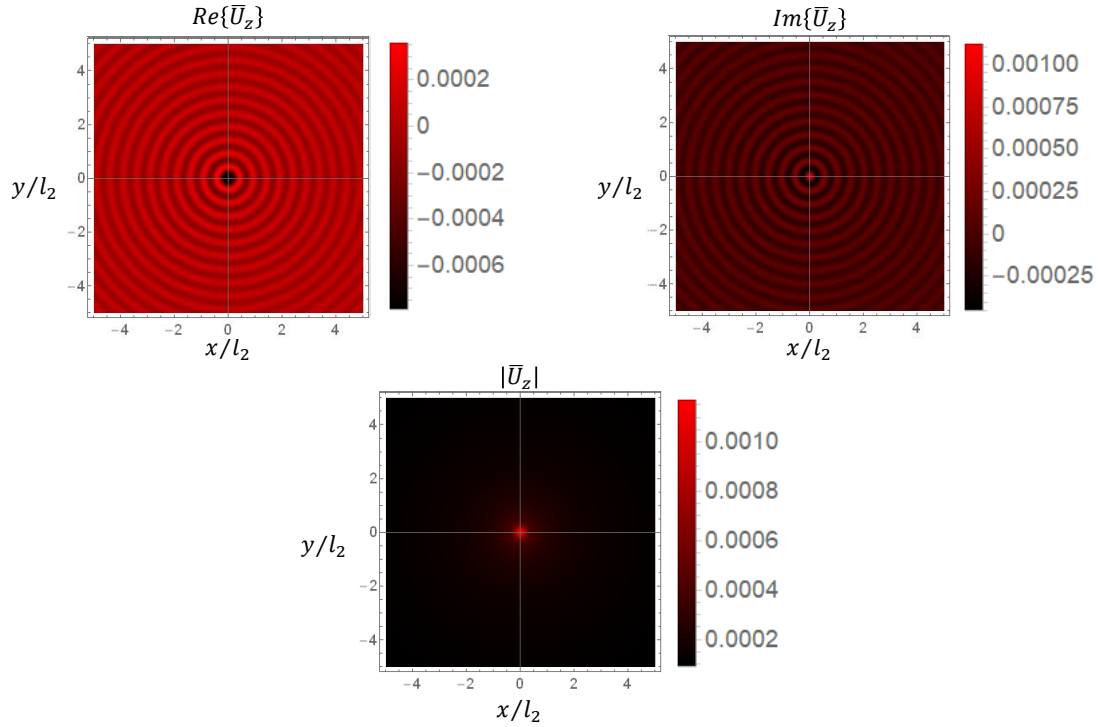

Figure 4.2.4.8: Displacement contours for $H = 0.1$, $K_2 = 100$, (anomalous dispersion).

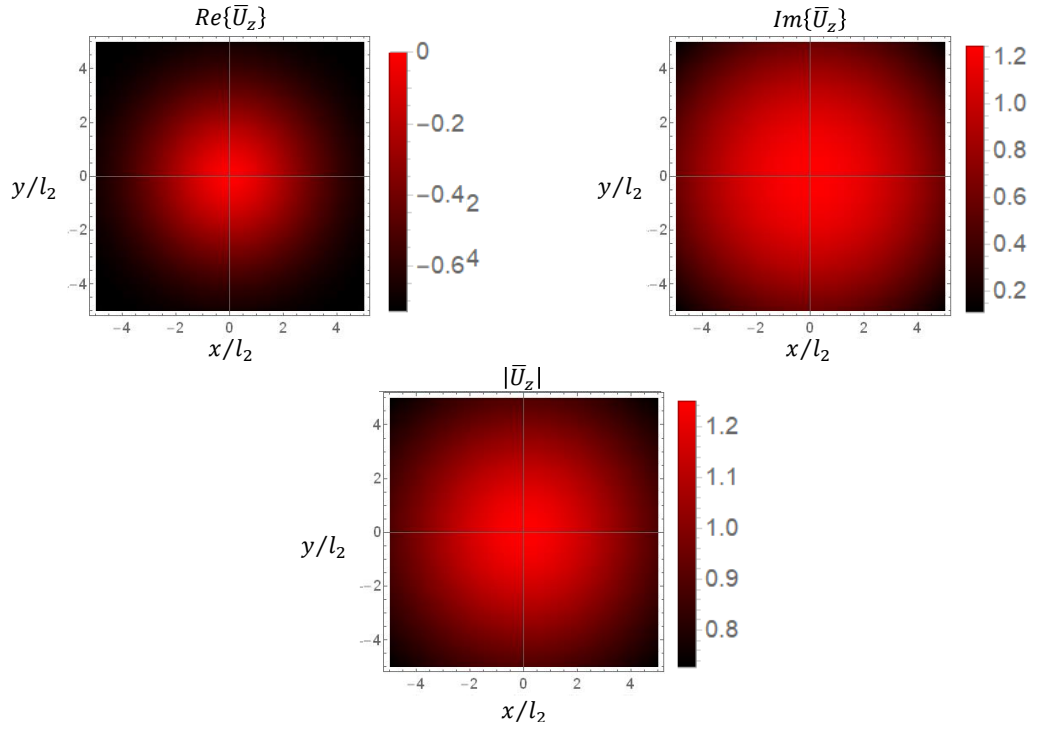

Figure 4.2.4.9: Displacement contours for $H = 10$, $K_2 = 0.1$, (normal dispersion).

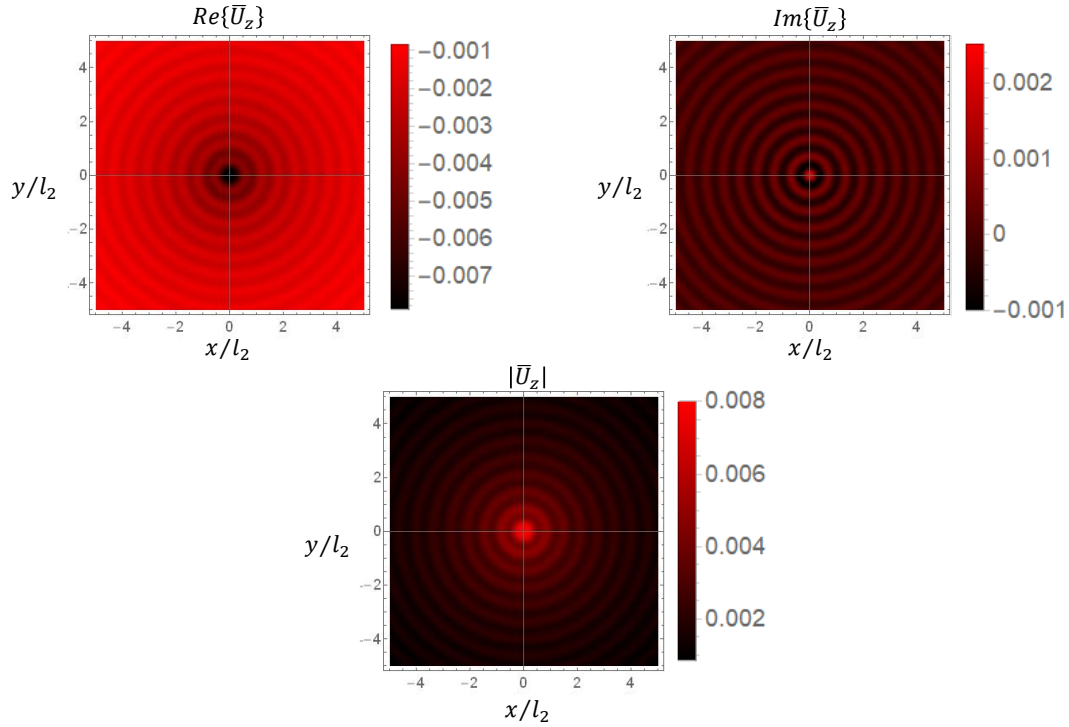

Figure 4.2.4.10: Displacement contours for $H = 10$, $K_2 = 1$, (normal dispersion).

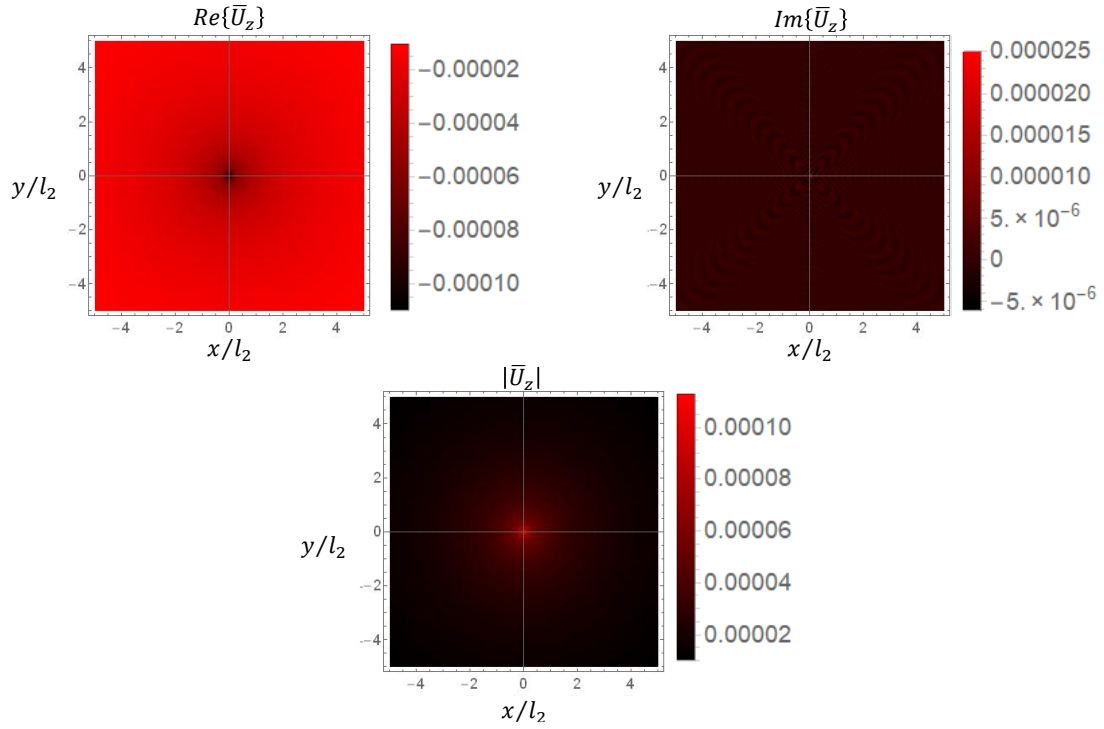

Figure 4.2.4.11: Displacement contours for $H = 10$, $K_2 = 10$, (normal dispersion).

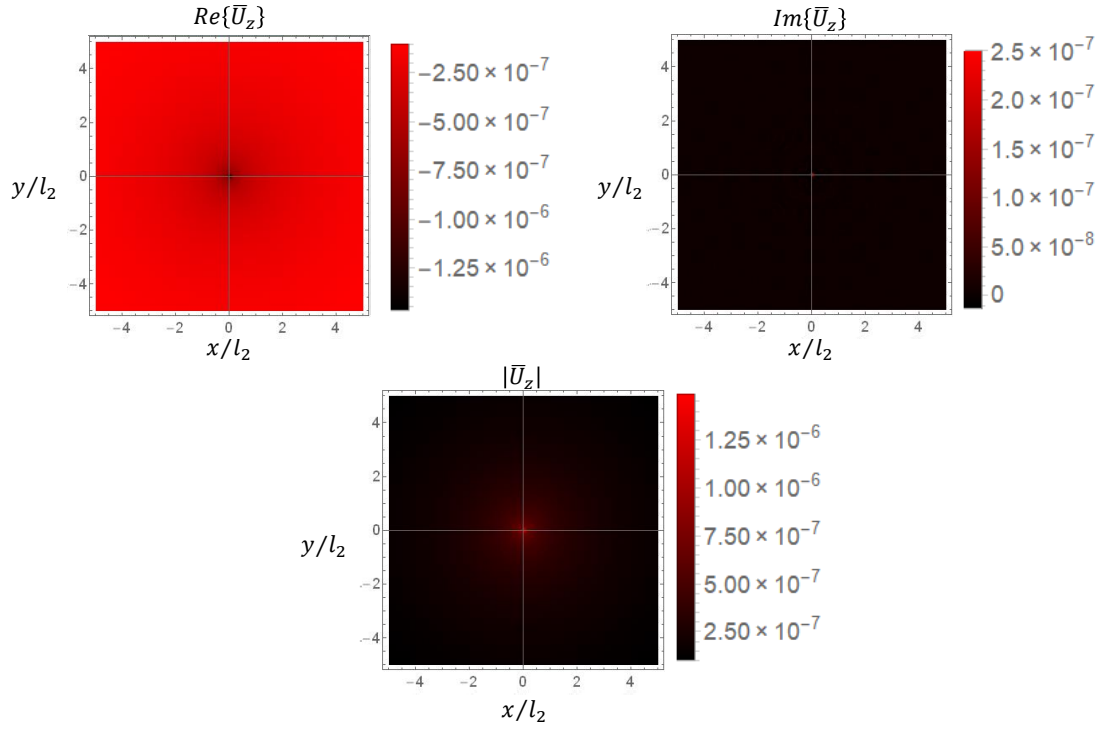

Figure 4.2.4.12: Displacement contours for $H = 10$, $K_2 = 100$, (normal dispersion).

The following conclusions are obtained by observing the above figures:

• Unlike the case of classical elasticity where the Green's function of the corresponding problem is singular at the point where the body force is applied, here the value of the Green's function is finite.

• For a fixed value of H the non-dimensional displacement decrease as the value of K_2 increases.

• In the cases of anomalous dispersion and no dispersion for $K_2 \leq 1$ the non-dimensional displacement contours are practically the same for a fixed value of K_2, regardless the value of H.

• Qualitatively the response of the system does not depend from the values of H, K_2. However, in the scattering problems that will be examined later, which are formulated using the problem's Green's function, it will be shown that the response of the system will be affected from the values of H, K_2 both quantitatively and qualitatively, (i.e. bifurcations will appear as the system's parameters H, K_2 approach specific values).

4.3 Infinite Domain Under Plane Strain

4.3.1 Definition of the Problem

In the second problem that we examine, the infinite domain is under plane conditions, meaning that both P and SV waves will propagate inside the domain. From a mathematical point of view, this is much more challenging case compared to anti-plane shear because the differential equations of motion are coupled. For this reason, the theory of dipolar gradient elasticity is adopted in order to simplify the resulting equations as much as possible. The plane strain conditions for the displacements and the body forces are:

$$u_x = u_x(x, y, t), \quad u_y = u_y(x, y, t), \quad u_z = 0 \tag{4.3.1.1}$$

$$F_x = F_x(x, y, t), \quad F_y = F_y(x, y, t), \quad F_z = 0 \tag{4.3.1.2}$$

Substituting the above expressions into (3.3.3.7) results to the following system of coupled PDEs:

$$(\lambda+\mu)(1-l^2\nabla^2)\frac{\partial}{\partial x}\left(\frac{\partial u_x}{\partial x}+\frac{\partial u_y}{\partial y}\right)+\mu(1-l^2\nabla^2)\left(\frac{\partial^2 u_x}{\partial x^2}+\frac{\partial^2 u_x}{\partial y^2}\right)+F_x$$
$$=\rho\ddot{u}_x-I\left(\frac{\partial^2\ddot{u}_x}{\partial x^2}+\frac{\partial^2\ddot{u}_x}{\partial x^2}\right) \tag{4.3.1.3}$$

$$(\lambda+\mu)(1-l^2\nabla^2)\frac{\partial}{\partial y}\left(\frac{\partial u_x}{\partial x}+\frac{\partial u_y}{\partial y}\right)+\mu(1-l^2\nabla^2)\left(\frac{\partial^2 u_y}{\partial x^2}+\frac{\partial^2 u_y}{\partial y^2}\right)+F_y$$
$$=\rho\ddot{u}_y-I\left(\frac{\partial^2\ddot{u}_y}{\partial x^2}+\frac{\partial^2\ddot{u}_y}{\partial y^2}\right) \tag{4.3.1.4}$$

Once again, the displacement and body force components are supposed to have a harmonic time variation:

$$u_j(x,y,t)=U_j(x,y)e^{-i\omega t},\quad j=x,y \tag{4.3.1.5}$$

$$F_j(x,y,t)=P_j(x,y)e^{-i\omega t},\quad j=x,y \tag{4.3.1.6}$$

The equations of motion for time harmonic conditions are obtained by substituting (4.3.1.5), (4.2.3.6) into (4.2.1.3), (4.2.1.4):

$$(\lambda+\mu)(1-l^2\nabla^2)\frac{\partial}{\partial x}\left(\frac{\partial U_x}{\partial x}+\frac{\partial U_y}{\partial y}\right)+\mu(1-l^2\nabla^2)\left(\frac{\partial^2 U_x}{\partial x^2}+\frac{\partial^2 U_x}{\partial y^2}\right)$$
$$-I\omega^2\left(\frac{\partial^2 U_x}{\partial x^2}+\frac{\partial^2 U_x}{\partial x^2}\right)+\rho\omega^2 U_x+F_x=0 \tag{4.3.1.7}$$

$$(\lambda+\mu)(1-l^2\nabla^2)\frac{\partial}{\partial y}\left(\frac{\partial U_x}{\partial x}+\frac{\partial U_y}{\partial y}\right)+\mu(1-l^2\nabla^2)\left(\frac{\partial^2 U_y}{\partial x^2}+\frac{\partial^2 U_y}{\partial y^2}\right)$$
$$-I\omega^2\left(\frac{\partial^2 U_y}{\partial x^2}+\frac{\partial^2 U_y}{\partial y^2}\right)+\rho\omega^2 U_y+F_y=0 \tag{4.3.1.8}$$

Equations (4.3.1.7), (4.3.1.8) compose the system of PDEs that describe the problem and will be solved using the double Fourier transform. It worth noting that the corresponding problem of classical elasticity was solved by Eason, Fulton and Sneddon [84] and the solution that is presented here is identical to theirs.

4.3.2 Derivation of the Green's Function - Purely Displacement Formulation

By applying the double Fourier transform in (4.3.1.7), (4.3.1.8) for the case where $P_i(x,y,t) = \delta(x)\delta(y)p_i$, $i = x,y$ we obtain the following expressions for the transformed displacement components:

$$\hat{\hat{U}}_x = \frac{L}{N}, \quad \hat{\hat{U}}_y = \frac{M}{N} \tag{4.3.2.1}$$

Where:

$$\begin{aligned} L = &\left\{\left[\mu\xi^2 + (\lambda+2\mu)\eta^2\right]\left[l^2\left(\xi^2+\eta^2\right)+1\right] - \left[I\left(\xi^2+\eta^2\right)+\rho\right]\omega^2\right\}p_x \\ &- \xi\eta\left(\lambda+\mu\right)\left[l^2\left(\xi^2+\eta^2\right)+1\right]p_y \end{aligned} \tag{4.3.2.2}$$

$$\begin{aligned} M = &\left\{\left[(\lambda+2\mu)\xi^2 + \mu\eta^2\right]\left[l^2\left(\xi^2+\eta^2\right)+1\right] - \left[I\left(\xi^2+\eta^2\right)+\rho\right]\omega^2\right\}p_y \\ &- \xi\eta\left(\lambda+\mu\right)\left[l^2\left(\xi^2+\eta^2\right)+1\right]p_x \end{aligned} \tag{4.3.2.3}$$

$$\begin{aligned} N = &\left\{\mu\left(\xi^2+\eta^2\right)\left[l^2\left(\xi^2+\eta^2\right)+1\right] - \left[I\left(\xi^2+\eta^2\right)+\rho\right]\omega^2\right\} \\ &\times\left\{(\lambda+2\mu)\left(\xi^2+\eta^2\right)\left[l^2\left(\xi^2+\eta^2\right)+1\right] - \left[I\left(\xi^2+\eta^2\right)+\rho\right]\omega^2\right\} \end{aligned} \tag{4.3.2.4}$$

Substituting (3.3.3.8) into (4.3.2.2) - (4.3.2.4) and dividing the resulting expression with the density ρ yields:

$$\begin{aligned} \frac{L}{\rho} = &\left\{\left(v_2^2\xi^2 + v_1^2\eta^2\right)\left[l^2\left(\xi^2+\eta^2\right)+1\right] - \left[h^2\left(\xi^2+\eta^2\right)+1\right]\omega^2\right\}p_x \\ &- \xi\eta\left(v_1^2 - v_2^2\right)\left[l^2\left(\xi^2+\eta^2\right)+1\right]p_y \end{aligned} \tag{4.3.2.5}$$

$$\begin{aligned} \frac{M}{\rho} = &\left\{\left(v_1^2\xi^2 + v_2^2\eta^2\right)\left[l^2\left(\xi^2+\eta^2\right)+1\right] - \left[h^2\left(\xi^2+\eta^2\right)+1\right]\omega^2\right\}p_y \\ &- \xi\eta\left(v_1^2 - v_2^2\right)\left[l^2\left(\xi^2+\eta^2\right)+1\right]p_x \end{aligned} \tag{4.3.2.6}$$

$$\begin{aligned} \frac{N}{\rho} = &\rho\left\{v_2^2\left(\xi^2+\eta^2\right)\left[l^2\left(\xi^2+\eta^2\right)+1\right] - \left[h^2\left(\xi^2+\eta^2\right)+1\right]\omega^2\right\} \\ &\times\left\{v_1^2\left(\xi^2+\eta^2\right)\left[l^2\left(\xi^2+\eta^2\right)+1\right] - \left[h^2\left(\xi^2+\eta^2\right)+1\right]\omega^2\right\} \end{aligned} \tag{4.3.2.7}$$

Where v_1^2 and v_2^2 are the propagation velocities of the primary and the secondary as they are defined in classical elasticity:

$$v_1 = \sqrt{\frac{\lambda+2\mu}{\rho}} \tag{4.3.2.8}$$

$$v_2 = \sqrt{\frac{\mu}{\rho}} \tag{4.3.2.9}$$

Dividing (4.3.2.5) - (4.3.2.7) with v_2^2 results to:

$$\begin{aligned}\frac{L}{\mu} = &\left\{\left(\xi^2+\beta^2\eta^2\right)\left[l^2\left(\xi^2+\eta^2\right)+1\right]-\left[h^2\left(\xi^2+\eta^2\right)+1\right]\beta^2k_1^2\right\}p_x\\ &-\xi\eta\left(\beta^2-1\right)\left[l^2\left(\xi^2+\eta^2\right)+1\right]p_y\end{aligned} \tag{4.3.2.10}$$

$$\begin{aligned}\frac{M}{\mu} = &\left\{\left(\beta^2\xi^2+\eta^2\right)\left[l^2\left(\xi^2+\eta^2\right)+1\right]-\left[h^2\left(\xi^2+\eta^2\right)+1\right]\beta^2k_1^2\right\}p_y\\ &-\xi\eta\left(v_1^2-v_2^2\right)\left[l^2\left(\xi^2+\eta^2\right)+1\right]p_x\end{aligned} \tag{4.3.2.11}$$

$$\begin{aligned}\frac{N}{\mu} = &\,\mu\left\{\left(\xi^2+\eta^2\right)\left[l^2\left(\xi^2+\eta^2\right)+1\right]-\left[h^2\left(\xi^2+\eta^2\right)+1\right]\beta^2k_1^2\right\}\\ &\times\left\{\beta^2\left(\xi^2+\eta^2\right)\left[l^2\left(\xi^2+\eta^2\right)+1\right]-\left[h^2\left(\xi^2+\eta^2\right)+1\right]\beta^2k_1^2\right\}\end{aligned} \tag{4.3.2.12}$$

Where β is the ratio of the propagation velocities and k_i are the wavenumbers that describe the motions of the primary and secondary defined in the same sense as in classical elasticity:

$$\beta = \frac{v_1}{v_2} \tag{4.3.2.13}$$

$$k_i = \frac{\omega}{v_i}, \quad i = 1,2 \tag{4.3.2.14}$$

To determine the expressions of the displacement components, we write (4.3.2.1) as the sum of the displacements caused by a force acting in the x and y directions separately, i.e.:

$$\hat{\hat{U}}_x = \hat{\hat{U}}_x^{p_x} + \hat{\hat{U}}_x^{p_y} \tag{4.3.2.15}$$

$$\hat{\hat{U}}_y = \hat{\hat{U}}_y^{p_x} + \hat{\hat{U}}_y^{p_y} \tag{4.3.2.16}$$

In view of (4.3.2.1), (4.3.2.10) - (4.3.2.12), (4.3.2.15), (4.3.2.16), the expressions of $\hat{\hat{U}}_i^{p_j}$ are given by:

$$\hat{\hat{U}}_x^{p_x} = \frac{\left\{\left(\xi^2+\beta^2\eta^2\right)\left[l^2\left(\xi^2+\eta^2\right)+1\right]-\left[h^2\left(\xi^2+\eta^2\right)+1\right]\beta^2k_1^2\right\}p_x}{N} \tag{4.3.2.17}$$

$$\hat{\hat{U}}_x^{p_y} = -\frac{\xi\eta\left(\beta^2-1\right)\left[l^2\left(\xi^2+\eta^2\right)+1\right]p_y}{N} \tag{4.3.2.18}$$

$$\hat{\hat{U}}_y^{p_x} = -\frac{\xi\eta\left(\beta^2-1\right)\left[l^2\left(\xi^2+\eta^2\right)+1\right]p_x}{N} \tag{4.3.2.19}$$

$$\hat{\hat{U}}_y^{p_y} = \frac{\left\{\left(\beta^2\xi^2+\eta^2\right)\left[l^2\left(\xi^2+\eta^2\right)+1\right]-\left[h^2\left(\xi^2+\eta^2\right)+1\right]\beta^2k_1^2\right\}p_y}{N} \tag{4.3.2.20}$$

The numerator of (4.3.2.17) can be written as:

$$\begin{aligned}&\left(\xi^2+\beta^2\eta^2\right)\left[l^2\left(\xi^2+\eta^2\right)+1\right]-\left[h^2\left(\xi^2+\eta^2\right)+1\right]\beta^2k_1^2=\beta^2\left(\xi^2+\eta^2-k_1^2\right)\\&-\left(\beta^2-1\right)\xi^2+l^2\left[\beta^2\left(\xi^2+\eta^2-\frac{h^2}{l^2}k_1^2\right)-\left(\beta^2-1\right)\xi^2\right]\left(\xi^2+\eta^2\right)\end{aligned} \tag{4.3.2.21}$$

Respectively, the numerator of (4.3.2.20) can be written as:

$$\begin{aligned}&\left(\beta^2\xi^2+\eta^2\right)\left[l^2\left(\xi^2+\eta^2\right)+1\right]-\left[h^2\left(\xi^2+\eta^2\right)+1\right]\beta^2k_1^2=\beta^2\left(\xi^2+\eta^2-k_1^2\right)\\&-\left(\beta^2-1\right)\eta^2+l^2\left[\beta^2\left(\xi^2+\eta^2-\frac{h^2}{l^2}k_1^2\right)-\left(\beta^2-1\right)\xi^2\right]\left(\xi^2+\eta^2\right)\end{aligned} \tag{4.3.2.22}$$

Because of (4.3.2.12), (4.3.2.21) and (4.3.2.22), the terms $\hat{\hat{U}}_i^{p_j}$ can now be expressed as:

$$\begin{aligned}\hat{\hat{U}}_x^{p_x} = \frac{p_x}{\mu\beta^2\left(\xi^2+\eta^2\right)}&\left\{\frac{\xi^2}{\left(\xi^2+\eta^2\right)\left[l^2\left(\xi^2+\eta^2\right)+1\right]-\left[h^2\left(\xi^2+\eta^2\right)+1\right]k_1^2}\right.\\&\left.+\frac{\beta^2\eta^2}{\left(\xi^2+\eta^2\right)\left[l^2\left(\xi^2+\eta^2\right)+1\right]-\left[h^2\left(\xi^2+\eta^2\right)+1\right]\beta^2k_1^2}\right\}\end{aligned} \tag{4.3.2.23}$$

$$\begin{aligned}\hat{\hat{U}}_x^{p_y} = \frac{p_y}{\mu\beta^2\left(\xi^2+\eta^2\right)}&\left\{\frac{1}{\left(\xi^2+\eta^2\right)\left[l^2\left(\xi^2+\eta^2\right)+1\right]-\left[h^2\left(\xi^2+\eta^2\right)+1\right]k_1^2}\right.\\&\left.-\frac{\beta^2}{\left(\xi^2+\eta^2\right)\left[l^2\left(\xi^2+\eta^2\right)+1\right]-\left[h^2\left(\xi^2+\eta^2\right)+1\right]\beta^2k_1^2}\right\}\end{aligned} \tag{4.3.2.24}$$

$$\begin{aligned}\hat{\hat{U}}_y^{p_x} = \frac{p_x}{\mu\beta^2\left(\xi^2+\eta^2\right)}&\left\{\frac{1}{\left(\xi^2+\eta^2\right)\left[l^2\left(\xi^2+\eta^2\right)+1\right]-\left[h^2\left(\xi^2+\eta^2\right)+1\right]k_1^2}\right.\\&\left.-\frac{\beta^2}{\left(\xi^2+\eta^2\right)\left[l^2\left(\xi^2+\eta^2\right)+1\right]-\left[h^2\left(\xi^2+\eta^2\right)+1\right]\beta^2k_1^2}\right\}\end{aligned} \tag{4.3.2.25}$$

$$\hat{U}_y^{p_y} = \frac{p_y}{\mu\beta^2\left(\xi^2+\eta^2\right)}\left\{\frac{\eta^2}{\left(\xi^2+\eta^2\right)\left[l^2\left(\xi^2+\eta^2\right)+1\right]-\left[h^2\left(\xi^2+\eta^2\right)+1\right]k_1^2} + \frac{\beta^2\xi^2}{\left(\xi^2+\eta^2\right)\left[l^2\left(\xi^2+\eta^2\right)+1\right]-\left[h^2\left(\xi^2+\eta^2\right)+1\right]\beta^2k_1^2}\right\} \tag{4.3.2.26}$$

By applying the inverse double Fourier transform in (4.3.2.23) - (4.3.2.26) we obtain:

$$U_x^{p_x} = \frac{p_x}{4\pi^2\mu\beta^2}\left\{\int_{-\infty}^{+\infty}\int_{-\infty}^{+\infty}\frac{\xi^2\left(\xi^2+\eta^2\right)^{-1}e^{i(\xi x+\eta y)}}{\left(\xi^2+\eta^2\right)\left[l^2\left(\xi^2+\eta^2\right)+1\right]-\left[h^2\left(\xi^2+\eta^2\right)+1\right]k_1^2}\,d\xi\,d\eta + \int_{-\infty}^{+\infty}\int_{-\infty}^{+\infty}\frac{\beta^2\eta^2\left(\xi^2+\eta^2\right)^{-1}e^{i(\xi x+\eta y)}}{\left(\xi^2+\eta^2\right)\left[l^2\left(\xi^2+\eta^2\right)+1\right]-\left[h^2\left(\xi^2+\eta^2\right)+1\right]\beta^2k_1^2}\,d\xi\,d\eta\right\} \tag{4.3.2.27}$$

$$U_x^{p_y} = \frac{p_y}{4\pi^2\mu\beta^2}\left\{\int_{-\infty}^{+\infty}\int_{-\infty}^{+\infty}\frac{\xi\eta\left(\xi^2+\eta^2\right)^{-1}e^{i(\xi x+\eta y)}}{\left(\xi^2+\eta^2\right)\left[l^2\left(\xi^2+\eta^2\right)+1\right]-\left[h^2\left(\xi^2+\eta^2\right)+1\right]k_1^2}\,d\xi\,d\eta - \int_{-\infty}^{+\infty}\int_{-\infty}^{+\infty}\frac{\beta^2\xi\eta\left(\xi^2+\eta^2\right)^{-1}e^{i(\xi x+\eta y)}}{\left(\xi^2+\eta^2\right)\left[l^2\left(\xi^2+\eta^2\right)+1\right]-\left[h^2\left(\xi^2+\eta^2\right)+1\right]\beta^2k_1^2}\,d\xi\,d\eta\right\} \tag{4.3.2.28}$$

$$U_y^{p_x} = \frac{p_x}{4\pi^2\mu\beta^2}\left\{\int_{-\infty}^{+\infty}\int_{-\infty}^{+\infty}\frac{\xi\eta\left(\xi^2+\eta^2\right)^{-1}e^{i(\xi x+\eta y)}}{\left(\xi^2+\eta^2\right)\left[l^2\left(\xi^2+\eta^2\right)+1\right]-\left[h^2\left(\xi^2+\eta^2\right)+1\right]k_1^2}\,d\xi\,d\eta - \int_{-\infty}^{+\infty}\int_{-\infty}^{+\infty}\frac{\beta^2\xi\eta\left(\xi^2+\eta^2\right)^{-1}e^{i(\xi x+\eta y)}}{\left(\xi^2+\eta^2\right)\left[l^2\left(\xi^2+\eta^2\right)+1\right]-\left[h^2\left(\xi^2+\eta^2\right)+1\right]\beta^2k_1^2}\,d\xi\,d\eta\right\} \tag{4.3.2.29}$$

$$U_y^{p_y} = \frac{p_y}{4\pi^2\mu\beta^2}\left\{\int_{-\infty}^{+\infty}\int_{-\infty}^{+\infty}\frac{\eta^2\left(\xi^2+\eta^2\right)^{-1}e^{i(\xi x+\eta y)}}{\left(\xi^2+\eta^2\right)\left[l^2\left(\xi^2+\eta^2\right)+1\right]-\left[h^2\left(\xi^2+\eta^2\right)+1\right]k_1^2}\,d\xi\,d\eta + \int_{-\infty}^{+\infty}\int_{-\infty}^{+\infty}\frac{\beta^2\xi^2\left(\xi^2+\eta^2\right)^{-1}e^{i(\xi x+\eta y)}}{\left(\xi^2+\eta^2\right)\left[l^2\left(\xi^2+\eta^2\right)+1\right]-\left[h^2\left(\xi^2+\eta^2\right)+1\right]\beta^2k_1^2}\,d\xi\,d\eta\right\} \tag{4.3.2.30}$$

The final four expressions can written in compacted form as:

$$U_x^{p_x} = -\frac{p_x}{4\pi^2\mu\beta^2}\left[\frac{\partial^2}{\partial x^2}I(x,y,k_1)+\beta^2\frac{\partial^2}{\partial y^2}I(x,y,\beta k_1)\right] \tag{4.3.2.31}$$

$$U_x^{p_y} = -\frac{p_y}{4\pi^2\mu\beta^2}\left\{\frac{\partial^2}{\partial x\partial y}\left[I(x,y,k_1)-\beta^2I(x,y,\beta k_1)\right]\right\} \tag{4.3.2.32}$$

$$U_y^{p_x} = -\frac{p_x}{4\pi^2\mu\beta^2}\left\{\frac{\partial^2}{\partial x\partial y}\left[I(x,y,k_1) - \beta^2 I(x,y,\beta k_1)\right]\right\} \tag{4.3.2.33}$$

$$U_y^{p_y} = -\frac{p_y}{4\pi^2\mu\beta^2}\left[\frac{\partial^2}{\partial y^2}I(x,y,k_1) + \beta^2\frac{\partial^2}{\partial x^2}I(x,y,\beta k_1)\right] \tag{4.3.2.34}$$

Where:

$$I = \int_{-\infty}^{+\infty}\int_{-\infty}^{+\infty}\frac{\left(\xi^2+\eta^2\right)^{-1}e^{i(\xi x+\eta y)}}{\left(\xi^2+\eta^2\right)\left[l^2\left(\xi^2+\eta^2\right)+1\right]-\left[h^2\left(\xi^2+\eta^2\right)+1\right]k_1^2}\,d\xi\,d\eta \tag{4.3.2.35}$$

In order to determine the integral presented in (4.3.2.35), we convert to polar coordinates (k,ϕ) using (4.2.3.5), (4.2.3.6):

$$I = \int_0^{2\pi}\int_0^{\infty}\frac{e^{-ikr[\cos(\phi)\cos(\theta)+\sin(\phi)\sin(\theta)]}}{k\left[k^2\left(l^2k^2+1\right)-\left(h^2k^2+1\right)k_1^2\right]}\,dk\,d\phi \tag{4.3.2.36}$$

The above integral can be simplified with the help of (4.2.3.8):

$$I = \int_0^{2\pi}\int_0^{\infty}\frac{e^{-ikr\cos(\phi-\theta)}}{k\left[k^2\left(l^2k^2+1\right)-\left(h^2k^2+1\right)k_1^2\right]}\,dk\,d\phi \tag{4.3.2.37}$$

By rearranging the terms in (4.3.2.37) we obtain:

$$I = 2\pi\int_0^{\infty}\frac{1}{k\left[k^2\left(l^2k^2+1\right)-\left(h^2k^2+1\right)k_1^2\right]}\left[\frac{1}{2\pi}\int_0^{2\pi}e^{-ikr\cos(\phi-\theta)}\,d\phi\right]dk \tag{4.3.2.38}$$

The term inside the brackets in (4.3.2.38) corresponds to the Bessel function of the first kind of order zero $J_0(kr)$ given in (4.2.3.12). Therefore (4.3.2.38) becomes:

$$I = 2\pi\int_0^{\infty}\frac{1}{k\left[k^2\left(l^2k^2+1\right)-\left(h^2k^2+1\right)k_1^2\right]}J_0(kr)\,dk \tag{4.3.2.39}$$

Differentiating (4.3.2.39) with respect to r yields:

$$\frac{\partial I}{\partial r} = 2\pi\int_0^{\infty}\frac{1}{k\left[k^2\left(l^2k^2+1\right)-\left(h^2k^2+1\right)k_1^2\right]}\frac{\partial J_0(kr)}{\partial r}\,dk \tag{4.3.2.40}$$

The derivative in (4.3.2.40) can be determined using the following identity:

$$\frac{\partial}{\partial x}\left[x^{-n}J_n(x)\right] = -x^{-n}J_{n+1}(x) \tag{4.3.2.41}$$

By setting $n = 0$, we retrieve the derivative of $J_0(kr)$:

$$\frac{\partial J_0(x)}{\partial x} = -J_1(x) \tag{4.3.2.42}$$

Where J_1 is the Bessel function of the first kind of order one. In view of (4.3.2.42), equation (4.3.2.40) becomes:

$$\frac{\partial I}{\partial r} = -2\pi \int_0^\infty \frac{1}{k^2\left(l^2k^2+1\right) - \left(h^2k^2+1\right)k_1^2} J_1(kr)\, dk \tag{4.3.2.43}$$

The roots of the denominator in (4.3.2.43) are:

$$p(k_1) = \pm\sqrt{\frac{h^2k_1^2 - 1 - \sqrt{4l^2k_1^2 + \left(h^2k_1^2-1\right)^2}}{2l^2}} \tag{4.3.2.44}$$

$$q(k_1) = \pm\sqrt{\frac{h^2k_1^2 - 1 + \sqrt{4l^2k_1^2 + \left(h^2k_1^2-1\right)^2}}{2l^2}} \tag{4.3.2.45}$$

It is noted that the denominator in (4.3.2.43) is the same as the dispersion equation of the primary waves (3.4.3.5), while the roots $p(k_1)$, $q(k_1)$ correspond to q_1 in (3.4.3.5). Also by setting $k_1 = \beta k_1$ in (4.3.2.44), (4.3.2.45) then the roots $p(\beta k_1) = p(k_2)$, $q(\beta k_1) = q(k_2)$ are the same as the roots of the dispersion equation q_2 of the secondary waves (3.4.3.6). By applying partial fraction decomposition the transformed function in (4.3.2.43) can be expressed as:

$$\frac{l^2}{(l^2k^2+1)k^2 - (h^2k^2+1)k_1^2} = \frac{A}{k-p(k_1)} + \frac{B}{k+p(k_1)} + \frac{\Gamma}{k-q(k_1)} + \frac{\Delta}{k+q(k_1)} \tag{4.3.2.46}$$

Where the coefficients A, B, Γ, Δ are given by:

$$\begin{aligned} A &= \frac{1}{2p(k_1)\left[p^2(k_1)-q^2(k_1)\right]}, \quad B = -\frac{1}{2p(k_1)\left[p^2(k_1)-q^2(k_1)\right]}, \\ \Gamma &= \frac{1}{2q(k_1)\left[q^2(k_1)-p^2(k_1)\right]}, \quad \Delta = -\frac{1}{2q(k_1)\left[q^2(k_1)-p^2(k_1)\right]} \end{aligned} \tag{4.3.2.47}$$

Therefore the transformed function in (4.3.2.43) can be written as:

$$\frac{l^2}{k^2\left(l^2k^2+1\right)-\left(h^2k^2+1\right)k_1^2} = \frac{1}{p^2(k_1)-q^2(k_1)}\left\{\frac{1}{\left[k^2-p^2(k_1)\right]}-\frac{1}{\left[k^2-q^2(k_1)\right]}\right\} \tag{4.3.2.48}$$

By substituting (4.3.2.48) into (4.3.2.43) we obtain:

$$\frac{\partial I}{\partial r} = -\frac{2\pi}{\left[p^2(k_1)-q^2(k_1)\right]l^2}\left[\int_0^\infty \frac{J_1(kr)}{k^2-p^2(k_1)}\,dk - \int_0^\infty \frac{J_1(kr)}{k^2-q^2(k_1)}\,dk\right] \tag{4.3.2.49}$$

The integrals that appear in (4.3.2.49) will be determined using (4.2.3.21). By setting in (4.2.3.21) $b=1$, $n=1$, $m=0$, we can construct the above integrals, however the inequality presented in (4.2.3.22) is not satisfied, for this reason in order to utilize (4.2.3.21) we first introduce the following decomposition.

$$-\int_0^\infty \frac{1}{k^2-\lambda^2}J_1(kr)\,dk = \frac{1}{\lambda^2}\int_0^\infty\left(1-\frac{k^2}{k^2-\lambda^2}\right)J_1(kr)\,dk \tag{4.3.2.50}$$

By setting in (4.3.2.50) $\lambda = p(k_1)$ and $\lambda = q(k_1)$ and substituting into (4.3.2.49) we obtain:

$$\begin{aligned} \frac{\partial I}{\partial r} = \frac{2\pi}{\left[p^2(k_1)-q^2(k_1)\right]l^2}\Bigg[&\frac{1}{p^2(k_1)}\left(\int_0^\infty J_1(kr)\,dk - \int_0^\infty \frac{k^2}{k^2-p^2(k_1)}J_1(kr)\,dk\right) \\ &-\frac{1}{q^2(k_1)}\left(\int_0^\infty J_1(kr)\,dk - \int_0^\infty \frac{k^2}{k^2-q^2(k_1)}J_1(kr)\,dk\right)\Bigg] \end{aligned} \tag{4.3.2.51}$$

The above equation can equivalently be written as:

$$\frac{\partial I}{\partial r} = \frac{2\pi}{[p^2(k_1) - q^2(k_1)]\, l^2} \left[\left(\frac{1}{p^2(k_1)} - \frac{1}{q^2(k_1)} \right) \int_0^\infty J_1(kr)\, dk \right.$$
$$\left. - \frac{1}{p^2(k_1)} \int_0^\infty \frac{k^2}{k^2 - p^2(k_1)} J_1(kr)\, dk + \frac{1}{q^2(k_1)} \int_0^\infty \frac{k^2}{k^2 - q^2(k_1)} J_1(kr)\, dk \right] \tag{4.3.2.52}$$

The coefficient of the first integral in (4.3.2.52) can be simplified to give:

$$\frac{2\pi}{[p^2(k_1) - q^2(k_1)]\, l^2} \left(\frac{1}{p^2(k_1)} - \frac{1}{q^2(k_1)} \right) = \frac{2\pi}{k_1^2} \tag{4.3.2.53}$$

In view of (4.3.2.53), equation (4.3.2.52) becomes:

$$\frac{\partial I}{\partial r} = \frac{2\pi}{k_1^2} \int_0^\infty J_1(kr)\, dk - \frac{2\pi}{[p^2(k_1) - q^2(k_1)]\, l^2} \left[\frac{1}{p^2(k_1)} \int_0^\infty \frac{k^2}{k^2 - p^2(k_1)} J_1(kr)\, dk \right.$$
$$\left. - \frac{1}{q^2(k_1)} \int_0^\infty \frac{k^2}{k^2 - q^2(k_1)} J_1(kr)\, dk \right] \tag{4.3.2.54}$$

The first integral in (4.3.2.54) can be determined using the following identity, (see formula 18, page 654 in [85]).

$$\int_0^\infty e^{-iar} J_1(kr)\, dk = \frac{1}{r} \left[1 - \frac{a}{(k^2 + a^2)^{1/2}} \right] \tag{4.3.2.55}$$

Equation (4.3.2.55) for $a = 0$ yields:

$$\int_0^\infty J_1(kr)\, dk = \frac{1}{r} \tag{4.3.2.56}$$

By setting in (4.2.3.21) $b = 3$, $n = 1$, $m = 0$ we obtain:

$$\int_0^\infty [(1 + e^{2i\pi}) J_1(kr) + i(1 - e^{2i\pi}) Y_1(kr)] \frac{k^2}{k^2 - \lambda^2}\, dk = i\pi\lambda H_1^{(1)}(\lambda r) \tag{4.3.2.57}$$

The above expression can be simplified with the help of Euler's formula, (see equation (4.2.3.24) for $x = 2\pi$):

$$\int_0^\infty \frac{k^2}{k^2-\lambda^2}\,dk = \frac{i\pi\lambda}{2}H_1^{(1)}(\lambda r) \tag{4.3.2.58}$$

The following result arises by setting in (4.3.2.58) $\lambda = p(k_1)$ and $\lambda = q(k_1)$ and substituting into (4.3.2.54):

$$\frac{\partial I}{\partial r} = \frac{2\pi}{k_1^2}\left\{\frac{1}{r} - \frac{i\pi k_1^2}{2\left[p^2(k_1)-q^2(k_1)\right]l^2}\left[\frac{H_1^{(1)}(p(k_1)r)}{p(k_1)} - \frac{H_1^{(1)}(q(k_1)r)}{q(k_1)}\right]\right\} \tag{4.3.2.59}$$

By applying the chain rule in (4.3.2.31) - (4.3.2.34) we obtain:

$$\begin{aligned} U_x^{p_x} = -\frac{p_x}{4\pi^2\mu\beta^2}\Bigg\{&\frac{\partial^2 I(r,\theta,k_1)}{\partial r^2}\left(\frac{\partial r}{\partial x}\right)^2 + \frac{\partial I(r,\theta,k_1)}{\partial r}\left(\frac{\partial^2 r}{\partial x^2}\right) \\ &+\beta^2\left[\frac{\partial^2 I(r,\theta,\beta k_1)}{\partial r^2}\left(\frac{\partial r}{\partial y}\right)^2 + \frac{\partial I(r,\theta,\beta k_1)}{\partial r}\left(\frac{\partial^2 r}{\partial y^2}\right)\right]\Bigg\} \end{aligned} \tag{4.3.2.60}$$

$$\begin{aligned} U_x^{p_y} = -\frac{p_y}{4\pi^2\mu\beta^2}\Bigg\{&\frac{\partial^2 I(r,\theta,k_1)}{\partial r^2}\left(\frac{\partial r}{\partial x}\frac{\partial r}{\partial y}\right) + \frac{\partial I(r,\theta,k_1)}{\partial r}\left(\frac{\partial^2 r}{\partial x\partial y}\right) \\ &+\beta^2\left[\frac{\partial^2 I(r,\theta,\beta k_1)}{\partial r^2}\left(\frac{\partial r}{\partial x}\frac{\partial r}{\partial y}\right) + \frac{\partial I(r,\theta,\beta k_1)}{\partial r}\left(\frac{\partial^2 r}{\partial x\partial y}\right)\right]\Bigg\} \end{aligned} \tag{4.3.2.61}$$

$$\begin{aligned} U_y^{p_x} = -\frac{p_x}{4\pi^2\mu\beta^2}\Bigg\{&\frac{\partial^2 I(r,\theta,k_1)}{\partial r^2}\left(\frac{\partial r}{\partial x}\frac{\partial r}{\partial y}\right) + \frac{\partial I(r,\theta,k_1)}{\partial r}\left(\frac{\partial^2 r}{\partial x\partial y}\right) \\ &+\beta^2\left[\frac{\partial^2 I(r,\theta,\beta k_1)}{\partial r^2}\left(\frac{\partial r}{\partial x}\frac{\partial r}{\partial y}\right) + \frac{\partial I(r,\theta,\beta k_1)}{\partial r}\left(\frac{\partial^2 r}{\partial x\partial y}\right)\right]\Bigg\} \end{aligned} \tag{4.3.2.62}$$

$$\begin{aligned} U_y^{p_y} = -\frac{p_y}{4\pi^2\mu\beta^2}\Bigg\{&\frac{\partial^2 I(r,\theta,k_1)}{\partial r^2}\left(\frac{\partial r}{\partial y}\right)^2 + \frac{\partial I(r,\theta,k_1)}{\partial r}\left(\frac{\partial^2 r}{\partial y^2}\right) \\ &+\beta^2\left[\frac{\partial^2 I(r,\theta,\beta k_1)}{\partial r^2}\left(\frac{\partial r}{\partial x}\right)^2 + \frac{\partial I(r,\theta,\beta k_1)}{\partial r}\left(\frac{\partial^2 r}{\partial x^2}\right)\right]\Bigg\} \end{aligned} \tag{4.3.2.63}$$

Differentiating (4.3.2.59) with respect to r yields:

$$\begin{aligned} \frac{\partial^2 I(r,\theta,k_1)}{\partial r^2} = -\frac{2\pi}{k_1^2}\Bigg\{&\frac{1}{r^2} + \frac{i\pi k_1^2}{2\left[p^2(k_1)-q^2(k_1)\right]l^2}\left[\frac{1}{p(k_1)}\frac{\partial H_1^{(1)}(p(k_1)r)}{\partial r}\right. \\ &\left.-\frac{1}{q(k_1)}\frac{\partial H_1^{(1)}(q(k_1)r)}{\partial r}\right]\Bigg\} \end{aligned} \tag{4.3.2.64}$$

The derivative of the Hankel function of the first kind can be determined using the following formula:

$$\frac{\partial H_n^{(1)}(z)}{\partial z} = \frac{nH_n^{(1)}(z)}{z} - H_{n+1}^{(1)}(z) \tag{4.3.2.65}$$

By setting in (4.3.2.65) $z = p(k_1)$, $z = q(k_1)$ and substituting the resulting expressions into (4.3.2.64) we obtain:

$$\begin{aligned}\frac{\partial^2 I(r,\theta,k_1)}{\partial r^2} = -\frac{2\pi}{k_1^2}\Bigg\{\frac{1}{r^2} + \frac{i\pi k_1^2}{2\left[p^2(k_1) - q^2(k_1)\right] l^2}\Bigg[\frac{H_1^{(1)}(p(k_1)r)}{p(k_1)r} - H_2^{(1)}(p(k_1)r) \\ - \frac{H_1^{(1)}(q(k_1)r)}{q(k_1)r} + H_2^{(1)}(q(k_1)r)\Bigg]\Bigg\}\end{aligned} \tag{4.3.2.66}$$

The first and second derivatives of r are:

$$\frac{\partial r}{\partial x} = \frac{x}{r} = \cos(\theta), \quad \frac{\partial r}{\partial y} = \frac{y}{r} = \sin(\theta) \tag{4.3.2.67}$$

$$\frac{\partial^2 r}{\partial x^2} = \frac{1}{r} - \frac{x^2}{r^3}, \quad \frac{\partial^2 r}{\partial x \partial y} = -\frac{xy}{r^3}, \quad \frac{\partial^2 r}{\partial y^2} = \frac{1}{r} - \frac{y^2}{r^3} \tag{4.3.2.68}$$

The expressions of the displacement components are finally obtained by setting in (4.3.2.66) $k_1 = \beta k_1$ and substituting the resulting expression into (4.3.2.60) - (4.3.2.63) along with (4.3.2.66) - (4.3.2.68):

$$\begin{aligned}U_x^{p_x} = \frac{p_x}{4\mu\beta^2 l^2 r} i \Bigg\{\frac{1}{p^2(k_1) - q^2(k_1)}\left[\frac{H_1^{(1)}(p(k_1)r)}{p(k_1)} - \frac{H_1^{(1)}(q(k_1)r)}{q(k_1)}\right] \\ + \frac{\beta^2}{p^2(\beta k_1) - q^2(\beta k_1)}\left[\frac{H_1^{(1)}(p(\beta k_1)r)}{p(\beta k_1)} - \frac{H_1^{(1)}(q(\beta k_1)r)}{q(\beta k_1)}\right]\Bigg\} \\ - \frac{1}{r}\Bigg\{\frac{x^2}{p^2(k_1) - q^2(k_1)}\left[H_2^{(1)}(p(k_1)r) - H_2^{(1)}(q(k_1)r)\right] \\ + \frac{\beta^2 y^2}{p^2(\beta k_1) - q^2(\beta k_1)}\left[H_2^{(1)}(p(\beta k_1)r) - H_2^{(1)}(q(\beta k_1)r)\right]\Bigg\}\Bigg\}\end{aligned} \tag{4.3.2.69}$$

$$U_x^{p_y} = -\frac{p_y xy}{4\mu\beta^2 l^2 r^2}\left\{\frac{1}{p^2(k_1)-q^2(k_1)}\left[H_2^{(1)}(p(k_1)r)-H_2^{(1)}(q(k_1)r)\right]\right.$$
$$\left.-\frac{\beta^2}{p^2(\beta k_1)-q^2(\beta k_1)}\left[H_2^{(1)}(p(\beta k_1)r)-H_2^{(1)}(q(\beta k_1)r)\right]\right\} \tag{4.3.2.70}$$

$$U_y^{p_x} = -\frac{p_x xy}{4\mu\beta^2 l^2 r^2}\left\{\frac{1}{p^2(k_1)-q^2(k_1)}\left[H_2^{(1)}(p(k_1)r)-H_2^{(1)}(q(k_1)r)\right]\right.$$
$$\left.-\frac{\beta^2}{p^2(\beta k_1)-q^2(\beta k_1)}\left[H_2^{(1)}(p(\beta k_1)r)-H_2^{(1)}(q(\beta k_1)r)\right]\right\} \tag{4.3.2.71}$$

$$U_y^{p_y} = \frac{p_y}{4\mu\beta^2 l^2 r} i\left\{\frac{1}{p^2(k_1)-q^2(k_1)}\left[\frac{H_1^{(1)}(p(k_1)r)}{p(k_1)}-\frac{H_1^{(1)}(q(k_1)r)}{q(k_1)}\right]\right.$$
$$+\frac{\beta^2}{p^2(\beta k_1)-q^2(\beta k_1)}\left[\frac{H_1^{(1)}(p(\beta k_1)r)}{p(\beta k_1)}-\frac{H_1^{(1)}(q(\beta k_1)r)}{q(\beta k_1)}\right]\Bigg\}$$
$$-\frac{1}{r}\left\{\frac{y^2}{p^2(k_1)-q^2(k_1)}\left[H_2^{(1)}(p(k_1)r)-H_2^{(1)}(q(k_1)r)\right]\right. \tag{4.3.2.72}$$
$$\left.\left.+\frac{\beta^2 x^2}{p^2(\beta k_1)-q^2(\beta k_1)}\left[H_2^{(1)}(p(\beta k_1)r)-H_2^{(1)}(q(\beta k_1)r)\right]\right\}\right\}$$

From (4.3.2.44), (4.3.2.45) it is clear that $\pm q(k_1)$ are the real routes of the dispersion equation, while $\pm p(k_1)$ are the imaginary routes of the dispersion equation. Having this in mind, (4.3.2.69) - (4.3.2.72) can be written in terms of Hankel functions and modified Bessel functions with real arguments using (4.2.3.28):

$$U_x^{p_x} = \frac{p_x}{4\mu\beta^2 l^2 r} i\left\{\frac{1}{P^2(k_1)+q^2(k_1)}\left[\frac{H_1^{(1)}(q(k_1)r)}{q(k_1)}-\frac{2i}{\pi}\frac{K_1(P(k_1)r)}{P(k_1)}\right]\right.$$
$$+\frac{\beta^2}{P^2(\beta k_1)+q^2(\beta k_1)}\left[\frac{H_1^{(1)}(q(\beta k_1)r)}{q(\beta k_1)}-\frac{2i}{\pi}\frac{K_1(P(\beta k_1)r)}{P(\beta k_1)}\right]\Bigg\}$$
$$+\frac{1}{r}\left\{\frac{x^2}{P^2(k_1)+q^2(k_1)}\left[\frac{2i}{\pi}K_2(P(k_1)r)-H_2^{(1)}(q(k_1)r)\right]\right. \tag{4.3.2.73}$$
$$\left.\left.+\frac{\beta^2 y^2}{P^2(\beta k_1)+q^2(\beta k_1)}\left[\frac{2i}{\pi}H_2^{(1)}(P(\beta k_1)r)-H_2^{(1)}(q(\beta k_1)r)\right]\right\}\right\}$$

$$U_x^{p_y} = \frac{p_y xy}{4\mu\beta^2 l^2 r^2}\left\{\frac{1}{P^2(k_1)+q^2(k_1)}\left[\frac{2i}{\pi}K_2(P(k_1)r)-H_2^{(1)}(q(k_1)r)\right]\right.$$
$$\left.+\frac{\beta^2}{P^2(\beta k_1)+q^2(\beta k_1)}\left[\frac{2i}{\pi}H_2^{(1)}(P(\beta k_1)r)-H_2^{(1)}(q(\beta k_1)r)\right]\right\} \tag{4.3.2.74}$$

$$U_y^{p_x} = \frac{p_x xy}{4\mu\beta^2 l^2 r^2}\left\{\frac{1}{P^2(k_1)+q^2(k_1)}\left[\frac{2i}{\pi}K_2(P(k_1)r)-H_2^{(1)}(q(k_1)r)\right]\right.$$
$$\left.+\frac{\beta^2}{P^2(\beta k_1)+q^2(\beta k_1)}\left[\frac{2i}{\pi}H_2^{(1)}(P(\beta k_1)r)-H_2^{(1)}(q(\beta k_1)r)\right]\right\} \tag{4.3.2.75}$$

$$
\begin{aligned}
U_y^{p_y} = \frac{p_y}{4\mu\beta^2 l^2 r} i \Bigg\{ & \frac{1}{P^2(k_1)+q^2(k_1)} \left[\frac{H_1^{(1)}(q(k_1)r)}{q(k_1)} - \frac{2i}{\pi} \frac{K_1(P(k_1)r)}{P(k_1)} \right] \\
& + \frac{\beta^2}{P^2(\beta k_1)+q^2(\beta k_1)} \left[\frac{H_1^{(1)}(q(\beta k_1)r)}{q(\beta k_1)} - \frac{2i}{\pi} \frac{K_1(P(\beta k_1)r)}{P(\beta k_1)} \right] \Bigg\} \\
& + \frac{1}{r} \Bigg\{ \frac{y^2}{P^2(k_1)+q^2(k_1)} \left[\frac{2i}{\pi} K_2(P(k_1)r) - H_2^{(1)}(q(k_1)r) \right] \\
& + \frac{\beta^2 x^2}{P^2(\beta k_1)+q^2(\beta k_1)} \left[\frac{2i}{\pi} H_2^{(1)}(P(\beta k_1)r) - H_2^{(1)}(q(\beta k_1)r) \right] \Bigg\} \Bigg\}
\end{aligned} \tag{4.3.2.76}
$$

Where $p(k_1) = iP(k_1)$. Since all the arguments in (4.3.2.73) - (4.3.2.76) are real we conclude that the $H_n^{(1)}$ terms are associated with outgoing waves, while the K_n terms are associated with evanescent modes. By shifting the coordinate system and for convenience setting $p_x = p_y = 1$, the problems Green's function can be written in matrix form:

$$
\mathbf{G}(\mathbf{r};\mathbf{r}') = \frac{1}{4\mu\beta^2 l^2} i \left[\Psi(s)\mathbf{I} + X(s)\hat{\mathbf{s}} \otimes \hat{\mathbf{s}} \right] \tag{4.3.2.77}
$$

In (4.3.2.77) $\mathbf{s}$ is a vector in the direction $\mathbf{s} = \mathbf{r} - \mathbf{r}'$, $s = |\mathbf{s}|$ is the magnitude of $\mathbf{s}$, $\hat{\mathbf{s}} = \mathbf{s}/|\mathbf{s}|$ is the unit vector n the direction $\mathbf{s} = \mathbf{r} - \mathbf{r}'$ and $X(s)$, $\Psi(s)$ are scalar functions given by:

$$
X(s) = \left\{ \frac{1}{s} \left[A(s,k_1) + \beta^2 A(s,\beta k_1) \right] + \beta^2 B(s,\beta k_1) \right\} \tag{4.3.2.78}
$$

$$
\Psi(s) = B(s,k_1) + \beta^2 B(s,\beta k_1) \tag{4.3.2.79}
$$

Where:

$$
A(s,k_1) = \frac{1}{P^2(k_1)+q^2(k_1)} \left[\frac{2i}{\pi} K_2(P(k_1)s) - H_2^{(1)}(q(k_1)s) \right] \tag{4.3.2.80}
$$

$$
B(s,k_1) = \frac{1}{P^2(k_1)+q^2(k_1)} \left[\frac{H_1^{(1)}(q(k_1)s)}{q(k_1)} - \frac{2i}{\pi} \frac{K_1(P(k_1)s)}{P(k_1)} \right] \tag{4.3.2.81}
$$

It is also noted that (4.3.2.77) is bounded in the limit where $\mathbf{r} \to \mathbf{r}'$:

$$
\mathbf{G}(\mathbf{r};\mathbf{r}') \sim \frac{1}{8\mu l^2 \pi} \left\{ \frac{i\pi + ln(P(k_1)/q(k_1))}{\beta^2 \left[P^2(k_1)+q^2(k_1) \right]} + \frac{i\pi + ln(P(\beta k_1)/q(\beta k_1))}{P^2(\beta k_1)+q^2(\beta k_1)} + O(s^2) \right\} \mathbf{I} \tag{4.3.2.82}
$$

4.3.3 Derivation of the Green's Function - Lamé Potentials

In order to verify the validity of (4.3.2.7) the problem is also solved using Lamé potentials. We begin setting $l_1 = l_2 = l$, $h_1 = h_2 = h$, $\tilde{v}_1 = v_1$, $\tilde{v}_2 = v_2$ in (3.4.2.22), (3.4.2.23), so that they hold for dipolar gradient elasticity:

$$\nabla^4\phi - \frac{1}{l^2}\nabla^2(\phi + \frac{h^2}{v_1^2}\ddot{\phi}) - \frac{1}{l^2}F = -\frac{1}{l^2 v_1^2}\ddot{\phi} \tag{4.3.3.1}$$

$$\nabla^4\boldsymbol{\psi} - \frac{1}{l^2}\nabla^2(\boldsymbol{\psi} + \frac{h^2}{v_2^2}\ddot{\boldsymbol{\psi}}) - \frac{1}{l^2}\mathbf{G} = -\frac{1}{l^2 v_2^2}\ddot{\boldsymbol{\psi}} \tag{4.3.3.2}$$

In the case of plane strain, the displacement and body force components are given by (4.3.1.1), (4.3.1.2), since the vector potentials $\boldsymbol{\psi}$, $\mathbf{G}$ are related with the displacement and body force vectors through (3.4.1.1), (3.4.1.3), then they must be in the form of:

$$\boldsymbol{\psi} = (0, 0, \psi), \quad \mathbf{G} = (0, 0, G) \tag{4.3.3.3}$$

Consequently, (4.3.3.2) degenerates to a scalar differential equation:

$$\nabla^4\psi - \frac{1}{l^2}\nabla^2(\psi + \frac{h^2}{v_2^2}\ddot{\psi}) - \frac{1}{l^2}G = -\frac{1}{l^2 v_2^2}\ddot{\psi} \tag{4.3.3.4}$$

For time harmonic conditions the displacement and body force components are in the form of (4.3.1.5), (4.3.1.6), in the same sense the displacement and body force potentials also exhibit a time harmonic variation:

$$\phi(x, y, t) = \phi(x, y)e^{-i\omega t}, \quad \psi(x, y, t) = \psi(x, y)e^{-i\omega t} \tag{4.3.3.5}$$

$$F(x, y, t) = F(x, y)e^{-i\omega t}, \quad G(x, y, t) = G(x, y)e^{-i\omega t} \tag{4.3.3.6}$$

The Lame potential differential equations for time harmonic conditions are obtained by inserting (4.3.3.5), (4.3.3.6) into (4.3.3.1), (4.3.3.4)

$$\nabla^4\phi - \frac{1}{l^2}\left(1 - \frac{h^2\omega^2}{v_1^2}\right)\nabla^2\phi - \frac{1}{l^2 v_1^2}\phi = \frac{1}{l^2}F \tag{4.3.3.7}$$

$$\nabla^4\psi - \frac{1}{l^2}\left(1 - \frac{h^2\omega^2}{v_2^2}\right)\nabla^2\psi - \frac{1}{l^2 v_2^2}\psi = \frac{1}{l^2}G \tag{4.3.3.8}$$

The expressions of F, G can be determined using (3.4.1.3), (3.4.2.6), (4.3.1.6) and Corollary 3.4.1.1, which is a result of the Helmholtz decomposition theorem:

$$F(\mathbf{r}) = \frac{1}{4\pi\rho v_1^2}\int_V \frac{\nabla_{\mathbf{r}'}\cdot\mathbf{P}(\mathbf{r}')}{|\mathbf{r}-\mathbf{r}'|}\,dV' \tag{4.3.3.9}$$

$$\mathbf{G}(\mathbf{r}) = \frac{1}{4\pi\rho v_2^2}\int_V \frac{\nabla_{\mathbf{r}'}\times\mathbf{P}(\mathbf{r}')}{|\mathbf{r}-\mathbf{r}'|}\,dV' \tag{4.3.3.10}$$

The above equations can be modified, so that F, G can be determined directly. To achieve this we will use the following vector identities:

$$\nabla\cdot(a\mathbf{v}) = \mathbf{v}\cdot\nabla a + a\nabla\cdot\mathbf{v}, \quad \forall a, \mathbf{v} \tag{4.3.3.11}$$

$$\nabla\times(a\mathbf{v}) = -\mathbf{v}\times\nabla a + a\nabla\times\mathbf{v}, \quad \forall a, \mathbf{v} \tag{4.3.3.12}$$

In view of (4.3.3.11), (4.3.3.12), equations (4.3.3.9), (4.3.3.10) became:

$$F(\mathbf{r}) = \frac{1}{4\pi\rho v_1^2}\int_V \nabla_{\mathbf{r}'}\cdot\frac{\mathbf{P}(\mathbf{r}')}{|\mathbf{r}-\mathbf{r}'|}\,dV' - \frac{1}{4\pi\rho v_1^2}\int_V \mathbf{P}(\mathbf{r}')\cdot\nabla_{\mathbf{r}'}\frac{1}{|\mathbf{r}-\mathbf{r}'|}\,dV' \tag{4.3.3.13}$$

$$\mathbf{G}(\mathbf{r}) = \frac{1}{4\pi\rho v_2^2}\int_V \nabla_{\mathbf{r}'}\times\frac{\mathbf{P}(\mathbf{r}')}{|\mathbf{r}-\mathbf{r}'|}\,dV' + \frac{1}{4\pi\rho v_2^2}\int_V \mathbf{P}(\mathbf{r}')\times\nabla_{\mathbf{r}'}\frac{1}{|\mathbf{r}-\mathbf{r}'|}\,dV' \tag{4.3.3.14}$$

The divergence theorem for vector fields is:

$$\int_R \nabla\cdot\mathbf{v}\,dV = \oint_{\partial R}\mathbf{n}\cdot\mathbf{v}\,dS \tag{4.3.3.15}$$

By setting $\mathbf{v} = \mathbf{a}\times\mathbf{v}$ in (4.3.3.15) we obtain:

$$\int_R \nabla\cdot(\mathbf{a}\times\mathbf{v})\,dV = \oint_{\partial R}\mathbf{n}\cdot(\mathbf{a}\times\mathbf{v})\,dS \tag{4.3.3.16}$$

Sifting the terms in (4.3.3.16) yields:

$$\int_R -\mathbf{a}\cdot(\nabla\times\mathbf{v})\,dV = \oint_{\partial R} -\mathbf{a}\cdot(\mathbf{n}\times\mathbf{v})\,dS, \quad \forall\mathbf{a},\mathbf{v} \tag{4.3.3.17}$$

Since (4.3.3.16) holds $\forall\mathbf{a},\mathbf{v}$ we can write:

$$\int_R \nabla\times\mathbf{v}\,dV = \oint_{\partial R} \mathbf{n}\times\mathbf{v}\,dS, \quad \forall\mathbf{a},\mathbf{v} \tag{4.3.3.18}$$

By substituting (4.3.3.17) into (4.3.3.13) and (4.3.3.18) into (4.3.3.14) we obtain:

$$F(\mathbf{r}) = -\frac{1}{4\pi\rho v_1^2}\int_V \mathbf{P}(\mathbf{r}')\cdot\nabla_{\mathbf{r}'}\frac{1}{|\mathbf{r}-\mathbf{r}'|}\,dV' + \frac{1}{4\pi\rho v_1^2}\oint_{\partial V}\mathbf{n}'\cdot\frac{\mathbf{P}(\mathbf{r}')}{|\mathbf{r}-\mathbf{r}'|}\,dS' \tag{4.3.3.19}$$

$$\mathbf{G}(\mathbf{r}) = \frac{1}{4\pi\rho v_2^2}\int_V \mathbf{P}(\mathbf{r}')\times\nabla_{\mathbf{r}'}\frac{1}{|\mathbf{r}-\mathbf{r}'|}\,dV' + \frac{1}{4\pi\rho v_2^2}\oint_{\partial V}\mathbf{n}'\times\frac{\mathbf{P}(\mathbf{r}')}{|\mathbf{r}-\mathbf{r}'|}\,dS' \tag{4.3.3.20}$$

Due to the assumptions of Corollary 3.4.1.1 the surface integrals can be neglected in (4.3.3.19), (4.3.3.20):

$$F(\mathbf{r}) = -\frac{1}{4\pi\rho v_1^2}\int_V \mathbf{P}(\mathbf{r}')\cdot\nabla_{\mathbf{r}'}\frac{1}{|\mathbf{r}-\mathbf{r}'|}\,dV' \tag{4.3.3.21}$$

$$\mathbf{G}(\mathbf{r}) = \frac{1}{4\pi\rho v_2^2}\int_V \mathbf{P}(\mathbf{r}')\times\nabla_{\mathbf{r}'}\frac{1}{|\mathbf{r}-\mathbf{r}'|}\,dV' \tag{4.3.3.22}$$

Where:

$$\nabla_{\mathbf{r}'}\frac{1}{|\mathbf{r}-\mathbf{r}'|} = -\nabla_{\mathbf{r}}\frac{1}{|\mathbf{r}-\mathbf{r}'|} \tag{4.3.3.23}$$

Substituting (4.3.3.23) into (4.3.3.21), (4.3.3.22) yields:

$$F(\mathbf{r}) = \frac{1}{4\pi\rho v_1^2}\int_V \mathbf{P}(\mathbf{r}')\cdot\nabla_{\mathbf{x}}\frac{1}{|\mathbf{r}-\mathbf{r}'|}\,dV' \tag{4.3.3.24}$$

$$\mathbf{G}(\mathbf{r}) = -\frac{1}{4\pi\rho v_2^2}\int_V \mathbf{P}(\mathbf{r}'\times\nabla_{\mathbf{r}}\frac{1}{|\mathbf{r}-\mathbf{r}'|}\,dV' \tag{4.3.3.25}$$

In the above equations the gradient operator can be moved outside of the integrals:

$$F(\mathbf{r}) = \frac{1}{4\pi\rho v_1^2}\nabla_{\mathbf{r}} \cdot \int_V \frac{\mathbf{P}(\mathbf{r}')}{|\mathbf{r}-\mathbf{r}'|}\, dV' \tag{4.3.3.26}$$

$$\mathbf{G}(\mathbf{r}) = -\frac{1}{4\pi\rho v_2^2}\nabla_{\mathbf{r}} \times \int_V \frac{\mathbf{P}(\mathbf{r}')}{|\mathbf{r}-\mathbf{r}'|}\, dV' \tag{4.3.3.27}$$

The integrals that appear in (4.3.3.26), (4.3.3.27) are related to the Green's function of the Poison equation $\nabla^2 g = f$, which for the two-dimensional case is:

$$g(\mathbf{r};\mathbf{r}') = -\frac{1}{4\pi}\int_V \frac{f(\mathbf{r}')}{|\mathbf{r}-\mathbf{r}'|}\, dV' \tag{4.3.3.28}$$

When $\mathbf{P}$ is considered as a point body force $\mathbf{P} = \delta(\mathbf{r}')\mathbf{p}$, equations (4.3.3.26), (4.3.3.27) take the form:

$$F(\mathbf{r}) = \frac{1}{4\pi\rho v_1^2}\nabla_{\mathbf{r}} \cdot \int_V \frac{\mathbf{p}\delta(\mathbf{r}')}{|\mathbf{r}-\mathbf{r}'|}\, dV' \tag{4.3.3.29}$$

$$\mathbf{G}(\mathbf{r}) = -\frac{1}{4\pi\rho v_2^2}\nabla_{\mathbf{r}} \times \int_V \frac{\mathbf{p}\delta(\mathbf{r}')}{|\mathbf{r}-\mathbf{r}'|}\, dV' \tag{4.3.3.30}$$

Where $\mathbf{p} = (p_x, p_y)$ is a constant vector. Also, when $f(\mathbf{r}) = \delta(\mathbf{r}')$, (4.3.3.28) yields:

$$g(\mathbf{r};\mathbf{r}') = -\frac{1}{4\pi}\int_V \frac{\delta(\mathbf{r}')}{|\mathbf{r}-\mathbf{r}'|}\, dV' = \frac{1}{2\pi}\ln(|\mathbf{r}-\mathbf{r}'|) \tag{4.3.3.31}$$

In the following equations the norm of vector r will be denoted as: $r = |\mathbf{r}| = \sqrt{x^2+y^2}$. By substituting (4.3.3.31) into (4.3.3.29), (4.3.3.30) we obtain:

$$F(\mathbf{r}) = -\frac{1}{2\pi\rho v_1^2}\nabla \cdot \ln(r)\mathbf{p} \tag{4.3.3.32}$$

$$\mathbf{G}(\mathbf{r}) = \frac{1}{2\pi\rho v_2^2}\nabla \times \ln(r)\mathbf{p} \tag{4.3.3.33}$$

Executing the differentiations in (4.3.3.32), (4.3.3.33) yields:

$$F(\mathbf{r}) = -\frac{xp_x + yp_y}{2\pi(x^2+y^2)\rho v_1^2} \tag{4.3.3.34}$$

$$\mathbf{G}(\mathbf{r}) = G(\mathbf{r}) = \frac{xp_y - yp_x}{2\pi(x^2+y^2)\rho v_2^2} \tag{4.3.3.35}$$

Inserting (4.3.3.34), (4.3.3.35) into (4.3.3.7), (4.3.3.8) gives:

$$\nabla^4\phi - \frac{1}{l^2}\left(1 - \frac{h^2\omega^2}{v_1^2}\right)\nabla^2\phi - \frac{1}{l^2 v_1^2}\phi = -\frac{xp_x + yp_y}{2\pi(x^2+y^2)\rho v_1^2 l^2} \tag{4.3.3.36}$$

$$\nabla^4\psi - \frac{1}{l^2}\left(1 - \frac{h^2\omega^2}{v_2^2}\right)\nabla^2\psi - \frac{1}{l^2 v_2^2}\psi = \frac{xp_y - yp_x}{2\pi(x^2+y^2)\rho v_2^2 l^2} \tag{4.3.3.37}$$

By applying the double Fourier transform in (4.3.3.36), (4.3.3.37) we obtain the following expressions for the transformed displacement components

$$\hat{\hat{\phi}} = \frac{\xi p_x + \eta p_y}{\left(\xi^2+\eta^2\right)\left\{(\lambda+2\mu)\left(\xi^2+\eta^2\right)\left[l^2\left(\xi^2+\eta^2\right)+1\right] - \left[\rho h^2\left(\xi^2+\eta^2\right)+\rho\right]\omega^2\right\}} i \tag{4.3.3.38}$$

$$\hat{\hat{\psi}} = \frac{-\xi p_x + \eta p_y}{\left(\xi^2+\eta^2\right)\left\{\mu\left(\xi^2+\eta^2\right)\left[l^2\left(\xi^2+\eta^2\right)+1\right] - \left[\rho h^2\left(\xi^2+\eta^2\right)+\rho\right]\omega^2\right\}} i \tag{4.3.3.39}$$

Equations (4.3.3.38), (4.3.3.39) can equivalently be written as:

$$\hat{\hat{\phi}} = \frac{\xi p_x + \eta p_y}{\left(\xi^2+\eta^2\right)\left\{v_1^2\left(\xi^2+\eta^2\right)\left[l^2\left(\xi^2+\eta^2\right)+1\right] - \left[h^2\left(\xi^2+\eta^2\right)+1\right]\omega^2\right\}\rho} i \tag{4.3.3.40}$$

$$\hat{\hat{\psi}} = \frac{-\xi p_x + \eta p_y}{\left(\xi^2+\eta^2\right)\left\{v_2^2\left(\xi^2+\eta^2\right)\left[l^2\left(\xi^2+\eta^2\right)+1\right] - \left[h^2\left(\xi^2+\eta^2\right)+1\right]\omega^2\right\}\rho} i \tag{4.3.3.41}$$

In view of (4.3.2.14), equations (4.3.3.40), (4.3.3.41) become:

$$\hat{\hat{\phi}} = \frac{\xi p_x + \eta p_y}{\left(\xi^2+\eta^2\right)\left\{\left(\xi^2+\eta^2\right)\left[l^2\left(\xi^2+\eta^2\right)+1\right] - \left[h^2\left(\xi^2+\eta^2\right)+1\right]k_1^2\right\}(\lambda+2\mu)} i \tag{4.3.3.42}$$

$$\hat{\hat{\psi}} = \frac{-\xi p_x + \eta p_y}{\left(\xi^2+\eta^2\right)\left\{\left(\xi^2+\eta^2\right)\left[l^2\left(\xi^2+\eta^2\right)+1\right] - \left[h^2\left(\xi^2+\eta^2\right)+1\right]k_2^2\right\}\mu} i \tag{4.3.3.43}$$

Using (4.3.2.13), we can prove that $\lambda + 2\mu = \beta^2\mu$, which results in:

$$\hat{\hat{\phi}} = \frac{\xi p_x + \eta p_y}{\left(\xi^2+\eta^2\right)\left\{\left(\xi^2+\eta^2\right)\left[l^2\left(\xi^2+\eta^2\right)+1\right] - \left[h^2\left(\xi^2+\eta^2\right)+1\right]k_1^2\right\}\beta^2\mu} i \tag{4.3.3.44}$$

$$\hat{\hat{\psi}} = \frac{-\xi p_x + \eta p_y}{\left(\xi^2+\eta^2\right)\left\{\left(\xi^2+\eta^2\right)\left[l^2\left(\xi^2+\eta^2\right)+1\right] - \left[h^2\left(\xi^2+\eta^2\right)+1\right]\beta^2 k_1^2\right\}\mu} i \tag{4.3.3.45}$$

By applying the inverse Fourier transform in (4.3.3.44), (4.3.3.45)

$$\begin{aligned}\phi = &\frac{p_x}{4\pi^2\mu\beta^2}\int_{-\infty}^{+\infty}\int_{-\infty}^{+\infty}\frac{\xi\left(\xi^2+\eta^2\right)^{-1}e^{i(\xi x+\eta y)}}{\left(\xi^2+\eta^2\right)\left[l^2\left(\xi^2+\eta^2\right)+1\right] - \left[h^2\left(\xi^2+\eta^2\right)+1\right]k_1^2}\,d\xi\,d\eta \\ &+\frac{p_y}{4\pi^2\mu\beta^2}\int_{-\infty}^{+\infty}\int_{-\infty}^{+\infty}\frac{\eta\left(\xi^2+\eta^2\right)^{-1}e^{i(\xi x+\eta y)}}{\left(\xi^2+\eta^2\right)\left[l^2\left(\xi^2+\eta^2\right)+1\right] - \left[h^2\left(\xi^2+\eta^2\right)+1\right]k_1^2}\,d\xi\,d\eta\end{aligned} \tag{4.3.3.46}$$

$$\begin{aligned}\psi = &\frac{p_y}{4\pi^2\mu}\int_{-\infty}^{+\infty}\int_{-\infty}^{+\infty}\frac{\eta\left(\xi^2+\eta^2\right)^{-1}e^{i(\xi x+\eta y)}}{\left(\xi^2+\eta^2\right)\left[l^2\left(\xi^2+\eta^2\right)+1\right] - \left[h^2\left(\xi^2+\eta^2\right)+1\right]\beta^2k_1^2}\,d\xi\,d\eta \\ &-\frac{p_x}{4\pi^2\mu}\int_{-\infty}^{+\infty}\int_{-\infty}^{+\infty}\frac{\xi\left(\xi^2+\eta^2\right)^{-1}e^{i(\xi x+\eta y)}}{\left(\xi^2+\eta^2\right)\left[l^2\left(\xi^2+\eta^2\right)+1\right] - \left[h^2\left(\xi^2+\eta^2\right)+1\right]\beta^2k_1^2}\,d\xi\,d\eta\end{aligned} \tag{4.3.3.47}$$

The final two equations can be written in compacted form as:

$$\phi = \frac{1}{4\pi^2\mu\beta^2}\left[p_x\frac{\partial}{\partial x}I(x,y,k_1) + p_y\frac{\partial}{\partial y}I(x,y,k_1)\right] \tag{4.3.3.48}$$

$$\psi = \frac{\beta^2}{4\pi^2\mu\beta^2}\left[p_y\frac{\partial}{\partial y}I(x,y,\beta k_1) - p_x\frac{\partial}{\partial x}I(x,y,\beta k_1)\right] \tag{4.3.3.49}$$

Where I is given by (4.3.2.35), while it's polar coordinate representation is given by (4.3.2.39). By applying the chain rule in (4.3.3.48), (4.3.3.49) we obtain:

$$\phi = \frac{1}{4\pi^2\mu\beta^2}\left[p_x\frac{\partial I(r,\theta,k_1)}{\partial r}\left(\frac{\partial r}{\partial x}\right) + p_y\frac{\partial I(r,\theta,k_1)}{\partial r}\left(\frac{\partial r}{\partial y}\right)\right] \tag{4.3.3.50}$$

$$\psi = \frac{\beta^2}{4\pi^2\mu\beta^2}\left[p_y\frac{\partial I(r,\theta,\beta k_1)}{\partial r}\left(\frac{\partial r}{\partial y}\right) - p_x\frac{\partial I(r,\theta,\beta k_1)}{\partial x}\left(\frac{\partial r}{\partial x}\right)\right] \tag{4.3.3.51}$$

The expressions $\partial I/\partial r$ and the first derivatives of r are given by (4.3.2.59) and (4.3.2.67) respectively. Finally, the Lamé potentials are obtained by substituting the aforementioned equations into (4.3.3.50), (4.3.3.51)

$$\phi = \frac{p_x x + p_y y}{2\pi k_1^2 \mu \beta^2 r^2} - \frac{p_x x + p_y y}{4l^2 \mu \beta^2 \left[p^2(k_1) - q^2(k_1)\right] r} i \left[\frac{H_1^{(1)}(p(k_1)r)}{p(k_1)} - \frac{H_1^{(1)}(q(k_1)r)}{q(k_1)} \right] \tag{4.3.3.52}$$

$$\psi = \frac{p_y x - p_x y}{2\pi k_1^2 \mu \beta^2 r^2} + \frac{p_y x - p_x y}{4l^2 \mu \left[p^2(\beta k_1) - q^2(\beta k_1)\right] r} i \left[\frac{H_1^{(1)}(p(\beta k_1)r)}{p(\beta k_1)} - \frac{H_1^{(1)}(q(\beta k_1)r)}{q(\beta k_1)} \right] \tag{4.3.3.53}$$

The displacement components are obtained by substituting (4.3.3.52), (4.3.3.52) into (3.4.1.1). The resulting expressions match those given in equations (4.3.2.69) - (4.3.2.72), indicating that both methods lead to the same outcome.

4.3.4 Displacement Fields

For plotting the distributions of the displacement components it is convenient to introduce the following non-dimensional variables:

$$H = \frac{h}{l} \tag{4.3.4.1}$$

$$K_1 = l k_1 \tag{4.3.4.2}$$

$$X = \frac{x - x'}{l} = \frac{(x - x')k_1}{K_1} \tag{4.3.4.3}$$

$$Y = \frac{y - y'}{l} = \frac{(y - y')k_1}{K_1} \tag{4.3.4.4}$$

$$R = \frac{s}{l} = \frac{s k_1}{K_1}, \quad R^2 = X^2 + Y^2 \tag{4.3.4.5}$$

$$\bar{U}_x^{p_x} = \frac{\tilde{\mu} U_x^{p_x}}{p_x}, \quad \bar{U}_x^{p_y} = \frac{\tilde{\mu} U_x^{p_y}}{p_y}, \quad \bar{U}_y^{p_x} = \frac{\tilde{\mu} U_y^{p_x}}{p_x}, \quad \bar{U}_y^{p_y} = \frac{\tilde{\mu} U_y^{p_y}}{p_y} \tag{4.3.4.6}$$

Where H is the non-dimensional characteristic length of the material, K_1 is a non-dimensional wave number, X is the non-dimensional x coordinate, Y is the non-dimensional y coordinate, R is the non-dimensional radial coordinate and $\bar{U}_i^{p_j}$ are the non-dimensional components of the Green's function. Also, due to (4.3.2.15), (4.3.2.16) and (4.3.4.6), the non-dimensional displacement components are:

$$\bar{U}_x = \bar{U}_x^{p_x} + \bar{U}_x^{p_y}, \quad \bar{U}_y = \bar{U}_y^{p_x} + \bar{U}_y^{p_y} \tag{4.3.4.7}$$

By substituting (4.3.4.1) - (4.3.4.5) into (4.3.2.44), (4.3.2.45) the following expressions for the roots of the dispersion equation arise:

$$p(k_1) = \pm\sqrt{\frac{H^2K_1^2 - 1 - \sqrt{4K_1^2 + \left(H^2K_1^2 - 1\right)^2}}{2K_1^2}k_1^2} \tag{4.3.4.8}$$

$$q(k_1) = \pm\sqrt{\frac{H^2K_1^2 - 1 + \sqrt{4K_1^2 + \left(H^2K_1^2 - 1\right)^2}}{2K_1^2}k_1^2} \tag{4.3.4.9}$$

In view of (4.2.3.27), (4.3.4.1) - (4.3.4.6) the non-dimensional Green's function is:

$$\bar{\mathbf{G}}(\mathbf{r};\mathbf{r}') = \frac{1}{4\beta^2}i\left[\Psi(s)\mathbf{I} + X(s)\hat{\mathbf{s}}\otimes\hat{\mathbf{s}}\right] \tag{4.3.4.10}$$

Where:

$$p^2(k_1) - q^2(k_1) = -\sqrt{\frac{4K_1^2 + \left(H^2K_1^2 - 1\right)^2}{l^2}} \tag{4.3.4.11}$$

$$p(k_1)s = \pm\sqrt{\frac{H^2K_1^2 - 1 - \sqrt{4K_1^2 + \left(H^2K_1^2 - 1\right)^2}}{2}R} \tag{4.3.4.12}$$

$$p(k_1)s = \pm\sqrt{\frac{H^2K_1^2 - 1 + \sqrt{4K_1^2 + \left(H^2K_1^2 - 1\right)^2}}{2}R} \tag{4.3.4.13}$$

The expressions of $p(k_1)$, $q(k_1)$ are now given by (4.3.4.8), (4.3.4.9) and when (4.3.4.10), (or (4.3.2.73) - (4.3.2.77)) are used only the positive roots are taken into account. It is also noted that in view of (4.3.4.11) - (4.3.4.13), the radial coordinate s and the gradient coefficient l do not appear in (4.3.4.10). The non-dimensional displacement contours are determined using (4.3.4.10), we distinguish the cases of normal ($H > 1$), anomalous ($H < 1$) and no dispersion ($H = 1$) by adjusting the value of H and β. It will be shown that β depends only from the Poisson ratio v, thus the systems parameters are H, K_1, v. In view of (4.3.2.8), (4.3.2.9), (4.3.2.13) we obtain:

$$\beta = \sqrt{\frac{\lambda + 2\mu}{\mu}} = \sqrt{1 + \frac{1}{1 - 2v}} \tag{4.3.4.14}$$

In the figures that follow the contours of the norm of the displacement components and the norm of the total displacement are presented, for the case where the body force is applied at the origin of the coordinate system. Unlike the case of anti - plane shear, the response is not explored in detail here due to the greater number of parameters involved and results are given only for characteristic values of the systems parameters. The reason that results are given only for $v = 0.25$ is that for fixed values of H, K_1 the qualitative response of the system does not depend from the value of the Poisson ratio.

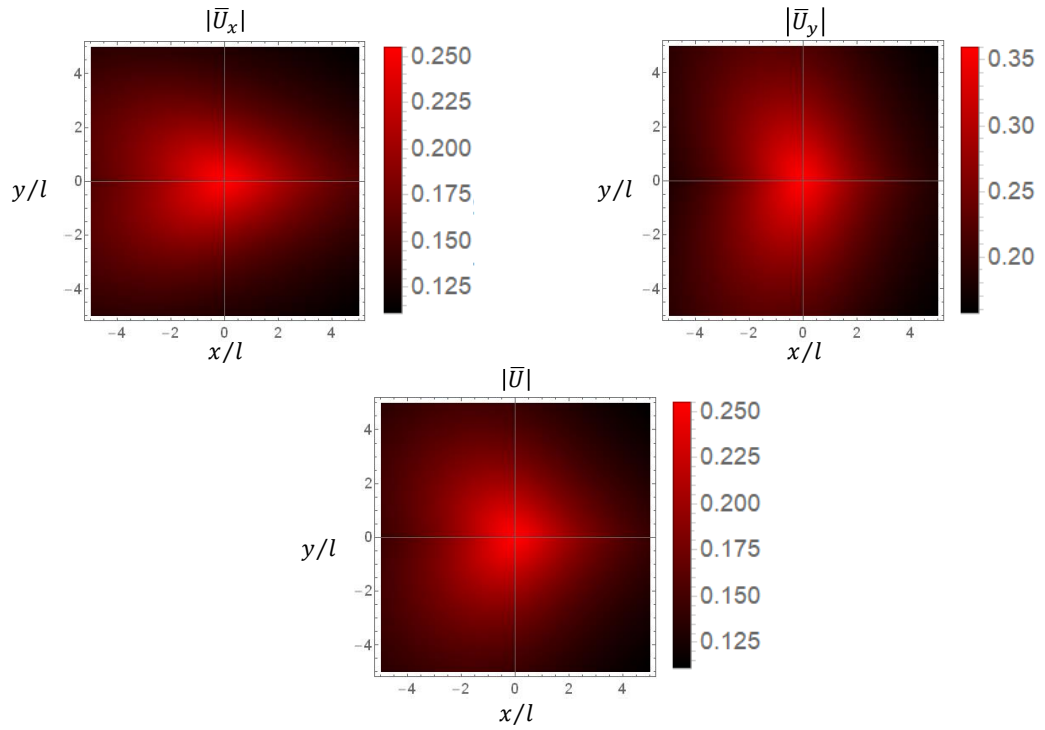

Figure 4.3.4.1: Displacement contours for $H = 1$, $K_1 = 0.1$, $v = 0.25$, (no dispersion).

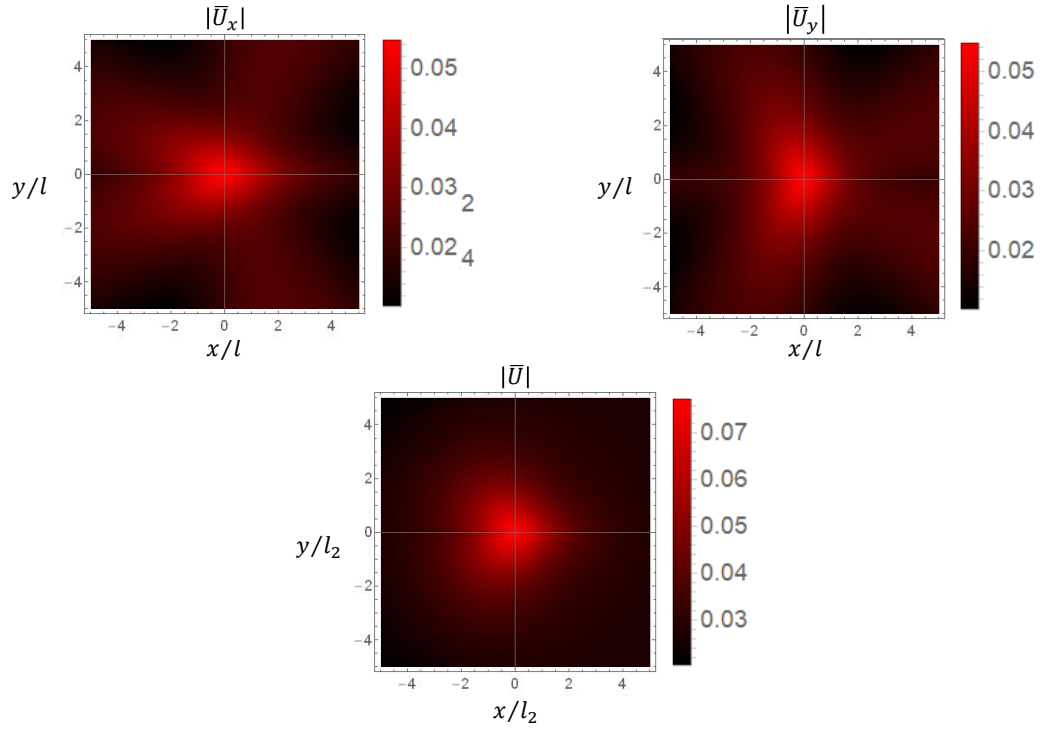

Figure 4.3.4.2: Displacement contours for $H = 1$, $K_1 = 1$, $v = 0.25$, (no dispersion).

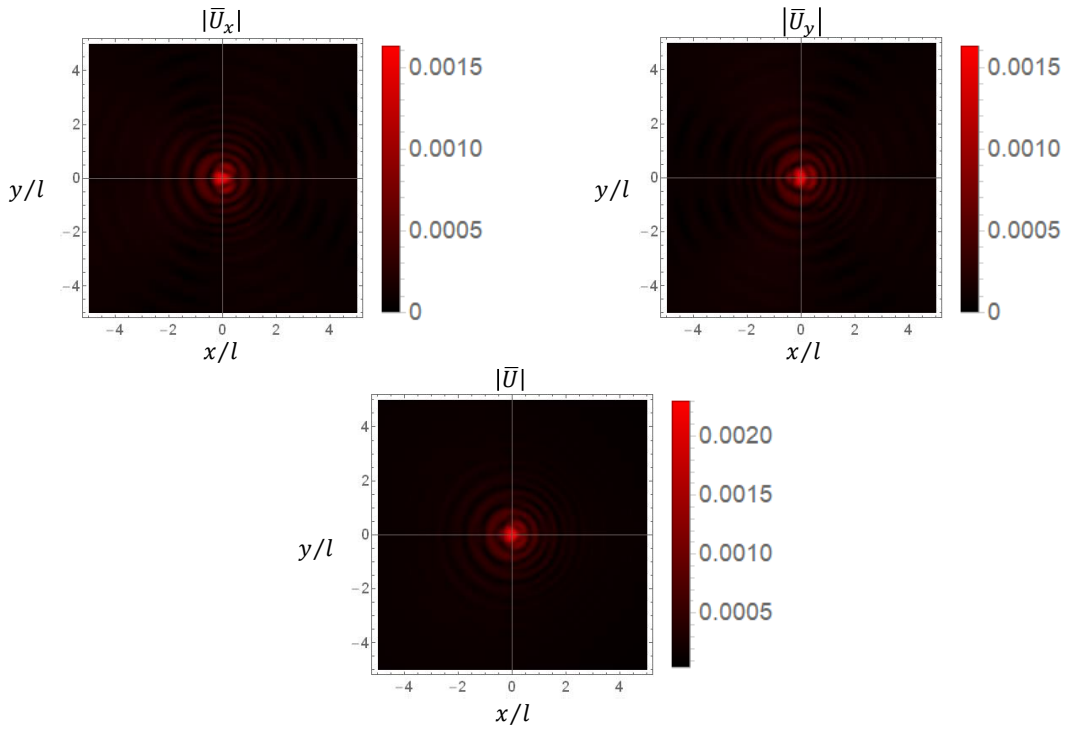

Figure 4.3.4.3: Displacement contours for $H = 1$, $K_1 = 10$, $v = 0.25$, (no dispersion).

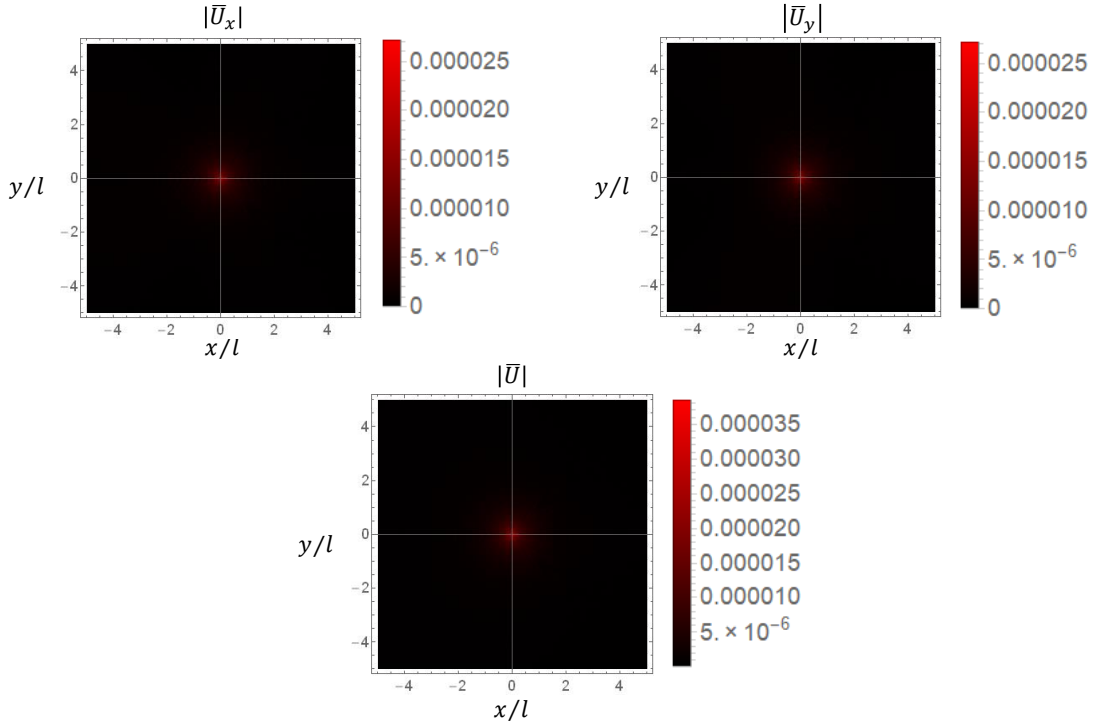

Figure 4.3.4.4: Displacement contours for $H = 1$, $K_1 = 100$, $v = 0.25$, (no dispersion).

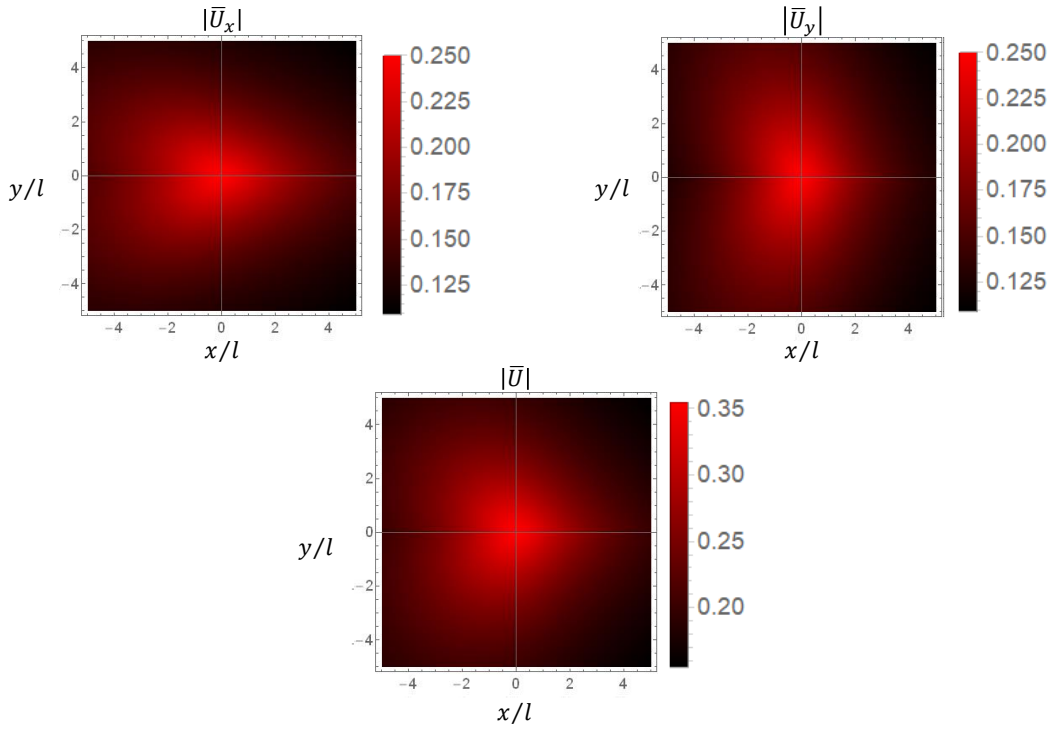

Figure 4.3.4.5: Displacement contours for $H = 0.1$, $K_1 = 0.1$, $v = 0.25$, (anomalous dispersion).

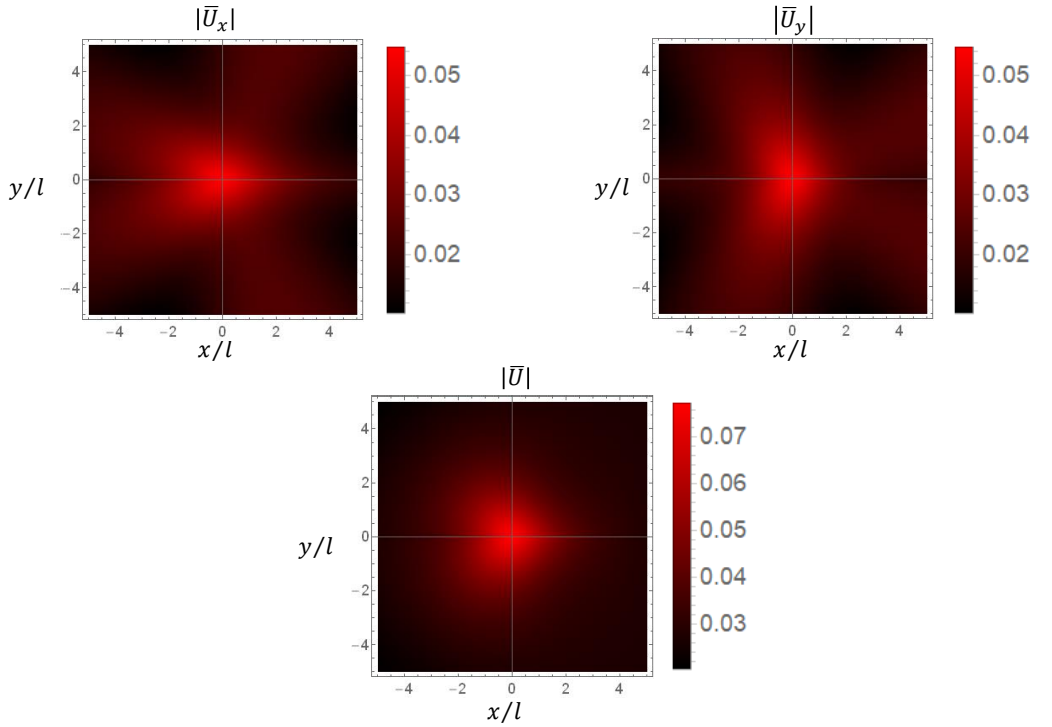

Figure 4.3.4.6: Displacement contours for $H = 0.1$, $K_1 = 1$, $v = 0.25$, (anomalous dispersion).

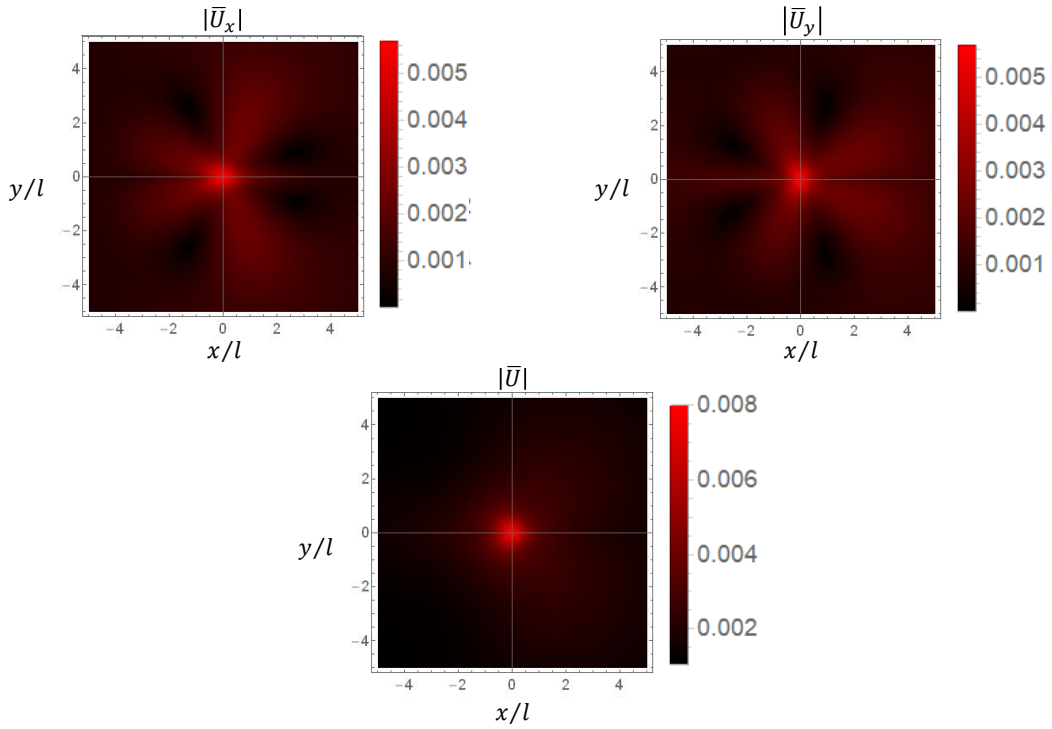

Figure 4.3.4.7: Displacement contours for $H = 0.1$, $K_1 = 10$, $v = 0.25$, (anomalous dispersion).

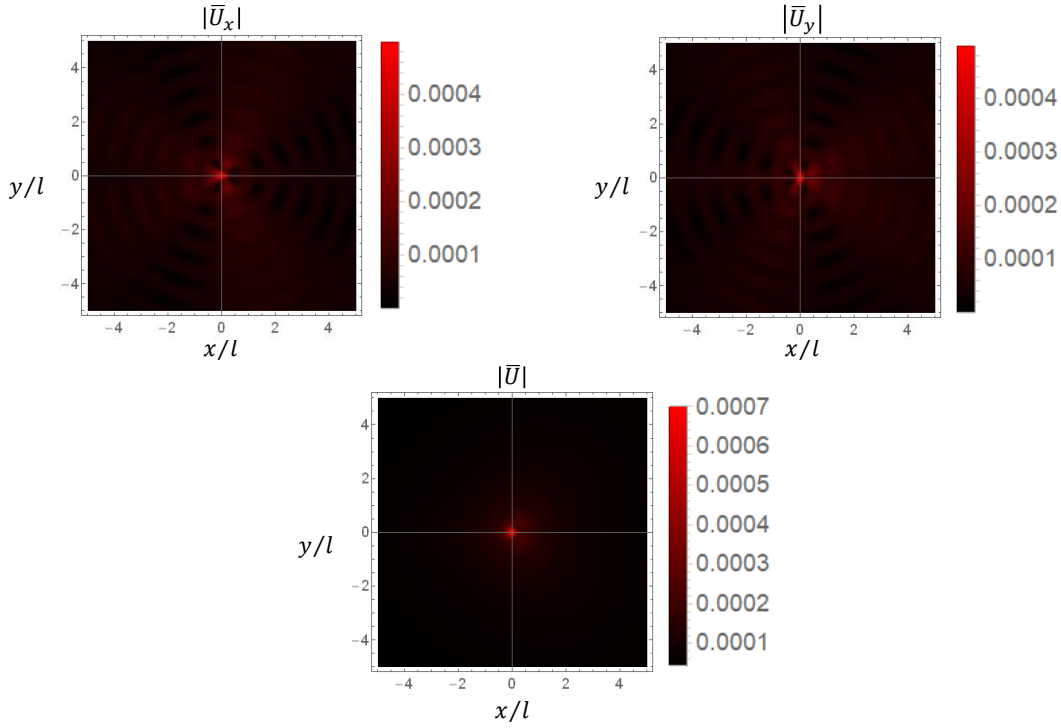

Figure 4.3.4.8: Displacement contours for $H = 0.1$, $K_1 = 100$, $v = 0.25$, (anomalous dispersion).

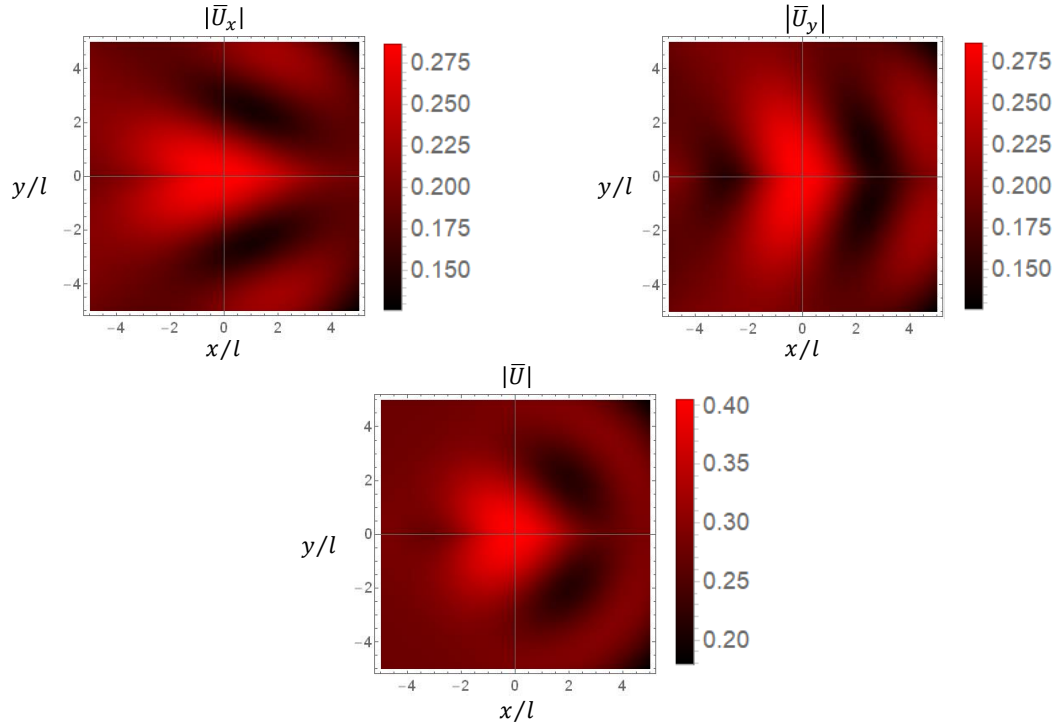

Figure 4.3.4.9: Displacement contours for $H = 10$, $K_1 = 0.1$, $v = 0.25$, (normal dispersion).

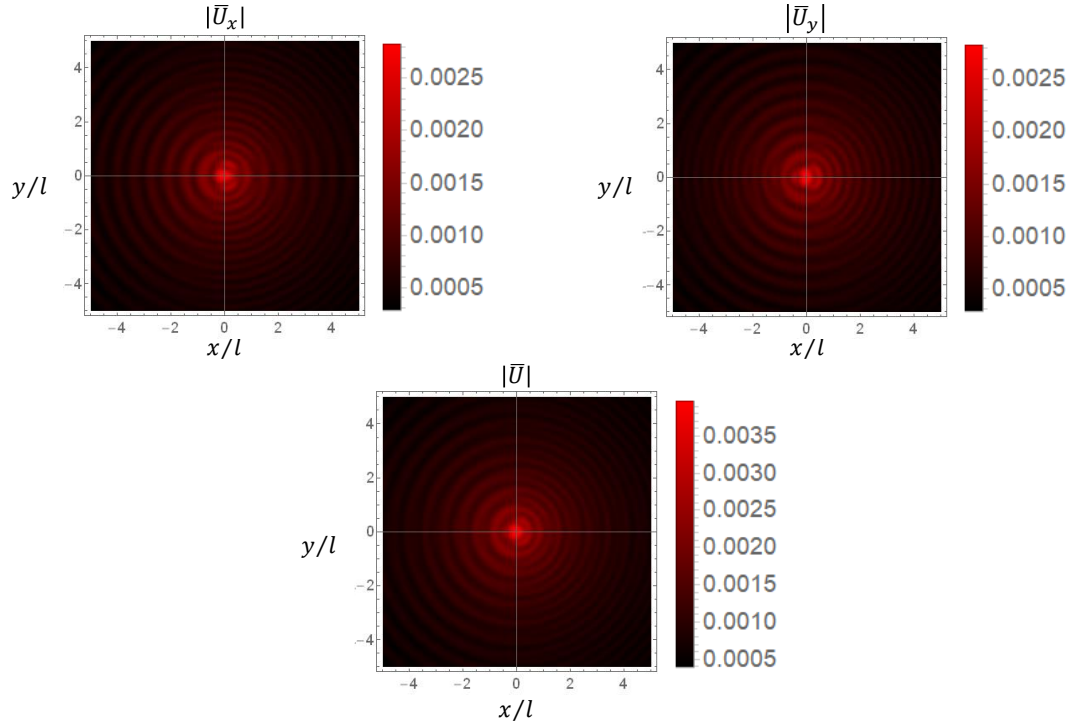

Figure 4.3.4.10: Displacement contours for $H = 10$, $K_1 = 1$, $v = 0.25$, (normal dispersion).

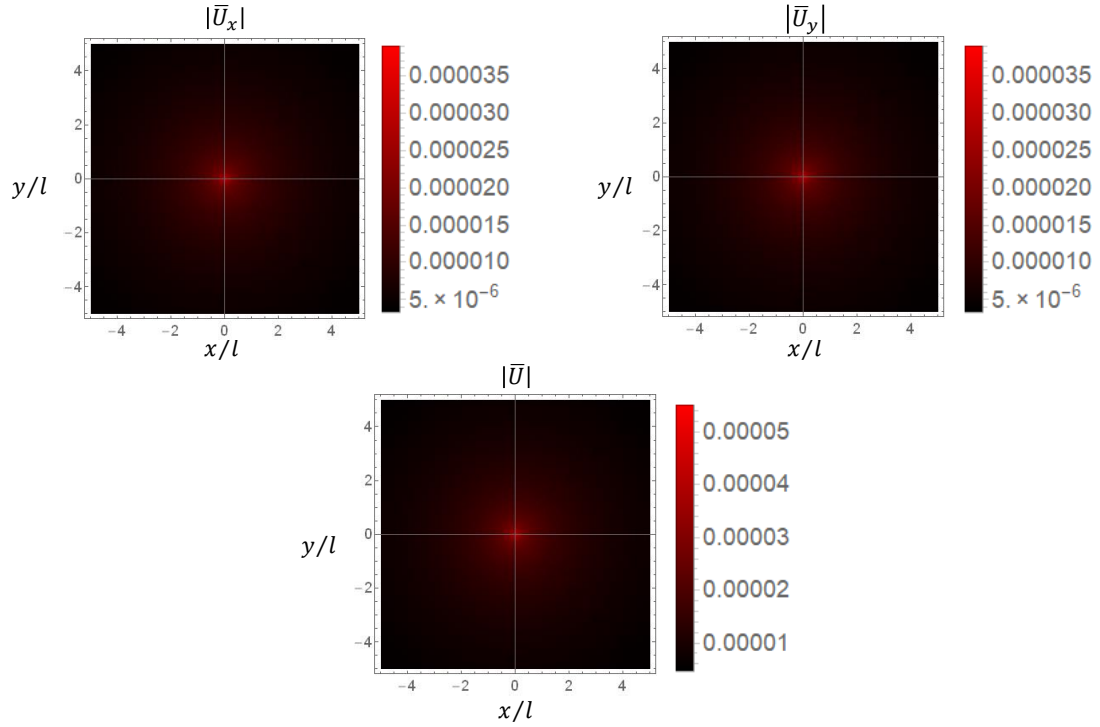

Figure 4.3.4.11: Displacement contours for $H = 10$, $K_1 = 10$, $v = 0.25$, (normal dispersion).

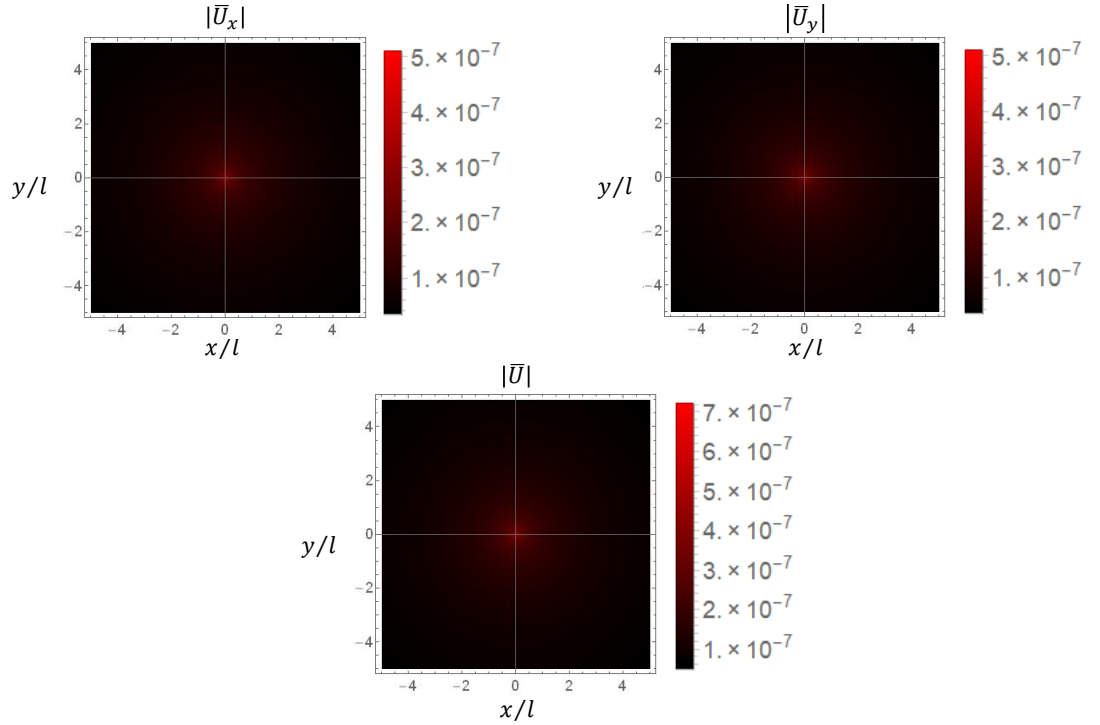

Figure 4.3.4.12: Displacement contours for $H = 10$, $K_1 = 100$, $v = 0.25$, (normal dispersion).

5 Scattering Problems

5.1 Introduction

In this part of the thesis the two fundamental solutions that where derived in the previous chapter are applied in order to formulate scattering problems in the context of gradient continua. In the problems that are examined the scattering is caused by a number of obstacle points (or pins) which are modelled as concentrated body forces. When these configurations of points form the corners of closed geometrical shapes such as polygons, then in some cases exotic behaviours are observed in relation to the response of the system. For example, for specific values of the waves frequency the system's motions can be limited either inside or outside these configurations. The idea behind this concept is similar to well known Faraday cage where a electromagnetic field is trapped inside an enclosure. The reason why this idea cannot be applied in the context of classical continua is because in classical elasticity the corresponding Green's functions are singular at the point where the body force is applied and as a consequence the displacements are infinite in these points, however as it was shown in the previous chapter that the Green's functions that where derived are finite. For the case of plane strain, due to the computational load that arises from the extensive expression of the corresponding Green;s function, geometrically simple configurations of pins are considered for circles consisting of 12, 24 and 64 pins. The case of anti-plane shear has much less computational load, since the problem is scalar, which allows the consideration of more complex configurations such as fractals. Specifically results are given for the case where the pins form the corners of Koch's snowflake [86]. To the knowledge of the author both problems have never been attempted before in the context of sub-theories of Mindlin's general one and present interests both from a scientific and a practical point of view as related applications where presented in the first chapter of the thesis.

5.2 Scattering by Points

5.2.1 Scattering by a Single Point Under Anti-Plane Shear

In this work, the wave scattering for the case of anti-plane strain is formulated having as a mathematical background a paper published by Evans and Porter in 2007 [87]. In their work Evans and Porter modelled the scattering of flexural waves by pined elastic plates in vacuo and floating on water, which is a similar concept to the one indicated in this thesis.

In its equilibrium position an infinite domain governed by form II of Mindlin's general theory occupies the $x-y$ plane and when excited by an incident wave field of unit amplitude, undergoes a displacement normal to itself of the following form:

$$\mathcal{R}\{u_{in}(\mathbf{r})e^{-i\omega t}\} \tag{5.2.1.1}$$

Where ω is the circular frequency of the incident excitation given by (3.4.3.6) and $\mathbf{r} = (x, y) = (r\cos(\theta), r\sin(\theta))$. A solution of the systems homogeneous equation of motion (4.2.1.8) describing a long-crested incident wave is:

$$u_{in}(\mathbf{r}) = e^{iq[x\cos(\psi)+y\sin(\psi)]} = e^{iqr\cos(\theta-\psi)} \tag{5.2.1.2}$$

Where q is the positive real root of the dispersion equation given by (4.2.3.15) and ψ is the angle defined by the positive x-axis and the direction of wave propagation. Also, since the Green's function of anti-plane shear has been written in a non-dimensional form (4.2.4.7), it is necessary to express (5.2.1.2) using the same non-dimensional parameters that are defined by (4.2.4.1) - (4.2.4.3).

For an infinite domain under anti-plane shear, pinned by a single pin at a point with position vector $\mathbf{r}' = (x', y')$, the non-dimensional displacement $U(\mathbf{r})$ can be expressed as the displacement generated by the incident wave given by (5.2.1.2) and the displacement due to the existence of the pin. Since the pin can be considered as a consecrated body force, the displacement field that it generates can be determined using the Green's function of the anti-plane shear, which in non-dimensional form is given by (4.2.4.7).

$$U(\mathbf{r}) = u_{in}(\mathbf{r}) + A\bar{g}(\mathbf{r};\mathbf{r}') \tag{5.2.1.3}$$

If the infinite domain is constrained at the position where the pin is placed, the constant A can be determined by setting (5.2.1.3) equal to zero for $\mathbf{r} = \mathbf{r}'$:

$$A = -\frac{u_{in}(\mathbf{r}')}{\bar{g}(\mathbf{r}';\mathbf{r}')} \tag{5.2.1.4}$$

In other words, in order for a point (x', y') to remain stationary during the deformation, a pin that generates a displacement equal and opposite to the one generated by the incident wave must be inserted at the same point.

5.2.2 Scattering by a Finite Number of Arbitrary Points Under Anti-Plane Shear

We now consider the case where the infinite domain is pined by N_p pins at points with position vectors $\mathbf{r'}_n$. The non-dimensional displacement $U(\mathbf{r})$ is now given as as the displacement generated by the incident wave given by (5.2.1.2) and the displacement due to the existence of all the pins:

$$U(\mathbf{r}) = u_{in}(\mathbf{r}) + \sum_{n=1}^{N_p} \left[A_n \bar{g}(\mathbf{r}_m; \mathbf{r'}_n)\right] \tag{5.2.2.1}$$

Again, if the infinite domain is constrained at the position where the pins are placed, the constants A_n can be determined by setting (5.2.2.1) equal to zero for $\mathbf{r}_m = \mathbf{r'}_n$ and solving the following N_p simultaneous algebraic equations:

$$0 = u_{in}(\mathbf{r}_m) + \sum_{n=1}^{N_p} \left[A_n \bar{g}(\mathbf{r}_m; \mathbf{r'}_n)\right], \quad m = 1, 2, ..., N_p \tag{5.2.2.2}$$

The solution to the system of equations (5.2.2.2) can be expressed in matrix form as:

$$\mathbf{A} = -\bar{\mathbf{G}}^{-1}\mathbf{U}_{in} \tag{5.2.2.3}$$

Where $\mathbf{A}$ is a $N_p \times 1$ vector with components the scaling factors A_n, $\bar{\mathbf{G}}$ is a $N_p \times N_p$ symmetric matrix with components $\bar{g}(\mathbf{r}_m; \mathbf{r}_n)$, (i.e. the problems Green matrix) and $\mathbf{U}_{in}$ is a $N_p \times 1$ vector with components $u_{in}(\mathbf{r}_m)$, (i.e. the non-dimensional displacement at each pin location, caused by an incident wave, in an unpinned infinite domain).

$$\mathbf{A} = \begin{bmatrix} A_1 \\ A_2 \\ \vdots \\ A_n \end{bmatrix}, \; \bar{\mathbf{G}} = \begin{bmatrix} \bar{g}(\mathbf{r}_1; \mathbf{r'}_1) & \bar{g}(\mathbf{r}_1; \mathbf{r'}_2) & \cdots & \bar{g}(\mathbf{r}_1; \mathbf{r'}_n) \\ \bar{g}(\mathbf{r}_2; \mathbf{r'}_1) & \bar{g}(\mathbf{r}_2; \mathbf{r'}_2) & \cdots & \bar{g}(\mathbf{r}_2; \mathbf{r'}_n) \\ \vdots & \vdots & \ddots & \vdots \\ \bar{g}(\mathbf{r}_n; \mathbf{r'}_1) & \bar{g}(\mathbf{r}_n; \mathbf{r'}_2) & \cdots & \bar{g}(\mathbf{r}_n; \mathbf{r'}_n) \end{bmatrix}, \; \mathbf{U}_{in} = \begin{bmatrix} u_{in}(\mathbf{r}_1) \\ u_{in}(\mathbf{r}_2) \\ \vdots \\ u_{in}(\mathbf{r}_n) \end{bmatrix} \tag{5.2.2.4}$$

The constants A_n are used to scale the value of the Green's function at the position of each pin so that they satisfy (5.2.2.2), but they also scale the Green's function at every other location, as observed in the plate deflection equation. Therefore, in order to maximise the displacements in an area of the plate defined by a configuration of pins, the absolute values

of the constants A_n should be maximised. Since $\mathbf{U}_{in}$ depends only from the characteristics of the incident wave and the geometry of the pins, by observing (5.2.2.3) it is clear that the maximization of $\mathbf{A}$ occurs when $|\det(\bar{\mathbf{G}}^{-1})|$ is maximized. In the bibliography this condition is stated by demanding that $|\det(\bar{\mathbf{G}}^{-1})|$ is maximized as this defines the scaling factor applied to $\mathbf{U}_{in}$. Equivalently, $|\det(\bar{\mathbf{G}})|$ should be minimised. Although a detailed prof of the last proposition has not yet been given, it has been established in many works that the resonances appear when $|\det(\bar{\mathbf{G}})|$ is minimised.

For a given configuration of pins, $\bar{\mathbf{G}}$ depends only on the non-dimensional wave number K_2 of the incident wave. Therefore the local minima points can be identified by plotting $|\det(\bar{\mathbf{G}})|$ as a function of K_2. The wave numbers corresponding to these points caused the largest displacements in the infinite domain and as it will be shown later resonances appear. It is important to highlight that the method presented here for detecting resonant modes is not an approximate one and if the computations are sufficiently dense then the local minima points are determined with practically zero error. Regarding the computing part of the problem, the detection of the local minima points is the operation with the biggest computational cost. A good practice for reducing the computational load is initially to plot $|\det(\bar{\mathbf{G}})|$ as a function of K_2 using a sufficiently large step size, ensuring that no local minima are overlooked. Then, increase the calculation density (reduce the step size) around the identified local minima.

5.2.3 Scattering by a Single Point Under Plane Strain

For an infinite domain under plane stain, the idea is identical as in the case of anti-plane shear, with the only difference being that the Green's function is of matrix form. Consequently, an incident wave field which includes both primary and secondary waves is given by:

$$\begin{aligned}\mathbf{u}_{in}(\mathbf{r}) = \mathbf{e}_1 \left(e^{iq(k_1)[x\cos(\psi)+y\sin(\psi)]} + e^{iq(\beta k_1)[x\cos(\psi)+y\sin(\psi)]}\right) \\ + \mathbf{e}_2 \left(e^{iq(k_1)[x\cos(\psi)+y\sin(\psi)]} + e^{iq(\beta k_1)[x\cos(\psi)+y\sin(\psi)]}\right)\end{aligned} \tag{5.2.3.1}$$

Where $q(k_1)$ and $q(\beta k_1)$ are the positive real roots of the dispersion equations of the primary and secondary waves respectively given by (4.3.2.45). It is also noted that if the incident wave field consists solely of primary or secondary waves, only the corresponding terms in (5.2.3.1) are considered.

For an infinite domain under plane strain, pinned by a single pin at a point with position vector $\mathbf{r}' = (x', y')$, the non-dimensional displacement $\mathbf{U}(\mathbf{r})$ can be expressed as the displacement generated by the incident wave field given by (5.2.3.1) and the displacement due to the existence of the pin. Since the pin can be considered as a consecrated body force, the displacement field that it generates can be determined using the Greens function of the plane strain, which in non-dimensional form is given by (4.3.4.10).

$$\mathbf{U}(\mathbf{r}) = \mathbf{u}_{in}(\mathbf{r}) + \bar{\mathbf{G}}(\mathbf{r};\mathbf{r}')\mathbf{A} \tag{5.2.3.2}$$

If the infinite domain is constrained at the position where the pin is placed, the coefficient vector $\mathbf{A}$ can be determined by setting (5.2.3.2) equal to zero for $\mathbf{r} = \mathbf{r}'$:

$$\mathbf{A} = -\bar{\mathbf{G}}^{-1}(\mathbf{r}';\mathbf{r}')\mathbf{u}_{in}(\mathbf{r}') \tag{5.2.3.3}$$

Where $\mathbf{A}$ is a 2×1 vector, $\bar{\mathbf{G}}$ is a 2×2 symmetric matrix and $\mathbf{u}_{in}$ is a 2×1 vector. It is also worth mentioning the similarity between (5.2.2.3) and (5.2.3.3)

5.2.4 Scattering by a Finite Number of Arbitrary Points Under Plane Strain

In view of (5.2.1.1,) for the case where the infinite domain is pined by N_p pins at points with position vectors $\mathbf{r'}_n$. The non-dimensional displacement $\mathbf{U}(\mathbf{r})$ is now by:

$$\mathbf{U}(\mathbf{r}) = \mathbf{U}_{in}(\mathbf{r}) + \bar{\mathbf{G}}(\mathbf{r};\mathbf{r}')\mathbf{A} \tag{5.2.4.1}$$

If the infinite domain is constrained at the position where the pins are placed, the constant vector $\mathbf{A}$ can be determined by setting (5.2.4.1) equal to zero for $\mathbf{r}_m = \mathbf{r'}_n$ and solving the following $2N_p$ simultaneous algebraic equations:

$$\bar{\mathbf{A}} = -\bar{\bar{\mathbf{G}}}^{-1}\mathbf{U}_{in} \tag{5.2.4.2}$$

Now $\mathbf{A}$ is a $2N_p \times 1$ vector with components the scaling factors A_n^j, (or equivalently a 2×1 block vector with components $\mathbf{A}^j$), $\bar{\mathbf{G}}$ is a $2N_p \times 2N_p$ symmetric block matrix with components $\bar{\mathbf{U}}^{ij}(\mathbf{r}_m;\mathbf{r}_n)$, (i.e. the problems Green matrix) and $\mathbf{U}_{in}$ is a $2N_p \times 1$ vector with components $u_{in}^j(\mathbf{r}_m)$, (or equivalently a 2×1 block vector with components $\mathbf{u}_{in}^j(\mathbf{r}_m)$, (i.e. the non-dimensional displacement at each pin location, caused by an incident wave, in an unpinned infinite domain).

$$\bar{\mathbf{A}} = \left[\begin{array}{c} \mathbf{A}^x \\ \hline \mathbf{A}^y \end{array}\right], \quad \bar{\bar{\mathbf{G}}} = \left[\begin{array}{c|c} \bar{\mathbf{U}}^{xx} & \bar{\mathbf{U}}^{xy} \\ \hline \bar{\mathbf{U}}^{yx} & \bar{\mathbf{U}}^{yy} \end{array}\right], \quad \mathbf{U}_{in} = \left[\begin{array}{c} \mathbf{u}_{in}^x \\ \hline \mathbf{u}_{in}^y \end{array}\right] \tag{5.2.4.3}$$

The expressions of the components of the above block matrices are given bellow:

$$\mathbf{A}^j = \begin{bmatrix} A_1^j \\ A_2^j \\ \vdots \\ A_n^j \end{bmatrix}, \quad \mathbf{u}_{in}^j = \begin{bmatrix} u_{in}^j(\mathbf{r}_1) \\ u_{in}^j(\mathbf{r}_2) \\ \vdots \\ u_{in}^j(\mathbf{r}_n) \end{bmatrix} \tag{5.2.4.4}$$

$$\bar{\mathbf{U}}^{ij} = \begin{bmatrix} \bar{U}_i^{p_j}(\mathbf{r}_1;\mathbf{r'}_1) & \bar{U}_i^{p_j}(\mathbf{r}_1;\mathbf{r'}_2) & \cdots & \bar{U}_i^{p_j}(\mathbf{r}_1;\mathbf{r'}_n) \\ \bar{U}_i^{p_j}(\mathbf{r}_2;\mathbf{r'}_1) & \bar{U}_i^{p_j}(\mathbf{r}_2;\mathbf{r'}_2) & \cdots & \bar{U}_i^{p_j}(\mathbf{r}_2;\mathbf{r'}_n) \\ \vdots & \vdots & \ddots & \vdots \\ \bar{U}_i^{p_j}(\mathbf{r}_n;\mathbf{r'}_1) & \bar{U}_i^{p_j}(\mathbf{r}_n;\mathbf{r'}_2) & \cdots & \bar{U}_i^{p_j}(\mathbf{r}_n;\mathbf{r'}_n) \end{bmatrix} \tag{5.2.4.5}$$

It is noted that the subscripts and superscripts in the above equations are not related to covariant and contravariant notation. They are used solely to make the equations more compact when expressed with block matrices. The subscripts refer to the points where the pins are placed, while the superscripts indicate the directions of the body forces and displacements.

Regarding the interpretation of the above matrices, it is the same as the corresponding ones of the anti-plane shear case. Also, the maximization of $\bar{\mathbf{A}}$ occurs when $|\det(\bar{\bar{\mathbf{G}}})^{-1}|$ is maximized due to the similarity between (5.2.2.3) and (5.2.4.2).

5.3 Scattering Under Plane Strain

5.3.1 Scattering by Circular Configurations

For the plane strain case circular configurations consisting of 12, 24, and 48 pins are considered. The systems parameters are the non-dimensional wave number K_1, the material's internal length ratio H, the Poisson's ration v and the angle ψ formed by the direction of propagation and the horizontal x axis, (the definitions of H, K_1 are given in (4.3.4.1), (4.3.4.2)). The effect of the angle ψ is not considered because the circular configurations have radial symmetry. This means that the displacement fields generated by waves propagating in an oblique direction can be obtained by rotating the fields from a reference direction. In order to analyse the system's response, the distribution of the determinant of the Green's matrix with respect to K_1 is plotted for various values of H that correspond to normal, anomalous and no dispersion. As shown in the following figures, minima occur only in the case of anomalous dispersion ($H < 1$) and thus, resonances are observed only under this condition. Additionally, in the case anomalous dispersion as the number of pins inserted increases the amount of local minima also increases.

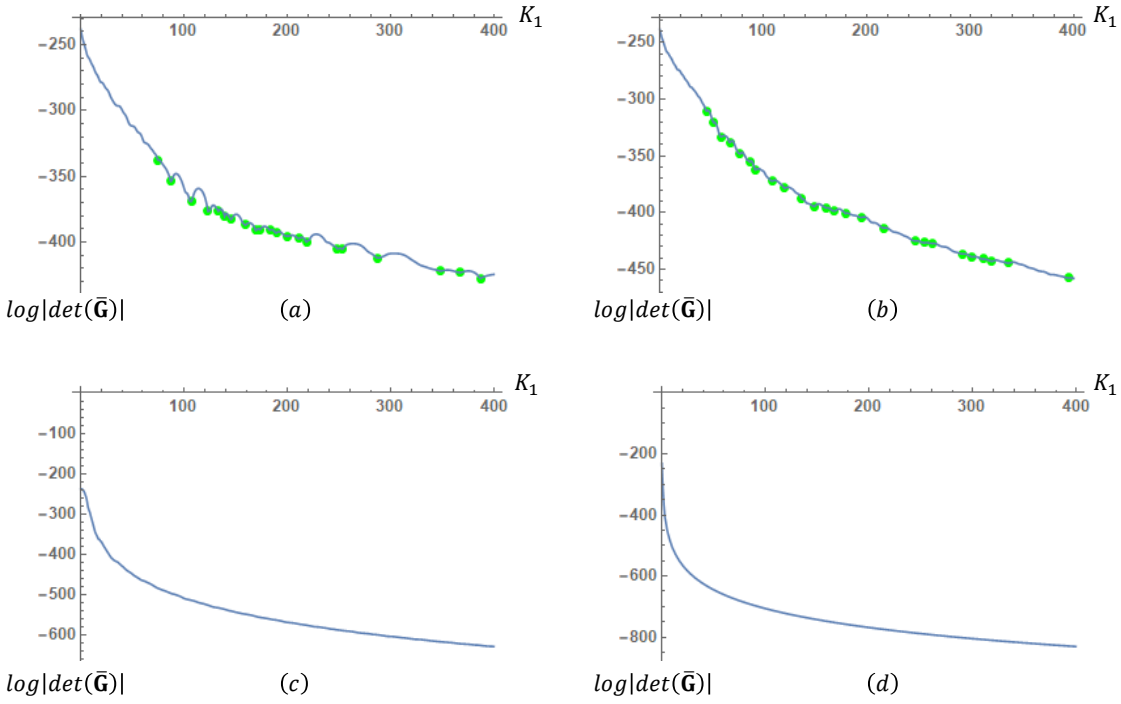

Figure 5.3.1.1: $\log(|\det(\bar{\mathbf{G}})|) - K_2$ diagram for a circular configuration consisting of 24 pins (a) $H = 0.01$, (b) $H = 0.1$, (c) $H = 1$ and (d) $H = 10$, $v = 0.25$.

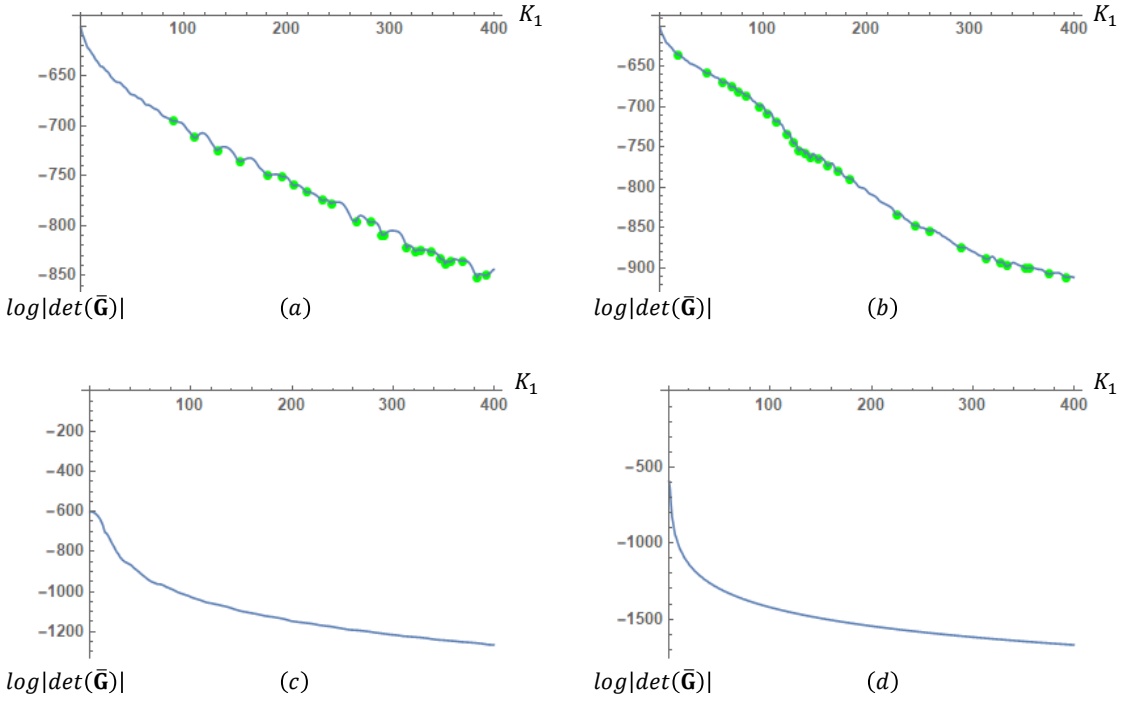

Figure 5.3.1.2: $\log(|\det(\bar{\mathbf{G}})|) - K_2$ diagram for a circular configuration consisting of 48 pins (a) $H = 0.01$, (b) $H = 0.1$, (c) $H = 1$ and (d) $H = 10$, $v = 0.25$.

The effect of the Poisson's ratio on the system's response is analysed by using a circular configuration with 48 pins. The determinant of the Green's matrix is plotted as a function of K_1 for a fixed value of H while varying the Poisson's ratio within the range $(-1, 0.5)$. As shown in the following figures, the number of minima generally remains constant as the Poisson's ratio increases. However, near the value of 0.5, there is a significant increase in the number of minima as the Poisson's ratio rises.

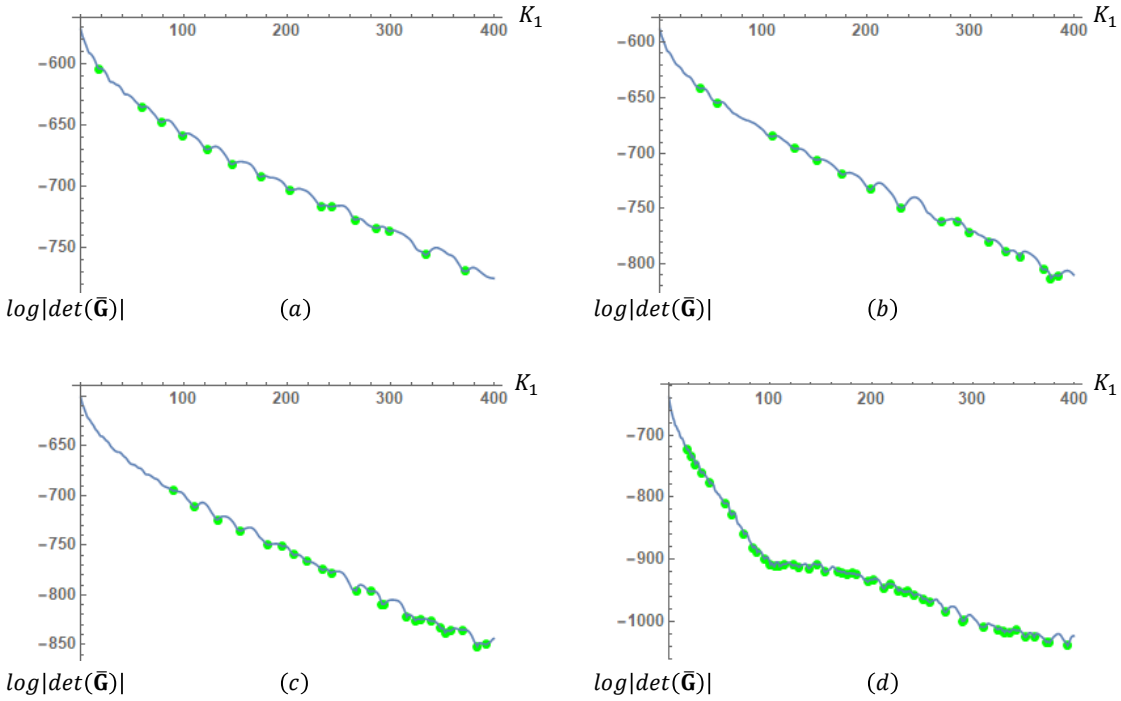

Figure 5.3.1.3: $\log(|\det(\bar{\mathbf{G}})|) - K_2$ diagram for a circular configuration consisting of 48 pins (a) $v = -0.99$, (b) $v = 0$, (c) $v = 0.25$ and (d) $v = 0.49$, $H = 0.01$.

The analysis revealed that during the resonances, the displacement's increase significantly more when the incident wave is of S type. The results presented below for anomalous dispersion highlight the strongest resonances observed in circular configurations with 12, 24 and 48 pins, this displacement fields are generated by S waves propagating along the horizontal x axis. For the cases of normal and no dispersion, where there are no local minima, results are given for the most interesting cases that were detected.

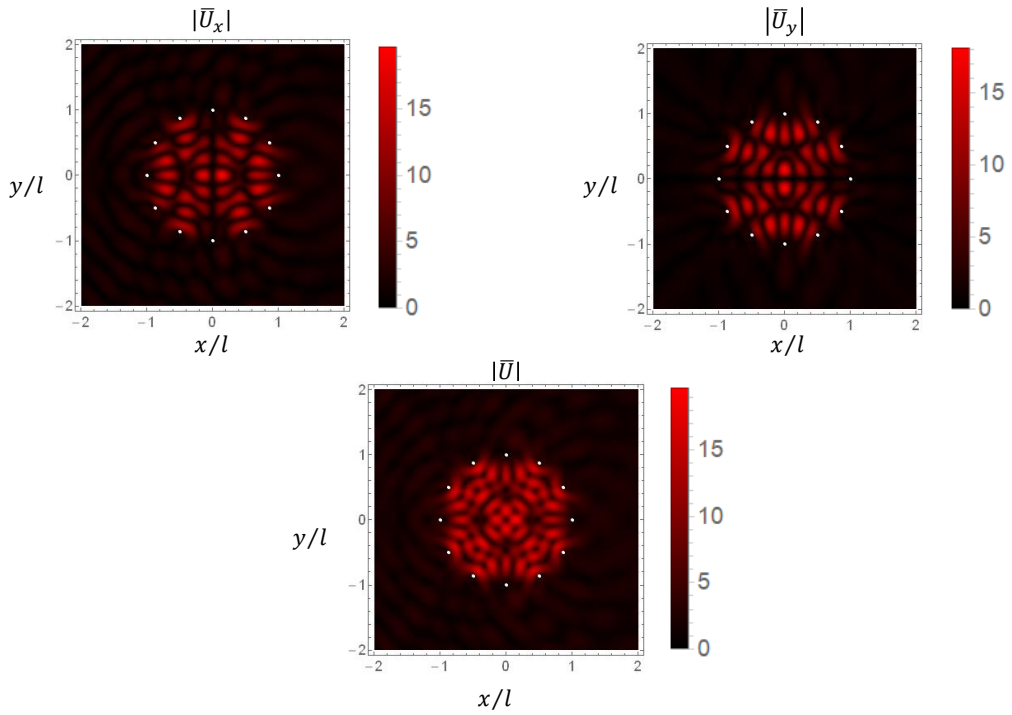

Figure 5.3.1.4: Displacement contours for a circle with 12 pins, $H = 0.01$ (anomalous dispersion), $v = 0.49$, $K_1 = 37.103$ (7th minima).

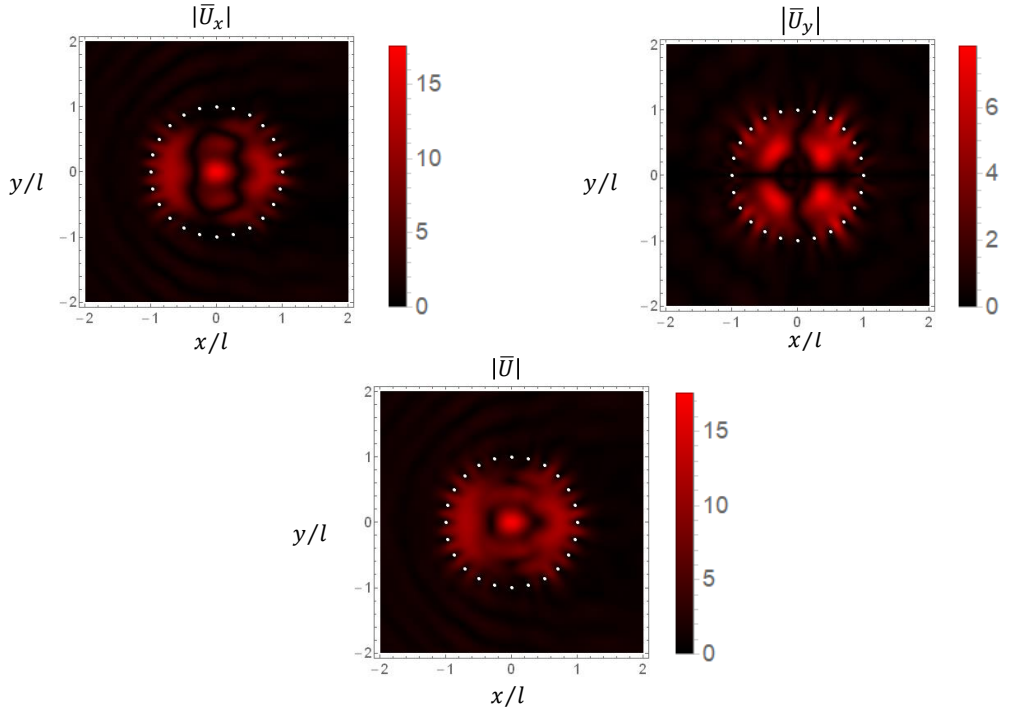

Figure 5.3.1.5: Displacement contours for a circle with 24 pins, $H = 0.01$ (anomalous dispersion), $v = 0.49$, $K_1 = 28.054$ (1st minima).

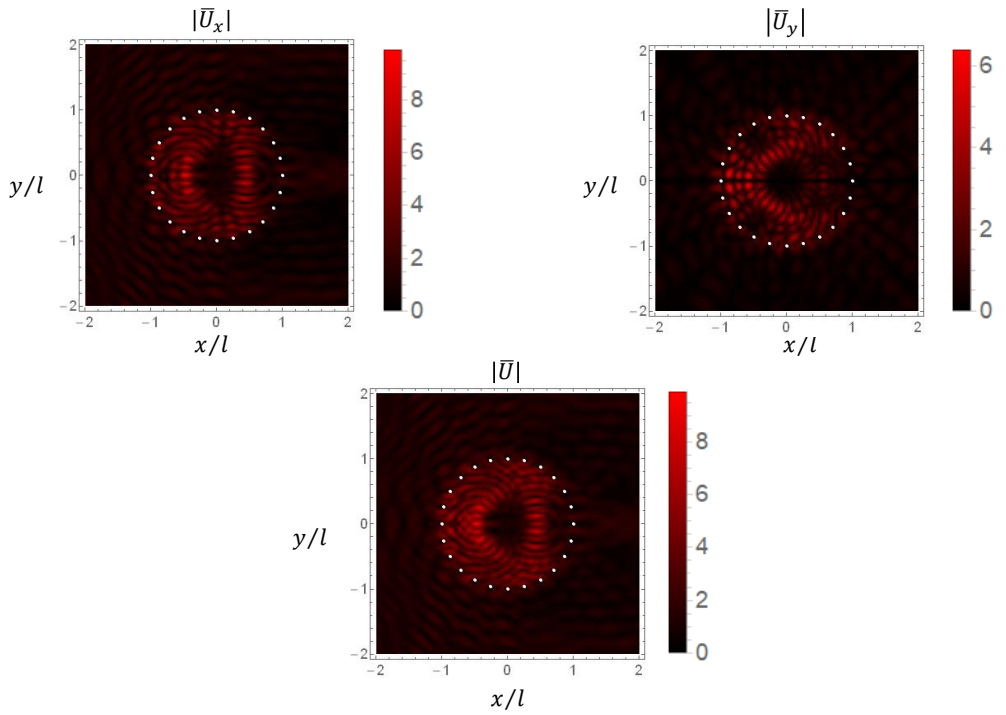

Figure 5.3.1.6: Displacement contours for a circle with 24 pins, $H = 0.01$ (anomalous dispersion), $v = 0.49$, $K_1 = 105.051$ (13th minima).

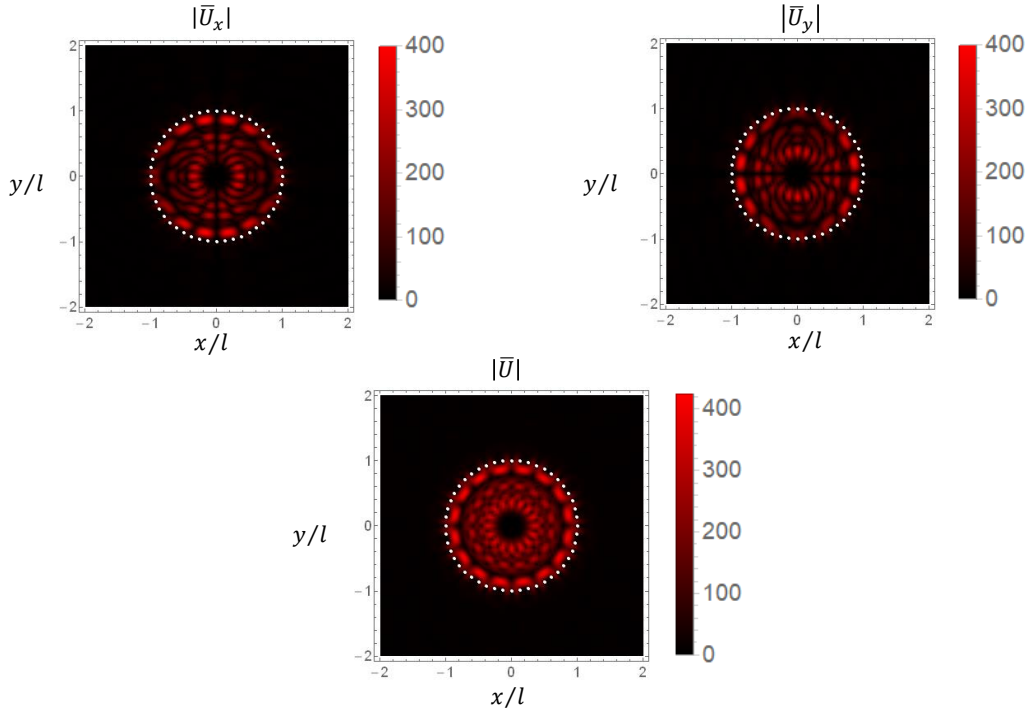

Figure 5.3.1.7: Displacement contours for a circle with 48 pins, $H = 0.01$ (anomalous dispersion), $v = 0.49$, $K_1 = 93.848$ (11th minima).

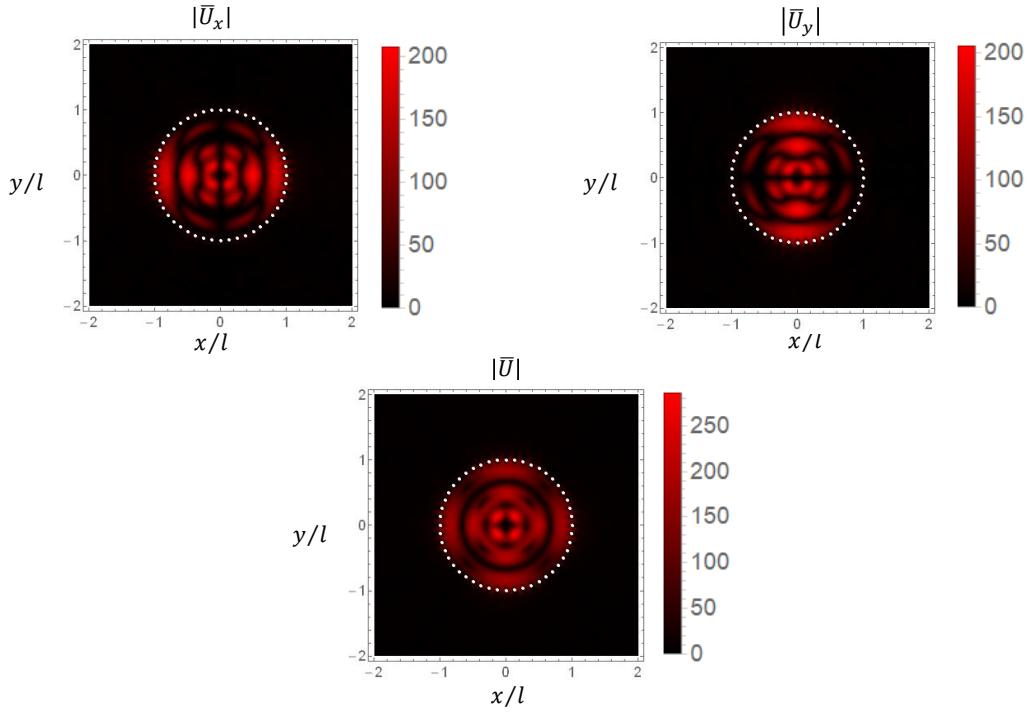

Figure 5.3.1.8: Displacement contours for a circle with 48 pins, $H = 0.01$ (anomalous dispersion), $v = 0.49$, $K_1 = 100.264$ (12th minima).

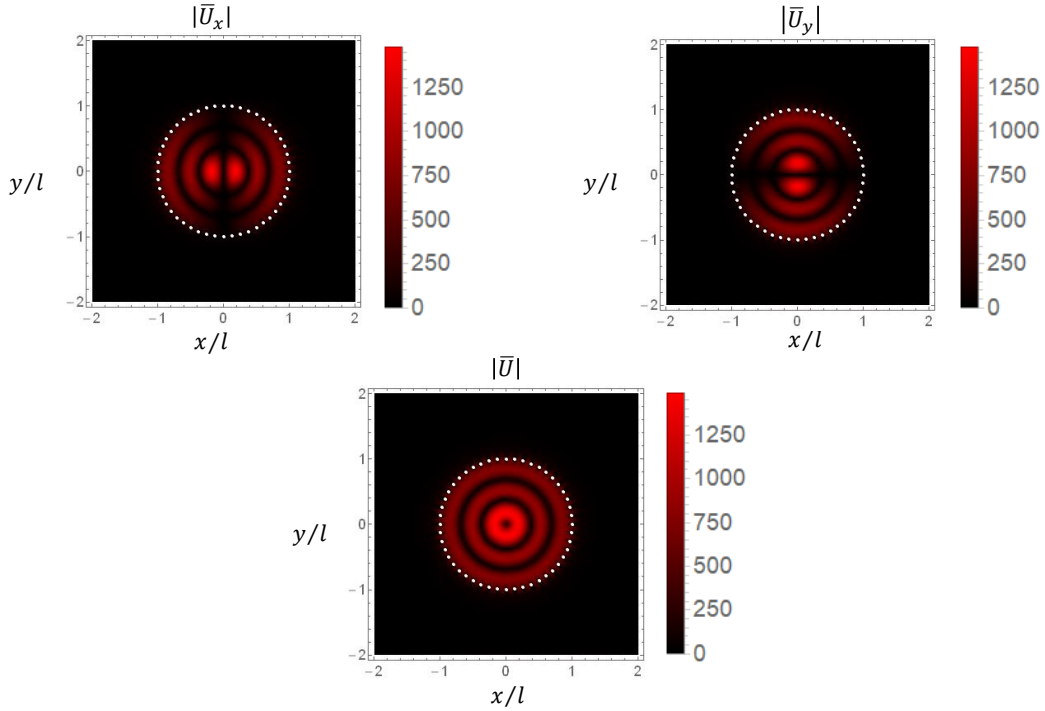

Figure 5.3.1.9: Displacement contours for a circle with 48 pins, $H = 0.01$ (anomalous dispersion), $v = 0.49$, $K_1 = 103.770$ (13th minima).

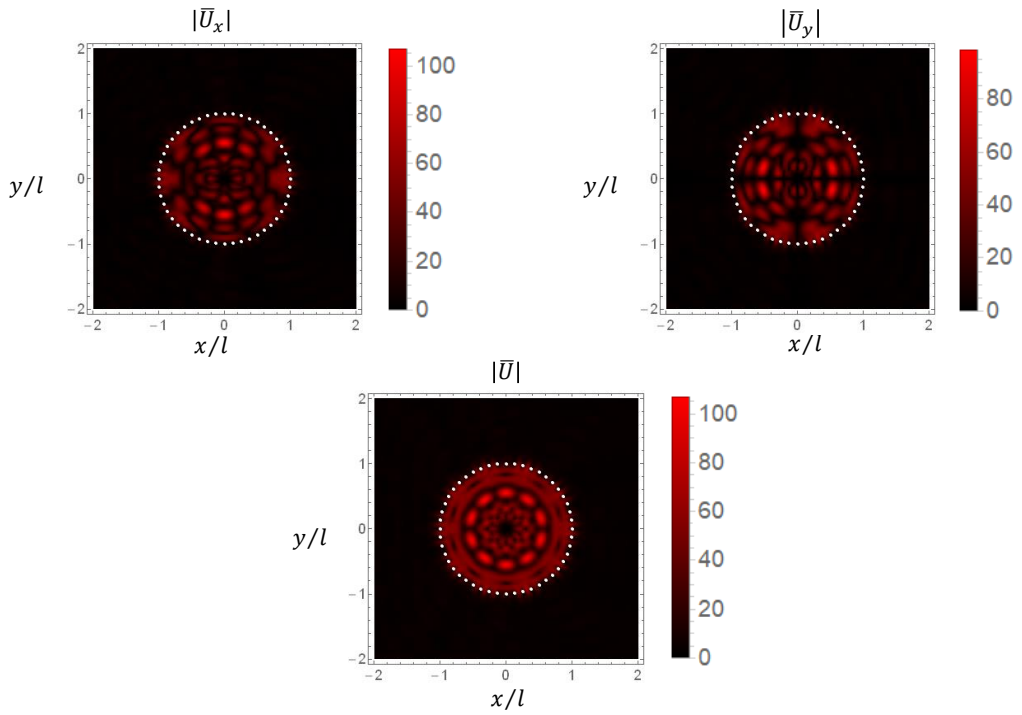

Figure 5.3.1.10: Displacement contours for a circle with 48 pins, $H = 0.01$ (anomalous dispersion), $v = 0.49$, $K_1 = 109.244$ (14th minima).

As shown in the figures above, at all resonances, the wave motion is largely confined within the pin configuration, meaning the waves are trapped inside. In most cases, where $\bar{U}_x$ is maximized within the configuration, $\bar{U}_y$ is minimized and vice versa. Additionally, increasing the number of pins results in larger displacements, as the reduced spacing between pins makes it more difficult for the trapped waves to escape the configuration.

To demonstrate that the local minima correspond to resonances, the non-dimensional displacements are shown for a value of K_1 that lies between two local minima, where the resonances are notably strong. For a circular configuration with 48 pins and parameters $H = 0.01$, $v = 0.49$, the system's response appears to be significantly different from the responses shown in the figures above for $K_1 = 100.264$ (12th minima) and $K_1 = 103.770$ (13th minima).

To further illustrate the effectiveness of the pins, the distribution of the norm of the non-dimensional displacement $\bar{U}$ along the x axis is plotted.

In the following diagrams the distribution of the norm of the non-dimensional displacement $\bar{U}$ along the x axis, for a circle with 12 pins is shown for (a) a wide range of the non-dimensional coordinate x/l and (b), (c) close to the pins. The line $y = 1$ is included because the incident wave has a unit amplitude. Two pins are positioned along the x axis axis at points $(-1, 0)$ and $(1, 0)$, where the displacement magnitude is zero. The displacement function is smooth and continuous on both sides of the pins, with similar patterns observed for circles with more pins.

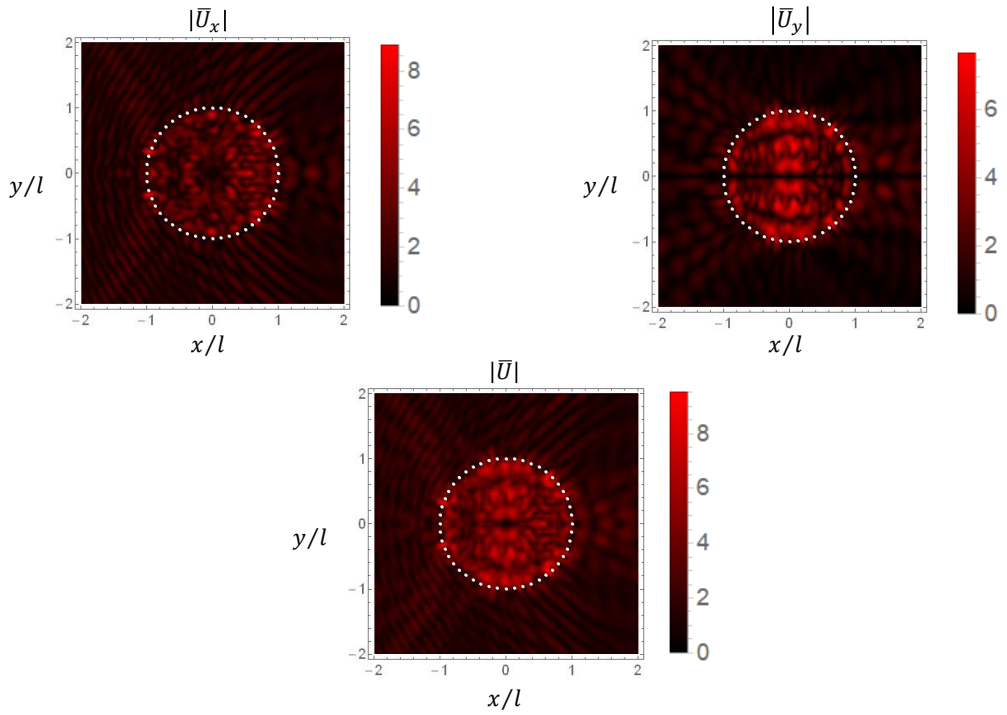

Figure 5.3.1.11: Displacement contours for a circle with 48 pins, $H = 0.01$ (anomalous dispersion), $v = 0.49$, $K_1 = 102$ (between the 12th and 13th minima).

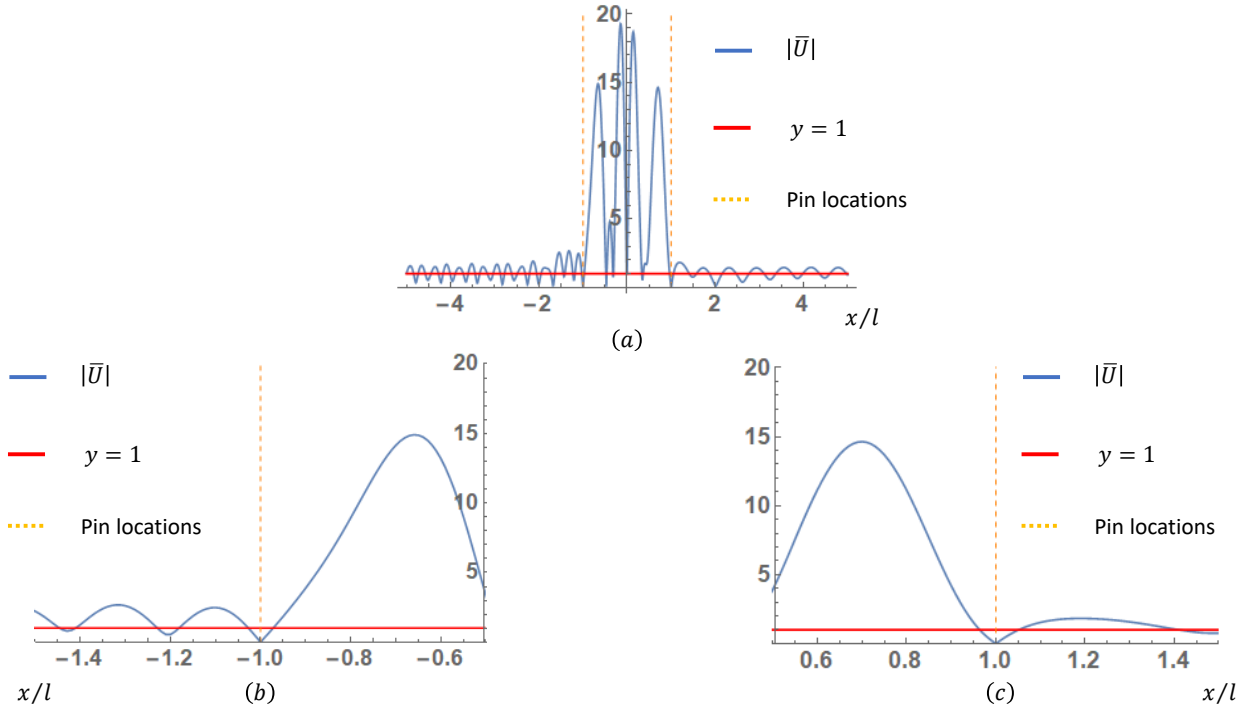

Figure 5.3.1.12: Distribution of $\bar{U}$, for a circle with 12 pins, $H = 0.01$, $v = 0.49$, $K_1 = 37.103$ (7th minima), $y = 0$: (a) wide range of x/l and (b), (c) close to the pins.

In the cases of normal and no dispersion, no local minima are observed, and as a result, no resonances occur. The system's response remains the same for different values of the non-dimensional wave number K_1, regardless of the number of pins inserted. Additionally, the parameters v and H do not significantly affect the system's response. However, it is important to note that the system's response differs significantly in the case of anomalous dispersion, particularly for values of K_1 that do not correspond to local minima. Under anomalous dispersion, the motion of wave particles is largely confined within the pin configuration, regardless of the value of K_1. For specific values of K_1, the displacements are maximized, whereas in normal and no dispersion, the waves are not trapped within the pin configuration.

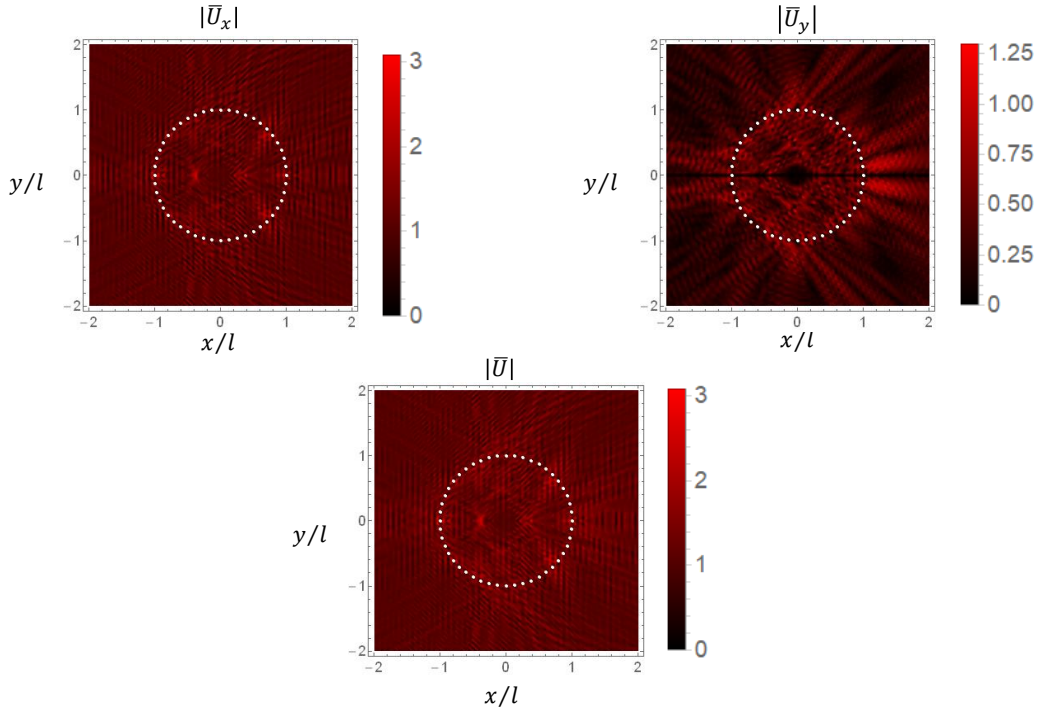

Figure 5.3.1.13: Displacement contours for a circle with 48 pins, $H = 1$ (no dispersion), $v = 0.49$, $K_1 = 10$.

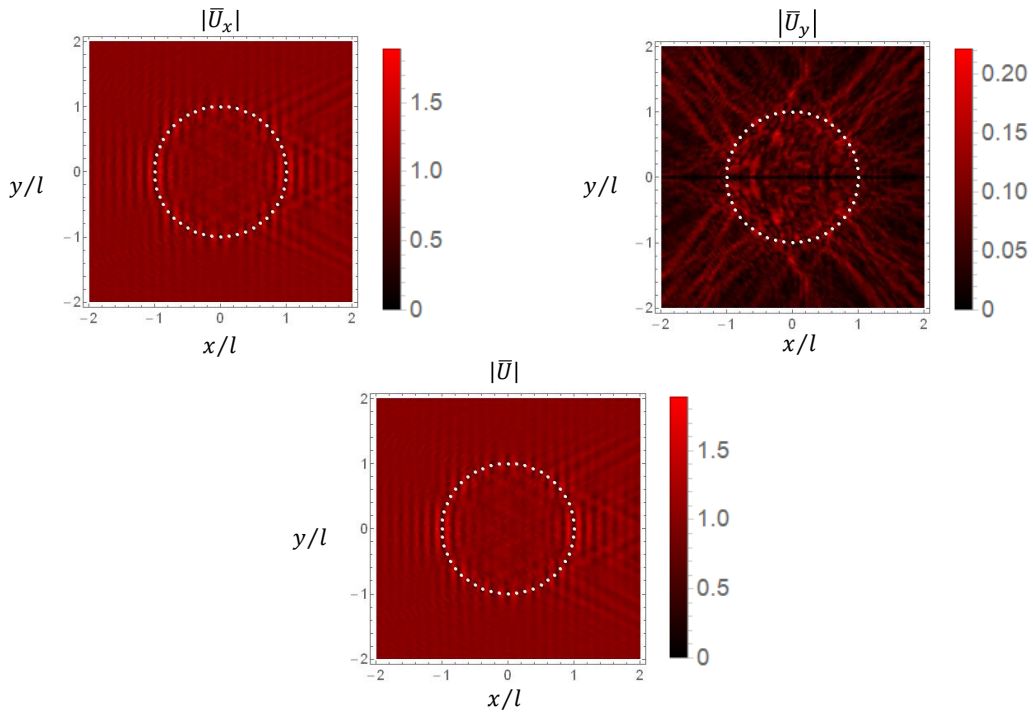

Figure 5.3.1.14: Displacement contours for a circle with 48 pins, $H = 10$ (normal dispersion), $v = 0.49$, $K_1 = 10$.

5.4 Scattering Under Anti-Plane Shear

5.4.1 Fractals - Koch's Snowflake

The relative simplicity of the anti-plane shear Green's function permits the consideration of complicated configurations of pins. For this reason, Koch's snowflake (a fractal curve) is considered in order to examine the effect of the fractional dimension of the configurations. The term fractal refers to a geometric shape containing detailed structure at arbitrarily small scales, usually having a fractional dimension strictly exceeding the topological dimension. Koch's snowflake is one of the earliest fractals to have been described and it is based on the Koch's curve, which appeared in 1904 by the Swedish mathematician Helge von Koch [88]. The Koch snowflake can be built up through an iterative process, in a sequence of stages. Initially, there is an equilateral triangle, and each successive stage is formed by adding outward bends to each side of the previous stage, making smaller equilateral triangles.

The Koch snowflake can be constructed by starting with an equilateral triangle, then recursively altering each line segment as follows: Initially the straight segments are divided into three segments of equal length. Then, an outward pointing equilateral triangle that has the middle segment of the previous iteration as its base is drawn and finally the line segment that coincides with base of the triangle is removed. The Koch snowflake poses several geometrical properties the most important of which are presented below.

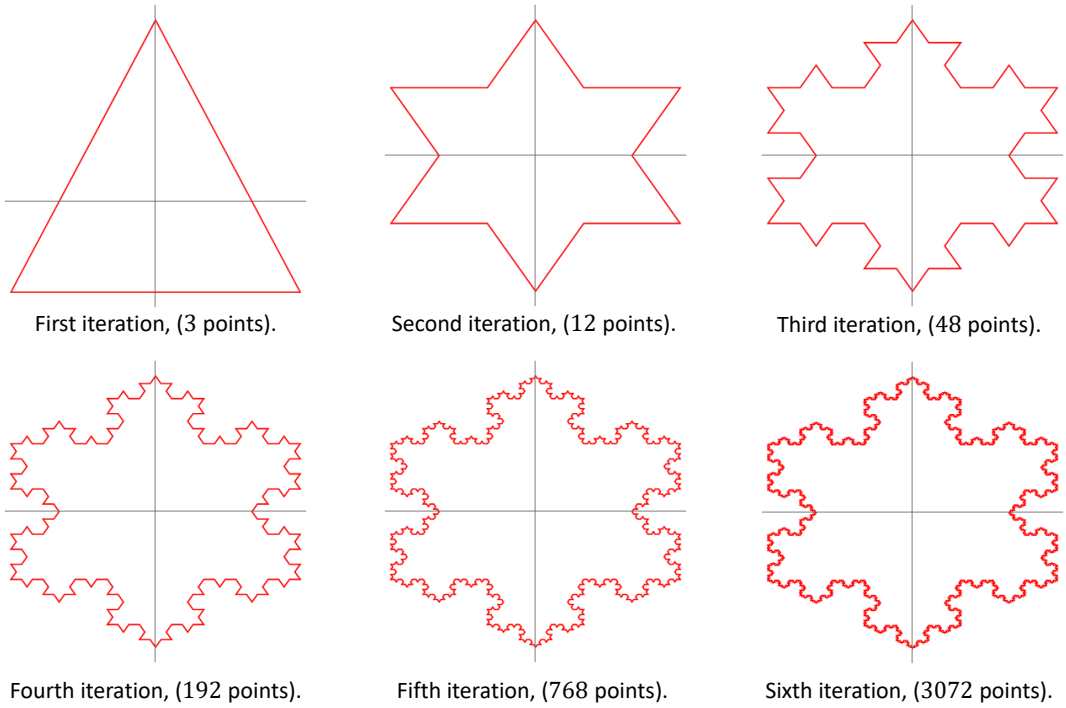

Figure 5.4.1.1: The first six iterations of Koch's snowflake.

In each iteration the number of sides and corners is increased by four times compared to the previous iteration, so the number of sides and corners after n iterations is given by:

$$N_n = 3 \cdot 4^n, \quad n \geq 0 \tag{5.4.1.1}$$

If the original equilateral triangle has sides of length s, the length of each side of the snowflake after n iterations is:

$$S_n = \frac{S_{n-1}}{3} = \frac{s}{3^n}, \quad n \geq 1, \quad S_0 = s \tag{5.4.1.2}$$

Since each side of the snowflake has the same length, the perimeter of the snowflake after n iterations is given by multiplying the number of sides N_n by the side length S_n:

$$P_n = N_n \cdot S_n = 3 \cdot s \cdot \left(\frac{4}{3}\right)^n, \quad n \geq 0 \tag{5.4.1.3}$$

From (5.4.1.3) it is clear that the perimeter of the curve is unbounded, as n tends to infinity.

$$\lim_{n\to\infty}(P_n) = \lim_{n\to\infty}\left[3 \cdot s \cdot \left(\frac{4}{3}\right)^n\right] = \infty \tag{5.4.1.4}$$

For determining the area of Koch's snowflake it is convenient to formulate first an expression for calculating the area of each new triangle added in an iteration. In each iteration a new triangle is added on each side of the previous iteration, so the number of new triangles added in iteration n is:

$$T_n = N_{n-1} = 3 \cdot 4^{n-1}, \quad n \geq 0 \tag{5.4.1.5}$$

Let a_0 denote the area of the original equilateral triangle. The area of each new triangle added in an iteration is 1/9 of the area of each triangle added in the previous iteration, so the area of each triangle added in iteration n is:

$$a_n = \frac{a_{n-1}}{9} = \frac{a_0}{9^n}, \quad n \geq 1 \tag{5.4.1.6}$$

The additional area added in iteration n therefore is:

$$b_n = T_n \cdot a_n = \frac{3}{4} \cdot \frac{4}{9}^n \cdot a_0, \quad n \geq 1 \tag{5.4.1.7}$$

The total area of the snowflake after n iterations is:

$$A_n = a_0 + \sum_{k=1}^{n} b_k = a_0\left[1 + \frac{3}{4}\sum_{k=1}^{n}\left(\frac{4}{9}\right)^k\right] = a_0\left[1 + \frac{1}{3}\sum_{k=0}^{n-1}\left(\frac{4}{9}\right)^k\right] \tag{5.4.1.8}$$

Collapsing the geometric sum in (5.4.1.8) gives:

$$A_n = \frac{a_0}{5}\left[8 - 3\left(\frac{4}{9}\right)^n\right], \quad n \geq 1 \tag{5.4.1.9}$$

From (5.4.1.9) it is clear that the perimeter of the curve is unbounded, as n tends to infinity.

$$\lim_{n\to\infty}(A_n) = \frac{a_0}{5}\lim_{n\to\infty}\left[8 - 3\left(\frac{4}{9}\right)^n\right] = \frac{8}{5}a_0 \tag{5.4.1.10}$$

Finally, for defining the dimension of Koch's snowflake it necessary to first introduce a few definitions.

Definition 5.4.1.1. *Let S be a subset of an Euclidean space $\mathbb{R}^n$. Suppose that $N(\varepsilon)$ is the number of boxes of side length ε required to cover the set. Then the Minkowski–Bouligand dimension (or box-counting dimension) is defined as:*

$$\dim_{box}(S) := \lim_{\varepsilon \to 0} \left[\frac{\ln(N(\varepsilon))}{\ln(1/\varepsilon)} \right]$$

If the above limit does not exist, one may still take the limit superior and limit inferior, which respectively define the upper box dimension and lower box dimension. There is a more technical definition known as Hausdorff dimension which always exists for a bounded subset of $\mathbb{R}^n$, and which agrees with the box-counting dimension in most cases, but before defining the Hausdorff dimension, the diameter of metric space must be introduced.

Definition 5.4.1.2. *Let (X, ρ) be a metric space. For any subset $U \subset X$, the diameter of U, denoted as $diam(A_i)$, is defined as:*

$$diam(U) := \sup\{\rho(x, y) : x, y \in U\}, \quad diam(\emptyset) := 0$$

Two more important concepts for defining the Hausdorff dimension are the d-dimensional Hausdorff measure and the Hausdorff d-dimensional outer measure:

Definition 5.4.1.3. *Let S be a bounded subset of an Euclidean space $\mathbb{R}^n$ and X be a metric space. If $S \subset X$ and $d \in [0, \infty]$, then d-dimensional Hausdorff measure is defined as:*

$$H^d_\delta(S) := \inf\{\sum_{i=1}^{\infty} [diam(U_i))]^d : \bigcup_{i=1}^{\infty} U_i \supseteq S, diam(U_i) < \delta\}$$

While the Hausdorff d-dimensional outer measure is defined as:

$$\mathcal{H}^d(S) := \lim_{\delta \to 0} \left[H^d_\delta(S) \right]$$

Definition 5.4.1.4. *The Hausdorff dimension $\dim_H(X)$ is defined as:*

$$\dim_H(X) := \inf\{d \geq 0 : \mathcal{H}^d(X) = 0\}$$

The dimension of Koch's snowflake can be easily determined using Definition 5.4.1.1. After an iteration a line segment is substituted by four new line segments, meaning that after n iterations the total amounts of line segments that the snowflake will have is 4^n, while the

length of the side segments is $1/3^n$. From the aforementioned we conclude that $\varepsilon = 1/3$ and $N(\varepsilon) = 4^n$. Using these values for the case where S is Koch's snowflake we obtain:

$$\dim_{box}(S) = \lim_{n\to 0}\left[\frac{\ln(4^n)}{\ln(3^n)}\right] = \frac{\ln(4)}{\ln(3)} \tag{5.4.1.11}$$

The above value can be verified using the definition of Hausdorff dimension, however it is much easier to determine the fractals dimension using the more heuristic definition of box-counting dimension.

5.4.2 Scattering by Koch's Snowflake

Unlike the circular configurations where the $\log(|\det(\bar{\bar{\mathbf{G}}})|) - K_1$ diagram changes noticeably when pins are added, the local minima positions in the case of Koch's snowflake under anomalous dispersion remain practically unchanged across different iterations, over a wide range of non-dimensional wavenumbers K_2.

For the first iteration no minima are formed in the $\log(|\det(\bar{\mathbf{G}})|) - K_2$ diagram because the number of points is too low. Consequently, results for this case are not presented, as they are not particularly meaningful.

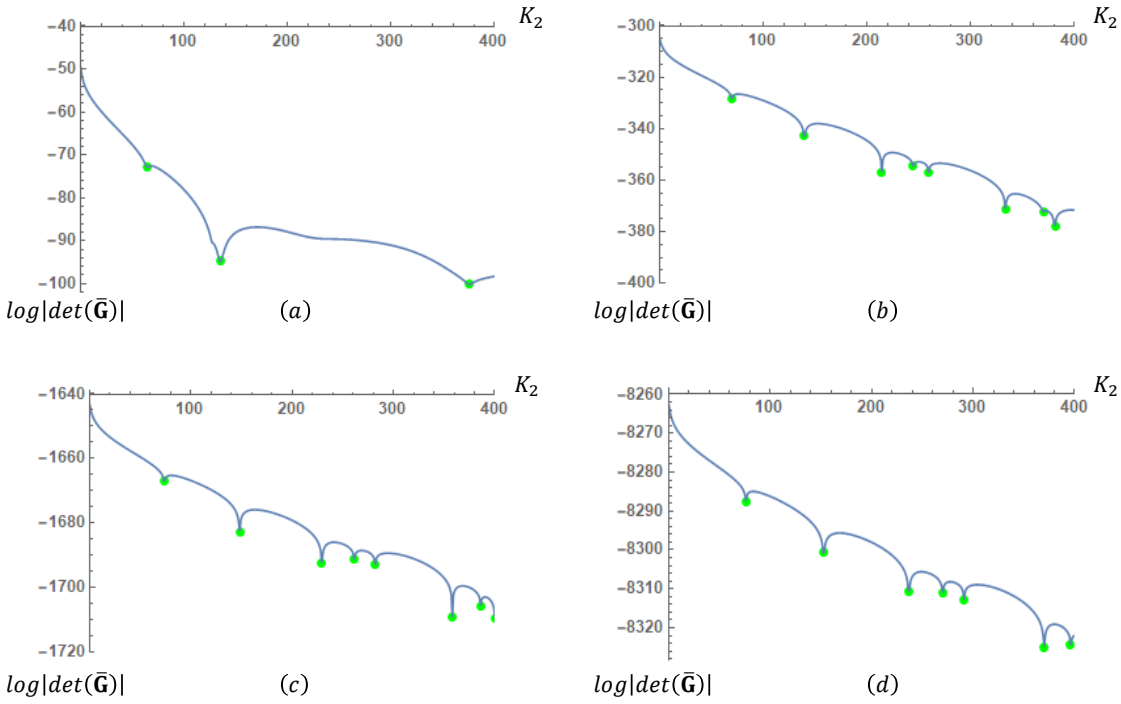

Figure 5.4.2.1: $\log(|\det(\bar{\mathbf{G}})|) - K_2$ diagram for the (a) second, (b) third, (c) fourth and (d) fifth iterations of Koch's snowflake, $H = 0.01$.

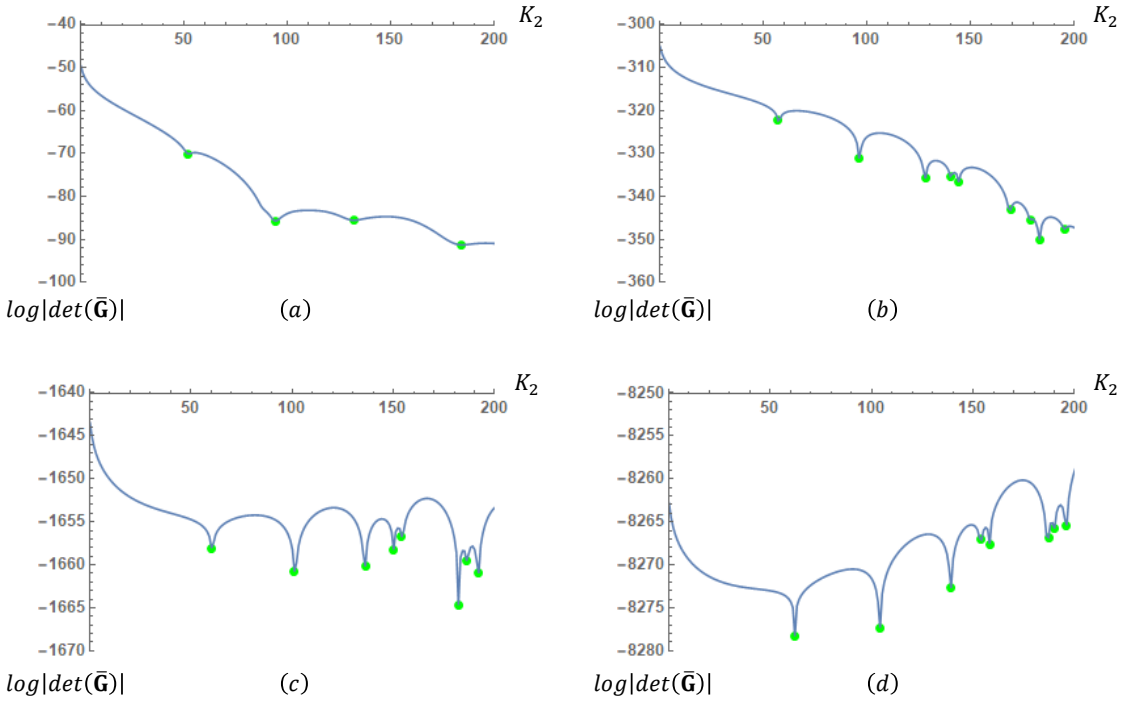

Figure 5.4.2.2: $\log(|\det(\bar{\mathbf{G}})|) - K_2$ diagram for the (a) second, (b) third, (c) fourth and (d) fifth iterations of Koch's snowflake, $H = 0.1$.

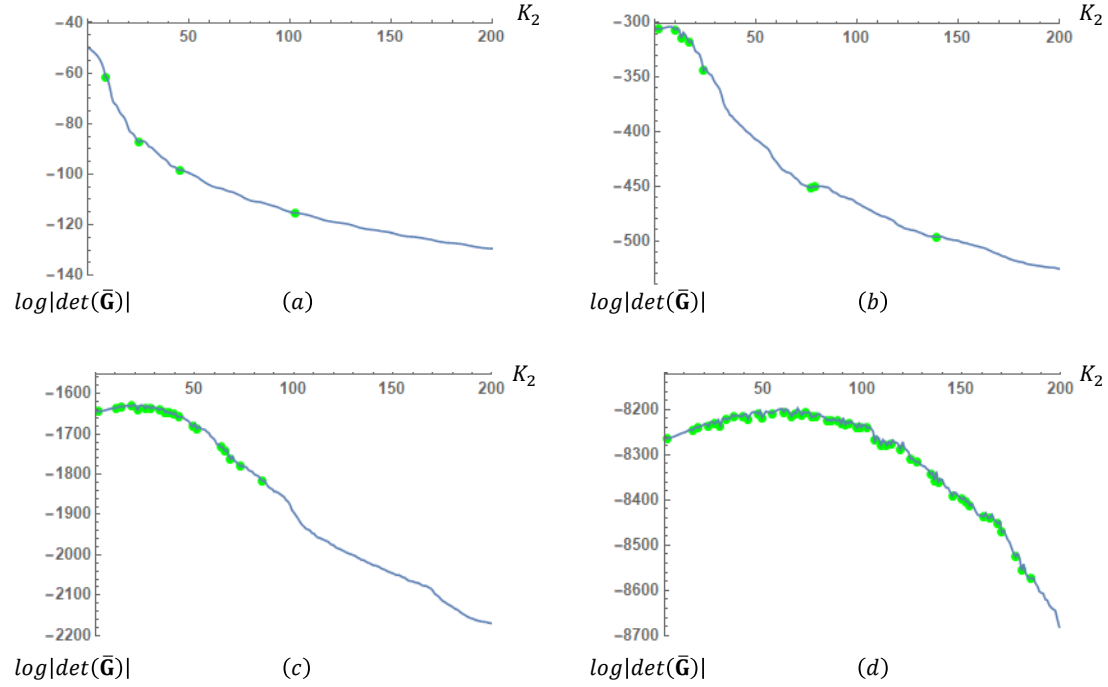

Figure 5.4.2.3: $\log(|\det(\bar{\mathbf{G}})|) - K_2$ diagram for the (a) second, (b) third, (c) fourth and (d) fifth iterations of Koch's snowflake, $H = 1$.

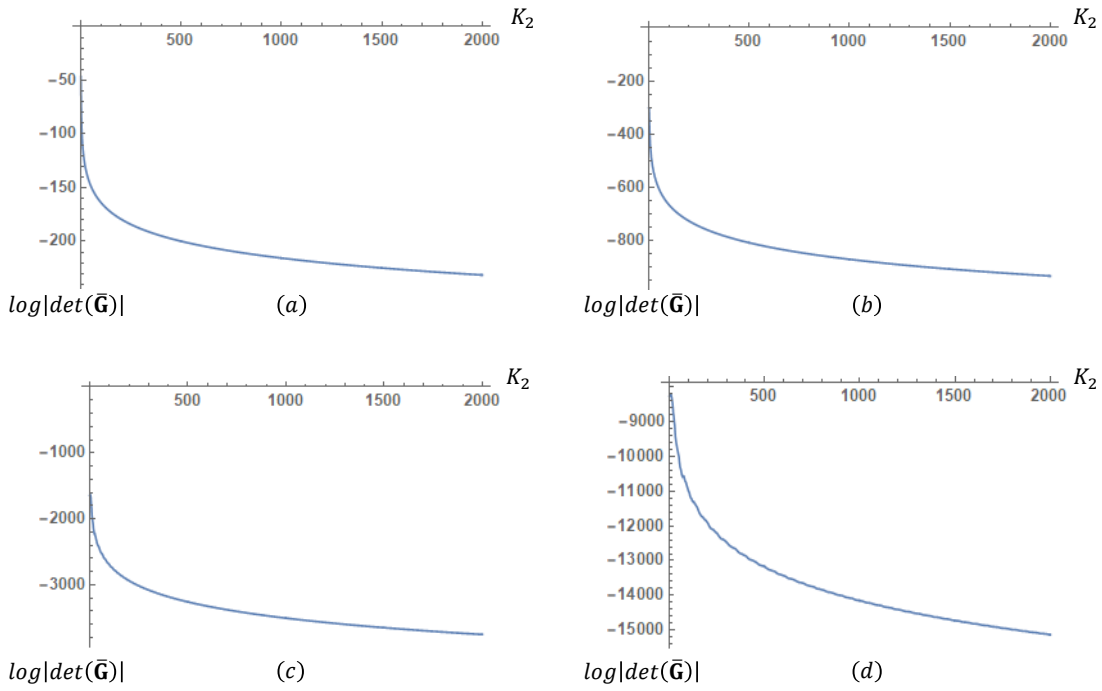

Figure 5.4.2.4: $\log(|\det(\bar{\mathbf{G}})|) - K_2$ diagram for the (a) second, (b) third, (c) fourth and (d) fifth iterations of Koch's snowflake, $H = 10$.

In the case of anomalous dispersion, starting from the third iteration onward, the positions of the local minima remain nearly constant, over a given range of non-dimensional wavenumbers K_2. This indicates that the resonant modes can be determined with high precision using only a small number of pins. In contrast, when the dispersion is normal, no minima are observed and as a result, no resonant modes are present, while in the case of no-dispersion the number of local minima increases rapidly with each iteration and beyond a certain point, discrete minima no longer exist. The difference in the $\log(|\det(\bar{\mathbf{G}})|) - K_2$ diagram for various values of H, greater than and less than $H = 1$ is reflected in the system's response, both qualitative and quantitatively, as different types of resonant modes appear and the values of the non-dimensional displacements differ dramatically.

The system's response is examined by considering the first five iterations of Koch's snowflake, with the value of H adjusted for each iteration, the side length of the original equilateral triangle is set to $a = l$, while the effect of the angle formed by the direction of propagation with the horizontal x axis is not considered. Once again the system's response undergoes qualitative changes depending on the type of dispersion. Specifically, for the case of anomalous dispersion results are given for the first four local minima for $H = 0.1$ and $H = 0.01$. This allows for a comparison of the system's response at the corresponding minima throughout the iteration process. Further analysis revealed that for $H < 0.01$ and $H > 10$, the results remain virtually unchanged. For the cases of normal and no-dispersion results are given for values of K_2 that either correspond to local minima or do not, focusing on the most significant cases identified in the analysis.

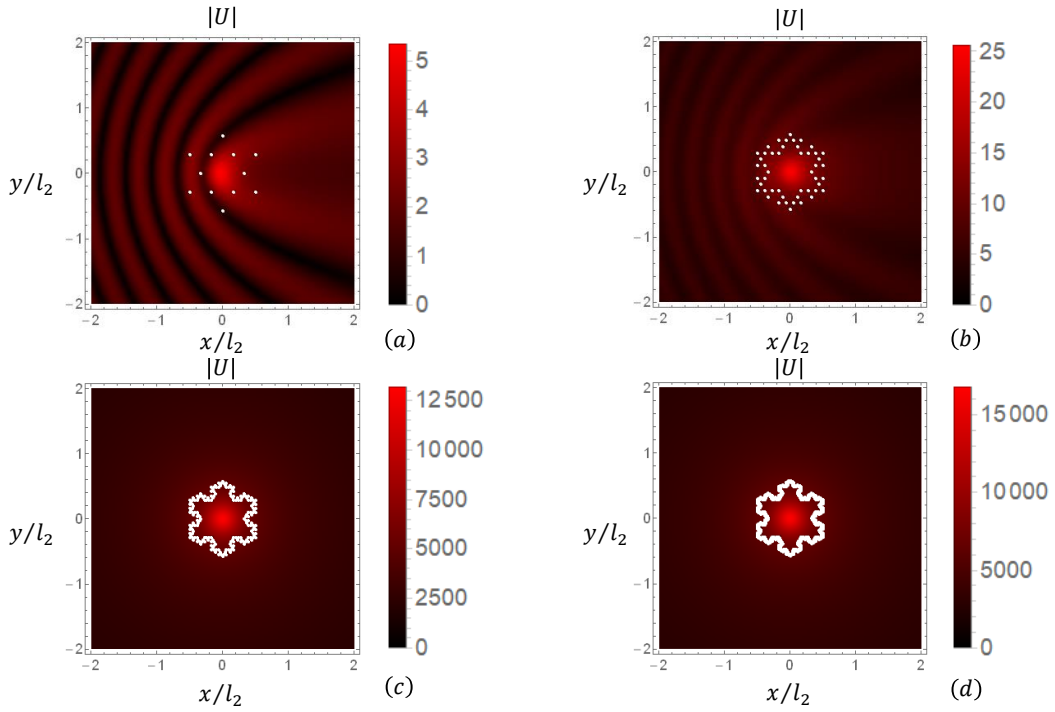

Figure 5.4.2.5: Displacement contours for $H = 0.01$, (anomalous dispersion), first minima: (a) $K_2 = 64.265$, (b) $K_2 = 69.547$, (c) $K_2 = 73.566$, (d) $K_2 = 75.879$.

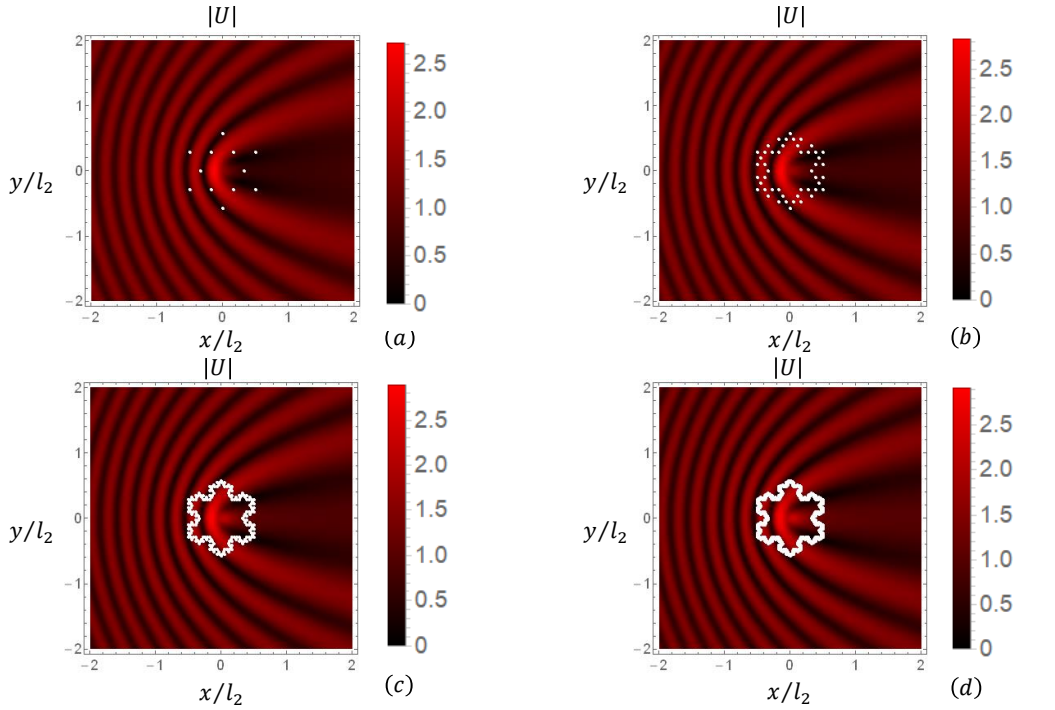

Figure 5.4.2.6: Displacement contours for $H = 0.01$, (anomalous dispersion), second minima: (a) $K_2 = 134.975$, (b) $K_2 = 139.520$, (c) $K_2 = 147.902$, (d) $K_2 = 152.569$.

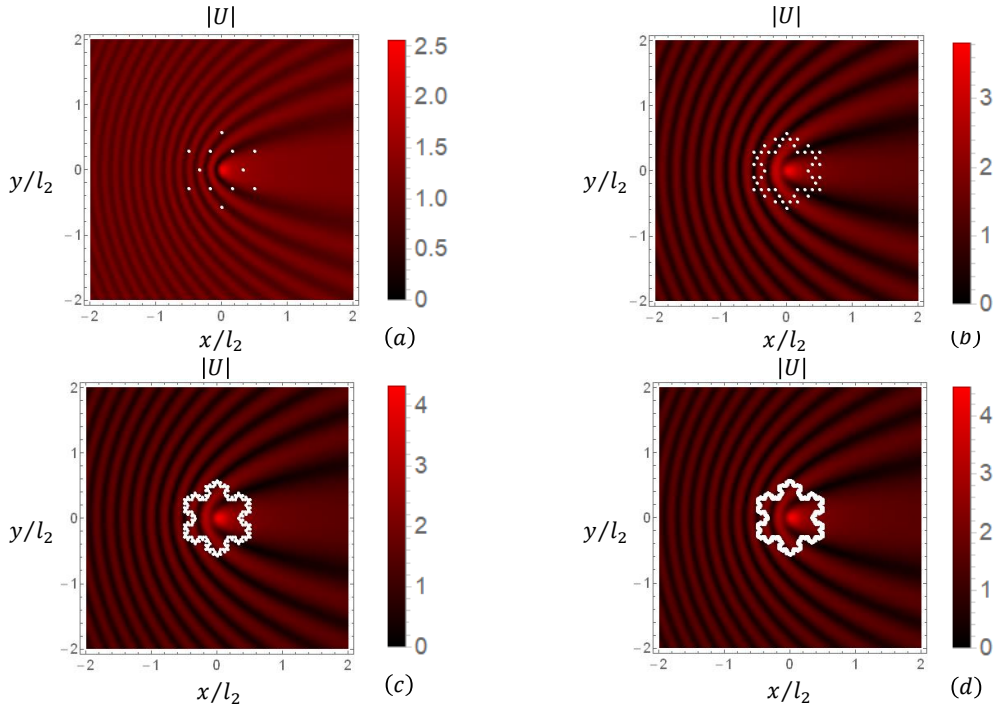

Figure 5.4.2.7: Displacement contours for $H = 0.01$, (anomalous dispersion), third minima: (a) $K_2 = 375.460$, (b) $K_2 = 214.042$, (c) $K_2 = 229.299$, (d) $K_2 = 236.518$.

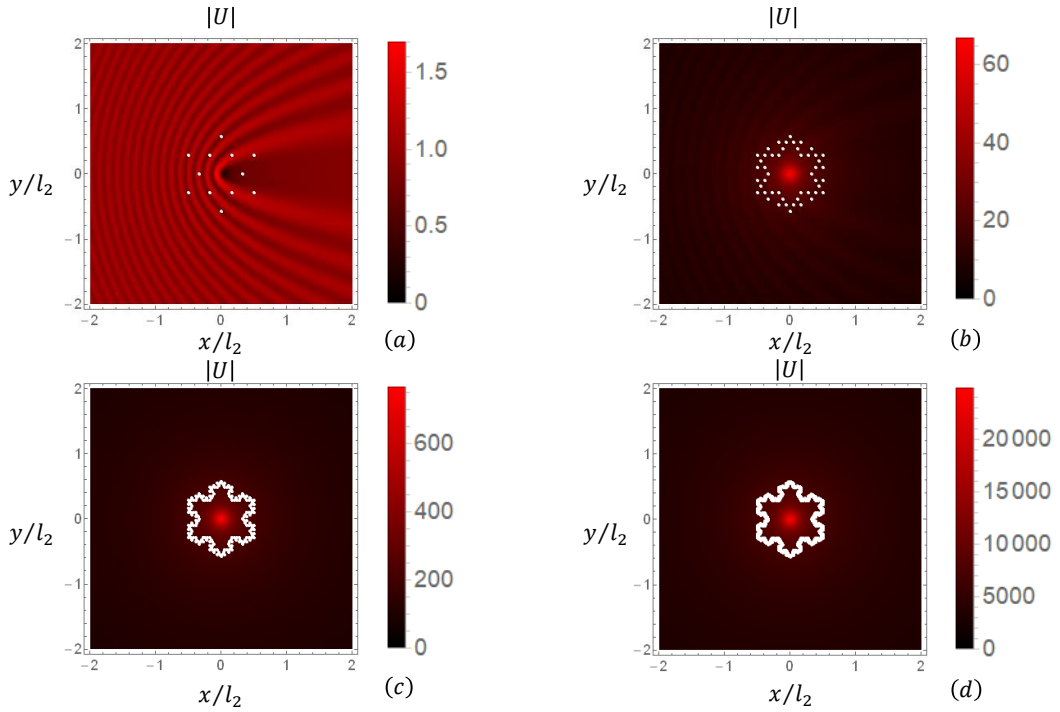

Figure 5.4.2.8: Displacement contours for $H = 0.01$, (anomalous dispersion), fourth minima: (a) $K_2 = 511.805$, (b) $K_2 = 244.559$, (c) $K_2 = 261.285$, (d) $K_2 = 269.893$.

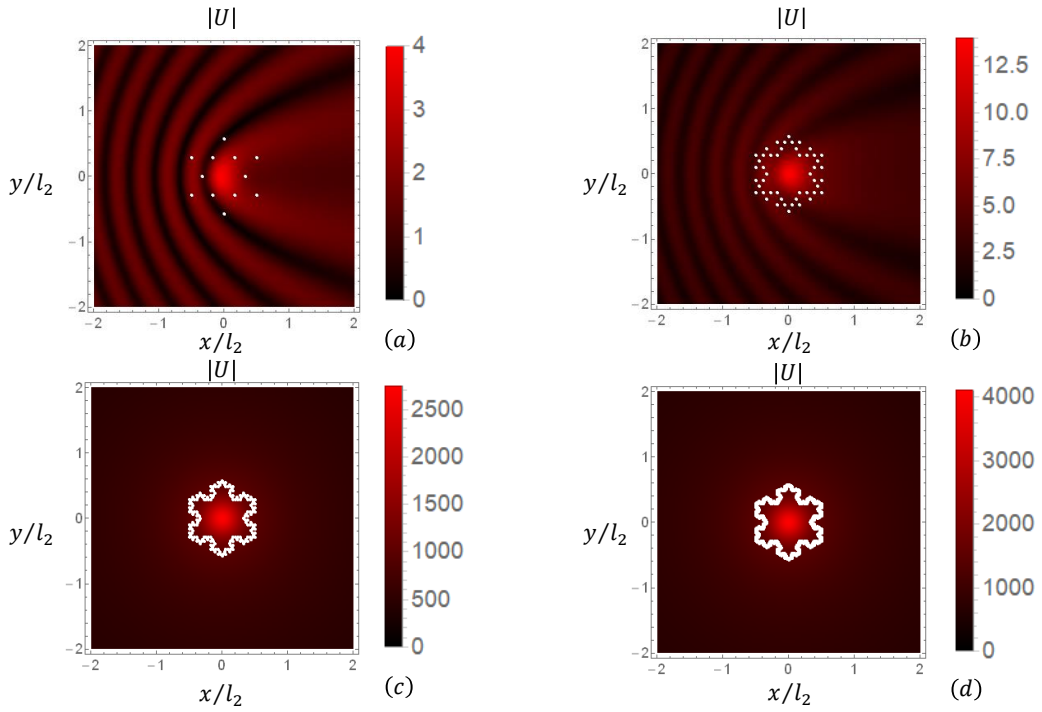

Figure 5.4.2.9: Displacement contours for $H = 0.1$, (anomalous dispersion), first minima: (a) $K_2 = 52.047$, (b) $K_2 = 57.435$, (c) $K_2 = 60.4621$, (d) $K_2 = 62.068$.

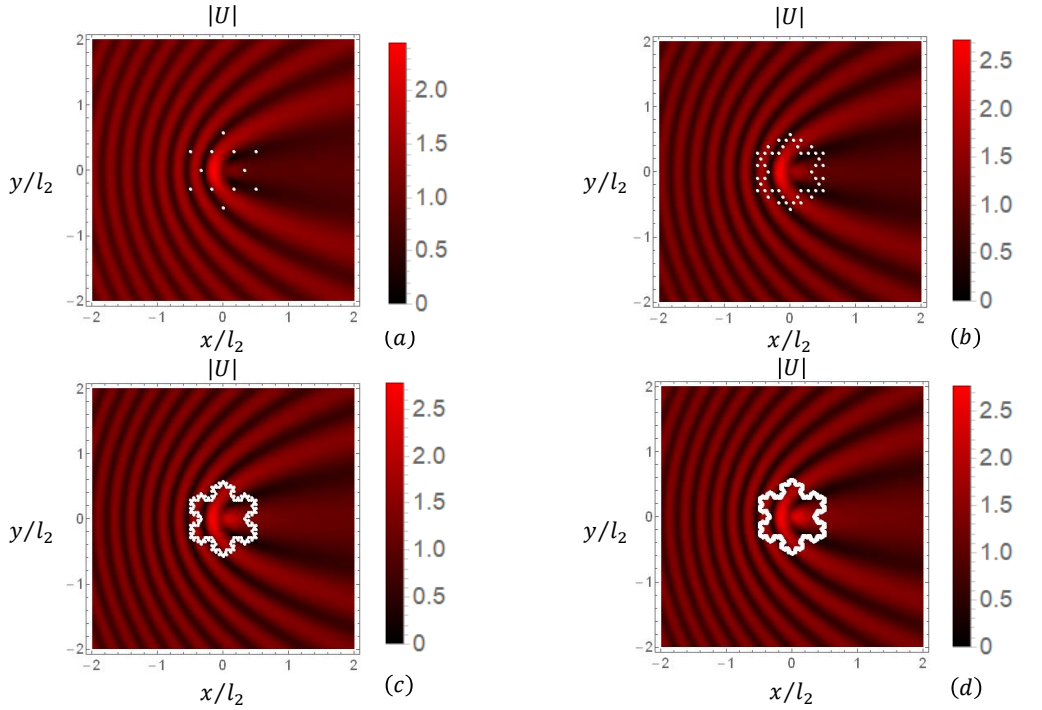

Figure 5.4.2.10: Displacement contours for $H = 0.1$, (anomalous dispersion), second minima: (a) $K_2 = 94.144$, (b) $K_2 = 96.301$, (c) $K_2 = 101.480$, (d) $K_2 = 103.924$.

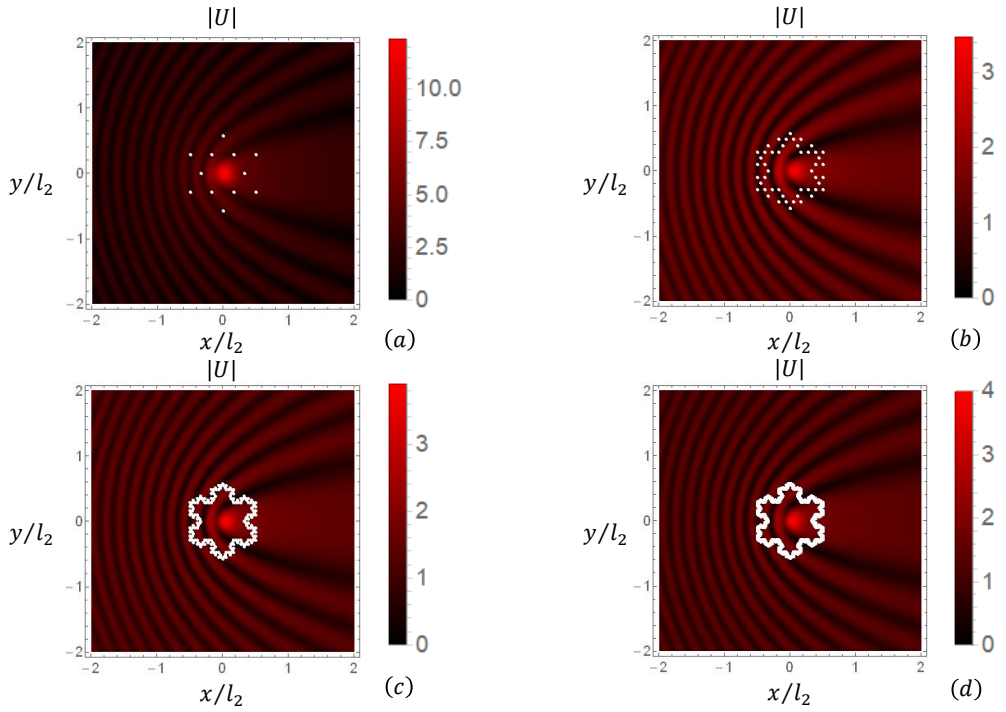

Figure 5.4.2.11: Displacement contours for $H = 0.1$, (anomalous dispersion), third minima: (a) $K_2 = 131.981$, (b) $K_2 = 127.831$, (c) $K_2 = 135.769$, (d) $K_2 = 138.872$.

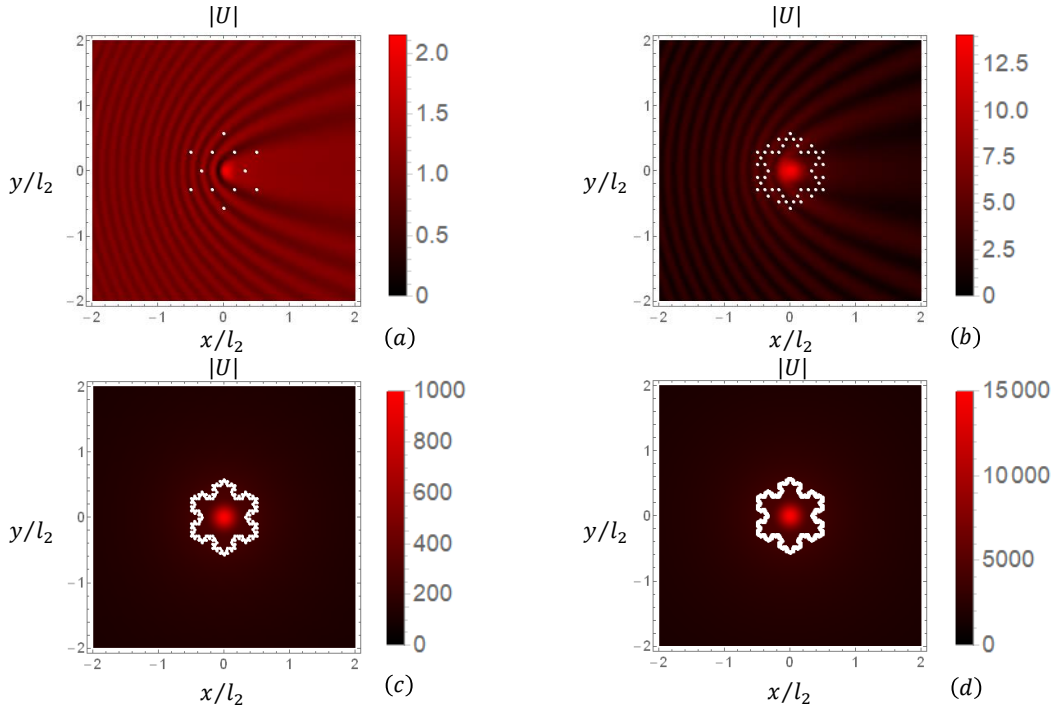

Figure 5.4.2.12: Displacement contours for $H = 0.1$, (anomalous dispersion), fourth minima: (a) $K_2 = 184.300$, (b) $K_2 = 140.283$, (c) $K_2 = 149.982$, (d) $K_2 = 153.657$.

Based on the figures above, the following conclusions can be made for the case of anomalous dispersion:

• In the vast majority of cases, the percentage change in the minima value between consecutive iterations decreases.

• Two types of resonant modes are identified: (a) modes in which waves propagate along discrete paths and (b) trapping modes, where the motion is mostly confined within the arrangement of pins.

• The non-dimensional displacements values increase as the number of pins increases.

• The system's response at the resonant modes where paths are formed remains nearly unchanged both qualitatively and quantitatively, even as the iterations increase. In contrast, at the trapping modes, the qualitative response stays consistent, but the non-dimensional displacements within the pin configuration increase significantly with more iterations.

• When dispersion is anomalous, a decrease in the value of H leads to an increase in the non-dimensional displacement.

• From the fourth iteration and on, when waves are trapped inside the configuration of pins, the non-dimensional displacement increases unrealistically. This behaviour can be explained by the structure of Koch's snowflake, which contains many corners. With each iteration, the number of corners quadruples. A configuration with numerous corners promotes successive wave reflections, leading to increased superposition and consequently, larger displacements.

• Similar responses are observed for all other detected minima.

When there is no dispersion, the local minima correspond to resonances where either discrete wave paths are formed, or the wave motion is confined predominantly inside the configuration of pins. However, there is a qualitative difference in the displacement field compared to the case of anomalous dispersion. In particular, the paths along which the waves propagate change behind the configuration, while In the trapping modes, concentric circles form outside the arrangement of pins, a pattern that does not occur in the anomalous dispersion case. For all other cases of local minima, the system's response is similar to what is shown in the following figure.

In the case of normal dispersion, there are no local minima, and thus no resonances. The system's response remains almost unchanged, regardless of the number of pins inserted. Additionally, the values of H and K_2 have minimal impact on the system's behaviour. Cloaking modes, where the wave path is redirected around the pin configuration making the pins appear absent or ineffective form at every value of K_2. These paths are vertical and extremely narrow, resulting in nearly uniform displacements across the entire infinite domain.

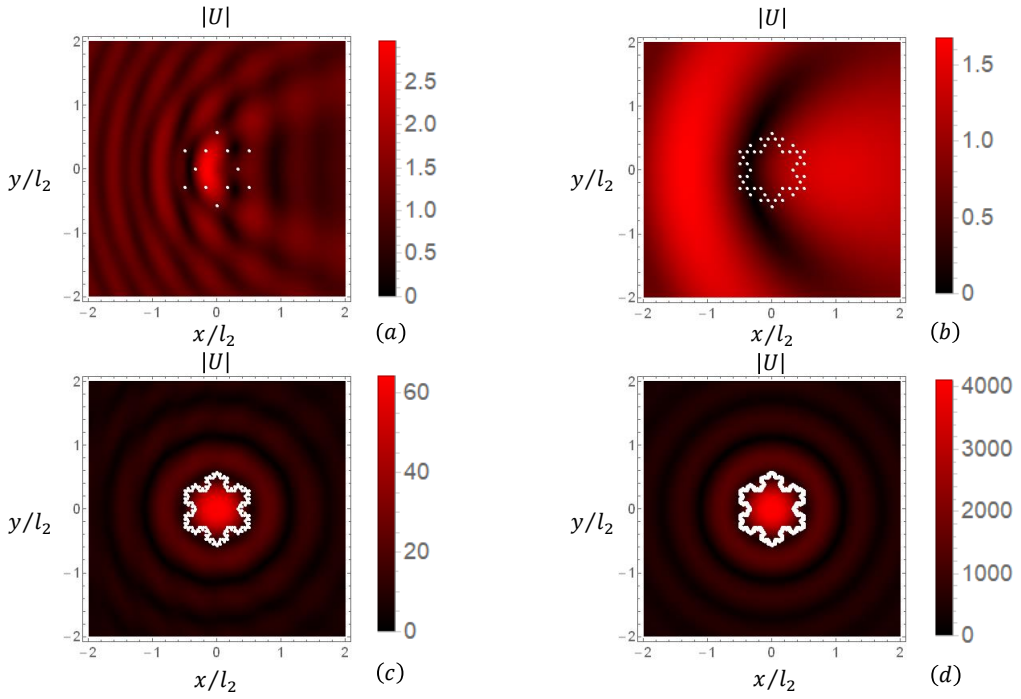

Figure 5.4.2.13: Displacement contours for $H = 1$, (no dispersion): (a) $K_2 = 8.797$ (1st minima), (b) $K_2 = 1.819$ (1st minima), (c) $K_2 = 10.325$ (2nd minima), (d) $K_2 = 13.951$ (2nd minima).

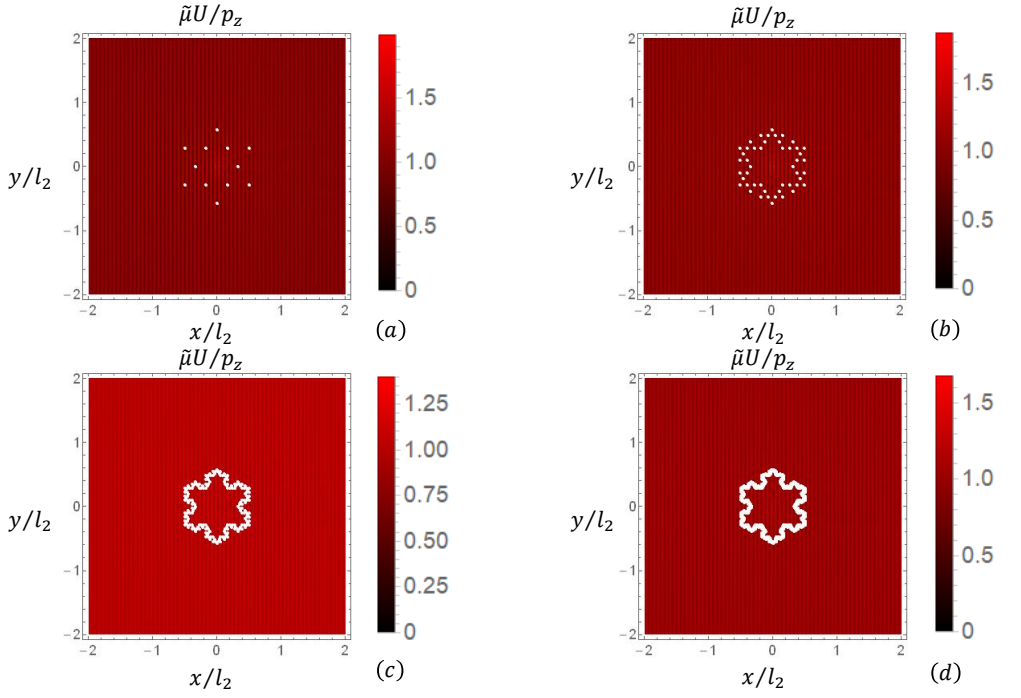

Figure 5.4.2.14: Displacement contours for $H = 10$, (normal dispersion), $K_2 = 10$.

.

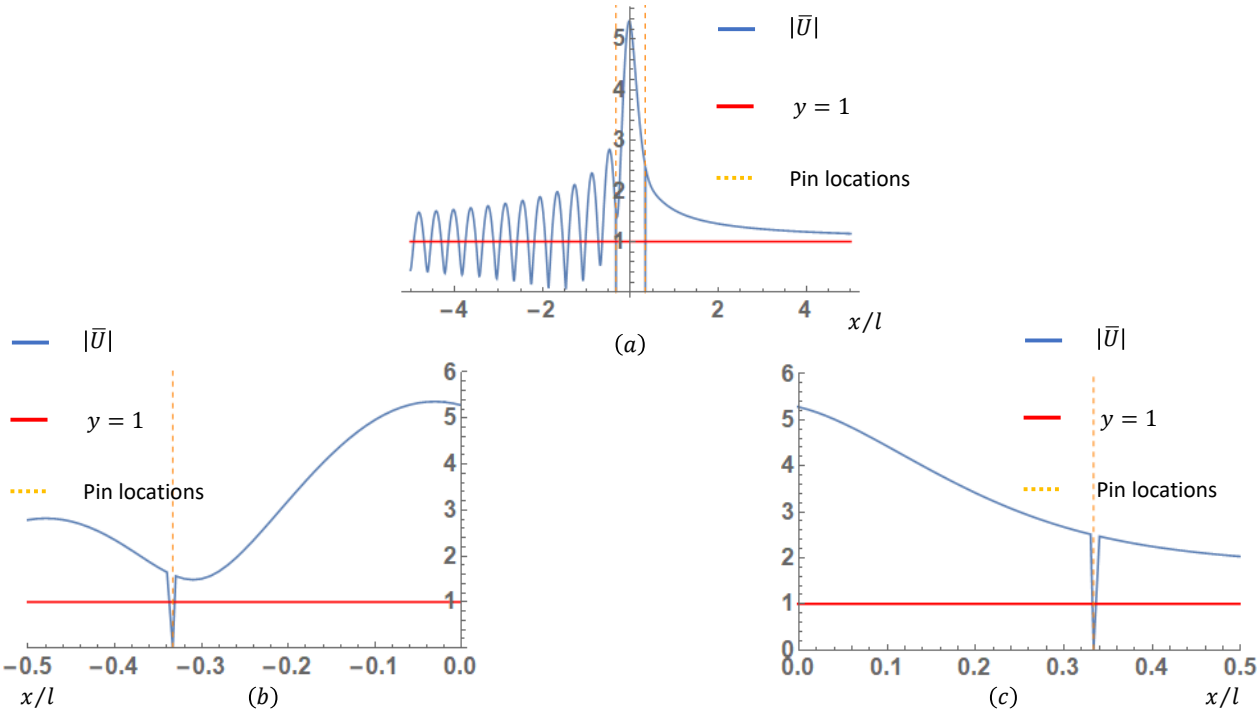

Figure 5.4.2.15: Distribution of U, for the second iteration of Koch's snowflake (12) pins, $H = 0.01$ (anomalous dispersion), $K_2 = 64.265$ (1st minima), $y = 0$: (a) wide range of x/l_2 and (b), (c) close to the pins.

.

In the above diagrams the distribution of the norm of the non-dimensional displacement U along the x axis, for the second iteration of Koch's snowflake is presented. The line $y = 1$ is also shown because the incident wave has a unit amplitude. Two pins are positioned at points $(-1/3, 0)$ and $(1/3, 0)$, where the displacement magnitude is zero. However, unlike the case of plane strain where the displacements are smooth and continuous functions in the areas where the pins are placed, when the infinite domain is under anti-plane shear, jumps are created in the displacements close to the pins, regardless the number of pins inserted or the type of resonance that occurs, while the value of K_2, as long as it corresponds to a local minimum, has little impact on the displacement discontinuities. Another useful information that is extracted from the above diagrams is that the norm of the non-dimensional displacement U does not reach zero behind the configuration of pins, instead it approaches $y = 1$ asymptotically.

5.5 Remarks

In conclusion, in this work two Green's function are derived for infinite media, subjected to a point load with time harmonic variation, under plane strain and anti-plane shear, within simplified versions of Mindlin's general theory. These Green's functions are finite at the origin and are used to formulate problems involving wave scattering caused by point obstacles (pins), which are modelled as concentrated body forces. When the pins are placed in the infinite domain, configurations of obstacles are formed whose geometry affects the system's response both quantitatively and qualitatively.

For the plane strain case, circular configurations with 12, 24 and 48 pins were considered, while for the anti-plane shear case, analyses were conducted for the first five iterations of Koch's snowflake to illustrate the potential impact of a fractal configuration of pins on the system's response. The results show that, in the case of anomalous dispersion, resonances can occur, leading to a significant local increase in displacements within the infinite domain. For the anti-plane shear state, resonances can also occur even in the absence of dispersion. When the system resonates, either discrete wave paths form, or the motion of particles becomes largely confined within the configuration of pins. The magnitude of these resonances can be controlled by adjusting the number of pins and the material's (non-dimensional) characteristic length H, while details on how the parameters can be selected to tune the system are thoroughly presented in this work

The concepts presented in this thesis have considerable potential for engineering applications, such as designing seismic shields for earthquake protection and controlling tsunamis to safeguard coastlines. Significant research has been conducted in these areas over the past few years, though the approach has primarily been numerical and experimental. The theoretical framework in most cases raised many questions, as it was either lacking or, at best, based on classical plate theory. While classical plate theory shares similarities with generalized continuum theories, as presented in this thesis it is a technical theory that invokes a lot of assumptions that rational theories of generalized elasticity do not. The two main limitations of the derived Green's functions are that they apply only to infinite domains, making them unsuitable for cases where boundary conditions influence the system's response. Additionally, they are specific to deformation states that rarely occur in nature. However, these Green's functions can still be highly valuable when used to complement numerical solutions or experiments.

The aim of this work is not to tackle practical problems as the ones mentioned above from an analytical point of view, but to explore scattering from point obstacles in elasticity theory, which cannot be addressed in classical elasticity due to the singularity of the corresponding Green's functions, as well as to highlight potential applications where these concepts could be applied. This thesis also contributes to the bibliography of generalized continua by introducing a new Green's function for the plane strain case. Additionally, it presents a formulation and proof of the generalized version of the completeness theorem that holds for all three forms of Mindlin's general theory, which, to the author's knowledge, does not exist in the current literature.

References

[1] G. A. Maugin, A. V. Metrikine, Mechanics of generalized continua (2010).

[2] J. Mac Cullagh, An essay towards a dynamical theory of crystalline reflexion and refraction, The Transactions of the Royal Irish Academy 21 (1846) 17–50.

[3] W. T. B. Kelvin, P. G. Tait, Treatise on natural philosophy, Vol. 1, Claredon Press, 1867.

[4] W. Voigt, Theoretische studien über die elasticitätsverhältnisse der krystalle, Königliche Gesellschaft der Wissenschaften zu Göttingen, 1887.

[5] E. M. P. Cosserat, F. Cosserat, Théorie des corps déformables, A. Hermann et fils, 1909.

[6] E. Kröner, Mechanics of generalized continua, Springer, 1968.

[7] E. Aero, E. Kuvshinskii, Fundamental equations of the theory of elastic media with rotationally interacting particles, Soviet Physics-Solid State 2 (7) (1961) 1272–1281.

[8] W. Nowacki, Couple-stresses in the theory of thermoelasticity, in: Irreversible Aspects of Continuum Mechanics and Transfer of Physical Characteristics in Moving Fluids: Symposia Vienna, June 22–28, 1966, Springer, 1968, pp. 259–278.

[9] G. A. Maugin, Micromagnetism and polar media, Princeton University, 1971.

[10] C. Truesdell, R. Toupin, The classical field theories, Springer, 1960.

[11] R. D. Mindlin, H. Tiersten, Effects of couple-stresses in linear elasticity, Archive for Rational Mechanics and analysis 11 (1962) 415–448.

[12] R. Toupin, Elastic materials with couple-stresses, Archive for rational mechanics and analysis 11 (1) (1962) 385–414.

[13] A. Eringen, Nonlinear theory of continuous media, 1962, New York: McGraw.

[14] A. C. Eringen, E. Suhubi, Nonlinear theory of simple micro-elastic solids—i, International Journal of Engineering Science 2 (2) (1964) 189–203.

[15] E. Suhubl, A. C. Eringen, Nonlinear theory of micro-elastic solids—ii, International Journal of Engineering Science 2 (4) (1964) 389–404.

[16] A. C. Eringen, Simple microfluids, International Journal of Engineering Science 2 (2) (1964) 205–217.

[17] A. C. Eringen, Mechanics of micromorphic materials, in: Applied Mechanics: Proceedings of the Eleventh International Congress of Applied Mechanics Munich (Germany) 1964, Springer, 1966, pp. 131–138.

[18] R. D. Mindlin, Micro-structure in linear elasticity, Archive for rational mechanics and analysis 16 (1964) 51–78.

[19] A. E. Green, R. S. Rivlin, Multipolar continuum mechanics, Archive for rational mechanics and analysis 17 (1964) 113–147.

[20] V. Pal'mov, Fundamental equations of the theory of asymmetric elasticity, Journal of Applied Mathematics and Mechanics 28 (3) (1964) 496–505.

[21] S. Forest, Mechanics of generalized continua: construction by homogenizaton, Le Journal de Physique IV 8 (PR4) (1998) Pr4–39.

[22] G. A. Maugin, Nonlinear waves in elastic crystals, Oxford University Press, 1999.

[23] M. Cyrot, Ginzburg-landau theory for superconductors, Reports on Progress in Physics 36 (2) (1973) 103.

[24] B. Rosenstein, D. Li, Ginzburg-landau theory of type ii superconductors in magnetic field, Reviews of modern physics 82 (1) (2010) 109–168.

[25] V. Baidakov, G. S. Boltachev, S. Protsenko, G. Chernykh, The van der waals theory of capillarity and computer simulation, Colloid Journal 64 (2002) 661–670.

[26] J. D. Van der Waals, The thermodynamic theory of capillarity under the hypothesis of a continuous variation of density, Journal of Statistical Physics 20 (2) (1979) 200–244.

[27] F. Dell'Isola, D. J. Steigmann, Discrete and continuum models for complex metamaterials, Cambridge University Press, 2020.

[28] C. Sansour, S. Skatulla, A strain gradient generalized continuum approach for modelling elastic scale effects, Computer methods in applied mechanics and engineering 198 (15-16) (2009) 1401–1412.

[29] J. Fernández-Sáez, A. Morassi, L. Rubio, R. Zaera, Transverse free vibration of resonant nanoplate mass sensors: Identification of an attached point mass, International Journal of Mechanical Sciences 150 (2019) 217–225.

[30] S. Forest, Continuum thermomechanics of nonlinear micromorphic, strain and stress gradient media, Philosophical Transactions of the Royal Society A 378 (2170) (2020) 20190169.

[31] S. C. Cowin, Bone mechanics handbook, CRC press, 2001.

[32] Z. Hashin, S. Shtrikman, A variational approach to the theory of the elastic behaviour of multiphase materials, Journal of the Mechanics and Physics of Solids 11 (2) (1963) 127–140.

[33] S. M. Mousavi, Dislocation-based fracture mechanics within nonlocal and gradient elasticity of bi-helmholtz type–part i: Antiplane analysis, International Journal of Solids and Structures 87 (2016) 222–235.

[34] M. Jirásek, Non-local damage mechanics with application to concrete, Revue française de génie civil 8 (5-6) (2004) 683–707.

[35] D. L. McDowell, Multiscale modeling of interfaces, dislocations, and dislocation field plasticity, Mesoscale Models: From Micro-Physics to Macro-Interpretation (2019) 195–297.

[36] S. Brûlé, E. Javelaud, S. Enoch, S. Guenneau, Experiments on seismic metamaterials: molding surface waves, Physical review letters 112 (13) (2014) 133901.

[37] S. Brule, S. Enoch, S. Guenneau, Flat lens for seismic waves, arXiv preprint arXiv:1602.04492 (2016).

[38] Y. Achaoui, B. Ungureanu, S. Enoch, S. Brûlé, S. Guenneau, Seismic waves damping with arrays of inertial resonators, Extreme Mechanics Letters 8 (2016) 30–37.

[39] S. Brûlé, S. Enoch, S. Guenneau, Role of nanophotonics in the birth of seismic megastructures, Nanophotonics 8 (10) (2019) 1591–1605.

[40] K. Kathiresan, N. Rajendran, Coastal mangrove forests mitigated tsunami, Estuarine, Coastal and shelf science 65 (3) (2005) 601–606.

[41] F. Danielsen, M. K. Sørensen, M. F. Olwig, V. Selvam, F. Parish, N. D. Burgess, T. Hiraishi, V. M. Karunagaran, M. S. Rasmussen, L. B. Hansen, et al., The asian tsunami: a protective role for coastal vegetation, Science 310 (5748) (2005) 643–643.

[42] T. Rasmeemasmuang, J. Sasaki, Wave reduction in mangrove forests: general information and case study in thailand, in: Handbook of Coastal Disaster Mitigation for Engineers and Planners, Elsevier, 2015, pp. 511–535.

[43] D. M. Alongi, Mangrove forests: resilience, protection from tsunamis, and responses to global climate change, Estuarine, coastal and shelf science 76 (1) (2008) 1–13.

[44] H.-O. Peitgen, H. Jürgens, D. Saupe, M. J. Feigenbaum, Chaos and fractals: new frontiers of science, Vol. 106, Springer, 2004.

[45] B. B. Mandelbrot, The fractal geometry of nature/revised and enlarged edition, New York (1983).

[46] P. Cvitanovic, R. Artuso, R. Mainieri, G. Tanner, G. Vattay, N. Whelan, A. Wirzba, Chaos: classical and quantum, ChaosBook. org (Niels Bohr Institute, Copenhagen 2005) 69 (2005) 25.

[47] M. Senechal, Quasicrystals and geometry, cambridge univ (1995).

[48] Y. Zhang, J. Wang, C. Wang, Y. Zeng, T. Chen, Crashworthiness of bionic fractal hierarchical structures, Materials & Design 158 (2018) 147–159.

[49] T. Vicsek, Fractal growth phenomena, World scientific, 1992.

[50] P. Meakin, Fractals, scaling and growth far from equilibrium, Vol. 5, Cambridge university press, 1998.

[51] A. Carpinteri, Fractal nature of material microstructure and size effects on apparent mechanical properties, Mechanics of materials 18 (2) (1994) 89–101.

[52] C. Atzeni, G. Pia, U. Sanna, N. Spanu, A fractal model of the porous microstructure of earth-based materials, Construction and Building Materials 22 (8) (2008) 1607–1613.

[53] G. P. Cherepanov, A. S. Balankin, V. S. Ivanova, Fractal fracture mechanics—a review, Engineering Fracture Mechanics 51 (6) (1995) 997–1033.

[54] A. Yavari, S. Sarkani, E. Moyer Jr, On fractal cracks in micropolar elastic solids, J. Appl. Mech. 69 (1) (2002) 45–54.

[55] J. Li, M. Ostoja-Starzewski, Fractals in elastic-hardening plastic materials, Proceedings of the Royal Society A: Mathematical, Physical and Engineering Sciences 466 (2114) (2010) 603–621.

[56] B. B. Mandelbrot, Fractals in physics: squig clusters, diffusions, fractal measures, and the unicity of fractal dimensionality, Journal of Statistical Physics 34 (1984) 895–930.

[57] M. Angel Martín, F. Javier Taguas, Fractal modelling, characterization and simulation of particle-size distributions in soil, Proceedings of the Royal Society of London. Series A: Mathematical, Physical and Engineering Sciences 454 (1973) (1998) 1457–1468.

[58] G. McDowell, M. Bolton, D. Robertson, The fractal crushing of granular materials, Journal of the Mechanics and Physics of Solids 44 (12) (1996) 2079–2101.

[59] S. Moeini, T. J. Cui, Fractal coding metamaterials, Annalen der Physik 531 (2) (2019) 1800134.

[60] R. H. Bilal, M. Naveed, M. Baqir, M. Ali, A. A. Rahim, Design of a wideband terahertz metamaterial absorber based on pythagorean-tree fractal geometry, Optical Materials Express 10 (12) (2020) 3007–3020.

[61] A. Misra, L. Placidi, F. dell'Isola, E. Barchiesi, Identification of a geometrically nonlinear micromorphic continuum via granular micromechanics, Zeitschrift für angewandte Mathematik und Physik 72 (2021) 1–21.

[62] A. Bedford, A. Bedford, Hamilton's principle in continuum mechanics, Vol. 139, Springer, 1985.

[63] A. Montanaro, D. Pigozzi, On weakly isotropic tensors, International journal of nonlinear mechanics 29 (3) (1994) 295–309.

[64] H. Weyl, The classical groups princeton university press, New Jersey (1946).

[65] E. A. Kearsley, J. T. Fong, Linearly independent sets of isotropic cartesian tensors of ranks up to eight, J. Res. Natl. Bur. Stand., Sect. B 79 (1975) 49.

[66] G. Racah, Determinazione del numero dei tensori isotropi indipendenti di rango n, G. Bardi, 1933.

[67] J. Ignaczak, Tensorial equations of motion for elastic materials with microstructure, Trends in elasticity and thermoelasticity (1971) 89–111.

[68] H. Georgiadis, D. Anagnostou, Problems of the flamant–boussinesq and kelvin type in dipolar gradient elasticity, Journal of Elasticity 90 (2008) 71–98.

[69] P. Gourgiotis, H. Georgiadis, Plane-strain crack problems in microstructured solids governed by dipolar gradient elasticity, Journal of the Mechanics and Physics of Solids 57 (11) (2009) 1898–1920.

[70] D. Anagnostou, P. Gourgiotis, H. Georgiadis, The cerruti problem in dipolar gradient elasticity, Mathematics and Mechanics of Solids 20 (9) (2015) 1088–1106.

[71] H. Georgiadis, P. Gourgiotis, D. Anagnostou, The boussinesq problem in dipolar gradient elasticity, Archive of Applied Mechanics 84 (2014) 1373–1391.

[72] H. Georgiadis, The mode iii crack problem in microstructured solids governed by dipolar gradient elasticity: static and dynamic analysis, J. Appl. Mech. 70 (4) (2003) 517–530.

[73] H. Georgiadis, I. Vardoulakis, E. Velgaki, Dispersive rayleigh-wave propagation in microstructured solids characterized by dipolar gradient elasticity, Journal of Elasticity 74 (2004) 17–45.

[74] H. Georgiadis, C. Grentzelou, Energy theorems and the j-integral in dipolar gradient elasticity, International journal of Solids and Structures 43 (18-19) (2006) 5690–5712.

[75] C. Grentzelou, H. Georgiadis, Balance laws and energy release rates for cracks in dipolar gradient elasticity, International Journal of Solids and Structures 45 (2) (2008) 551–567.

[76] A. E. Giannakopoulos, S. Petridis, D. S. Sophianopoulos, Dipolar gradient elasticity of cables, International Journal of Solids and Structures 49 (10) (2012) 1259–1265.

[77] J. Achenbach, Wave propagation in elastic solids, Elsevier, 2012.

[78] E. Sternberg, On the integration of the equations of motion in the classical theory of elasticity, Division of Applied Mathematics, Brown University, 1959.

[79] P. Gourgiotis, H. Georgiadis, I. Neocleous, On the reflection of waves in half-spaces of microstructured materials governed by dipolar gradient elasticity, Wave Motion 50 (3) (2013) 437–455.

[80] A. Love, H.: The small free vibrations and deformation of a thin elastic shell, philos, Tech. rep., TR Soc. A, 179, 491–546, https://doi. org/10.1098/rsta (1888).

[81] G. Kirchhoff, Über das gleichgewicht und die bewegung einer elastischen scheibe., Journal für die reine und angewandte Mathematik (Crelles Journal) 1850 (40) (1850) 51–88.

[82] J. N. Reddy, Theory and analysis of elastic plates and shells, CRC press, 2006.

[83] G. N. Watson, A treatise on the theory of Bessel functions, Vol. 2, The University Press, 1922.

[84] G. Eason, J. Fulton, I. N. Sneddon, The generation of waves in an infinite elastic solid by variable body forces, Philosophical Transactions of the Royal Society of London. Series A, Mathematical and Physical Sciences 248 (955) (1956) 575–607.

[85] L. Debnath, D. Bhatta, Integral transforms and their applications, Chapman and Hall/CRC, 2016.

[86] H. Von Koch, On a continuous curve without tangents constructive from elementary geometry, in: Classics on fractals, CRC Press, 2019, pp. 24–45.

[87] D. Evans, R. Porter, Penetration of flexural waves through a periodically constrained thin elastic plate in vacuo and floating on water, Journal of Engineering Mathematics 58 (2007) 317–337.

[88] H. v. Koch, On a continuous curve without tangent constructable from elementary geometry, Classics on fractals (1904).